Biosynthesis of polyhydroxyalkanoates and its medical applications.

Ranjana Rai

School of Life Sciences

UNIVERSITY OF WESTMINSTER

Biosynthesis of Polyhydroxyalkanoates and its Medical Applications

Ms. Ranjana Rai

Department of Molecular and Applied Biology, University of Westminster, UK

A thesis submitted for the degree of Doctor of Philosophy, (Ph.D)

University of Westminster

July, 2010

Declaration

This thesis is a presentation of my original research work. Wherever contributions of others are involved, every effort is made to indicate this clearly, with due reference to the literature, and acknowledgement of collaborative research and discussions.

Ms. Ranjana Rai

Acknowledgement

I would first like to express my deepest gratitude to the University of Westminster's Scholarship Department. Without its financial support I would not have been able to pursue my Ph.D research.

My heartfelt gratitude to my supervisor Dr.Ipsita Roy without whose guidance, support and encouragement this research would not have been possible. I would also like to thank my second supervisor Professor Taj Keshavarz for all his support and guidance.

I am also indebted to Dr. Mike Gordge, Dr. Ian Locke from the Univerisity of Westminster and our collaborators Professor Aldo Boccaccini, Dr. Mohamad Darmawati Yonus from Imperial College, London, Professor Jonathan Knowles, Dr.Vehid Salih, Dr. George Georgiou and Dr. Graham Palmer from UCl Eastman Dental Institute, UK, Professor Steve Howdle, Ian Barker from University of Nottingham, UK and Dr. Aine McCormick from St.Thomas Hospital, UK for their help and support.

I would also like to thank for the support received from Dr.Thakoor Tandel, Neville Antonio and Dr. Zhi Song. I am also indebted to many of my colleagues past and present and special thanks to all my friends Maria, Anu, Sheryl and Diluka for their friendship, for patiently listening to me all through these years and for their support.

This Ph.D has been a long journey, of commitment and dedication. It would not have been possible without the constant love, support and encouragement from my parents, sisters and particularly my husband.

Dedication

I would like to dedicate this work to my parents (Aama and Daddy) for making me the person I am, to my sisters (Josna and Sarojna) for always believing in me, supporting me and my husband, Anup for always being there for me.

Abstract

Polyhydroxyalkanoates are polyesters of 3-hydroxyalkanoic acids produced by numerous Gram positive and Gram negative bacteria under nutrient limiting conditions. Once extracted, the PHAs exhibit a variety of properties from thermoplastic to flexible elastomeric nature. Biodegradability and bicompatibility of PHAs are also well established. Owing to these properties PHAs are increasingly attracting interest for commercial exploitation in various agricultural, industrial and particularly medical applications.

The main aim of this study was to investigate PHA production in microorganisms and utilise the PHA produced for medical applications. Nutrient limitations play a pivotol role in PHA production, hence studies were carried out on the effects of nitrogen, phosphorous, potassium and sulphate limitations on the short chain length, scl-PHA (C_3-C_5 carbon chain length) accumulation by *B. cereus* SPV. The organism accumulated P(3HB) under nitrogen (38 % dcw), sulphur (13.15 % dcw), phosphorous (33.33 % dcw) and P(3HB-co-3HV) under potassium limitations (13.4 % dcw).

Studies were also carried out on the production of medium chain length, mcl-PHAs (C_6-C_{14} carbon chain length) using five different *Pseudomonas* sp., *P. aeruginosa, P. putida, P. fluorescens, P. oleovorans* and *P. mendocina.* GC-MS analysis confirmed the presence of the monomer 3-hydroxyoctanoate in the polymer extracted from *P. putida.* However the result could not be confirmed with NMR. *P. oleovorans* was shown to accumulate copolymers of 3HO and 3-hydroxyhexanoate. *P. aeruginosa* accumulated a novel copolymer containing the monomers 3-hydroxyoctanoate and 2-hydroxydodecanoate, P(3HO-co-2HDD) when grown in octanoate. Occurrence of monomers other than 3-hydroxyacid is rare hence accumulation of P(3HO-co-2HDD) by the organism was interesting. *P. fluorescens* did not accumulate any polymer.

P. mendocina was the main organism that was focussed on for mcl-PHA production because of it being relatively unexplored amongst other *Pseudomonas* producers. The organism showed interesting mcl-PHA biosynthetic capability. It accumulated a homopolymer of P(3HO) (31.3 % dcw) when grown in octanoate. This is the first time that an absolute homopolymer of P(3HO) has been produced. *P. mendocina* also accumulated a copolymer of P(3HB-co-3HO) when grown in sucrose. Such copolymers containing both scl and mcl monomers occur rarely.

A detailed study on the effects of different extraction methods on the yield, molecular weight, thermal properties and lipopolysaccharide (LPS) content of P(3HO) was carried out. An optimised extraction method using a dispersion of hypochlorite and chloroform combined with an optimised polymer purification was found to extract P(3HO) efficiently and also reduce the amount of LPS to an FDA approved level of 0.35 EU/mL.

The homopolymer P(3HO) was also studied as a potential biomaterial for medical applications. The polymer was fabricated into neat P(3HO) films to be used a biomaterial for pericardial patch application. Bioactive nanobioglass particles (n-BG) of the type 45S5 Bioglass® were incorporated as a filler in the polymer matrix to form P(3HO)/n-BG composite films. The P(3HO)/n-BG composite films were to be used as a multifunctional wound dressing which would act both as a biomaterial for skin regeneration and also provide a haemostatic effect. Yes, the P(3HO) in combination with n-BG i.e. the P(3HO)/n-BG composite film was studied for wound dressing. This has been pointed out in Chapter 5: sections 5.1.2. and 5.3.5 The n-BG was found to accelerate blood clotting time confirming the haemostatic effect. The roughness, wettability and Young's modulus of the neat films was increased by the incorporation of the n-BG. Both the neat and composite films were flexible and elastomeric in nature. The E value of the 5 wt% neat film (1.4 MPa) was suitable for its use as a pericardial patch material. The flexible

nature of the P(3HO)/n-BG composite film would make it suitable for applications in difficult contours of the body. Both the neat and composite films were able to support the attachment, growth and proliferation of the HaCaT cells. However, biocompatibility was improved for the P(3HO)/n-BG composites. *In vitro* degradation studies revealed the films both neat and composite underwent hydrolytic degradation which started at the surface and that aged with time.

Modification of P(3HO) was also carried out. This was done by exposing P(3HO) to UV rays, incorporating n-BG into the UV treated polymer matrix to form composites by and blending the flexible elastomeric P(3HO) with the hard and brittle Poly-3-hydroxybutyrate, P(3HB) produced from *B. cereus* SPV and incorporating n-BG into this blend polymer matrix. UV treatment of the polymer increases it hydrophilicity and surface roughness. However, UV treatment also caused P(3HO) chain scissions which increased its surface roughness and also caused cross linking of polymer chains. Both the UV P(3HO) neat and UV P(3HO)/n-BG composite (neat and composite films) made from UV treated P(3HO) showed improved biocompatibility over the non UV treated polymer counterparts for the seeded HaCaT cells. The films showed signs of polymer ageing and underwent slow hydrolytic degradation possibly because of the cross linked P(3HO) chains.

For the blend films the surface properties was greatly affected by the amount of P(3HB) incorporated. The roughness was higher for the blend film containing higher wt% of P(3HB). The roughness was further increased with the incorporation of n-BG into this blend matrix. The stiffness of P(3HO) increased due to the incorporation of P(3HB). *In vitro* degradation studies revealed that the fabricated blend and composite blend films underwent hydrolytic degradation.

Table of content

List of Figures

List of Tables:

Chapter 1: Introduction

1.1. Introduction

Synthetic plastics are imposing a serious threat to our environment. Since its first marked debut in the 1950s, plastics have become an absolute necessity in our lives. However, these plastics are not degradable. Non biodegradable plastics accumulate at the rate of 25 million tons per year and have therefore become one of the main environmental hazards. This problem is compounded with the fact that the resources for crude oil is also decreasing. Therefore, in the present scenario when global warming, climate change and dwindling fossil carbon resources have taken a centre stage; scientists from all over the world are looking for greener ecofriendly alternatives to petrochemical derived plastics. This alternative has come in the form of biodegradable plastics and one such family of polymers attracting considerable interest is the polyhydroxyalkanoates, PHAs (Anderson and Dawes, 1990; Lee, 1995; Sudesh *et al.*, 2000)

Polyhydroxyalkanoates (PHAs) are polyesters of hydroxyalkanoates (HAs) which have the general structure as shown in **Figure 1.1**(Lee *et al.,* 1995). In these polymers, the carboxyl group of one monomer forms an ester bond with the hydroxyl group of the neighbouring monomer (Madison and Huisman, 1999). PHAs are synthesised by numerous Gram positive bacteria; aerobic (cyanobacteria) and anaerobic (non-sulfur and sulfur purple bacteria) photosynthetic bacteria, Gram negative bacteria as well as some archaebacteria. These are produced through the fermentation of carbon and serve as intracellular carbon and energy storage compounds (Anderson and Dawes, 1990; Sudesh *et al.*, 2000). PHAs are accumulated by bacteria as water insoluble cytoplasmic inclusions, the number per cell and size of which varies among different species (Anderson and Dawes, 1990; Doi, 1990; Lee *et al.*, 1995). Usually, bacteria produce these granules when subjected to an unbalanced growth condition with excess carbon and simultaneous limitation

of nutrient(s) such as oxygen, nitrogen, sulphur, magnesium and phosphorous (Anderson and Dawes, 1990; Doi, 1990; Lee, 1995). Some bacteria however, produce them without being subjected to any kind of nutritional constraints for example, *Alcaligenes latus* (Anderson and Dawes, 1990; Doi, 1990).

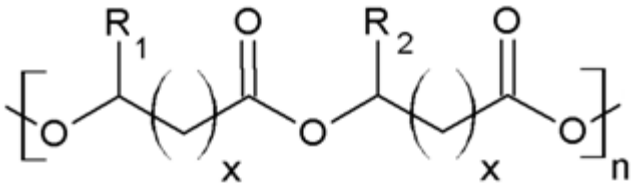

Figure 1.1: The general structure of Polyhydroxyalkanoates

R_1/R_2 = alkyl groups C_1–C_{13}, x = 1–4, n = 100–30 000.

PHAs make an ideal carbon-energy storage material due to their low solubility and high molecular weight, which exerts negligible osmotic pressure on the bacterial cell (Sudesh *et al.*, 2000; Peters and Rehm, 2005). Depending on the number of carbon atoms in the monomeric unit, PHAs are classified as short chain length PHAs, scl-PHAs, that contain 3-5 carbon atoms, example poly(3-hydroxybutyrate), P(3HB), poly(4-hydroxybutyrate), P(4HB) and medium chain length PHAs, mcl-PHAs, that contain 6-14 carbon atoms, example poly(3-hydroxyhexanoate), P(3HHx) and poly(3-hydroxyoctanoate), P(3HO). Also, depending on the kind of monomer present, PHAs can be a homopolymer containing only one type of hydroxyalkanoate as the monomer unit, e.g., P(3HB), P(3HHx) or a heteropolymer containing more than one kind of hydroxyalkanoate as monomer units, e.g., poly(3-hydroxybutyrate-co-3-hydroxyvalerate), P(3HB-co-3HV), poly(3-hydroxyhexanoate-co-3-hydroxyoctanoate), P(3HHx-co-3HO) and poly-(3-hydroxybutyrate-co-3-hydroxyhexanoate), P(3HB-co-3HHx) (Byrom, 1987; Asrar *et al.*, 2002).

In terms of the physical properties exhibited by these two PHA families, mcl-PHAs e.g. P(3HO) with different mol % of 3-hydroxyhexanoate, 3(HHx)

having melting temperature, (T_m) values ranging between 40°C and 60°C , glass transition temperature, (T_g) values between -50 and -25°C, are thermoelastomers having low crystallinity, low tensile strength and high elongation to break (Holmes, 1988). Scl-PHAs for example P(3HB), with a T_m of 180°C and a T_g, of 4°C, is highly crystalline, brittle and stiff and has tensile strength comparable with that of polypropylene (Martin and Williams, 2003). Introduction of a comonomer into the P(3HB) backbone, as in the case of a heteropolymer, greatly affects the polymer properties by increasing its flexibility, toughness and decreasing its stiffness (Valappil *et al.,* 2006). For example, a copolymer like poly(3-hydroxybutyrate-co-3-hydroxyhexanoate), P(3HB-co-3HHx), has a lower melting temperature, crystallinity and is more malleable than P(3HB). In fact P(3HB-co-3HHx) has similar mechanical properties to one of the representative commercial polymers, low density polyethylene (LDPE) which are used for making articles that require low temperature flexibility, toughness and durability (Doi *et al.,* 1995). The properties of PHAs vary considerably depending on their monomer content and hence can be tailored by controlling their compositions. For example, when *P. putida* GPO1 was grown on octanoate and varying mole % of 10-undecenoate, the organism accumulated copolymers of mcl-PHAs with varying mole % of individual monomers, all of which exhibited different thermal and molecular properties (Hartmann *et al.,* 2006). PHAs are biodegradable, recyclable, natural materials which under aerobic conditions degrade into carbon dioxide and water and under anaerobic conditions degrade into carbon dioxide and methane. In nature, microorganisms are able to degrade PHAs mainly using PHA depolymerase (Jendrossek and Handrick, 2002; Choi *et al.*, 2004; Verlinden *et al.*, 2007). These are also biocompatible, exhibit piezoelectricity which stimulates bone growth, aids in wound healing and exhibits wide ranging physical and mechanical properties that arise from the diversity in their chemical structures. Owing to these properties, PHAs are increasingly becoming popular as a natural polymer and attracting

attention for a number of applications in industry, agriculture and as biomaterials for medical applications (Philip *et al.*, 2007). In fact, a major milestone in the medical application of PHAs has been the approval from Food and Drug Administration, FDA, for P(4HB), produced by Tepha FLEX as a biomaterial for use as an absorbable suture (Chen and Qiong, 2005).

1.2. PHA production in microorganisms

The first PHA to be discovered was the short chain length PHA, poly(3-hydroxybutyrate), P(3HB), in *B. megaterium* by a French scientist Francois Lemoigne in 1926 (Lemoigne, 1926) and is one of the most well studied PHA. Mcl-PHA was only discovered in 1983 when *P. oleovorans* was grown in octane (de Smet *et al.,* 1983). Since the first discovery of PHA, more than 90 different genera of archae and eubacteria has been reported to accumulate PHAs (Zinn *et al.,* 2001). The molecular structure of the PHA produced is directly dependent on the organism used, culture conditions for the organism's growth and the carbon feed (Anderson and Dawes, 1990).

1.2.1. Medium chain length, mcl-PHA production using *Pseudomonas* sp.

Since the first discovery of mcl-PHA, many fluorescent *Pseudomonas* sp belonging to the rRNA homology group I have been used for their production (Diard *et al.*, 2002). To date more than 150 units of mcl-PHA monomers have been produced by culturing various *Pseudomonas* strains on different carbon substrates (Kim *et al.,* 2007). The versatility of *Pseudomonas* sp. in using a range of carbon sources and the low substrate specificity of the mcl-PHA synthase, the key enzyme involved in the polymerisation of medium chain length hydroxyacyl CoA into mcl-PHA, leads to the diversity in mcl-PHA monomers. *Pseudomonas* species can be grown on both structurally related

and unrelated carbon sources for producing PHAs. Structurally related carbon sources like alkanes, alkenes, and aldehydes produce precursor substrates that exhibit structures related to the constituents of the mcl-PHAs (de Smet *et al.,* 1983; Brandl *et al.,* 1988; Durner *et al.,* 2001). For example when *P. oleovorans* was grown in hexane, it produced a copolymer containing 83 mol % of 3(HHx), 12 mol % of (3HO) and 4.9 mol % of 3-hydroxydecanoate, 3(HD); in heptane the organism produced 97.5 mol % of 3-hydroxyheptanoate, (3HP), 2.5 mol % of (3HV) and in octane it accumulated 87.8 mol % of (3HO) and 12.2 mol % of (HHx) (Preusting *et al.,* 1990). Structurally unrelated carbon sources provide precursor substrates that are not similar to its structure; these are also relatively cheaper and less toxic as opposed to fatty acids. For example non alkyl based carbon sources like glucose and glucanoate provide precursors such as acetyl-CoA that in turn form the monomeric units. When *P. putida* KT2442 was grown on glucose it was able to accumulate mcl-PHA containing predominantly (3HD) and minor constituents of (3HHx), (3HO) and 3-hydroxydodecanoate, 3(HDD). 3-hydroxyoctanoate is produced as the main monomer when the organisms are grown on carbon sources containing even number of carbon atoms e.g. C_6 ,C_8, C_{10}, C_{12}, C_{14} and 3-hydroxynonanoate when the organisms are grown on carbon sources containing odd number of carbon atoms e.g. C_7, C_9 and C_{11} (Kim *et al.,* 2007).

However, there are some exceptions, for example *Pseudomonas* sp DSY-82, *Pseudomonas stutzeri*, *Pseudomonas* sp. 61-3, and *Pseudomonas* sp. A33, that do not accumulate only mcl-PHA monomers but also copolymers containing monomers of both short chain length and medium chain length, e.g. P(3HB-co-3HHx) (Chen *et al.*, 2004; Chen *et al.*, 2006). Some of these microorganisms are able to accumulate these monomers only when grown using structurally related carbon souces. For example *Pseudomonas nitroreducens* produces P(3HB-co-3HO) containing 93 mol % of 3HO and 7 mol % of 3HB when grown in octanoic acid. Similarly *Pseudomonas pseudoalkaligenus* YSI accumulated

P(3HB-co-3HO-co-3HD) when grown using octanoic acid as the sole carbon source (Hang *et al.,* 2002). Some organisms have been found to produce scl-mcl copolymers when grown using both structurally related and unrelated carbon sources. For example *Pseudomonas* sp. 61-3 accumulated copolymers of 3HB and mcl-monomers when grown in glucanoate as well as alkanoic acids (Kato, 1996). Similarly *Pseudomonas* sp. A33 was able to accumulate the copolymers containing 3(HB) and nine other mcl monomers like 3-hydroxyhexadecanoate, 3(HHD), 3-hydroxydodecenoate, 3(HDDE), 3-hydroxytetradecenoate, 3(HTDE) and 3-hydroxyhexadecenoate, 3(HHDE) when grown using both fatty acid and glucose (Lee *et al.*, 1995). Such organisms that are able to produce scl-mcl copolymers of PHAs are rare in comparison to the organisms able to produce only scl-PHAs and or mcl-PHAs. Hence, these copolymers of scl-mcl-PHAs occur less frequently in nature than scl or mcl-PHAs (Kim *et al.*, 2007).

Some *Pseudomonas* sp. have also been observed to accumulate aliphatic and aromatic PHAs from aromatic hydrocarbons for example, *P. putida, P. oleovorans P. citronellolis, P. fluorescens* and *Pseudomonas* j*essenii* (Tobin and O' Connor, 2005). *P. putida* CA-3 has the ability to accumulate a copolymer of mcl-PHA containing the monomers, 3-hydroxyhexanoic acid, 3-hydroxyoctanoic acid, and 3-hydroxydecanoic acid from styrene and phenyl acetic acid (Ward *et al.,* 2005). Styrene is a major toxic environmental pollutant and hence its utilisation for PHA production can prevent environmental pollution as well as produce environmentally friendly degradable polymer.

1.2.2. Short chain length, scl-PHA production using *Bacillus* sp.

The genus *Bacillus* has been widely studied for the production of PHAs. Properties of short generation time, absence of endotoxins and the presence of both amylase and proteinase which enables it to use even food waste as a substrate, make this genus an important candidate for PHA production (Law and Slepecky, 1961). Findlay and White in 1983 showed the presence of P(3HB) in *B. megaterium* by acid ethanolysis followed by GCMS analysis of the resulting 3-hydroxyalkanoic acid ethyl esters (Findlay and White, 1983). **'Dave *et al.*, (1996)** reported that P(3HB) accumulates to up to 70 % of the dry cell weight in optimum culture conditions for *Bacillus* sp. IPCB-403 It is seen that *Bacillus* sp. can accumulate wide ranging monomers in their polymer chains depending upon the carbon substrate. *Bacillus* sp. INT005 accumulated PHAs ranging from P(3HB), P(3HB-co-3HV): copolymer of 3-hydroxybutyrate and 3-hydroxyvalerate, P(3HB-co-3HHx): copolymer of 3-hydroxybutyrate and 3-hydroxyhexanoate, P(3HB-co-4HB-co-3HHx): copolymer of 3-hydroxybutyrate, 4-hydroxybutyrate and 3-hydroxyhexanoate to P(3HB-co-6HHx-co-3HHx): a terpolymer of 3-hydroxybutyrate, 6-hydroxyhexanoate and 3-hydroxyhexanoate when grown in butyrate, valerate, hexanoate, octanoate, decanoate and β- capralactone (Tajima *et al.,* 2003). *B. cereus* UW85 could produce a terpolymer of 3-hydroxybutyrate, 3-hydroxyvalerate and 6-hydroxyhexanoate when grown using β-capralactone (Labuzek and Radecka, 2001). Borah *et al.* (2002) studied the influence of nutritional and environmental conditions on the accumulation of P(3HB) in *B. mycoides* RLJB-017 and found that sucrose, glucose and fructose were more suitable for the organism growth and P(3HB) accumulation (Borah *et al.,* 2002). Studies on *B. cereus* SPV have shown that the organism is versatile in using a broad spectrum of substrates ranging from fatty acids, plant oils and carbohydrates to accumulate PHAs. When grown in glucose, fructose,

sucrose and gluconate the organism accumulated PHAs such as P(3HB) upto 38 % dcw, poly(3-hydroxybutyrate-co-4-hydroxybutyrate), P(3HB-co-4HB) upto 40.25 % dcw, P(3HB-co-4HB) upto 38.40 % dcw and poly(3-hydroxybutyrate-co-3-hydroxyvalerate-co-4-hydroxybutyrate), P(3HB-co-3HV-4HB) upto 41.90 % dcw respectively (Valappil *et al.*, 2006). When grown in n-alkanoates containing C_3 to C_{12} carbon atoms the organism had the highest yield of P(3HB) upto 80.14 % dcw for decanoate (Valappil *et al.*, 2006).

1.3. The enzymology of PHA production and organisation of the PHA biosynthetic genes

PHA producton is catalysed by the enzyme 'PHA synthase which uses, hydroxyacyl-CoA, (HACoA) molecules as substrate. The reaction catalysed by this enzyme is shown in **Figure 1.2**. The PHA synthase enzyme is encoded by the *phaC* gene (Rehm, 2003).

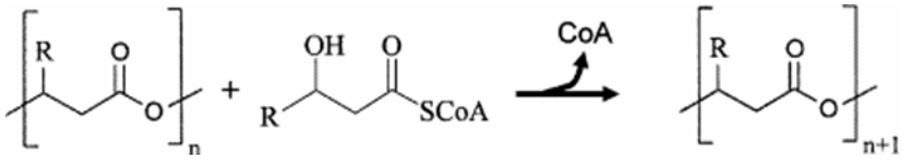

Figure 1.2: Reaction catalysed by the PHA synthase enzyme (Rehm, 2003).

Currently the sequences of 88 PHA synthases have been carried out including two from the halobacterial species *Haloarcula marismortui* and *Haloferax mediterranei* (Grage *et al.*, 2009; Grage, 2009). Based on the amino acid sequences, the substrate ranges of the enzymes, molecular mass and subunit compositions, PHA synthases have been grouped into four classes i.e. Class I, II, III and IV (Rehm, 2003; Grage *et al.*, 2009). The genetic organisation of these PHA synthase genes are shown in **Figure 1.3**.

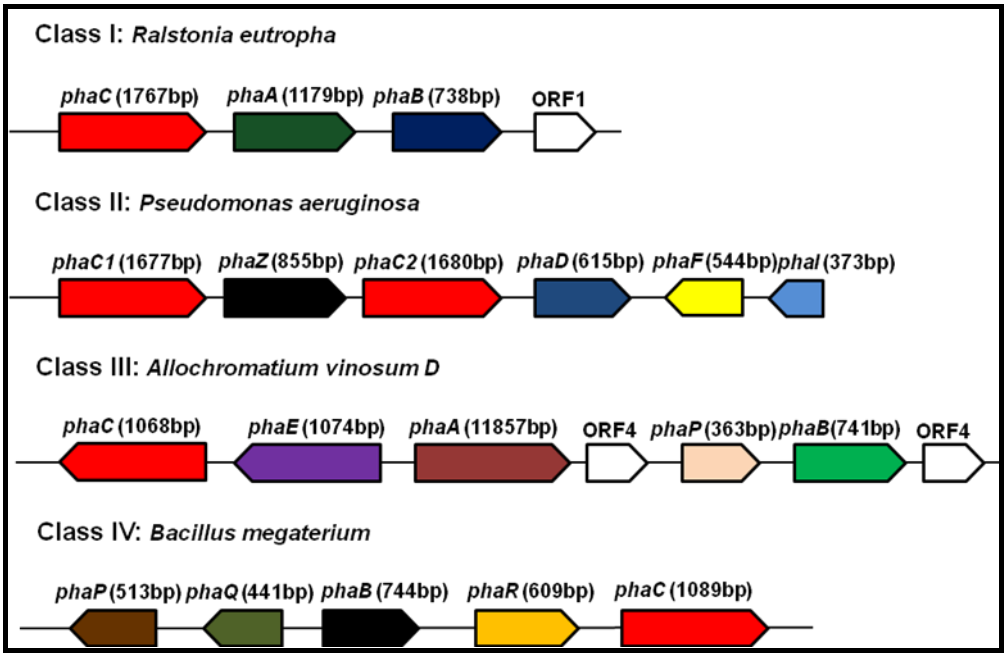

Figure 1.3: Genetic organisation of the PHA synthase genes (Rehm, 2003)

The Class I PHA synthase (prototype: *Cupriavidus necator*) consist of only one type of subunit (PhaC). Its molecular weight ranges between 61 and 73 kDa and catalyzes polymerization of short chain length hydroxyacidCoAs, HACoAs (Qi and Rehm, 2001). In this class, the genes encoding for the PHA synthase (*phaC*), ß-ketothiolase (*phaA*) and NADPH dependent acetoacetyl-CoA reductase (*phaB*) constitute the *phaCAB* operon (Peoples and Sinskey, 1989). The ß-ketothiolase enzyme catalyses the condensation of two acetyl-CoA molecules to form the acetoacetyl-CoA. This acetoacetyl-CoA molecule formed is then converted to (R)-3-hydroxybutyryl-CoA by the NADPH dependent acetoacetyl-CoA reductase (Peoples and Sinskey, 1989).

The Class II PHA synthase (prototype: *Pseudomonas aeruginosa*) is encoded by two different genes, *phaC1 and phaC2*, again 61 to 73 kDa in size. Each catalyse the polymerisation of medium chain length hydroxyacyl CoA substrates, to form mcl-PHAs (Rehm, 2003). The two *phaC* genes are separated by the *phaZ* gene, encoding the PHA depolymerase. Further downstream of the synthase operon, the *phaD* gene is collinearly located

along with the genes *phaI* and *phaF*, which are transcribed in the opposite direction. Both *phaF* and *phaI* code for granule associated structural proteins phasins (Ren *et al.,* 2009). The *phaF* gene is also involved in the transcriptional regulation of *phaC1* gene expression (Prieto *et al.,* 1999). PhaF encoded by *phaF* is a granule associated protein which in the absence of substrates for PHA production remains free in the cytoplasm as no PHA granule is formed. Thus it binds to the promoter region upstream of the *phaC1* gene thereby inhibiting the transcription of the *phaC1* gene. However, in the presence of PHA producing substrates, the phaF is bound to the PHA granule and therefore the *phaC1* gene gets expressed (Prieto *et al.*, 1999; Kessler and Witholt, 2001). The *phaD* gene product plays a role in the regulation of the size and number of PHA granules formed (Klinke *et al.*, 2000)

The Class III PHA synthase (prototype: *Allochromatium vinosum, Thiocystis violacea, Thiocapsa pfennigii*) is a heteromer containing two subunits of 40 kDa, each encoded by the genes *phaC* and *phaE*. The subunits do not show any homology to each other. Both are required for the functional activity of the PHA synthase which catalyses the polymerization of short chain length HACoAs (Liebergesell *et al.,* 1992). *phaP* codes for the granule associated structural protein called phasins. These proteins have been observed to have an influence on the granule size, number and also on the molecular weights of the synthesized PHA (Klinke *et al.*, 2000). *phaA* and *phaB* encodes for the ß-ketothiolase and an NADPH dependent acetoacetyl-CoA reductase, respectively, as described above.

The Class IV PHA synthase (prototype: *Bacillus megaterium*) is a heterodimer containing two subunits of 40 kDa and 20 kDa each, encoded by the *phaC* and *phaR* genes respectively. This enzyme catalyses the polymerisation of scl-HACoA substrates to form scl-PHAs (Mc Cool and Cannon, 2001). In this class, the *phaC* and *phaR* genes are separated by the

phaB gene. Here the *phaRBC* operon is transcribed as a tricistronic operon. The *phaP* and *phaQ* genes located upstream are transcribed in an opposite direction. Here too, the PhaP proteins are associated with the PHA granules and are called phasins. In *Cupriavidus necator*, PhaP have been found to regulate P(3HB) production by regulating the surface/volume ratio of P(3HB) granules and by interacting directly with the PHA synthase (York *et al.,* 2001). PhaQ in *B. megaterium,* is found to be a transcriptional regulator that negatively controls expression of the *phaQ* and *phaP* genes (Lee *et al.,* 2004).

1.4 Metabolic pathways for PHA production

The biosynthesis of PHA involves two major steps, the first step leads to the generation of hydroxyacyl CoA substrates and the second leads to the polymerisation of these substrates leading to the formation of the PHA. Three metabolic pathways (Pathway I: Chain elongation reaction; Pathway II: Fatty acid ß-oxidation; Pathway III: Fatty acid *de novo* biosynthesis) are known to be utilised by different organisms to produce these substrates hydroxyacyl-CoA, (HACoA) and polymerise them into PHAs (**Figure 1.4**).

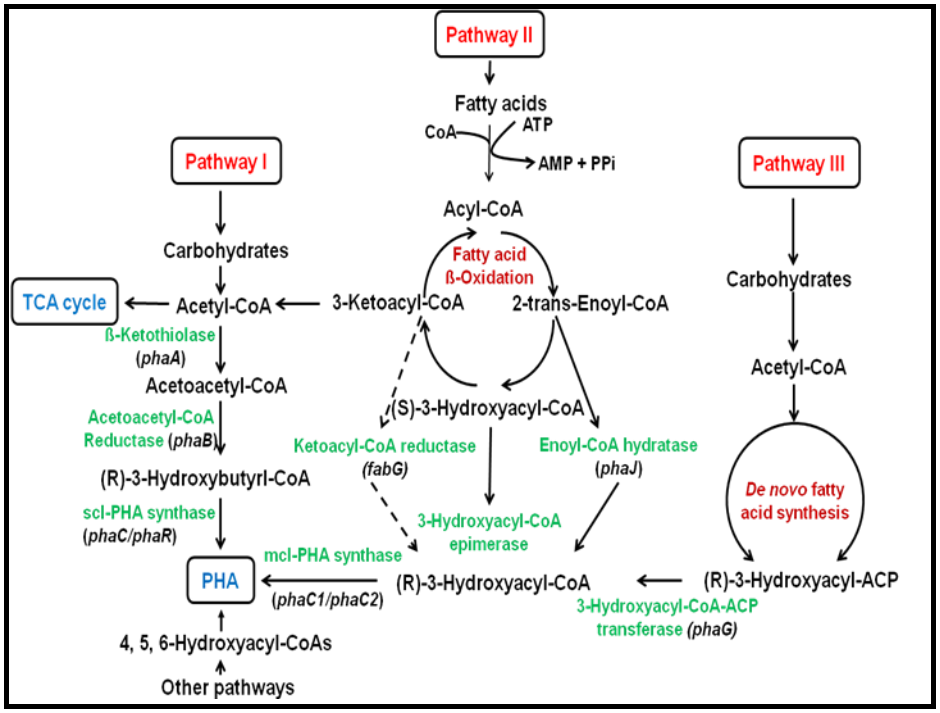

Figure 1.4: Metabolic pathways for the production of PHAs. (Adapted from Kim *et al.*, 2007)

Pathway I, that of the chain elongation reaction, is the best known among the PHA biosynthetic pathway and is represented by *Cupriavidus necator* (Sudesh *et al.,* 2000; Taguchi *et al.,* 2001). Here, the condensation of two acetyl-CoA molecules from the tricarboxylic acid (TCA) cycle takes place to form acetoacetyl-CoA with the help of the enzyme ß-ketothiolase (*phaA*) (Senior and Dawes, 1971; Senior and Dawes, 1973; Philip *et al.*, 2006). Acetoacetyl-CoA is then converted to (R)-3-hydroxybutyryl-CoA by the (R)-specific acetoacetyl-CoA reductase (*phaB*) which is NAPH dependent. Finally, the PHA synthase enzyme catalyses the polymerisation via esterification of 3-hydroxybutyryl-CoA into poly(3-hydroxybutyrate), P(3HB) (Philip *et al.,* 2006).

Pathway II, the fatty acid ß-oxidation pathway, was deciphered when fluorescent *Pseudomonas*, such as *Pseudomonas oleovorans*, *Pseudomonas putida* and *Pseudomonas aeruginosa* were found to accumulate PHA

consisting of mcl-(*R*)-3HA units from alkanes, alcohols, alkanoates and oils (Huisman *et al.,* 1989; Taguchi *et al.,* 2001), (Huisman *et al.,* 1989; Taguchi *et al.,* 2001). Here, the fatty acids are first converted to the corresponding acyl-CoA thioesters which are then oxidised by fatty acid ß-oxidation via trans-2-enoyl-CoA and (*S*)-3-hydroxyacyl-CoA to form 3-ketoacyl-CoA. 3-ketoacyl-CoA is then cleaved by a ß- ketothiolase to form acetyl-CoA and an acyl-CoA comprising of two less carbon atoms as compared to the acyl-CoA that entered the first cycle. Subsequent cycles follow until the original acyl-CoA is completely converted to acetyl-CoA. The enzymes enoyl-CoA hydratase (encoded by *phaJ*) and 3-ketoacyl-CoA reductase (encoded by *fabG)* take active part in converting the fatty acid ß-oxidation intermediates into suitable substrates i.e. (R)-3-Hydroxyacyl-CoA for the PHA synthase to polymerise.

Fatty acid *de novo* biosynthesis is involved in pathway III and is of significant interest because it helps generate PHA monomers from structurally unrelated, simple, inexpensive carbon sources such as glucose, sucrose and fructose (Philip *et al.,* 2006), (**Figure 1.4**). *Pseudomonas* sp. reported to have this pathway are *P. aeruginossa, P. aureofaciens, P. citronellolis* and *P. putida*. In this pathway, the enzyme acyl-CoA-ACP transferase (encoded by *phaG*) transfers the hydroxyacyl moiety from (R)-3-hydroxy-acyl carrier protein to coenzyme A, thus forming (R)-3-hydroxyacyl-CoA, which acts as the substrate for the PHA synthase enzyme. Overexpression of transacylating enzymes such as malonyl-CoA-ACP transacylase (*fabD*) is also known to generate monomers for PHA biosynthesis (Taguchi *et al.,* 1999; Sudesh *et al.,* 2000).

The particular pathway for PHA production used by the organism is primarily governed by the metabolic pathway that is active in the organism and the carbon source provided. Pathway I is found in organisms such as *Cupriavidus necator* and *Bacillus cereus* for the production of scl-PHA using carbohydrates such as glucose. Organisms such as *Pseudomonas* sp. use pathway II and III

for the production of MCL-PHAs. Pathway II is used when grown on structurally related carbon sources such as fatty acids and pathway III is used when structurally unrelated carbon sources such as carbohydrates.

1.5. Role of nutrient limitations in PHA production

The role of nutrient limitations in the production of PHAs was first studied in 1958 by Macrae and Wilkinson. They observed that a sporogenous strain of *B. megaterium* accumulated more PHAs as the carbon to nitrogen ratio increased (Macrae and Wilkinson, 1958). Their results therefore suggested that like polyphosphate and carbohydrate reserves, PHA accumulation occurred in response to an imbalance in growth brought about by nutrient limitations (Sudesh *et al.,* 2000). It has now been established that PHA producers can accumulate PHAs not only in conditions of one limiting nutrient but in fact on simultaneous nutrient limitations at any one time. By nutrient limitation or limiting condition, it means that the limiting nutrient is present in an extremely low concentration which is just enough to support the organism's growth but at much lower concentrations when compared to carbon. Hence, the organisms accumulate the PHAs as an energy and carbon reserve during this nutrient(s) starvation. In fact, PHAs constitute an ideal carbon energy storage material due to low solubility and high molecular weight which exerts negligible osmotic pressure on the organism. Several studies have been carried out to study the relationship of nutrient limitations and PHA accumulation in both the scl and mcl-PHA producers, such as *B. cereus* SPV (Valappil *et al.,* 2007), *B. megaterium* and *Pseudomonas* sp (Ramsay *et al.*, 1991; Ramsay *et al.*, 1992; Huijberts and Eggink, 1996). Nitrogen 'N' and Phosphorous 'P' have been the most commonly used limiting nutrients for both scl and mcl production, however other nutrient limiting conditions of magnesium 'Mg', potassium 'K', sulphur 'S', carbon 'C' and oxygen 'O' have also been studied (lee and Chang, 1995; Lee *et al.*, 2000;

Ballistreri *et al.*, 2001). Limitation strategy for a nutrient, for example 'N', can be achieved either by adjusting the C/N ratio in the media as in case of batch fermentation or by adjusting both the C/N ratio and the nitrogen feed during fed batch and continuous fermentation. Limitations of other nutrients have been carried out using similar approaches

Study by Hazenberg and Witholt, (1997) found that *P. oleovorans* accumulated maximum PHA (33%, w/w) under 'N' limitation when compared to 'P' limitation (17 %, w/w), 'Mg' limitation (5-10 %, w/w), 'Fe' limitation (5-8 %, w/w) and 'O' limitation (5-10 %, w/w) when grown in n-octane (Hazenberg and Witholt, 1997). During fed batch culture of *P. putida* under phosphate limitation using oleic acid as the carbon source the organism accumulated mcl-PHA up to 51 % of the dcw (Lee *et al.,* 2000). In studies carried out by Kim *et al*, (2002), mcl-PHA accumulation of up to 75 % was reached when *P. oleovorans* was grown in fed batch using 20g octanoic acid per gram of ammonium nitrate (Kim, 2002). *Pseudomonas* sp. grown in nitrogen deficient E2 medium accumulated mcl-PHAs using aromatic carbon sources as the feed (Tobin and O' Connor, 2005). Limitation of oxygen has also been reported to stimulate both scl and mcl-PHAs. When *Azotobacter beijerinckii* was grown in a chemostat, oxygen limitation led to increased accumulation of the homopolymer P(3HB) and cell yield in both nitrogen limited and non nitrogen limited cultures (Senior *et al.*, 1972). Restricted oxygen supply has also been reported to trigger P(3HB) production in *Cupriavidus necator* (Vollbrecht *et al.*, 1979). Mcl-PHA producing *Pseudomonas* sp. have high oxygen demand to carry out various metabolic activities to support their growth. However, on being subjected to oxygen limitation these organisms accumulate PHAs. Therefore, to achieve high yield of PHA production Kim *et al.* in 1997 first grew *P. putida,* in a rich medium so that a high biomass could be achieved after which it was subjected to simultaneous limitation of nitrogen and oxygen to achieve PHA production. When single-stage continuous chemostat

cultivation of *P. oleovorans* was carried out in *n*-octane at a growth rate of 0.4 h^{-1}, *P. oleovorans* was able to accumulate PHAs with a yield of 22.9% dcw, under oxygen limitation. The organism was not able to produce any PHAs under 'P' limitation (Hazenberg and Witholt, 1997). Thus oxygen can be used as a limiting nutrient for the organisms to produce PHAs.

1.6. Detection, extraction and characterisation of PHAs

1.6.1. Traditional staining methods

PHAs are hydrophobic in nature, hence the traditional methods of detection has been used to stain these granules with lipophilic dyes such as Sudan black B (Schlegel *et al.,* 1970), Nile blue A (Ostle and Holt, 1982) and Nile red (Kranz *et al.,* 1997) . Such staining methods provide for easier identification between PHA accumulating and non accumulating strains. Nile blue A, a water soluble basic oxazine dye gives bright orange fluorescence at a wavelength of 460nm. This dye has an advantage over that of Sudan black in that, it does not stain other inclusion bodies such as glycogen and polyphosphate. Hence, it has more specific affinity to stain only PHAs (Ostle and Holt, 1982). Nile red has been observed to produce a strong orange fluorescence (emission maximum, 598 nm) with an excitation wavelength of 543 nm (maximum) upon binding to P(3HB) granules in cells of *Curiavidus necator* (Degelau *et al.,* 1995).

1.6.2. Extraction of PHAs

After fermentation, the cells containing PHAs are concentrated from their broth using conventional procedures such as centrifugation, filtration, or flocculation centrifugation. The harvested cells are then lyophilised and

subjected to various extraction methods that employ solvent extraction or non PHA biomass digestion (Wiliamson and Wilkinson, 1958).

Solvent extraction methods proposed for the recovery of both scl and mcl PHAs involve their extraction using chlorinated solvents such as methylene chloride, propylene carbonate, dichloroethane or chloroform. After extraction in these solvents, the polymer solution is filtered to remove cellular debris, concentrated and then PHA precipitated using cooled non solvents such as methanol or ethanol by vigorous shaking. However, such methods of extraction are limited by the fact that large volumes of solvents are required and are therefore commercially unattractive (Hahn *et al.*, 1993; Lee, 1995). Compared to scl-PHAs, mcl-PHAs are soluble in much broader solvent range and therefore cheaper and less toxic solvents such as hexane, acetone and dimethylcarbonate, (DMC) can be used for its extraction (Jiang *et al.*, 2006).

Digestion of the biomass other than PHA (de Koning *et al.*, 1997; de Koning and Witholt, 1997) typically consists of heat treatment, enzymatic solubilization, and surfactant washing. Sodium hypochlorite which solubilises non PHA material has been used for PHA extraction. It breaks open the bacterial cells and thus liberates the intracellular granules. However, sodium hypochlorite digestion causes severe degradation of the polymer, with up to 50% reduction in its molecular weight (Berger *et al.,* 1989). To combine the advantage of differential digestion and solvent extraction, dispersion of sodium hypochlorite and chloroform has also been used for PHA extraction. Here, the hypochlorite digests the cells releasing the PHA, which immediately dissolves in chloroform and thus gets protected from degradation (Hahn *et al.*, 1994)

The enzymatic digestion method developed by Imperial Chemical industries has also been used for the extraction of P(3HB). It involves the thermal treatment of biomass, enzymatic digestion using enzymes such as alcalase,

neutrase, lecitase, and lysozyme and washing with an anionic surfactant for example sodium dodecyl sulphate, (SDS) to solubilize non P(3HB) cellular material. Solubilized and non-solubilized cell compounds are separated by centrifugation following which washing with anionic surfactant and flocculation is carried out. After washing with an anionic surfactant and flocculation, P(3HB) is recovered by spray drying as awhite powder of about 200 μm particles (de Koning et al., 1997)

1.6.3. Characterisation of polyhydroxyalkanoates

1.6.3.1 Infrared spectroscopy

Detection of intracellular P(3HB) granules using dispersive infrared spectroscopy was established in the early 1960s (Rouf and Stokes, 1962). This method enables rapid identification of the polymer and requires very less sample about 0.5 to 1 mg (Kansiz *et al.*, 2000). Rapid screening of scl-PHAs such as P(3HB) in lyophilised bacterial cells has been carried out using FTIR Similarly rapid detection of mcl-PHAs in intact cells of *Pseudomonas* have also been carried out (Hong *et al.,* 1999). For scl-PHAs the band at 1185 cm^{-1} occurs due to C-O stretching and the band at 1282 cm^{-1} corresponding to –CH group (Kansiz *et al.*, 2000). Similarly for mcl-PHAs the characteristic marker ester carbonyl band occurs at 1742 cm^{-1} and the band at 1165 cm^{-1} which occurs due to C-O stretching (Randriamahefa *et al.*, 2003). Randriamahefa *et al*. 2003 used FTIR for rapid qualitative and quantitative analysis of mcl-PHAs in 27 strains of *Pseudomonas* grown in sodium octanoate (Randriamahefa *et al.,* 2003) Fourier transform infrared spectroscopy, (FTIR) enabled scientists to study in more details about the P(3HB) extracted from *Staphylococci*.

1.6.3.2. Ultraviolet spectroscopy

P(3HB) on heating with concentrated sulphuric acid gets converted to crotonic acid. The crotonic acid thus formed can be estimated by measuring the absorbance at 235 nm and therefore used for quantifying P(3HB) (Law and Slepecky, 1961). However, this method of estimation is limited because carbohydrates and chloroform soluble impurities in crude polymer which absorbs in the UV region may be retained even after acetone and alcohol washing, which would interfere with the assay giving incorrect values of P(3HB) concentration. This method is also not suitable for estimating other PHAs (Law and Slepecky, 1961).

1.6.3.3. Gas chromatography, (GC) and mass spectroscopy (MS)

(Braunegg *et al.,* 1978) developed a method that enabled detection of PHA at concentrations as low as 10 μM. In this method the lyophilised cells were subjected to direct acid or alkaline methanolysis, followed by gas chromatography (GC) of the methyl esters. Determination and quantification of PHAs in intact whole cells was carried out by Brandl *et al* in 1989. They subjected lyophilised cells to whole cell methanolysis for 140 minutes at 100^{o}C to produce methyl esters of the constituent 3-hydroxyalkanoic acid (Brandl *et al.,* 1989). Lageveen *et al*. (1988) and many others modified the GC technique to analyse the mcl-PHAs. They used 15% sulphuric acid in methanol as the transesterification reagent. The methyl esters were extracted into the chloroform phase after 140 minutes at 100^{o}C (Lageveen *et al.,* 1988) . However, sulphuric acid is of limited use as a general catalyst for transesterification reactions, due to further decomposition of the 3-hydroxy esters e.g., by acid catalyzed elimination. Also, since the reaction kinetics differ between scl and mcl PHAs, such methods of derivatisation which were initially developed for scl-PHAs, may lead to underestimation of the effective PHA content and to an incorrect copolymer composition determination

(Furrer *et al.,* 2007). Furrer *et al* in 1997 developed an effective method for transesterification of mcl-PHAs using the Lewis acid boron trifluoride in methanol as an effective transesterification reagent. In this method the mcl-PHA was boiled at 80^{o}C for 20 hrs. The polymeric phase was then dried using sodium sulphate and neutralised using sodium carbonate (Furrer *et al.,* 2007). This method has an advantage over using sulphuric acid; this is because sulphuric acid is limited in its use as a general catalyst for transesterification reactions due to further decomposition of the 3-hydroxy esters (Wallen and Rohwedder, 1974; Furrer *et al.*, 2007)

1.6.3.4. Nuclear magnetic resonance, (NMR) spectroscopy

Nuclear magnetic resonance, (NMR) spectroscopy such as ^{13}C, ^{1}H and 2D INADEQUATE (Incredible Natural Abundance Double Quantum Transfer Experiments) have been used for characterising and quantifying pure PHAs. NMR was used to determine the presence of the copolymer poly(3HB-co-3HV) in the PHA produced from *Cupriavidus necator* grown in acetate and propionate (Doi *et al.,* 1986).

1.7. Chemical structure of polyhydroxyalkanotes

The physical and material properties of PHAs are greatly influenced by their monomer composition and chemical structure i.e. the length of the pendant groups which extend from the polymer backbone, the chemical nature of this pendant group and the distance between the ester linkages in the polymer backbone. The short chain length PHAs, scl-PHAs, have monomeric units containing up to 5 carbon atoms. The most well known representative of this family is P(3HB). It has the simplest chemical structure with the methyl group as the pendant R-unit; shown as R_1/R_2 in **Figure 1.1**. Other monomers of this scl family are 4-hydroxybutyrate and 3-hydroxyvalerate (van der Walle *et al.,* 2001)

Mcl-PHAs are more structurally diverse than scl-PHAs. Here, the 'R' group can vary from propyl to tridecyl (e.g. 3-hydroxyhexanoate), may contain an aromatic group (e.g. mcl-PHA bearing para-methylphenoxy and meta-methylphenoxy groups) and the alkyl side chain can be saturated (e.g. 3-hydroxyoctanoate) and unsaturated (e.g. 4- hexenoic, 3-hydroxy-8-nonynoate and 3-hydroxy-10-undecynoate) (Kim *et al.,* 1999; Abraham *et al.,* 2001; Kim *et al.,* 1998). Some mcl-PHAs have also been found with the hydroxyl group on the C_2, C_4, C_5 and C_6 carbon atoms. Mcl-PHAs like rest of the PHA family are also hydrophobic, hence the presence of functional groups like halogens, carboxyl, hydroxyl, epoxy, phenoxy, cyanophenoxy, nitrophenoxy are particularly important, as they allow further chemical modifications of these PHAs leading to the production of novel biomaterial with tailorable properties. Till date more than 150 units of PHA monomers have been identified. The structures of some of these monomeric units and their names are shown in **Figure 1.5** and **Table 1.1** respectively.

Various types of monomers found in PHAs

3-Hydroxy acid	Butyric, Pentanoic, Hexanoic, Heptanoic, Octanoic, Nonanoic, Decanoic, Undecanoic, Dodecanoic, Tetradecanoic
3-Hydroxyacid (Unsaturated)	4-hexenoic, 5-Hexenoic, 6-Heptenoic, 6-Octenoic, 7-Octenoic, 8-Nonenoic, 9-Decenoic, 10-Undecenoic, 6-Dodocenoic, 5-Tetradecenoic, 5,8-Tetradecadienoic, 5,8,11-Tetradecatrienoic, 4-Hexadecenoic, 4,7-Hexadecadienoic
3-Hydroxy acid (Branched)	2,6-Dimethyl-5-Heptenoic, 4-Methylhexanoic, 5-Methylhexanoic, 4-Methyloctanoic, 5-Methyloctanoic, 6-Methyloctanoic, 6-Methylnonanoic, 7-Methylnonanoic, 8-Methylnonanoic, 7-Methyldecanoic
3-Hydroxy acids (Substituted side chain)	7-fluoroheptanoic, 9-fluorononanoic, 6-chlorohexanoic, 8-chlorooctanoic, 6-bromohexanoic, 8-bromooctanoic, 11-

	bromoundecanoic, 7-cyanoheptanolc, 9-cyanononanoic, 12-hydroxydodecanoic, Succinic methylester actd, Adipic acid methylester, Suberic acid methylester, Pimelic acid propylester.
Other then 3-Hydroxy acids	4-Hydroxybutanoic, 4-Hydroxyhexanoic, 4-Hydroxyoctanoic, 5-Hydroxyheptanoic, 5-Hydroxyhexanoic, 4-Hydroxyhexanoic, 2-Hydroxydodecanoic
Aromatic side groups	Dimethylesters of 3,6-Epoxy-7-nonenoic acid, 3-Hydroxyphenylhexanoic, 3-Hydroxyphenylheptanoic, 3-Hydroxyphenyloctanoic, 3-Hydroxy-6-p-methylphenoxyhexanoate
Other functional groups	3-Hydroxy-7-oxooctanoate, 3-Hydroxy-5-oxohexanoate, 8-Acetoxy-3-hydroxyoctanoate, 6-Acetoxy3-hydroxyhexanoate

References:(Lageveen *et al.*, 1988; Fritzsche and Lenz, 1990; Timm and Steinbuchel, 1990; Kim *et al.*, 1992; Kato, 1996; Kim *et al.*, 1996; Matsusaki *et al.*, 1998; Schmack *et al.*, 1998; Jung *et al.*, 2000; Kim *et al.*, 1998)

Table 1.1: The broad spectrum of monomers found in PHAs. (Adapted from Zinn et al., 2001)

3-Hydroxyacids

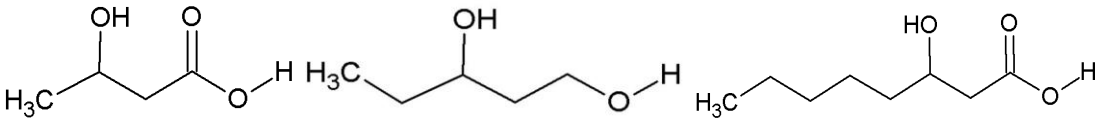

3-Hydroxybutric acid 3-Hydroxyvaleric acid 3-Hydroxyoctanoic acid

II. 3-Hydroxyacids (Unsaturated)

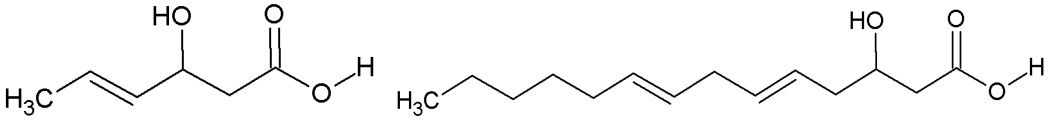

4-Hexenoic acid 5,8-Tetradecadenoic acid

III. 3-Hydroxyacid (Branched)

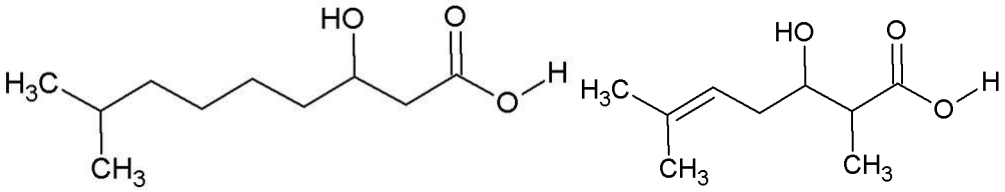

8-Methylnonanoic acid 2,6-Dimethyl-5-heptenoic acid

IV. 3-Hydroxyacids (Substituted side chain)

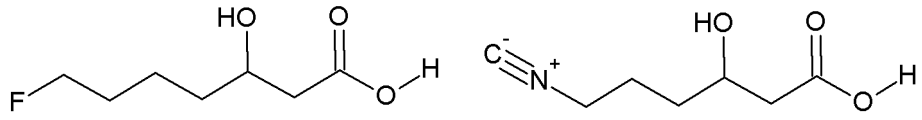

7-Fluroheptanoic acid 7-Cyanoheptanoic acid

V. Other than 3-Hydroxyacids

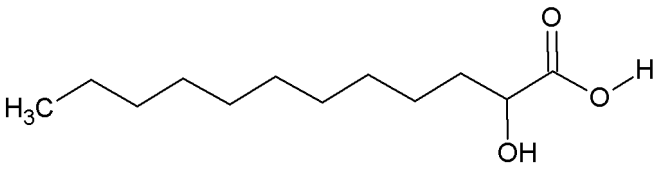

2-Hydroxydodecanoic acid

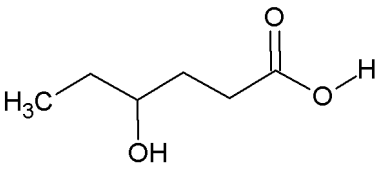

4-Hydroxyhexanoic acid

VI. Aromatic side group

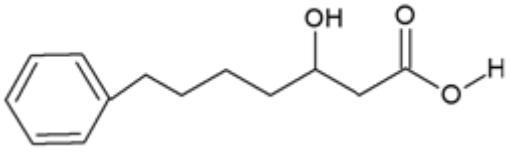

3-Hydroxyphenylheptanoic acid

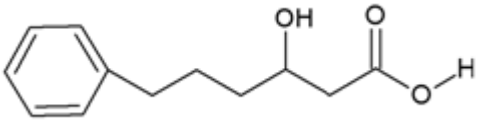

3-Hydroxyphenylhexanoic acid

VII. Other functional groups

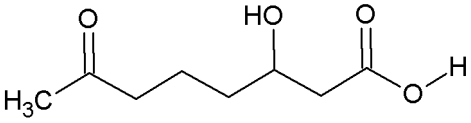

3-Hydroxy-7-oxooctanoic acid

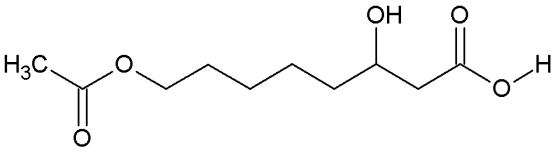

8-Acetoxy-3-hydroxyoctanoic acid

Figure 1.5: Compilation of some PHA monomer structures from Table 1

1.8. Physical properties of polyhydroxyalkanoates.

As descrbed in previous section, the chemical structure of the polymer greatly affects its physical and material properties. Scl-PHAs for example P(3HB), with a T_m of 180°C and a T_g, of 4°C, is highly crystalline, brittle and stiff (Martin and Williams, 2003). These are typically thermoplastic polymers

which become fluid and mouldable above their T_m. The brittleness of P(3HB) is largely due to the presence of large crystalline domains in the form of spherulites which form upon cooling of the melt (Barham and Keller, 1986; Marchessault *et al.*, 1990). P(3HB) with a Young's modulus of 3.5 GPa and tensile strength of 40 MPa has mechanical properties similar to that of polypropylene. However, the elongation to break is about 5%, which is significantly lower than that of polypropylene, 400 % (Lee, 1995). Another scl PHA, P(4HB) has a Young's modulus value of 149 MPa, tensile strength of 104 MPa and a high elongation to break value of 1000 %. The weight average molecular weight (M_w) of P(3HB) have been found to range between 530,000 to 1,100,000. and polydispersity to be around 1.75 (Valappil *et al.,* 2007).

Mcl-PHAs have melting temperatures (T_m values) ranging between 40^{o}C and 60^{o}C and glass transition temperatures (T_g values) ranging between -50^{o}C and -25^{o}C. Mcl-PHAs also have low crystallinity possibly due to the presence of large and irregular pendant side groups which inhibit close packing of the polymer chains in a regular three dimensional fashion to form a crystalline array (Sánchez *et al.,* 2003). This combination of T_g values below room temperature and a low degree of crystallinity imparts elastomeric behaviour to these polymers. In fact mcl-PHAs are the only microbially produced biopolymers which exhibit properties of thermoplastic elastomers and resemble natural rubbers produced by *H. brasiliensis* (Steinbüchel and Eversloh, 2003). However, mcl-PHAs act as true elastomers within a very narrow temperature range**.** At temperatures above or close to its T_m the polymer is completely amorphous and sticky (Steinbüchel and Eversloh, 2003) In mcl-PHAs the crystalline part acts as a physical crosslink and therefore they have mechanical properties such as tensile strength and elongation to break that are very different from that of scl-PHAs as shown in **Table 1.2** (Holmes, 1988). In mcl-PHAs M_w for both saturated and unsaturated pendant group containing polymers lie between the range of 60,000 and 412,000 and

the number average molecular weight, M_n, between 40,000 and 231,000 (Valappil *et al.,* 2007) . These values are relatively low, compared to that of scl-PHAs. The polydispersities of mcl-PHA copolymers are in the range of 1.6 to 4.4 with higher values for mcl-PHAs with unsaturated monomers than those with saturated monomers.

As discussed in section 1.1 introducing a comonomer into the polymer backbone alters the property of the polymer. PHAs are also biocompatible and biodegradable and exhibits wide ranging physical and mechanical properties that arise from the diversity in their chemical structures. The physical properties of some of the PHAs are shown in **Table 1.2**.

Polymer	Tensile strength	Modulus	Elongation to break (%)	Reference
P(3HB)	40 MPa	3.5 GPa	6	Lee *et al.*, 1995
P(4HB)	104 MPa	0.149 GPa	1000	Sudesh *et al.*, 1990
P(3HB-co-17%3HHx)	20 MPa	0.173 MPa	850	Hartman *et al.*, 2006
P(3HO-co-12%3HHx)	9 MPa	0.008 MPa	380	Preusting *et al.*, 1990
P(HO)	-	17 MPa	250-350	Marchessault *et al.*, 1990
P(3HO-co-12%3HHx-co-2%3HD)	9.3 MPa	7.6 MPa	380	Gagnon *et al.*, 1992
P(3HO-co-4.6%3HHx)	22.9 MPa	599.9 MPa	6.5	Asrar *et al.*, 2002
P(3HO-co-5.4%3HHx)	23.9 MPa	493.7 MPa	17.6	,,
P(3HO-co-7%HHx)	17.3 MPa	288.9 MPa	23.6	,,
P(3HO-co-8.5%HHx)	15.6 MPa	232.3 MPa	34.3	,,
P(3HO-co-9.5%HHx)	8.8 MPa	155.3 MPa	43.0	

Table 1.2: Mechanical properties of various PHAs.

1.9. Composites of polyhydroxyalkanoates

Interest in PHAs as biomaterials for various biomedical applications has increased in recent years because of their structural diversity, useful mechanical properties, biodegradability, piezoelectricity and biocompatibility (Zinn *et al.*, 2001; Williams and Martin, 2005; Nair and Laurencin, 2006). However, in recent years numerous studies have been carried out to study the cumulative effect of combining an inorganic phase with the polymer i.e. composite systems. PHAs are generally hydrophobic in nature and incorporation of such inorganic phases into the polymer matrix improves the hydrophilicity of the composite system. Extensive research is being carried out on the development of bioactive and biodegradable composite materials, both dense and porous systems, with the bioactive inorganic phase incorporated as either filler or coating (or both) into the biodegradable polymer matrix (Misra *et al.*, 2006). Although many bioceramic materials such as alumina and zirconia, bioactive glasses, glass-ceramics, hydroxyapatite, and resorbable calcium phosphates are available for composite preparaton; hydroxyapatite, wollastonite and bioactive glasses have been mainly studied in combination with PHAs to form composites (Li and Chang, 2004; Misra *et al.*, 2006; Misra *et al.*, 2007). Also, most work on composites has been carried out on scl-PHAs; the studies on mcl-PHA composites are limited to P(3HB-co-3HHx).

Composites of P(3HB) and bioactive silicate glass like 45S5 Bioglass® has been studied to develop scaffolds for bone tissue engineering (Misra *et al.*, 2007; Misra *et al.*, 2008; Misra *et al.*, 2009). These glasses have a high bioactivity index (Class A) are osteogenetic, osteoconductive and have the ability to bond with both soft and hard connective tissues (Chen *et al.*, 2008). Incorporation of 45S5 Bioglass® into P(3HB) has been shown to increase its bioactivity, protein adsorption and rate of degradation (Misra *et al.,* 2008).

Figures 1.6(a) and 1.7(b) show SEM images of the composite of Bioglass ® 45S5 and P(3HB).

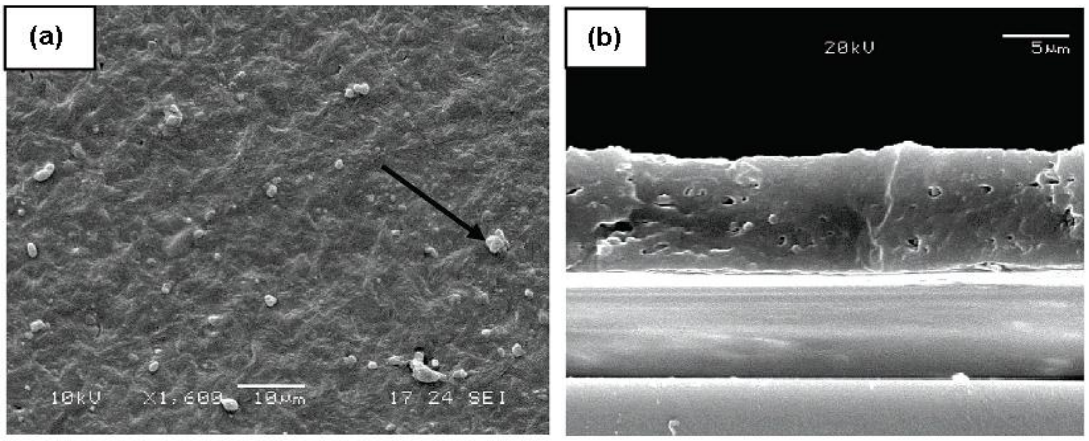

Figure 1. 6: SEM images of a Bioglass®/P(3HB) composite film. 6(a) Planar SEM images of Bioglass®/P(3HB) composite film and 6(b) cross section of Bioglass®/P(3HB) composite film (Misra *et al.*, 2007)

Xi *et al*. (2008) studied composites of hydroxyapatite (HA) and P(3HB-co-3HHx) which were prepared using phase separation and subsequent sublimation of the solvent. The porosity of the composite was more than 88 %. They found that the mechanical properties of P(3HB-co-3HHx)–HA composite scaffolds were improved compared to those of the P(3HB-co-3HHx) scaffolds. Both the compressive modulus, 0.6 MPa, and the maximum stress, 0.14 MPa of the composite scaffold were significantly higher than those of the P(3HB-co-3HHx) scaffold, measuring 0.38 MPa for compressive modulus and 0.1 MPa for maximum stress. Serum protein adsorption was significantly greater on the composite scaffolds (550 μg at 30 hrs), than on the P(3HB-co-3HHx) scaffolds (310 μg at 30 hrs) (Xi *et al.,* 2008). Protein preadsorption on the substrate modulates cell adhesion and survival (Webster *et al.,* 2000; Woo *et al.,* 2002; Xi *et al.,* 2008), hence it is of considerable importance in evaluating the effectiveness of a scaffold for tissue engineering. *In vitro* culture work also showed that the P(3HB-co-3HHx)–HA composite provided better cell attachment and proliferation of MC3T3-E1 osteoblast cells than the P(3HB-

co-3HHx) scaffold (Ramires *et al.,* 2001; Xi *et al.,* 2008). Studies carried out by Wang *et al*., 2005a, showed that blending of hydroxyapatite into P(3HB-co-3HHx) using salt leaching technique caused no remarkable change in its rate of degradation (Wang *et al.,* 2005). Proliferation assay using MTT showed that the osteoblast cells grew better on P(3HB-co-3HHx) scaffolds than P(3HB-co-3HHx)/HA composite scaffolds. Although HA exposed on the surface promoted osteoblast anchorage, SEM analysis revealed that the blending of HA into P(3HB-co-3HHx) resulted in a smooth surface of the P(3HB-co-3HHx)/HA composite. Thus, unlike in the previous study by Xi *et al*. (2008), here composite preparation by blending HA with P(3HB-co-3HHx) using salt leaching technique resulted in P(3HB-co-3HHx)/HAcomposite having smoother surface as compared to the neat polymer. As osteoblasts require surfaces with appropriate roughness for their growth, therefore, P(3HB-co-3HHx) with appropriate roughness supported better osteoblast growth when compared to P(3HB-co-3HHx)/HA composite (Wang *et al.,* 2005). Also, the degradability of HA may present a major limitation. A recent clinical report on a 6-7 year follow-up study confirmed that implanted crystalline HA was not biodegradable and remained in the body for extended periods with no visible signs of biomaterial resorption (Marcacci *et al.*, 2007; Chen, 2008). Therefore the kind of filler material used for composite preparation is crucial in assessing the over all properties of a composite system.

Composites of PHAs with carbon nanotubes have also been studied. Carbon nanotube-based biopolymer composites have improved mechanical properties and electrical current conductivity. Studies on composites of PHAs/ carbon nanotubes, CNTs, have been reported by Yun *et al*. (2008) and Misra *et al*. (2009). Poly(3-hydroxybutyrate), P(3HB) composites with bioactive glass particles and multiwall carbon nanotubes (MWCNTs) were prepared and used to identify whether the electrical properties of MWCNTs can be used to detect the bioactivity of P(3HB)/bioactive glass composites. The presence of

MWCNTs (2–7 wt.%) increased the surface roughness of the composites. The presence of MWCNTs in low quantity (2 wt %) enhanced MG-63 osteoblast-like cell attachment and proliferation compared to composites with higher concentration (4-7 wt%) of MWCNTs (Misra *et al.,* 2009). Yun and his group studied P(3HB)/SWCNTs (single wall carbon nanotubes) and P(3HO)/SWCNT composites with 0, 1 and 10 wt% concentrations of CNTs which were made using the solvent casting technique. Mechanical tests on these composites and the neat polymer showed that the Young's modulus, E and the hardness, H had increased for the composites. The Young's modulus, for P(3HO) increased from 0.12±0.01 GPa for the neat polymer to 0.53±0.05 GPa for P(3HO)/SWCNTs containing 10wt% SWCNTs. The hardness had also increased from 5.6±0.06x10^{-3} GPa for neat polymer to 13.7+0.6x10^{-3} GPa P(3HO)/SWCNTs containing 10wt% SWCNTs. Similarly for P(3HB), the Young's modulus increased from 5.66±0.17 GPa for neat polymer to 11.74±0.64 GPa for P(3HB)/SWCNTs containing 10wt% SWCNTs. The hardness also increased from 0.31±0.01 GPa for neat polymer to 0.35±0.01 GPa P(3HB)/SWCNTs containing 10wt% SWCNTs. Thus, the addition of SWCNTs increased the values of the Young's modulus and hardness of both polymers but the increase was found to be more significant for P(3HO) (Yun *et al.,* 2008).

1.10. Application of polyhydroxyalkanoates

1.10.1. Industrial application

PHAs have successfully been used for industrial applications. A blend of P(3HB) and P(3HO) is marketed by a US based company Metabolix. This polymer has an FDA approval for use as food additives (Clarinval and Halleux, 2005). Tsinghua University (China) in collaboration with Guangdong Jiangmen Center for Biotech Develpoment (China), KAIST (Korea) and

Procter & Gamble (USA) have carried out industrial production of P(3HB-3HHx) using *Aeromonas hydrophila*. The polymer produced is used to make flushables, nonwovens, binders, flexible packaging, thermoformed articles, synthetic paper and medical devices (Clarinval and Halleux, 2005). A German company Biomer produces P(3HB) industrially from *Alcaligene latus*. The polymer is used for making articles such as combs, pens, bullets and for use in classical transformation processes (Chen, 2005; Philip *et al.*, 2007). Metabolix (Cambridge. MA, USA) also manufactures BIOPOL®, a copolymer of P(3HB-co-3HV). BIOPOL® is used to coat paper and paperboards, blow moulding and film production. It has antistatic properties that can be exploited for electric and electronic packaging (Clarinval and Halleux, 2005). Nodax™ developed by Procter and Gamble is a copolymer of P(3HB) with small quantity of medium chain length monomers with side groups of at least three carbon units or more. This polymer can be used to make flushables that can degrade in septic systems and this would include hygienic wipes and tampon applicators. They can also be used to manufacture medical surgical garments, upholstery, carpet, packaging, compostable bags and lids or tubs for thermoformed articles. PHA based latex can be used for making water resistant surfaces to cover paper and cardboards (Pandey *et al.*, 2005).

1.10.2. Medical applications

PHAs have been studied as a biomaterial for scaffolds in tissue engineering of both hard and soft tissues. Encapsulation of drugs in controlled drug delivery using PHAs as a matrix material have also been carried out.

1.10.2.1. Tissue engineering

Tissue engineering is a multi-disciplinary field combining biology, materials science, and surgical reconstruction, to provide living tissue products that restore, maintain, or improve tissue function (Langer and Vacanti, 1993;

Williams *et al.*, 1999). PHAs are generally being used to make scaffolds on which cells can be seeded so as to induce new tissue growth. The PHA scaffold must be biocompatible, provide a conducive surface for the cells to adhere, must be able to guide and organise the cells in the desired manner and must support cell growth, without cell release, maintain cells in a viable state by proper diffusion of nutrients and passage of waste. Once the new tissue replacement is formed, the scaffold must be able to degrade and the degradation products must be non toxic and well tolerated (Williams *et al.,* 1999).

PHAs like P(3HB), P(3HB-co-3HHx) and blends of PHA with PDLLA have also been used as biomaterials for nerve regeneration. One of the early studies on P(3HB-co-3HHx) as conduit material for nerve regeneration was carried out by Yang *et al.,* in 2002. This study showed that the foetal mouse cerebral cortex cells were able to grow well when seeded on P(3HB-co-3HHx) films (Yang, 2002). In soft tissue engineering, P(3HB-co-3HHX) as a possible material for the construction of artificial oesophagus has been investigated. P(3HB-co-3HHX) based artificial oesophagus was implanted in dogs. The *in vivo* results showed that the copolymer did stimulate the regeneration of the removed oesophagus in the dog, however the biodegradation of the implanted P(3HB-co-3HHx) was almost undetected (Chen and Qiong, 2005).

Similarly PHAs have also been extensively explored for hard tissue engineering. P(3HB) and composites of P(3HB) with bioactive 45S5 Bioglass® (microsize and nanosize) have been extensively studied for bone tissue engineering. The composite P(3HB)/BG showed good biocompatibility with the seeded MG-63 human osteoblast cell line. Incorporation of vitamin E in the composite further enabled better attachment, proliferation and differentiation of the osteoblast cells (Misra *et al.,* 2007; Misra *et al.,* 2008; Misra *et al.,* 2009). Studies carried out by Wang and his group have shown that P(3HB-co-3HHx) is a more superior biomaterial for osteoblast attachment, proliferation

and differentiation for bone marrow cells when compared to poly(lactic acid), PLA and P(3HB) (Wang *et al.,* 2004) (**Figures 1.7(a), (b)** and **(c)**).

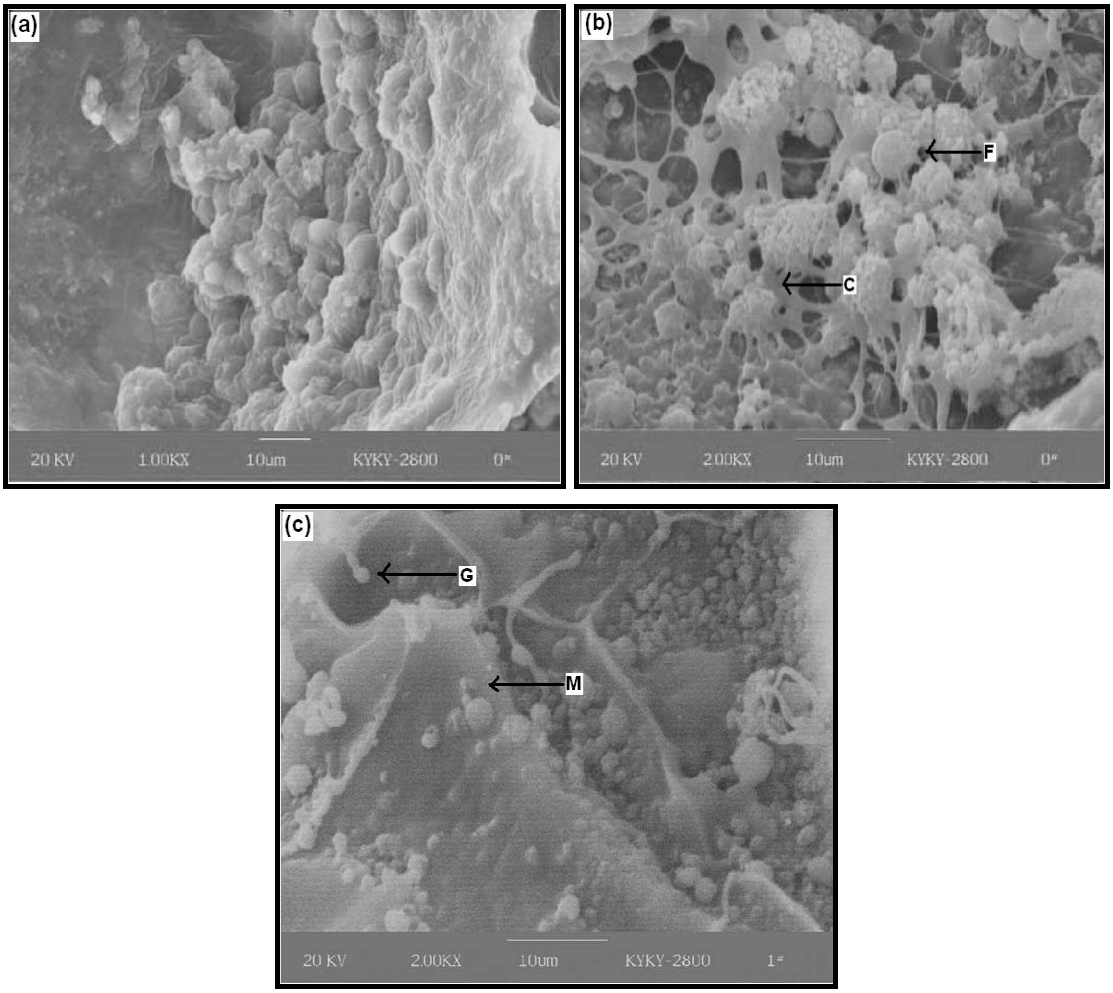

Figure 1.7: Scanning electron micrographs of rabbit bone marrow cells seeded on P(3HB-co-3HHx) scaffold after 10 days of incubation (1000 X): (a) Cell clumps; (b) Round cells with fibrillar collagen (F,C) attached by filapodia, (c) cells with extracellular matrix (M) and calcified globuli (G) (Wang *et al.*, 2004)

Wang at al. and others have shown that P(3HB-co-3HHx) with tailor made HHx content can be designed to meet the growth requirements of specific tissues for bone tissue engineering (Wang *et al.,* 2004; Wang *et al.,* 2005; Wang *et al.,* 2005).

Several investigations have been carried out on three dimensional polymer scaffold systems consisting of a blend of P(3HB) and P(3HB-co-3HHx) for

possible application as a matrix for cartilage tissue engineering (Deng *et al.,* 2002; Deng *et al.,* 2003; Zhao *et al.,* 2003). Biochemical analysis and RT-PCR confirmed that the polymer blend of P(3HB) / P(3HB-co-3HHx) was capable of initiating a redifferentiation process which allows chondrocytes to express and produce type II collagen more than the P(3HB) only scaffold (control). The P(3HB-co-3HHx) component in the blend P(3HB)/P(3HB-co-3HHx) scaffold provided better surface properties for anchoring type II collagen filaments and their penetration into internal layers of the scaffolds. These results suggested that the cells underwent chondrogenic differentiation on P(3HB-co-3HHx) containing scaffolds and that the presence of the right proportion of P(3HB-co-3HHx) in the blend system of P(3HB)/P(3HB-co-3HHx) highly favoured the production of the extracellular matrix of articular cartilage chondrocytes (Deng *et al.,* 2003).

1.10.2.2. Cardiac tissue engineering

Mcl-PHAs and its copolymers because of its elastomeric and flexible nature have been used for cardiac tissue engineering. PHAs have also been used for heart valve development. One of the early studies using an elastomeric P(3HO) (Tepha Inc) for the fabrication of a trileaflet heart valve scaffold was carried out by Sodian and his group in 2000. Vascular cells were harvested from ovine carotid arteries, expanded *in vitro* and seeded onto the heart valve scaffold. The study concluded that tissue engineered P(3HO) fabricated heart valve can be used for implantation in the pulmonary position with an appropriate function for 120 days in lambs (Sodian *et al.*, 2000; Chen and Qiong, 2005). In the same year Stock *et al*. 2000, evaluated the feasibility of creating 3-leaflet, valved, pulmonary conduits from autologous ovine vascular cells and thermoplastic P(3HO), (PHO 3836; TEPHA Inc., Cambridge, MA) in lambs. Scaffolds made using polyglycolic acid (PGA) and P(3HO) were formed into a conduit and 3 leaflets consisting of a monolayer of porous P(3HO) were sewn into the conduit as shown in **Figure 1.8(A). Figures 1.8(B)** and **1.8(C)**

show the appearance of tissue engineered seeded conduit 24 weeks *in vivo*. These results indicated that the remodelling of the tissue engineered structure continues for at least 24 weeks (Stock *et al.,* 2000). Stereolithography has also been used to construct P(4HB) and P(3HO) (Tepha, Inc., Cambridge, MA) heart valve scaffolds derived from X-ray computed tomography and specific software (CP, Aachen, Germany) (Sodian *et al.,* 2002). Using this technique, P(3HO) and P(4HB) could be moulded into a complete trileaflet valve scaffold without the need for suturing (Sodian *et al.*, 2002; Chen and Qiong, 2005). Novel hybrid valves which were fabricated from decellularized porcine aortic valves and coated with P(3HB-co-3HHx) were also developed. The results *in vivo* indicated that the P(3HB-co-3HHx) coating reduced calcification and promoted the repopulation of the hybrid valve with the recipient's cells, resembling native valve tissue (Wu *et al.,* 2007).

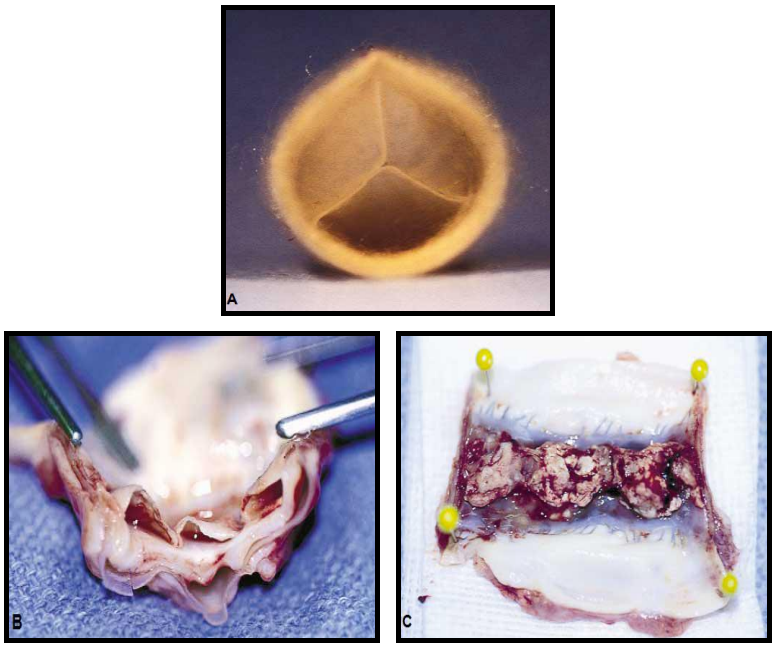

Figure 1.8: Tissue engineered seeded conduit 24 weeks *in vivo*. (a) P(3HO) scaffold frontal view, 18 mm in diameter and 20 mm in length. Three leaflets of porous P(3HO) were sutured into the conduit proximal view, (b) Gross appearance of tissue-engineered seeded conduit 24 weeks *in vivo* (distal view). Clear separation of all 3 leaflets from the conduit wall is shown. (c), Gross appearance of tissue-engineered unseeded conduit 4 weeks *in vivo* (proximal view)(Stock *et al.,* 2000)

1.10.2.3. Drug delivery

PHAs have been studied as drug carrier scaffolds for controlled drug delivery. The use of P(3HB-co-4HB) rods as antibiotic carriers for the treatment of osteomyelitis using Sulperazone™ or Ducoid was evaluated and compared with P(3HB-co-3HV) . P(3HB-co-4HB) was preferred as it was less rigid and easier to handle as opposed to P(3HB-co-3HV) (Türesin *et al.*, 2001). Hasirci and Keskin, also studied P(4HB) and P(3HB-co-4HB) as matrices for tetracycline release, because the physical properties like strength, modulus, and elongation of the scaffolds were comparable to that of other drug delivery systems. Transdermal drug delivery (TDD) is an ideal method for drug administration. However, in this method the hydrophobic stratum corneum represents a major barrier against hydrophilic ionisable drugs (Wang *et al.*, 2003). Studies were therefore carried out by Wang *et al.* (2003) to use mcl-PHAs for TDD. Tamsulosin was used as the model drug in this study; polyamidoamine dendrimer which acted as an enhancer was added to the polymer matrix. The dendimer acted as an enhancer by weakly enhancing the permeation of tamulosin by pretreatment. The dendrimer-containing PHA matrix achieved the clinically required amount of tamsulosin permeating through the skin model (Wang *et al.,* 2003). Graft copolymerised monoacrylate-poly(ethylene glycol), PEGMA and P(3HO), i.e. PEGMA-g-P(3HO) has been used to develop a swelling controlled release delivery system for Ibuprofen as a model drug (Kim *et al.,* 2005). In another study P(3HB-co-3HHx) spheres (**Figure 1.9**) was studied as a matrix for the controlled release of triamcinolone acetonide for possible treatment of cystoid macular oedema, (CMO) and acute posterior segment inflammation associated with uveitis (Bayram and Denbas, 2008).

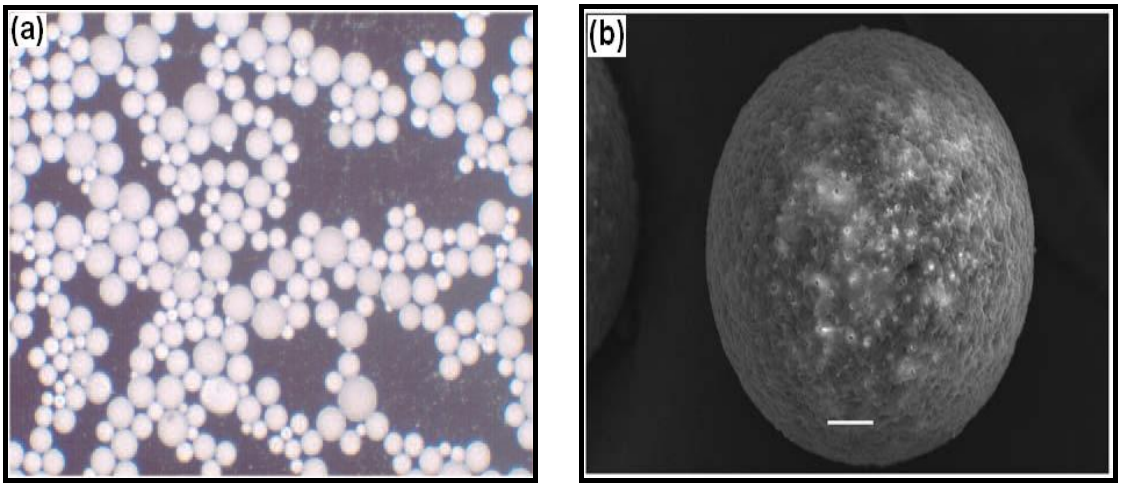

Figure 1.9: (a) Typical optical micrograph of P(3HB-co-3HHx)microspheres and (b) SEM micrograph of a single P(3HB-co3HHx) microsphere. (Bayram and Denbas, 2008)

1.10.2.4. Skin regeneration for wound healing

Research has been carried to use PHA scaffolds for skin regeneration and wound healing. In the studies carried out by Tang *et al*. 2008, copolymers of poly(3HB-co-5mol%3HHx), poly(3HB-co-7mol%-4HB) and poly(3HB-co-97mol%-4HB) were electrospun to fabricate scaffolds for skin tissue regeneration. The mechanical properties of all the scaffolds, tensile strength and Young's modulus had values between 5-30 MPa and 15-150 MPa, which were comparable to those of the human skin and hence suggest that they are mechanically stable in supporting regenerated tissues. Subcutaneous implantation of the scaffold fibres in rats was performed to investigate their bioabsorption behaviour and tissue response. Histological evaluation showed that subcutaneous implantation of the electrospun PHA scaffolds were well tolerated *in vivo,* however the tissue response increased with increasing 4HB content (Tang *et al.,* 2008). In the same year, nanofibrous matrices using a blend of P(3HB)/P(3HB-co-3HHx) and P(3HB)/P(3HB-co-4HB) were also prepared using the phase separation process. Three-dimensional interconnected fibrous networks were observed in these matrices with average fibre diameters of 50–500 nm, which are very similar to the major

extracellular matrix, (ECM) component collagen. Human keratinocyte cell line, HaCat, was seeded on these scaffolds and their response compared with HaCat seeded on solvent casted films of the same compositions. It was seen that cell behaviour including morphology, adhesion ability and viability on the nanofibrous matrices were better than those on the solvent casted films. The nanotopography of the matrix resembling that of collagen, a main component of the natural extracellular matrix, could have played a key role for eliciting this sort of cellular response (Li *et al.,* 2008).

1.11. Biocompatibility of PHAs

The biocompatibility of PHAs originates from the fact that some monomers incorporated into the polymer chain occur naturally in the human body. The monomer (R)-3-hydroxybutyric acid is a normal metabolite found in human blood. This hydroxyacid is present at concentrations of 3-10 mg per 100 mL blood in healthy adults (Hocking and Marchessault, 1994; Williams *et al.*, 1999). Also, low molecular weight PHAs are found complexed to other cellular macromolecules; hence called complexed PHAs (cPHAs). For example, cPHAs have been found in human tissues complexed with low density lipoproteins, carrier protein albumin and in the potassium channel (KcsA) of *Streptomyces lividans* (Nelson *et al.*, 1981; Reusch, 2002). Biocompatibility of PHAs like any other biomaterial is dependent on factors such as shape, surface porosity, surface hydrophilicity, surface energy, chemistry of the material and its degradation product (Yang *et al.,* 2002; Zhao *et al.,* 2003; Zheng *et al.,* 2005). In tissue engineering, it is also important to evaluate the biocompatibility of the degradation products of the implant material. To this end studies carried out by Sun and his group, on the cellular responses of mouse fibroblast cell line L929 to the PHA degradation products, oligohydroxyalkanoates (OHAs), showed that mcl-PHAs are more biocompatible than scl-PHAs (Sun *et al.,* 2007). Biocompatibilities of PHA scaffolds have also been enhanced by (1)

increasing the hydrophilicity of the polymer, for example by grafting acrylamide and carboxyl ions onto the P(3HO), P(3HB) and P(3HB-co-3HHx) films using plasma treatment (Kim *et al.,* 2002). (2) Surface modifications of PHAs using NaOH and enzyme treatment (Yang *et al.,* 2002; Zhao *et al.,* 2002). (3) Coating the polymer surface using a biocompatible compound. For example, the surface of both porous and dense P(3HB-co-3HHx) matrices was coated with a biocompatible protein, silk fibroin which is a natural protein generated from silk worm silk fibre (Mei *et al.,* 2006). Biomaterials intended for long-term contact with blood must not induce thrombosis, antigenic responses, destruction of blood components, and plasma protein. *In vitro* tests showed haemocompatibility of P(3HB-co-3HHx) as blood contact graft material that reduced thrombogenicity and adhesiveness of blood platelets (Qu *et al.*, 2006)

1.12. Biodegradation of polyhydroxyalkanoates

1.12.1. Factors affecting biodegradation

PHAs are biodegradable polymers that can degrade both under aerobic and anaerobic conditions. They can also be subjected to thermal degradation and enzymatic hydrolysis. In biological systems PHAs can be degraded using microbial depolymerases as well as by nonenzymatic and enzymatic hydrolysis in animal tissue (Philip *et al.,* 2007). Numerous factors affect the biodegradability of PHAs such as stereoregularity, molecular mass, monomeric composition and crystallinity of the polymer. Studies carried out by Mochizuki *et al.* (1997) and Tokiwa *et al.* (2004). showed that biodegradation of PHAs is influenced by the chemical structure i.e. presence of functional groups in the polymer chain, hydrophilicity/hydrophobicity balance and presence of ordered structure: like crystallinity, orientation and morphological properties (Mochizuki and Hirami, 1997; Tokiwa and Calabia,

2004). Usually, the degradation of the polymer decreases with the increase of highly ordered structure i.e. increasing crystallinity. Since more crystalline structures, also have higher melting temperature for the crystalline phase of the polymer, hence for PHAs, the degradation rate also decreases with increasing T_m. Thus mcl-PHAs with low crystallinity and T_m are more degradable than scl-PHAs which have comparatively higher crystallinity and T_m. Studies have also shown that the rate of hydrolysis of PHAs depends on the surface area of the polymer exposed. Hydrolysis starts on the surface and at physical lesions on the polymer and proceeds to the inner part of the material (Wang *et al.,* 2005).

1.12.2. Biodegradation in the environment

In nature, the microbial population present in a given environment and temperature also contribute to the biodegradability of the polymer. Microorganisms from the families *Pseudonocardiaceae, Micromonosporaceae, Thermomonosporaceae, Streptosporangiaceae* and *Streptomycetaceae* predominantly degrade P(3HB) in the environment. These microbes secrete extracellular enzymes that solubilise the polymer and these soluble products are then absorbed through their cell walls and utilised. Some PHA producing bacteria are able to degrade the polymer intracellularly. During intracellular degradation, the polymer is ultimately broken down to acetyl-CoA which under the aerobic conditions enters the citric acid cycle and is oxidised to CO_2 (Lee, 1995; Philip *et al.*, 2007). The enzyme involved in the degradation of the PHAs is the PHA depolymerase encoded by *phaZ* (Knoll *et al.,* 2009).

1.12.3. Biodegradation and biocompatibility in the medical context

It is of paramount importance that the rate of degradation of the PHA scaffold should equal that of the regenerative rate of the tissues. The *in vivo* and *in vitro* degradation of PHAs has been studied by a number of research groups and various biodegradation rates of PHAs observed (Wang *et al.*, 2005; Williams and Martin, 2005). Williams *et al*. (1999) observed that P(3HO-co-3HHx) degrades slowly *in vivo*. The subcutaneous implants of P(3HO-co-3HHx) in mice decrease in M_w from 137,000 on implantation to around 65,000 over 40 weeks (Williams *et al.,* 1999). Since the degradability of PHAs decreases with the overall increase in the crystallinity, hence when Wang *et al*. (2005) blended gelatin with P(3HO-co-3HHx) they found that blending of gelatin accelerated the degradation of P(3HO-co-3HHx). They concluded that the weight loss observed was first due to the reduction in the crystallinity of the blended polymer as confirmed by the weakening of its crystalline peak from X-ray diffraction (XRD) analysis. Secondly, blending with gelatin created a more porous polymer surface, which was exposed for hydrolytic attack as observed by scanning electron microscopy, (SEM) analysis (Wang *et al.,* 2005).

1.13. Aims and objectives

The aim of this study was to biosynthesise polyhydroxyalkanoates, PHAs, from bacteria and to initiate the utilisation of the PHAs produced for medical applications. This aim was achieved by the following objectives:

1. Exploration of the short chain length PHA, scl-PHA, production from *B. cereus* SPV. The organism was grown under different nutrient limiting conditions for scl-PHA production (Chapter 3)
2. Exploration of medium chain length PHA, mcl-PHA, production from different *Pseudomonas* sp. such as *P. aeruginosa, P. putida, P. fluorescens, P. oleovorans* and *P. mendocina* with a focussed detailed study on *P. mendocina* (Chapter 4).
3. Fabrication of the polymer, poly(3-hydroxyoctanoate), P(3HO), into two dimensional films and combining it with bioactive nanobioglass particles to produce the composite, P(3HO)/n-BG two dimensional films. In depth characterisation of these fabricated films for the proposed medical applications (Chapter 5).
4. Modification of P(3HO) using (i) UV rays and its fabrication into two dimentional films and P(3HO)/n-BG two dimensional composite films and (ii) Blending of P(3HO) with poly(3-hydroxybutyrate), P(3HB) and its fabrication into neat two dimensional and composite blend two dimensional films. In depth characterisation of these fabricated films (Chapter 6).

Chapter 2: Materials and methods

2.1. Bacterial strains and cell line

Short chain length polyhydroxyalkanoate, scl-PHA, production was studied using *Bacillus cereus* SPV obtained from the University of Westminster culture collection. Medium chain length, mcl-PHA production studies were done using five *Pseudomonas* strains: *P. aeruginosa, P. putida,* and *P. fluorescens*, which were also obtained from University of Westminster's culture collection. *P. mendocina* was bought from National Collection of Industrial and Marine Bacteria (NCIMB) and *P. oleovorans* from American type culture collection (ATCC). Cell culture studies were done using the keratinocyte cell line, HaCaT which was obtained from the University of Westminster's cell line collection.

2.2. Chemicals and reagents

The chemicals were obtained from Sigma-Aldrich or BDH Ltd UK unless otherwise stated. Bacterial media preparations were done using general purpose reagents. Analytical studies were carried out using analytical grade reagents. Chromatography grade reagents were used for Gas chromatography mass spectroscopy analysis, GC-MS, and nuclear magnetic resonance, NMR, analysis.

Cell culture studies, were done using cell culture grade media and reagents from Lonza, UK. Protein estimation was done using the BCA estimation kit from Sigma-Aldrich. Carbon estimation was done using the Fatty acid assay kit from Biovision, UK. For lipopolysaccharide, (LPS) estimation, *Limulus amebocute* lysate, (LAL) Kit from Cape Cod, USA was used.

2.3. Media

Different media compositions were used during this study which are listed below.

2.3.1. Inoculum growth medium

Nutrient broth media was used for the seed culture preparation according to the manufacturer's specifications. The medium contained the following concentration of nutrients:

Chemicals	Composition (g//L)
'Lab- Lemco' Powder	1.00 g
Yeast extract	2.00 g
Peptone	5.00 g
Sodium Chloride	5.00 g

Table 2.1: Chemical composition of inoculum growth medium

2.3.2. Short chain length, scl- PHA production media

B. cereus SPV was grown in different single nutrient limiting media to study the effects of these limiting nutrient conditions on its PHA accumulation behaviour.

2.3.2.1. Nitrogen deficient medium

A semi defined nitrogen limiting PHA production medium, Kannan and Rehacek was used for the nitrogen limiting study (Kannan and Rehacek, 1970). The medium contained the following concentration of nutrients:

Chemicals	Composition (g/L)
Glucose	20.00
Yeast extract	2.50
Potassium chloride	3.00
Ammonium sulphate	5.00
* Soybean dialysate	100 mL

Table 2.2: Chemical composition of nitrogen limiting medium

(* Soybean dialysate was prepared from 10 g of defatted soybean flour in 1000 mL of distilled water for 24 hrs at 4^{o}C).

2.3.2.2. Sulphur deficient medium

The Kannan and Rehacek medium was modified by removing ammonium sulphate and incorporating ammonium chloride to obtain a semi defined sulphur limiting medium. The medium contained the following concentration of nutrients:

Chemical	Composition(g/L)
Glucose	20.00
Yeast extract	2.50
Ammonium Chloride	8.00
*Soybean dialysate	100 mL

Table 2.3: Chemical composition of sulphur limiting medium

(* Soybean dialysate was prepared from 10 g of defatted soybean flour in 1000 mL of distilled water for 24 hrs at 4^{o}C).

2.3.2.3. Potassium deficient medium

A previously reported potassium deficient production medium was used for PHA production under potassium deficient conditions (Wakisaka *et al.,* 1982). The medium contained the following concentration of nutrients:

Chemicals	Composition (g/L)
Glucose	20.00
Peptone	10.00
Casein	5.00
NaCl	3.00

Table 2.4: Chemical composition of potassium limiting medium

2.3.2.4. Phosphate deficient medium

Phosphate deficient medium previously reported by Lopez *et al*. (1986) was used to study the PHA accumulation by the organism under phosphate deficient condition (Lopez *et al.,* 1986). The medium contained the following concentration of nutrients:

Chemicals	Chemicals (g/L)
Glucose	20.00
KNO_3	0.50
$MgSO_4.\ 7H_2O$	0.20
$CaCl_2$	0.10
NaCl	0.10
K_2HPO_4	8.00
KH_2PO_4	2.80

Table 2.5: Chemical composition of phosphate limiting medium

The final pH of all nutrient limiting PHA production media used during this study, was set to 6.8 using 1 M HCl or 1 M NaOH. In all the media, the carbon source glucose was autoclaved at 110^{o}C for 10 minutes while the remaining components of the media were sterilised by autoclaving at 121^{o}C

for 15 minutes. These different components were then added together under aseptic conditions before inoculation.

2.3.3. Medium chain length, mcl-PHA production media

Medium chain length, mcl-PHA production studies were done by growing the *Pseudomonas* strains in different defined mcl-PHA production media. These media contain carbohydrates at concentrations of 20 g/L or fatty acids at 20 mM as carbon feed. The media used are listed below along with their compositions.

2.3.3.1. E medium

A defined chemical medium previously reported by Vogel and Bonner in 1956 was used for the production of mcl-PHA (Vogel and Bonner, 1956). The medium contained the following concentration of nutrients:

Chemicals	Composition (g/L)
$NaNH_4HPO_4$	3.50
$K_2HPO_4.3H_2O$	7.50
KH_2PO_4	3.70
$C_6H_8O_7$	2.90
$MgSO_4.7H_2O$	100 mM: 1 mL/L

Table 2.6: Chemical composition of E medium

2.3.3.2. E2 medium

The E medium was modified by removing citric acid and incorporating trace element solution. The medium contained the following concentration of nutrients:

Chemicals	Composition (g/L)
$NaNH_4HPO_4$	3.50
$K_2HPO_4.3H_2O$	7.50

KH_2PO_4	3.70
$MgSO_4.7H_2O$	100 mM: 1 mL/L
Trace element solution	1 mL/L

Table 2.7: Chemical composition of E2 medium

2.3.3.3. Modified E2, ME2 medium

The E2 medium was modified further by reducing the concentration of the constituting salts excluding magnesium $MgSO_4.7H_2O$ by half. The concentrations of the nutrients are as follows:

Chemicals	Composition (g/L)
$NaNH_4HPO_4$	1.75
$K_2HPO_4.3H_2O$	3.75
KH_2PO_4	1.85
$MgSO_4.7H_2O$	100 mM: 1 mL/L
Trace element solution	1 mL/L

Table 2.8: Chemical composition of ME2 medium

2.3.3.4. Mineral salt medium, (MSM)

A defined mineral salt PHA production medium previously reported by Tian *et al*. (2000) was also used to study the accumulation of mcl-PHAs by the organisms (Tian *et al.,* 2000). The medium contained the following concentration of nutrients:

Chemicals	Composition (g/L)
$(NH_4)_2SO_4$	0.50
$MgSO_4$	0.40
Na_2HPO_4	3.80
KH_2PO_4	2.65
Trace element solution	1 mL/L

Table 2.9: Chemical composition of the MSM medium

2.3.3.5. Trace element solution

Trace element solution of E2, ME2 and MSM media had the following concentration of nutrients:

Chemicals	Composition (g/L)
$CoCl_2$	0.22
$FeCl_3$	9.70
$CaCl_2$	7.80
$NiCl_3$	0.12
$CrCl_6.H_2O$	0.11
$CuSO_4.5H_2O$	0.16

Table 2.10: Chemical composition of trace element solution

The trace element solution was prepared by dissolving the chemicals in 0.1 N HCl.

All the mcl-PHA production media, was set at a final pH of 7 using 1 M NaOH and 1 M HCl. The carbon sources (fatty acids or carbohydrates) and magnesium sulphate were sterilised separately. The remaining inorganic salt components of the media were sterilised together. Except for carbohydrates which were sterilized at 110^{o}C for 10 minutes, all other components were sterilised at 121^{o}C for 15 minutes. The trace element solution was filter sterilised. The different components of the medium were then mixed together aseptically before inoculation.

2.4. Production of PHAs

The production of PHAs involves four major steps **(Figure 2.1)**, these are:

1. Culturing of the organisms in suitable growth and PHA production medium.
2. Harvesting of the cultures at desired specific time points and then lyophilisation.
3. Extraction of PHAs from the dried bacterial biomass.
4. Characterisation of PHAs.

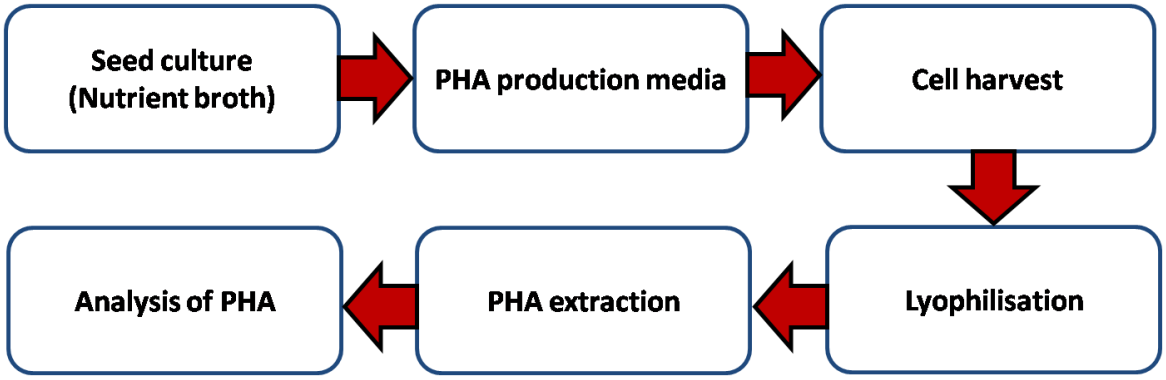

Figure 2.1: A flowchart for the production of PHAs.

2.4.1. Culturing of microorganisms.

2.4.1.1. PHA production at shaken flask level

Batch PHA production at shaken flask level was carried out using a two stage seed culture preparation for the *Pseudomonas* strains. The first seed culture was prepared by inoculating 30 mL of sterile nutrient broth (growth medium) in a 250 mL conical flask, using a single colony of the various *Pseudomonas* strains and growing it for 24 hrs in an orbital shaker (Stuart Scientific OrbitalShaker, S150) at 30°C and at a speed of 200 rev min^{-1}. This was then used for inoculating sterile PHA production medium, 300 mL in a 1L flask to prepare the second stage seed culture. The organism was again grown under the same culture conditions of 30°C and 200 rev min^{-1}. The growth of the organisms were monitored by measuring optical density (OD) readings at 450 nm. For OD values above 0.8, a tenfold diluted culture was used. The seed culture at an OD of 3.3 was used for all the *Pseudomonas* strains used throughout the study in order to inoculate specific PHA production medium and grown for different time periods, as appropriate, at 30°C and 200 rev min^{-1}.

Similarly, batch PHA production using *B. cereus* SPV was also carried out at shaken flask level. A one stage seed culture preparation was carried out

similar to that of the first seed culture for *Pseudomonas* sp. Sterile nutrient broth (growth medium), 30 mL in a 250 mL conical flask was inoculated using a single colony of *B. cereus* SPV. The organism was then grown at 30^{o}C, at a speed of 250 rev min^{-1}. The growth of the organism was monitored by taking OD readings at 600 nm and when the seed culture reached a final OD of 3.3, it was then used to inoculate the final respective PHA production medium and again grown for different time periods, as appropriate, at 30^{o}C and 250 rev min^{-1}.

Throughout the study, while inoculating the production medium, the inoculum volume used was 10% of the final working volume of the production medium.

Note: All the production studies were carried out in triplicates.

2.4.1.2. Optimisation of Poly(3-hydroxyalkanoate), P(3HO) production from *P. mendocina*

Optimisation of P(3HO) produced from *P. mendocina* using octanoate feed was done by designing conditions i.e. design of experiments, (DoE) using conditions generated from the partial factorial design. The three parameters chosen for the partial factorial design were: pH, carbon to nitrogen ratio and agitation speed of the stirrer i.e. rpm. The lower limit (-1) and the upper limit (+1) values chosen for pH were -1 = 6.8 and +1 = 7.5. Similarly -1 = 10:1(g/g) and +1 = 20:1(g/g) were the rates chosen for carbon to nitrogen ratio. The lower limit -1 value for rpm = 150 and upper limit +1 value was 250. **Table 2.11** lists the various fermentation conditions that were generated from the partial factorial design using the three parameters with their upper and lower limit values.

Parameters	rpm	C/N ratio	pH
Condition 1	(-1) 150	(-1) 10:1	(-1) 6.8
Condition 2	(+1) 250	(-1) 10:1	(+1) 7.5
Condition 3	(-1) 150	(+1) 20:1	(-1) 6.8
Condition 4	(+1) 250	(+1) 20:1	(+1) 7.5

Table 2.11: Fermentation conditions obtained from the partial factorial design.

All the optimisation studies for scaling up P(3HO) production was carried out in 2 L bioreactors. The working volume used in the 2 L fermenter was 1.7 L. The fermenter was sterilized at 121^{o}C for 30 minutes containing only the inorganic salts. The remaining components of the medium, carbon source sodium octanoate and magnesium sulphate were sterilized separately at 12^{o}C for 15 minutes. The trace element solution was filter sterilized. The different components of the medium were then mixed together under sterile conditions. The pH of the medium was maintained using 2M NaOH and 2M H_2SO_4.

Note: All the optimization studies were carried out in duplicates.

2.5. Extraction of PHA

The biomass was recovered by centrifuging the cultures at 4600 rev min^{-1} (Sorval, centrifuge) for 30 minutes and then lyophilised. The polymer was extracted from this dried bacterial biomass using various methods as described below.

2.5.1. Extraction using dispersion of chloroform ($CHCl_3$) and sodium hypochlorite (NaOCl)

In this method of extraction, two different hypochlorite concentrations, hypochlorite to chloroform ratios and incubation times were used. In the first method the dried bacterial biomass was incubated (orbital shaker from Stuart Scientific Orbital Shaker, S150) in a dispersion containing 30% NaOCl and

$CHCl_3$ in a 1:1 ratio at 30°C for two and a half hours and 150 rev min^{-1}. In the second improvised extraction method the dried bacterial biomass was incubated in a dispersion containing 80 % NaOCl and $CHCl_3$ in a 1:4 ratio at 30°C for two and a half hours and 150 rev min^{-1}. It was then centrifuged at 4000 g for 18 minutes following which three layers were formed. The topmost layer was that of hypochlorite, middle layer contained the cell debris and the bottom layer was the $CHCl_3$ containing the dissolved polymer. Polymer was then precipitated by introducing this $CHCl_3$ layer into 10 volumes of ice cold methanol with continuous stirring.

2.5.2. Temperature dependent extraction using hexane

This method was first described by Furrer *et al*. (2007). Here 1g of biomass in 15 mL of hexane was incubated for 24 hrs at 60°C with vigorous shaking. The solution was then kept at 5°C for 6 hrs for polymer precipitation after which the polymer was filtered and air dried.

2.5.3. Acetone extraction:

Recovered biomass was washed twice with water and lyophilised. It was then treated with methanol, (1 g in 20 mL methanol) for 5 minutes at 22±10°C at 140 g. This pre-treated biomass was then subjected to soxhlet extraction using five volumes of acetone for 5 hrs following which the polymer was finally precipitated using 10 volumes of chilled methanol with continuous stirring.

2.5.4. Soxhlet extraction

The dried biomass was incubated with 16 % NaOCl at 37°C for 1 hour. Incubation with NaOCl causes lysis of the cells. The cells were then

centrifuged at 4000 g, for 10 minutes, after which the residue was washed twice with 50 mL each of HPLC water, acetone, ethanol and diethylether. The residues obtained were freeze dried and then refluxed using $CHCl_3$ for 24 hrs. The polymer was finally precipitated using ten volumes of chilled methanol with continuous stirring.

2.5.5. Chloroform extraction

The dried biomass was incubated in $CHCl_3$ for 24 hrs at 30^{o}C with vigorous shaking. The $CHCl_3$ solution was then concentrated using a rotary vacuum evaporator (Rotary vacuum evaporator, from Perkin Elmer USA) followed by polymer precipitation in 10 volumes of chilled methanol with continuous stirring.

2.6. Polymer purification

The polymer extracted using the second optimised dispersion of hypochlorite and chloroform was subjected to sequential repeated steps of precipitation to reduce or remove the contaminating LPS. The polymer was first precipitated using a 70 % each of methanol and ethanol (1:1 ratio). The precipitated polymer was then repeatedly dissolved in acetone and again precipitated using the same methanol to ethanol mixture.

2.7. Wet scanning transmission electron microscopy, wet STEM analysis

The accumulated intracellular PHA inclusions were imaged using the wet STEM analysis. The sample for the imaging was prepared by centrifuging 1 mL of the culture at 4000 g for 10 minutes. The pelleted culture was then washed twice in 1 mL of distilled water again at 5217 g for 10 minutes. The

washed pellet was then suspended in 300 µl of distilled water. 0.5 µl of this culture suspension was then imaged in a FEI XL30 ESEM, equipped with a field-emission electron source. All transmission-mode images were acquired with an accelerating voltage of either 20 or 25 kV, spot-size 3. The analysis was carried out in collaboration with University of Cambridge, UK.

2.8. Other analytical studies

2.8.1. Biomass estimation

Estimation of the biomass was done by taking absorbance readings at 450nm using an Novespec II spectrophotometer (Pharmacia Biotech) and also by measuring the cell dry weights of the freeze dried cells.

2.8.2. Nitrogen estimation

The estimation of ammonium in the medium was done using the phenol-hypochlorite reaction method. The amount of 'N' in the 'NH_4' was then calculated. The sample for the test was prepared by first centrifuging the required volume of the culture at 8700 g for 10 minutes. The supernatant was used for carrying out the assay. After appropriate dilution, 1mL of phenol nitroprusside buffer was added to 2.5 mL of the sample and mixed by gentle swirling. To this, 1.5 mL of hypochlorite reagent was added promptly and mixed gently by inversion. The sample was then left standing for 45 minutes out of direct sunlight. The absorbance readings were then measured at 635 nm. Ammonium sulphate was used as the positive standard. The media components except ammoniums sulphate was used as a negative control. The assay was carried out in triplicates.

The reagents required for the assay was prepared as follows: For phenol nitroprusside buffer, 3 g of sodium phosphate tribasic ($Na_3PO_4.12H_2O$), 3 g of sodium citrate and 0.3 g ethylene diamine tetraacetic acid, EDTA were dissolved in HPLC water. The pH of the solution was set at 12. To this solution, 6 g of phenol and 20 mg of sodium nitroprusside ($Na_2[Fe(CN)_5NO].2H_2O$) was added. The alkaline hypochlorite reagent was prepared by adding 2.5 mL of sodium hypochlorite (NaOCl) solution containing 4 % chlorine to 40 mL of 1M NaOH solution. The final volume was then made up to 100 mL by adding HPLC water.

2.8.3. Octanoic acid estimation

Briefly the sample was prepared by centrifuging the culture at 8700 g for 10 minutes. The amount of free octanoic acid present in the supernatant i.e. medium was then determined as per the instructions using the fatty acid assay kit from Biovision, UK.

2.8.4. Carbohydrate estimation

2.8.4.1. Phenol sulphuric acid assay

Glucose estimation was carried out by the phenol sulphuric acid assay. For this, the culture was first centrifuged at 10,400 g for 10 minutes. Desired dilutions of the supernatant were carried out. 200 µl of 5 % phenol was added to 200 µl of the diluted sample. To this, 1 mL of H_2SO_4 was added immediately and left standing for 10 minutes. It was then vigorously mixed and once again left standing for 30 minutes at room temperature. Subsequently, the absorbance was read at 490 nm.

2.7.4.2. Dinitrosalicylic calorimetric assay

This method was used for the estimation of sucrose and or fructose present in the culture supernatant. The carbohydrates were first hydrolysed by adding 20 µl of concentrated HCl to 1 mL of the culture supernatant. The hydrolysis was allowed to proceed at 90^{o}C for 5 minutes. 50 µL of 5N KOH solution was then added to neutralize the acid. Post neutralisation, 1 mL of the dinitrosalicylic acid, DNS reagent (The dinitrosalicylic acid solution contained: dinitrosalicylic acid, 10 g; phenol, 2 g; sodium sulfite, 0.5 g and NaOH, 10 g in 1000 mL of H_2O) was added to 1 mL of the supernatant. The mixture was then heated at 90^{o}C for 5-15 minutes until the red brown colouration appeared. 1 mL of a 40 % potassium sodium tartarate (Rochelle salt) solution was then added to stabilize the colour. The reaction mixture was then cooled down to room temperature. The absorbance was then recorded, sucrose at 575 nm and fructose at 553 nm. Sucrose and fructose were used as the positive standards respectively. In each case complete media devoid of these sugars were used as negative control. The assay was carried out in triplicates.

2.8.4.3. Endotoxin assay

The lipopolysaccharide, LPS was extracted from the polymer using a method which was adapted from Furrer *et al*. (2007). 300 mg of the polymer in the powder form was first heated upto 60-70^{o}C for 24 hrs in a pyrogen free round bottom flask (50 mL size). To this melted polymer 6 mL of pyrogen free water was added and then incubated for 24 hrs at 150 rev min^{-1}.

The LPS extracted was then quantified using an FDA approved endotoxin test, Limulus amebocyte lysate, (LAL) test. Limulus amebocyte lysate (LAL)

is an aqueous extract of blood cells (amebocytes) from the horseshoe crab, *Limulus polyphemus*. In the presence of endotoxin LAL becomes turbid; this is because the LPS present in the bacterial cell wall reacts with enzymes located in the granules of the amebocytes initiating the clotting cascade. While the complete reaction mechanism is not understood, the last step is well described. The activated clotting enzymes cleaves the clotting protein (coagulogen); the insoluble cleavage products then coalesce by ionic interaction following which the turbidity of the reaction mixture increases (Bang, 1953; Levin and Bang, 1968)

In this study a kinetic turbidimetric LAL method, was used in which the time taken to reach a particular level of turbidity (the onset time) was determined. Higher endotoxin concentrations give shorter onset times. The assay was carried out as per the instructions using the LAL estimation kit. For the LAL assay, 100 µl of the, sample (water containing the extracted LPS) was incubated with 100 µl of the LAL at 37^{o}C. The assay was carried out on a 96 well plate using a plate reader VersaMax (Molecular design) and the software SoftMax Pro 5. The absorbance was read at 405 nm. The endotoxin was estimated from the endotoxin standard curve (concentration range between 0.03 to 1 EU/ml) Pyrogen free water was used as a negative control and standard endotoxins as positive control.

2.9. Characterisation of PHAs

2.9.1. Structural characterization

The structural charaterisation of the kind of PHA monomer accumulated by the organism was carried out by performing the following analysis.

2.9.1.1. Attenuated total reflectance fourier transform infrared, ATR-FTIR spectrometry

Preliminary analysis of the polymer was performed using ATR-FTIR. 2 mg of the polymer was used for the study. The analysis was performed under the following conditions: Spectral range 4000 to 400 cm^{-1}; window material, CsI: 16 scans and resolution 4 cm^{-1}. The analysis was carrid out at the Department of Biomaterials and Tissue engineering, Eastman Dental Institute, Univeristy College London, UK.

2.9.1.2. Gas Chromatography-Mass Spectroscopy, GC-MS

The PHA monomer was identified by carrying out GC-MS analysis of the methanolysed polymer. Two different methods for methanolysis or making the methyl esters of the polymer were used. The first method used was a slight modification of the gas chromatographic method of Huijberts *et al*. (1994). The reaction mixture contained 20 mg of the polymer, 100 µl of 1 mg/mL methyl benzoate, ($C_6H_5COOCH_3$), 2 mL of $CHCl_3$ and 2 mL of 15 % sulphuric acid in methanol. The reaction mixture was refluxed for 4 hrs, after the reaction, the tubes were cooled on ice for 5 min, 1.0 mL HPLC water was added and the tubes were vortexed for 1 min. After phase separation, the bottom organic phase was collected, dried over anhydrous sodium sulphate, filtered and analysed. (Huijberts *et al*., 1994). This method was used for the PHA extracted from *B. cereus* SPV and for PHA extracted from *P. aeruginosa* and *P. oleovorans*.

The methanolysis method developed by Furrer *et al*. (2007) was used for making methyl esters of the polymer extracted from *P. mendocina*. The reaction mixture contained 10 mg of polymer, 1 mL of methylene chloride containing 10 mg/mL of 2-ethyl-2-hydroxybutyric acid. The polymer was dissolved at room temperature for 1 hr. 1 mL of BF_3 in methanol (0.65 M) was also added, after which the tube was tightly sealed, vigorously shaken and

then heated for 20 h at 80°C. After the reaction, the tubes were cooled on ice for 5 min, 2 mL HPLC water was added and the tubes were vortexed for 1 min. After phase separation, the bottom organic phase was collected, dried over anhydrous Na_2SO_4 and neutralized by adding Na_2CO_3. It was then filtered and used for carrying out the GC-MS study (Furrer *et al.,* 2007). The samples were sent for GC-MS analysis at the School of Chemistry, University of Southampton, UK.

2.9.1.3. Nuclear Magnetic Resonance Spectroscopy, NMR

Structural characterisation of the PHA monomers, accumulated by the organism was also done using ^{13}C and ^{1}H and heteronuclear single quantum coherence, (HSQC) NMR. For these 20 mg of purified polymer was dissolved in 1 mL of the deuterated chloroform ($CDCl_3$) and analysed on a Bruker AV400 (400 MHz) spectrometer. Chemical shifts are referenced against residual solvent signal (7.26 ppm and 77.0 ppm for 1H and 13C respectively). Spectra were analysed using the MestRec software package. The samples were sent for NMR analysis at the Department of Chemistry, University of Nottingham, UK and Department of Chemistry, University College London, UK.

2.9.2. Mechanical properties

Tensile testing was carried out using a Perkin –Elmer dynamic mechanical analyzer at room temperature. The test was carried out on polymer strips of 10 mm length and 4 mm width cut from pressed and solvent casted polymer films . The initial load was set to 1 mN and then increased to 6000 mN at the rate of 200 mM min^{-1}. The test was carried out on 6 repeats of the samples. Young's modulus, stress and strain were recorded during the test.

Dynamic mechanical analysis was also carried out to study the viscoelastic properties of loss modulus, storage modulus and tan δ which were measured as a function of temperature. A temperature scan from -20 to 80^{o}C was applied at a heating rate of 4^{o}C min^{-1}. A frequency of 1 Hz was used, with a static tension control of 110% and a controlled dynamic strain of 0.2 %. Nitrogen was used as a purge. The test was carried out on 9 repeats of the samples. The analysis was carrid out at the Department of Biomaterials and Tissue engineering, Eastman Dental Institute, Univeristy College London, UK.

2.9.3. Crystallinity

A Phillips PW1700 series automated powder diffractometer was used for X-ray diffraction (XRD) analysis of P(3HO). Cu Kα radiation of 40 kV and 40 mA was obtained using a secondary crystal monochromator. Every scan was recorded in the range of 2θ = 10 - 40^{o} with the scan time running over 13 hrs. Crystallinity % of the polymer was calculated from mathematical model functions, Gauss and Lorentzian functions of the different aged polymer samples. The sample was sent for analysis at the Department of Biomaterials, Imperial College, UK.

2.9.4. Contact angle study

Static contact angle measurements were carried out to evaluate the wettability i.e. hydrophilicity of the fabricated films. A gas tight micro-syringe was used to place an equal volume of water (<10 μl) on every sample by means of forming a drop. Photos (frame interval of 1 second, number of frames = 100) were taken to record the shape of the drops. The water contact angles on the specimens were measured by analysing the recorded drop images using the Windows based KSVCam software. Six repeats for each

sample was carried out. The experiment was done on a KSV Cam 200 optical contact angle meter (KSV Instruments Ltd). The analysis was carrid out at the Department of Biomaterials and Tissue engineering, Eastman Dental Institute, Univeristy College London, UK.

2.9.5. Surface study

2.9.5.1. Scanning electron microscopy

Microstructural studies for the surface topography of the polymer was also carried out. The studies were done on the samples using a JOEL 5610LV scanning electron microscope (JOEL). The samples were placed on 8 mm diameter aluminium stubs and then coated with gold using the gold spluttering device (EMITECH-K550). The operating pressure of 7 x 10^{-2} bar and deposition current of 20 mA for 2 minute was used. The SEM images were taken with an acceleration voltage of 15 kV (maximum) to avoid incineration of the polymer due to the beam heat. The samples were sent for the analysis at the Department of Biomaterials, Imperial College, UK.

2.9.5.2. White light interferometry study using Zygyo

White light interferometry was used to obtain 3D imaging of the surface topography of samples by means of the analyzer ZYGO (New View 200 OMP 0407C). This, measurement allowed to investigate and quantify the roughness and topography of the surfaces. The samples were sent for the analysis at the Department of Biomaterials, Imperial College, UK.

2.9.6. Molecular weight analysis

The molecular weights of the polymer i.e. number average molecular weight, (M_n) and weight average molecular weight, (M_n) was determined by carrying out gel permeation chromatography analysis. Two PolarGel-M columns (30 cm) in series (Varian inc.) were calibrated to 377,000 – 580 Da using narrow molecular weight polystyrene standards. The eluent used was tetrahydrofuran, THF [$(CH_2)_4O$], 10 mg/mL of P(3HO) was introduced into the GPC system at a flow rate of 1 mL/min. The eluted polymer was detected with a differential refractometer. The data were collected and analysed using Viscotek 'Trisec 2000' and 'Trisec 3.0' software. The samples were sent for the analysis at the Department of Chemistry, University of Nottingham, UK

2.9.7. Thermal properties

The thermal properties of the polymer i.e. glass transition temperature (T_g) and melting temperature, (T_m) was studied by carrying out differential scanning calorimetry, (DSC) using a Perkin Elmer Pyris Diamond DSC (Perkin Elmer Instrument). The amount of the polymer used for the study ranged from 8-10 mg and were encapsulated in standard aluminium pans. All tests were carried out under inert nitrogen. The samples were heated/cooled/heated at a heating rate of $20^oC\ min^{-1}$ between -57 and 100^oC. The test was carried out on 9 repeats of the samples. The analysis was carrid out at the Department of Biomaterials and Tissue engineering, Eastman Dental Institute, Univeristy College London, UK.

2.10. UV treatment of poly(3-hydroxyoctanoate)

Shangguan *et al.* (2006) had carried out UV treatment of poly(3-hydroxybutyrate-co-3-hydroxyhexanoate), P(3HB-co-3HHx) to increase its

biodegradability and biocompatibility. Modification of P(3HO) was carried out to achieve increase biodegradability and biocompatibility by exposing it to UV rays. For UV treatment of P(3HO) polymer was exposed to two UV lamps of 15 W (435 to 500 nm) each, placed at a distance of 3 cm. UV exposure was carried out for 8 hrs.

2.11. X-ray photoelectron spectroscopy, XPS

UV treated P(3HO) was assessed using X-ray photoelectron spectroscopy (Thermo Escalab 220iXL). Measurements were performed using an Al Kα monochromated X-ray source and quantified using CASAXPS (Casa Software Ltd, Teignmouth, UK). For all the samples, both survey and high-resolution spectra were recorded. The samples were sent for analysis at the School of Chemistry, Cardiff University, UK.

2.12. Fabrication of Films

After the successful production and characterisation of the PHAs, fabrication of the PHAs into two dimensional films, 2D films was done for the purpose of medical applications. Two different types of 2D films were made:

A: Neat 2D films or films using only the polymer.

B: Composite 2D films made by introducing a bioactive nanosize 45S5 Bioglass® (n-BG) as a filler i.e. polymer/nanobioglass composite scaffold. The composition in wt% of the n-BG is given in the following Table 2.12.

	SiO_2	Na_2O	CaO	P_2O_5
nBG	46.08	22.96	27.18	3.77

Table 2.12: Chemical composition of nano size (30nm) 45S5 Bioglass®

The n-BG was obtained from our collaborator Professor Aldo Boccaccini from Imperial College, UK.

2.12.1. Fabricaton of P(3HO) pressed films

The homopolymer P(3HO) produced from *P. mendocina* when grown in octanoate was pressed to form circular film disks of about 15 mm diameter. To make the film 50 mg of the polymer was used.

2.12.2. P(3HO) neat and P(3HO)/ 45S5 Bioglass® nanosize, (n-BG) composite, 2D films-solvent casted

Amongst the mcl-PHAs, P(3HO) produced from *P. mendocina* using octanoate was fabricated into 2D films for its use as a biomaterial. P(3HO) neat films were fabricated by using 5 and 10 % of the polmer in 10 mL of $CHCl_3$. The polymer was well dissolved after which the polymer solution was filtered and the films made, by casting the polymer solution into glass petridishes. The solution was then left to air dry at room temperature for 1 week followed by freeze drying for 10 days.

Composite films in chloroform were prepared using 10 mL of 5 and 10 wt % polymer containing 1 wt/vol % of 45S5 Bioglass® (n-BG) each. The polymer was dissolved completely following which the polymer solution was filtered. To this, required amount of n-BG was added. The mixture was then sonicated using the sonicator (Philip Harris Scientific) for a total of 1-2 minutes. The sonication programme used was 5 pulses in 10 seconds. The films were then cast as described above. The total weight % of n-BG in the 5 wt% polymer film is 17 and in the 10 wt% polymer film is 9. These fabricated films will be referred as P(3HO) neat and P(3HO)/n-BG composite; where the weight % have to mentioned the films will be referred as 5 wt% neat and 10 wt% neat, 5 wt% composite and 10 wt% composite films.

2.12.3 UV treated P(3HO) neat and P(3HO)/ 45S5 Bioglass® nanosize (n-BG) composite, 2D films- solvent casted.

The UV treated P(3HO) polymer was also fabricated into 2D films. Neat and composite films of the UV treated polymer were made with the same compositions and methodology as described above. These fabricated films will be referred as UV P(3HO) neat and UV P(3HO)/n-BG composite; where the weight % have to mentioned the films will be referred as as UV 5 wt% neat and UV 10 wt% neat, UV 5 wt% composite and UV 10 wt% composite films.

2.12.4. Blends of Poly(3-hydroxybutyrate), P(3HB) and P(3HO)

2D films were also made by blending mcl P(3HO) with scl P(3HB) produced from *B. cereus* SPV under nitrogen limitation. Different weight percentages of P(3HB) and P(3HO) were tried and the best quality blend films were made by using: (1) a 5 wt % P(3HB) and 1 wt % P(3HO) solution in 10 mL $CHCl_3$ and (2) a 1 wt % P(3HB) and 5 wt% P(3HO) solution in 10 mL $CHCl_3$. Preparation of the blend films were done in the same manner as described above.

Composite blend films were also prepared by incorporating 1 wt % n-BG to the solution of CHCl3 containing 1 wt% P(3HB) and 5 wt% P(3HO). This composite blend film was also prepared in the same manner as described above.

2.13. *In vitro* degradation study

In vitro degradation studies of the fabricated 2D films were carried out. The P(3HO) neat and P(3HO)/n-BG composite films made from non UV treated

P(3HO) was studied for a period of 1, 2 and 4 months in phosphate buffer saline, (PBS), Dulbecco's Modified Eagles Medium, (DMEM) and Dulbecco's Modified Eagles Medium Knock Out, ($DMEM^{KT}$).

PBS was chosen as phosphate buffer system is one of the buffer system that regulates the acid or base balance in the body. DMEM media was chosen since the biocompatibility studies for the fabricated films were carried out using the keratinocyte cell line HaCaT, and DMEM is the most optimum media for the growth of these cells. Similarly, $DMEM^{KT}$ media was also chosen since for pericardial patch application, the films would be seeded with embryonic stem cells and $DMEM^{KT}$ is one of the most optimum media that supports the growth of these cells.

In vitro degradation studies of the UV P(3HO) neat and UV P(3HO)/n-BG composite films made from UV treated P(3HO) were also carried out. The study was done for a period of 1, 2 and 4 months, using DMEM and $DMEM^{KT}$ media.

In vitro degradation studies for the blend films was carried out for a period of 15 days, 30 days and 60 days using a cellular simulated body fluid (SBF). The chemical compositions for SBF is listed in **Table 2.13.**

Chemicals	**Compositons (g/L)**
NaCl	8.00
$NaHCO_3$	0.35
KCl	0.22
$K_2HPO_4.3H_2O$	0.22
$MgCl_2.6H_2O$	0.30
1N, HCl	40 mL
$CaCl_2$	0.28
Na_2SO_4	0.07
$(CH_2OH)_3CNH_2$	6.06
H20	1000 mL

Table 2.13: Chemical compositions for simulated body fluid.

The pH of SBF was adjusted to 7.25 at 36.5°C by using 1N HCl.

DMEM medium contained 4.5 g/L of glucose and was supplemented with 10% foetal calf serum, 1% glutamine and 1% penicillin and streptomycin solution.

Note: All the degradation related studies were carried out in triplicates.

2.13.1. Surface morphology

SEM analyses of the planar surface of the degraded films were carried out at the end of the 4 month study to see changes in the surface morphology of the films occurring due to its degradation. The sample preparation and methodology was the same as described in section 2.9.5.1.

2.13.2. Water uptake, weight loss and pH measurements

The degradation kinetics was also determined by measuring the % water uptake or absorption (% WA) and % weight loss (% WL). For these, all the samples were first weighed M_o dry (M_o, the initial weight of the sample), immersed in the respective media and kept under static conditions, at 37°C till the desired time point. The media was changed once a week. At each prescheduled incubation time points the films were collected and analysed for water uptake (% WA) and weight loss (% WL) behaviour. For measuring the water absorption (% WA) of the samples, the immersed samples were removed at given time points, the surface was gently wiped with a tissue paper and the weight was measured M_w, wet (M_w, the weight of the samples after immersion in the media). Similarly, for measuring the weight loss, the samples were withdrawn from the media, washed several times with deionised water and dried at 37°C overnight and subsequently weighed M_t, dry (M_t, the dry weight

of the samples after immersion in the media followed by drying). Water absorption and weight loss were calculated using the following equations:

$$\text{Water absorption (\% WA)} = [(M_w \text{ wet-} M_t \text{ dry})/M_t \text{ dry}\ ]100$$
$$\text{Weight loss (\% WL)} = [(M_o \text{ dry-} M_t \text{ dry})/M_o \text{ dry}]\ 100$$

The media in which the films were incubated were changed every one week. The pH changes of the media were then measured at the end of each incubation time point.

2.13.3. Thermal properties

Thermal analysis of the degrading samples at the end of each time point was also carried out to study changes in their thermal properties corresponding to T_m, ΔH_f and T_g, occurring due to degradation. The sample preparation and analysis was carried out as described in section 2.9.7.

2.13.4. Mechanical properties

Mechanical analysis of the degrading samples at the end of each time point was also carried out to study changes in their stiffness occurring due to degradation. The sample preparation and analysis was carried out as described in section 2.9.2.

2.14. Protein adsorption study

Protein adsorption assay was performed using foetal bovine serum, (FBS). The films 1 cm^2 were incubated in 400 µl of undiluted FBS at 37^oC for 24 hrs. After incubation the samples were rinsed with phosphate buffer saline, (PBS) thrice. The samples were then incubated in 1 mL of 2% sodium dodecyl sulfate (SDS) in PBS for 24 hrs at room temperature and under vigorous shaking to further collect the adsorbed proteins. The amount of total protein

adsorbed on the surface of the samples was quantified using a commercial protein quantification kit (Pierce, Rockford, IL). The optical density of the samples was measured spectrophotometrically at 562 nm against a calibration curve using bovine serum albumin as per the manufacturer's protocol. The samples incubated only in PBS were used as a negative control. The assay was carried out in triplicates.

2.15. Cell culture study

The *in vitro* cell culture studies were carried out on the P(3HO) neat and P(3HO)/n-BG composite films made from both UV treated and non UV treated P(3HO) using the keratinocyte cell line HaCaT. The cells were cultured in DMEM supplemented with 10 % foetal calf serum, 1 % penicillin and 1% streptomycin solution. The media, trypsin and dye were all filter sterilised prior to use and warmed at 37^{o}C for about 15 minutes. The cells were incubated at 37^{o}C in a humified atmosphere (5 % CO_2 in 95 % air). The culture medium was changed every 2 days.

2.15.1. Cell seeding on the test samples

The samples (1 cm^2 in area) were UV sterilised for 30 minutes on each side and passivated for 12 hrs prior in the culture media prior to seeding the cells. The cells were released on confluence using trypsinisation. Following cell detachment fresh medium was added to the cell suspension and pelleted by centrifugation at 1500 rev min^{-1} for 10 minutes. The pellet was then resuspended in fresh medium and transferred to either 75 cm^2 tissue culture flasks for further passages or used for carrying out the analysis. A cell density of, 20,000 cells were used to seed the samples kept in 24 well plates. The samples were held onto the surface of the plates using the circular crown™ disk obtained from Scaffdex, Finland. The cell seeded films were again

incubated in the humidified atmosphere as described above. The medium was changed every 2 days and the cells were analysed after 1, 4 and 7 days for cell adhesion and proliferation and SEM observation. Cell culture studies were carried out on quadraplet samples per experiment and were repeated twice.

2.15.2. Cell adhesion and proliferation

Cell adhesion and proliferation studies were carried out using the Nile Red (NR) assay. The cells were incubated in DMEM medium containing 40 μg/mL NR for 3 hrs to allow the viable uninjured cells to take up the dye. After incubation, the samples were transferred to new 24 well plates, and washed twice with 2 mL of solution A (fixative: containing 1 % $CaCl_2$, 0.5 % formaldehyde). 300 μl of solution B (1 % acetic acid and 50 % ethanol solution) was then added to each sample to extract the dye. The plate was then allowed to stand at room temperature for 10 minutes followed by rapid agitation on a microtitre plate shaker. The absorbance of the dye was read at 540 nm using a microtitre plate reader from Thermomax. The software used was SoftMax Pro version 4.8. The total NR uptake was a measure of the cell's viability and proliferation (% NR uptake is directly proportional to the number of live and uninjured cells). The % cell proliferation was therefore calculated as follows:

$$\% \text{ viability} = \frac{\text{Mean absorbance of samples}}{\text{Mean absorbance of control}} \times 100$$

Positive control (cells + medium in the tissue culture plates) were run alongside in every experiment. Negative control (medium + samples, no cells) was also used in all experiments to account for absorption of the NR by the samples on their own. Background absorbance of the negative control was deducted from that of the test samples. The positive control was normalised to 100%.

2.15.3. SEM preparation for cells

The P(3HO) neat and P(3HO)/n-BG composite films both UV treated and untreated were examined under SEM in order to observe the HaCaT cell spreading and attachment on the surface of the samples. The specimens were fixed in 0.1 M cacodylate buffer containing 3 % glutaraldehyde for 12 hrs at 4^{o}C. Subsequent dehydration using a series of graded ethyl alcohols 50 %, 70 %, 90 % twice and 100 % four times was performed. The samples were then left to air dry for half an hour in the fume cupboard for subsequent drying. The dried samples were then attached to aluminium stubs, gold coated and examined under SEM (JEOL 5610LV, JEOL, USA) at an acceleration voltage of 10-15 kV.

2.16. *In vitro* haemostatic study using Thromboelastography® (TEG®)

The haemostatic effect of the n-BG 45S5® was studied by thromboelastography using a TEG® 5000 series Hemostasis Analyzer (Medicell Ltd, London, UK). Briefly, 20 µl of 0.2M $CaCl_2$ was added to 360 µl of citrated whole blood, followed by controlled amounts of n-BG, the clotting parameters were then monitored. The following clotting parameters were then monitored using the R time (reflecting the time delay before the clotting process begins to be detectable), alpha angle (reflecting the rate at which clotting proceeds) and maximum amplitude (reflecting the strength of the formed clot). Three different amounts of n-BG 45S5® i.e. 1, 2 and 4 mg were used for the study, in order to look for dose-related changes.

2.17. Statistical analysis

All data sets have been expressed along with their mean standard deviation. The data, where appropriate, were compared using the student's t-test and

differences were considered significant when *p < 0.05, very significant **p < 0.01 and highly significant ***p < 0.001, respectively. A p-value higher than 0.05 (p > 0.05) was interpreted as indicating no significant difference.

Chapter 3: Production of PHAs from *B. cereus* SPV under different nutrient limitations

3.1. Introduction

Macrae and Wilkinson in 1958, while studying *B. megaterium* (Macrae and Wilkinson, 1958), first made the observation that unbalanced growth conditions with limiting nutrient(s) triggers PHA accumulation in short chain length (scl) and medium chain length (mcl) PHA producers. It is now understood that majority of the organisms that make and store PHAs do so when subjected to nutrient(s) limiting conditions for growth, in the presence of excess carbon source. Such PHA producers are therefore called "growth limited producers". An exception to these growth limited producers are *Cupriavidus necator* (formerly known *Ralstonia eutropha)* (Kim *et al.,* 1994; Ryu *et al.,* 1997) and *Methylobacterium organophilum* (Kim *et al.,* 1996) that do not require any nutrient limiting conditions to accumulate PHAs and hence are called "growth associated producers". *A. latus* during growth, accumulated P(3HB) which was less than 50 % of its dcw (Yamane *et al.,* 1996). However, when subjected to a nitrogen limiting condition during fed batch culture, the P(3HB) accumulation increased up to 88% of its dcw (Wang and Lee, 1997). Such studies have therefore also implicated that introducing nutrient limiting conditions help the organism to increase its yield of the PHA produced. Over the years studies have also revealed that a large diversity in the molecular structures of the PHAs synthesized can be obtained depending on the organism and the culture condition used (Caballero *et al.,* 1995). Culture conditions like the type of nutrient(s) limitation that an organism plays a profound role in the kind of monomers accumulated in the polymer chain.

Therefore, experiments were carried out with an objective to study the effects of different nutrient limiting conditions on the PHA accumulation behaviour of *B. cereus* SPV, which has been isolated in our laboratory. This study reports for the first time, the effect of a range of single nutrient limiting

condition such as nitrogen, sulphur, potassium, and phosphate on PHA accumulation by *B. cereus* SPV. The organism was grown in specialised PHA production medium which was limited in the nutrient to be studied. The composition of these specified nutrient limiting media are described in section 2.3.2. The polymer obtained was then extracted from the lyophilised bacterial cells using the hypochlorite dispersion method (section 2.5.1). The polymer obtained under all these different nutrient limiting conditions were then analysed using fourier transform infrared spectroscopy, FTIR (section 2.9.1.1.) and Gas chromatography mass spectroscopy, GCMS (section 2.9.1.2).

3.2. Results

3.2.1. PHA production under nitrogen limitation

To study the effect of nitrogen limitation on the accumulation of PHAs by *B. cereus* SPV, the organism was grown in the Kannan and Rehacek medium, a nitrogen limiting medium (Kannan and Rehacek, 1970). The organism grew rapidly, a maximum cell density of 2g dcw/L was attained within 24 hrs of cultivation, and then a gradual decrease in cell density was observed during the stationary phase of growth (**Figure 3.1, Table 3.1**). The pH of the culture medium decreased during the growth, from its initial value of 7 to a minimum of 4.5. Cessation of logarithmic growth coincided with the approach of the pH minimum and rapid consumption of glucose. The PHA accumulation increased rapidly during the stationary phase and reached a maximum concentration of 38 % of dry cell weight at 72 hrs of growth. Once maximal PHA concentration was achieved, the PHA concentration remained almost constant until 120 hrs.

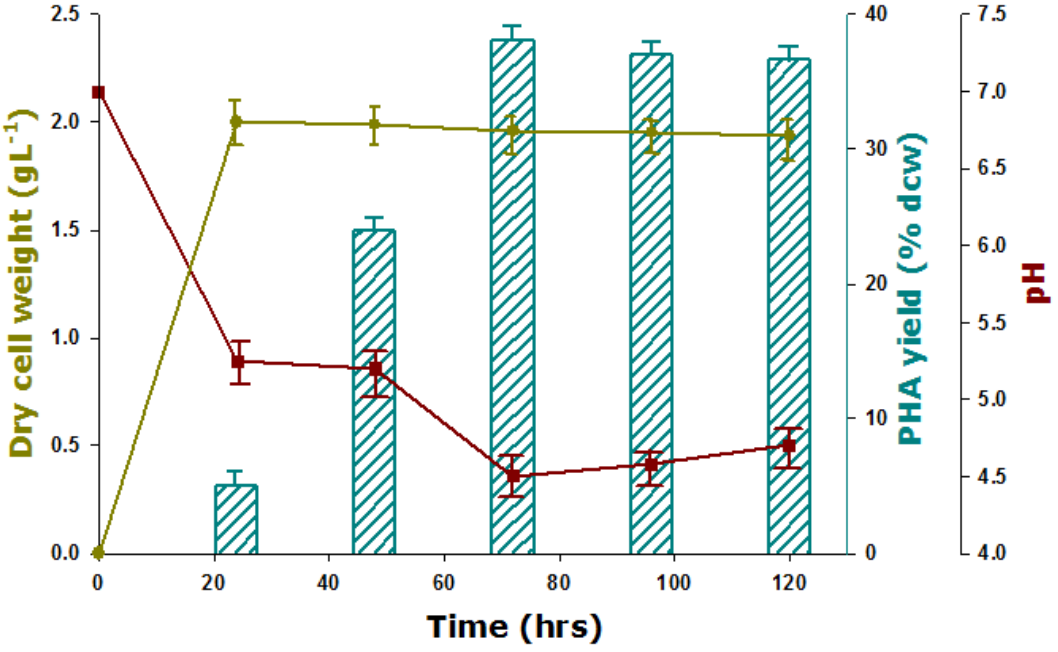

Figure 3.1: **Fermentation profile for P(3HB) production from *B. cereus* SPV in nitrogen limiting condition. [Dry cell weight (●), pH of the medium (♦), PHA yield (▨)]**

Limiting nutrient	PHA Monomers (mol %)	Growth parameters	Time (hrs)				
			24	48	72	96	120
Potassium	3HB (90)	Dry cell weight (g/L)	1.35 ± 0.01	1.71 ± 0.01	0.86 ± 0.01	1.01 ± 0.01	1.00 ± 0.01
	3HV (10)	PHA yield (% dcw)	3.70 ± 0.02	13.4 ± 0.02	4.20 ± 0.02	1.00 ± 0.01	ND
		pH	4.80 ± 0.03	4.60 ± 0.02	4.76 ± 0.02	4.88 ± 0.02	4.60 ± 0.02
Sulphur	3HB (100)	Dry cell weight (g/L)	1.25 ± 0.01	1.73 ± 0.01	1.51 ± 0.01	1.39 ± 0.02	0.95 ± 0.01
		PHA yield (% dcw)	ND	13.15 ± 0.02	1.29 ± 0.02	ND	ND
		pH	4.74 ± 0.02	4.75 ± 0.02	4.69 ± 0.03	4.53 ± 0.02	4.51 ± 0.03
Phosphate	3HB (100)	Dry cell weight (g/L)	0.10 ± 0.01	0.19 ± 0.01	0.18 ± 0.01	0.17 ± 0.01	0.15 ±0 .01
		PHA yield (% dcw)	ND	21.0 ± 0.04	33.33 ± 0.02	ND	ND
		pH	6.67 ± 0.02	6.63 ± 0.03	6.63 ± 0.02	6.64 ± 0.02	6.65 ± 0.02
Nitrogen	3HB (100)	Dry cell weight (g/L)	2.00 ± 0.02	1.99 ± 0.02	1.96 ± 0.01	1.95 ± 0.02	1.94 ± 0.02
		PHA yield (% dcw)	5.00 ± 0.02	24.0 ± 0.02	38.0 ± 0.03	37 ± 0.03	36.6 ± 0.03
		pH	5.25 ± 0.03	5.20 ± 0.02	4.50 ± 0.01	4.58 ± 0.01	4.7 ± 0.02

Table 3.1: Compilation of the growth parameters and kind of PHA monomers accumulated by *B. cereus* SPV when grown in different nutrient limiting conditions. ND: not determined. All the studies were carried out in triplicates.

Preliminary confirmation of the polymer identity was carried out using FTIR. FTIR analysis of the isolated polymer revealed absorption bands at 1724 cm^{-1}, corresponding to the ester carbonyl group and at 1281 cm^{-1} corresponding to the –CH group, characteristic of scl-PHAs (Sun *et al.*, 2007) (**Figure 3.2**), confirming the production of a scl-PHA.

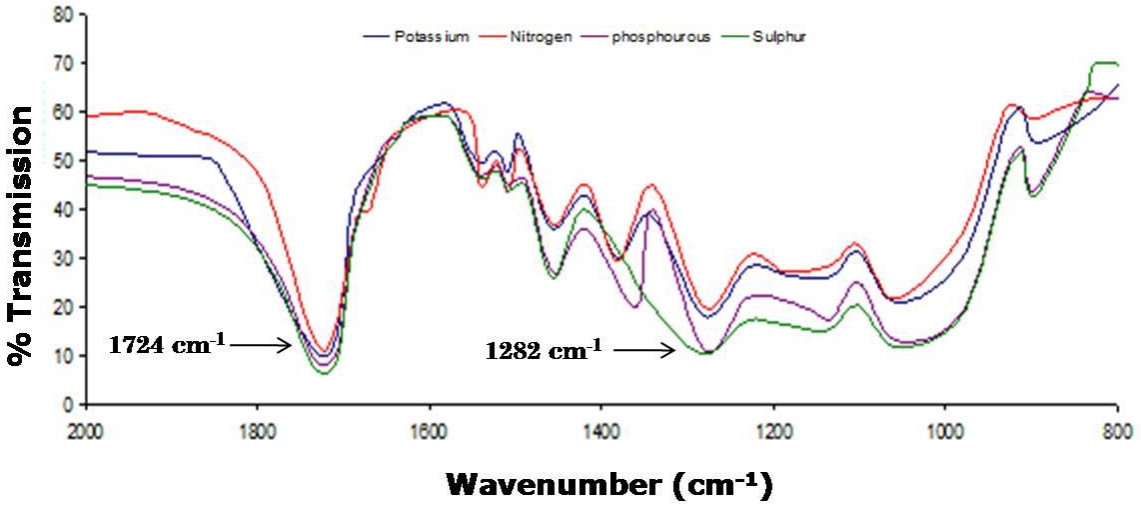

Figure 3.2: Combined FTIR spectra of the PHAs produced from different nutrient limiting conditions. Absorption bands at 1724 cm^{-1}, corresponds to the ester carbonyl group and at 1281 cm^{-1} to the –CH group, characteristics of scl-PHAs.

The actual monomeric characterisation of the polymer was done using GCMS. **Figure 3.3(A)** shows the total ion current chromatogram (TIC) for the methanolysis products of the isolated PHA with methyl benzoate added as an internal standard. Mass spectra analysis, showed that the peak with a retention time (R_t) of 6.81 minutes had an excellent similarity with the mass spectrum of methyl-3-hydroxybutyrate in the MS library as shown in **Figure 3.3(B)**. (The MS library used is from the National Institute of Science and Technology, NIST). Study on the fragmentation pattern for 3HB showed that the peak at m/z, 45.1 represented the hydroxyl end of the molecule which occurred due to the cleavage of the bond between C_3 and C_4. The peak at m/z

74.1 represented the carbonyl end of the molecule which also originated due to the cleavage between C_3 and C_4 following McLafferty rearrangement which involves γ-hydrogen rearrangement with a ß-cleavage reaction (McLafferty, 1956). Since only the methyl ester of hydroxybutyric acid was observed, it was concluded that a homopolymer of poly-3-hydroxybutyrate, P(3HB) was produced under this growth condition, the structure of the methyl ester of 3-hydroxybutyric acid is shown in **Figure 3.4**.

(A)

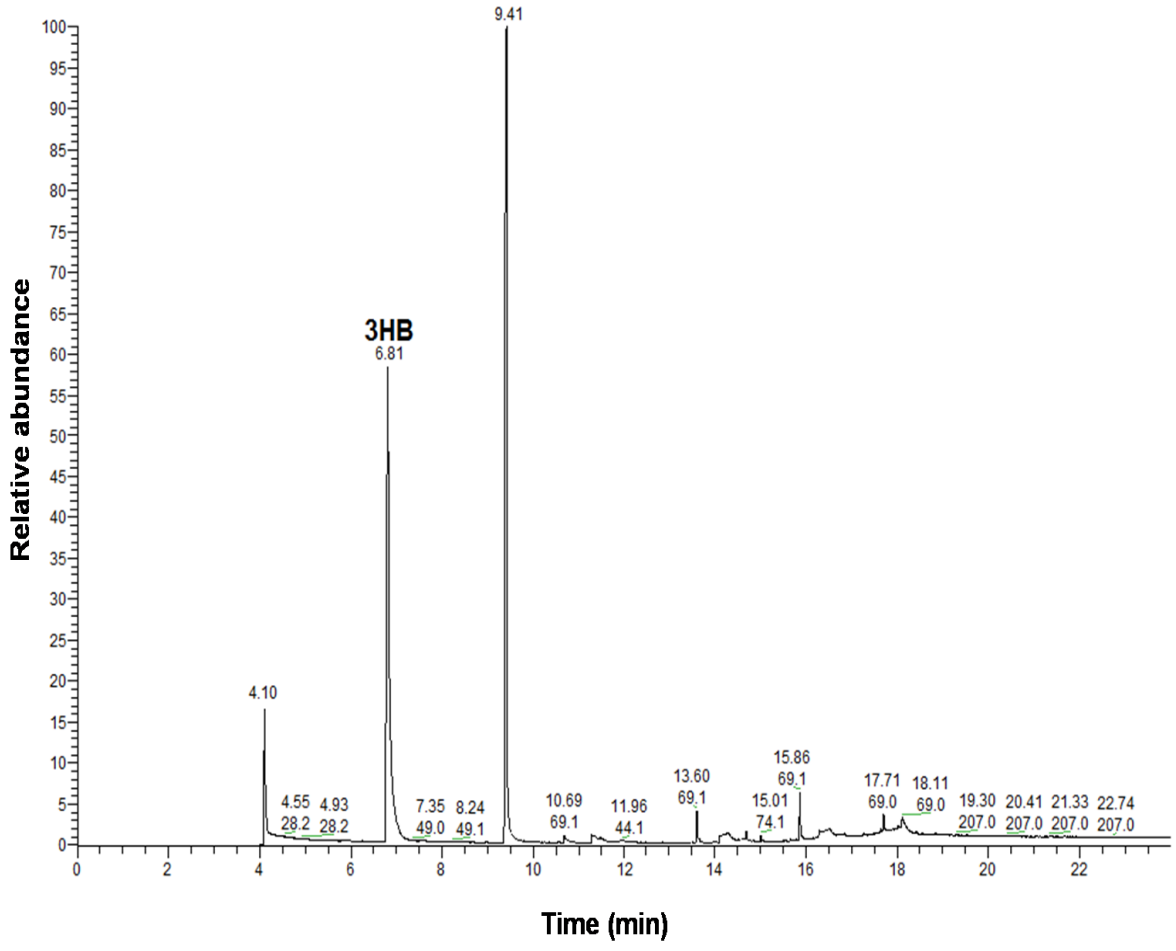

(B)

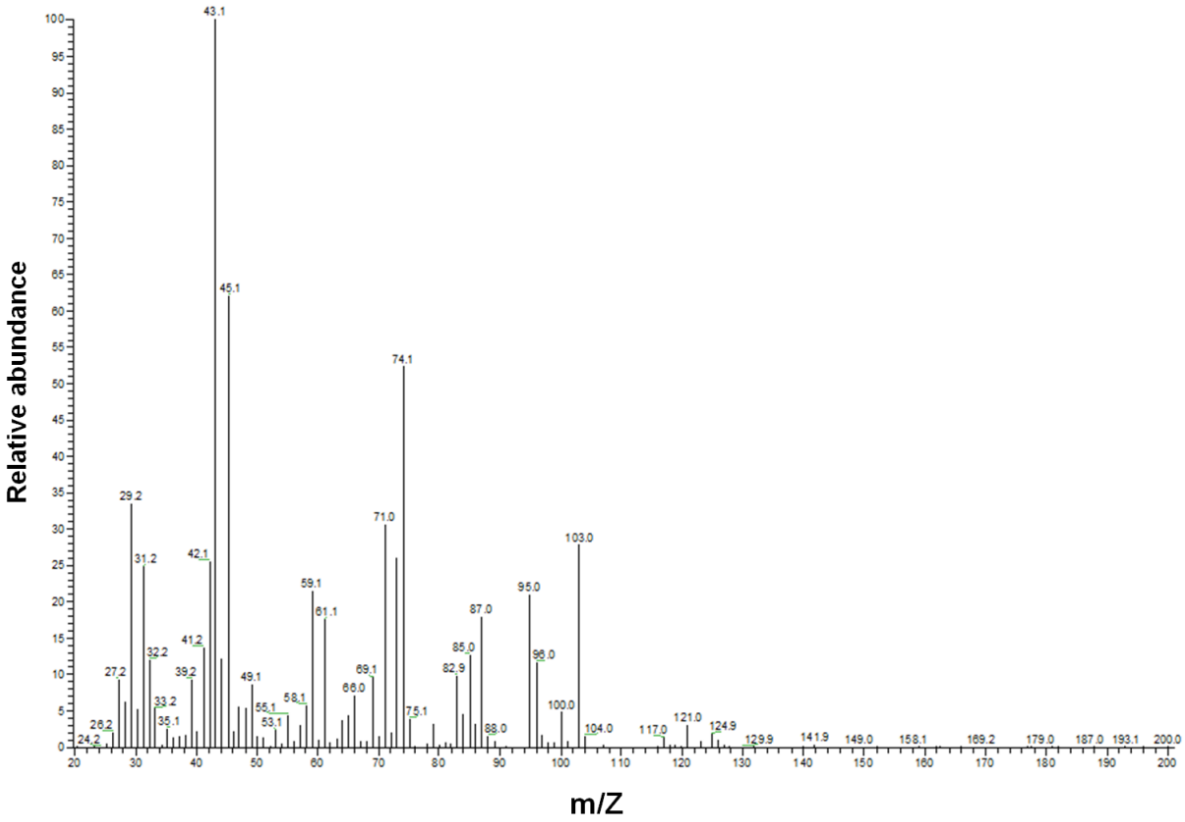

Figure 3.3: GC-MS analysis of the polymer produced when *B. cereus* SPV was grown under nitrogen limitation: (A) Total ion chromatogram for the methanolysis products of the PHA produced under this condition with methyl benzoate added as an internal standard). (B) Mass spectra of the monomer methyl-3-hydroxybutyric acid

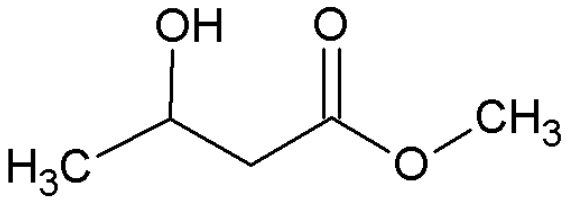

Figure 3.4: Structure of the methyl ester of 3-hydroxybutyric acid.

3.2.2. PHA production under potassium limitation

To study the effect of potassium limitation on the accumulation of PHA by *B. cereus* SPV, the organism was grown in the medium which was used by Wakisaka *et al.* (1982) to study PHA production in *B. thuringiensis*. Good growth was observed until 48 hrs (1.71g dcw/L), however, there was a sharp decrease in growth after 72 hrs (0.86g dcw/L). Surprisingly, the growth increased again and by the end of the fermentation the dry cell weight had increased to 1 g dcw/L (**Table 3.1, Figure 3.5**). The PHA yield increased up to a maximum of 13.4 % dcw at 48 hrs after which it decreased to 1 % dcw at 96 hrs. The polymer accumulation at 120 hrs could not be determined because of the low yield. The pH of the culture medium decreased as fermentation progressed from an initial value of 7 to 4.6 by 120 hrs i.e. the end of the fermentation.

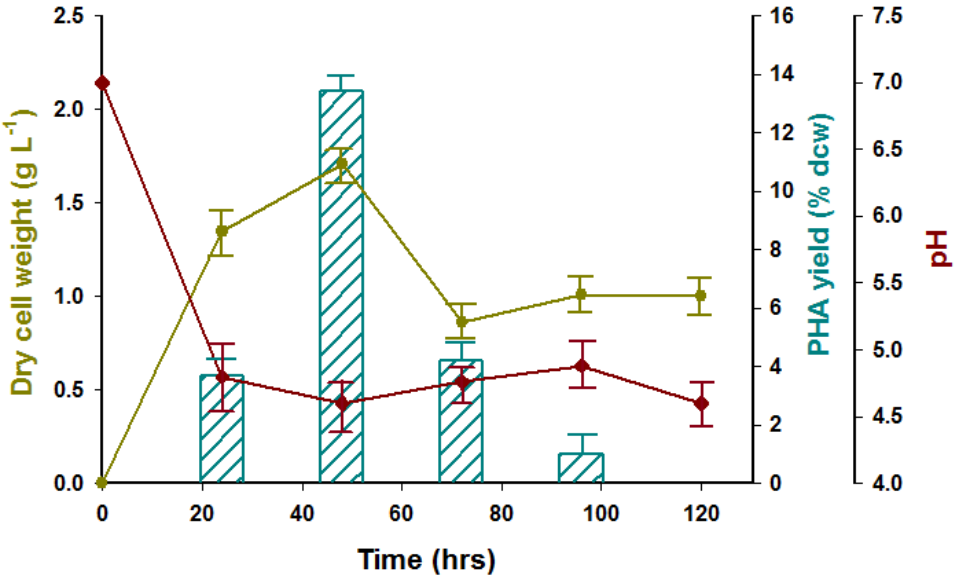

Figure 3.5: **Fermentation profile for P(3HB-co-3HV) production from *B. cereus* SPV in potassium limiting condition. [Dry cell weight (●), pH of the medium (♦), PHA yield (▨)]**

Preliminary analysis of the polymer was done using FTIR. The FTIR spectra showed the presence of the signature bands of scl-PHAs at 1724cm^{-1}, (ester carbonyl group) and 1281 cm^{-1} (-CH group) (Hong *et al.,* 1999) (**Figure 3.2**). The structural confirmation of the PHA monomers was done using GC-MS. GC-MS revealed that this growth condition led to the production of a copolymer containing 3HB and 3-hydroxyvalerate, 3HV. 3HB constituted 90 mol % of the polymer and 3HV made up to 10 mol %. **Figure 3.6 (A)** shows the total ion current chromatogram (TIC) for the methanolysis products of the isolated PHA with methyl benzoate added as an internal standard. Peaks at retention time (R_t) 6.94 and 8.09 minutes were identified as methyl-3-hydroxybutyrate and methyl-3-hydroxyvalerate. The fragmentation pattern of 3HB is the same as that seen for 3HB produced under nitrogen limitation, **Figure 3.6(B)**. The fragmentation pattern for 3HV showed that the peak at m/z 74 originated from the carbonyl end of the molecule due to McLafferty rearrangement (McLafferty, 1956). The peak at m/z 59.1 represented the hydroxyl end of the molecule which occurred due to the cleavage at bonds between C_3 and C_4 (**Figure 3.5(C**). **Figure 3.7** shows the structures of the methyl esters of these scl-PHA monomers.

(A)

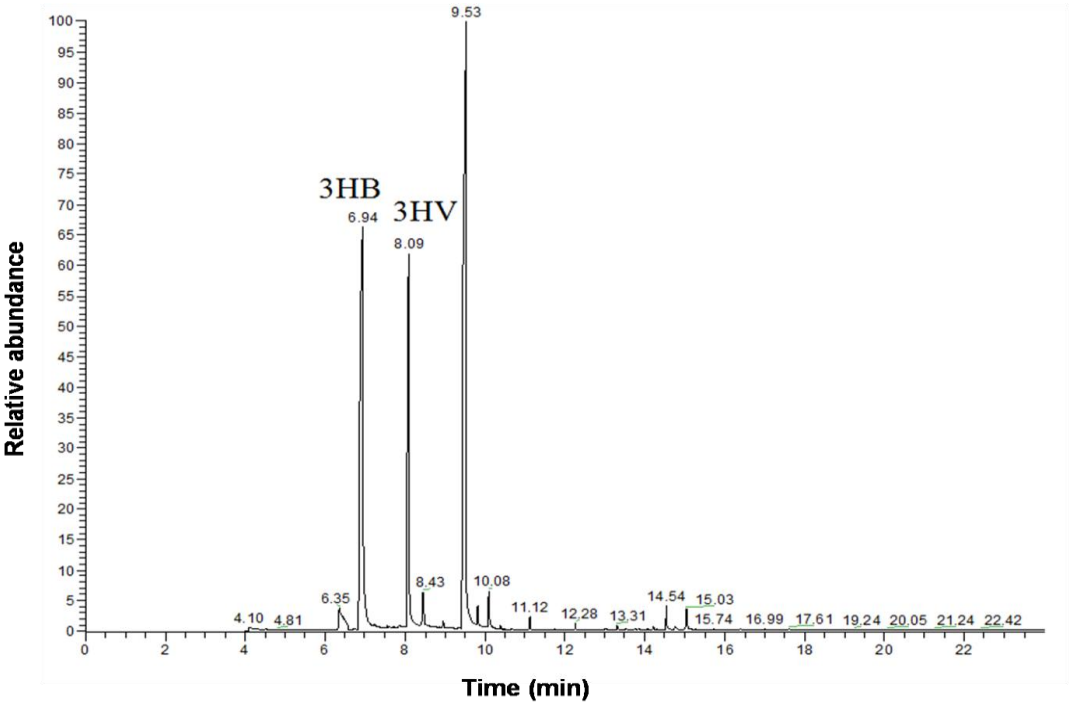
3HB
3HV
6.94
8.09
9.53
Relative abundance
Time (min)

(B)

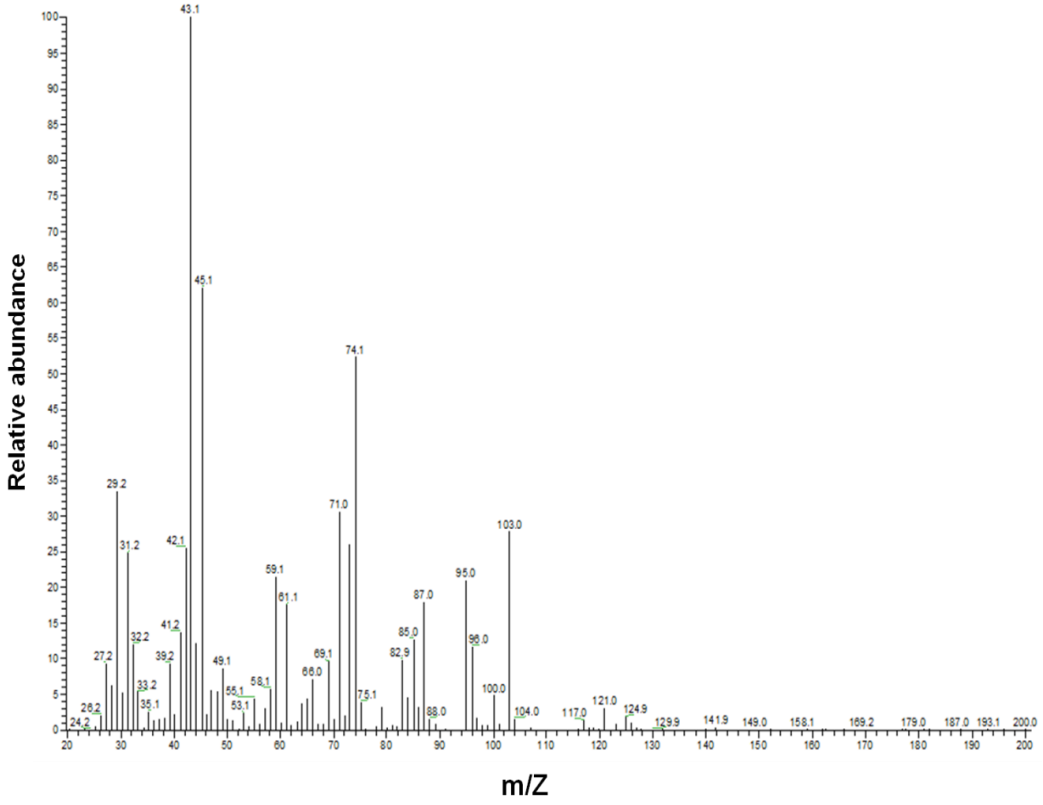
Relative abundance
m/Z

(C)

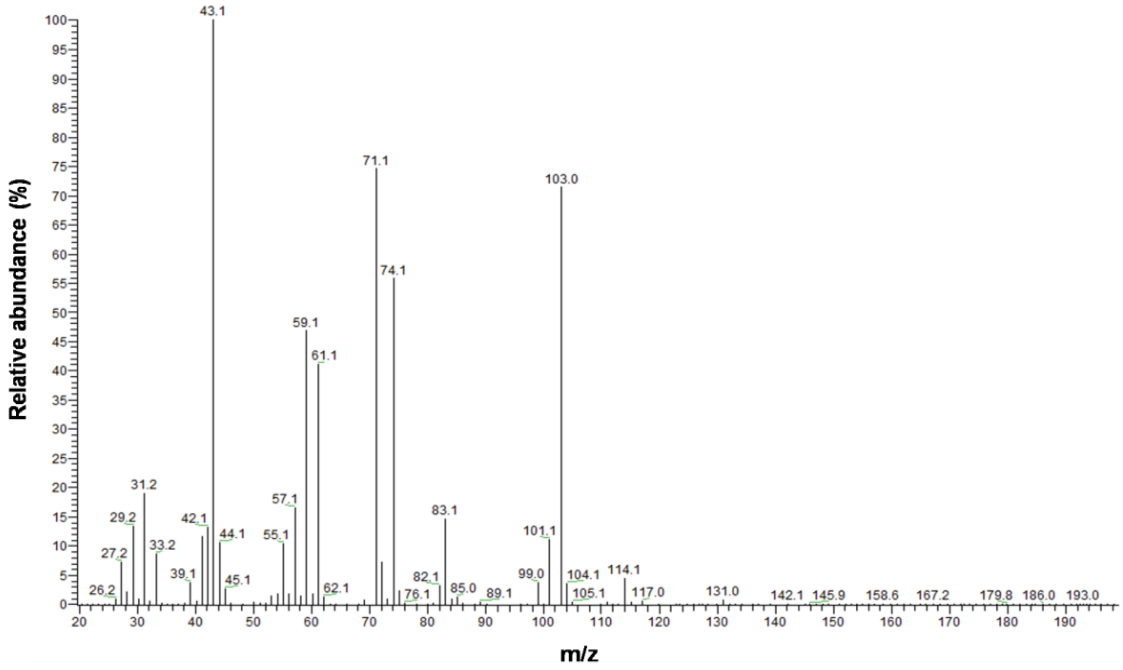

Figure 3.6: GC-MS of the polymer produced when *B. cereus* SPV was grown under potassium limitation: (A) Total ion chromatogram of the methanolysis products of the PHA isolated under this condition condition with methyl benzoate added as an internal standard. Mass spectra of the monomers (B) methyl-3-hydroxybutyric acid and (C) methyl-3-hydroxyvaleric acid produced.

(A) **(B)**

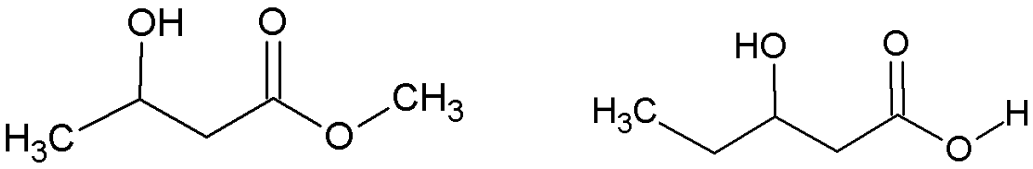

Figure 3.7: Structure of the methyl ester of (A) 3-hydroxybutyric acid and (B) methyl- 3-hydroxyvaleric acid

3.2.3. PHA production under sulphur limitation

PHA accumulation in *Bacillus cereus* SPV was also studied in a sulphur limiting medium. Here too, maximum cell growth was exhibited by the

organism at 48 hrs (1.73 g/L) (**Table 3.1**). The growth of the organism then decreased as reflected by decreasing dry cell weights (**Table 3.1, Figure 3.8**). The maximum PHA yield achieved was 13.15 % dcw at 48 hrs after which it decreased to 1.29 % dcw by 72 hrs. PHA production at 96 and 120 hrs was so low that the yield could not be determined. A decreasing pH of the medium was observed similar to that under nitrogen and potassium limiting conditions.

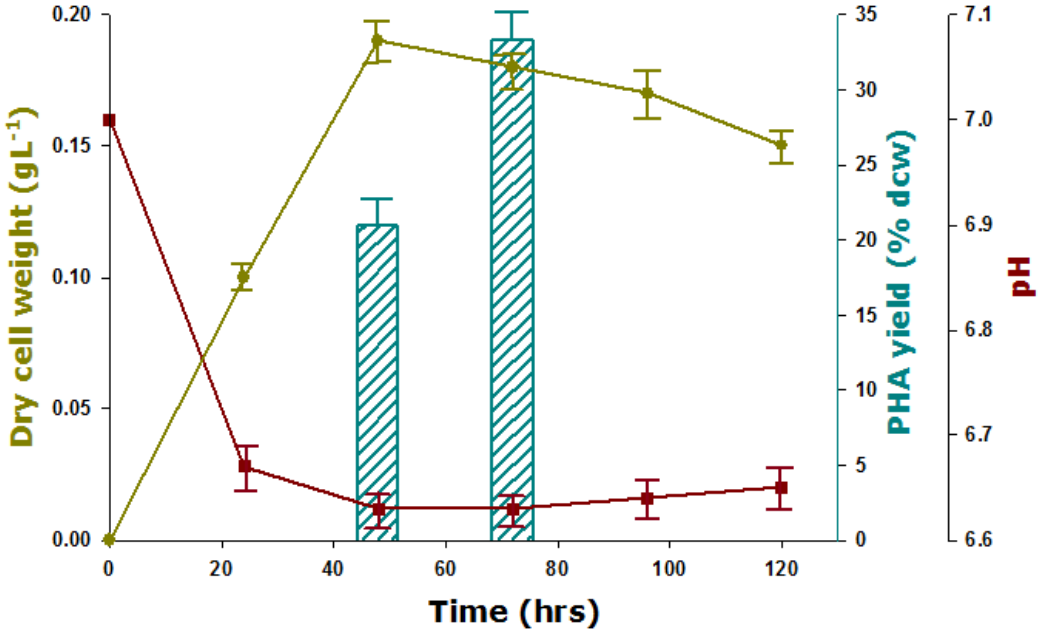

Figure 3.8: Fermentation profile for P(3HB) production from *B. cereus* SPV in sulphur limiting condition. [Dry cell weight (●), pH of the medium (♦), PHA yield (▨)]

Preliminary FTIR analysis of the polymer confirmed that it was an scl-PHA due to the presence of the scl signature bands of 1724cm^{-1}, (ester carbonyl group) and 1281 cm^{-1} (-CH group) (**Figure 3.2**). GCMS revealed that under sulphur limitation the organism accumulated P(3HB) inclusions. **Figure 3.9(A)** shows the total ion current chromatogram (TIC) for the methanolysis products of the isolated PHA under this condition. The fragmentation pattern

of methyl-3-hydroxybutyrate (R_t 6.81) showed excellent similarity to the corresponding standard mass spectra of 3-hydroxybutyric acid in the MS (NIST) library and to the fragmentation pattern observed for P(3HB) produced under nitrogen and potassium limitation (**Figure 3.9B**). The structure methyl-3-hydroxybutyrate is shown in **Figure 3.2**.

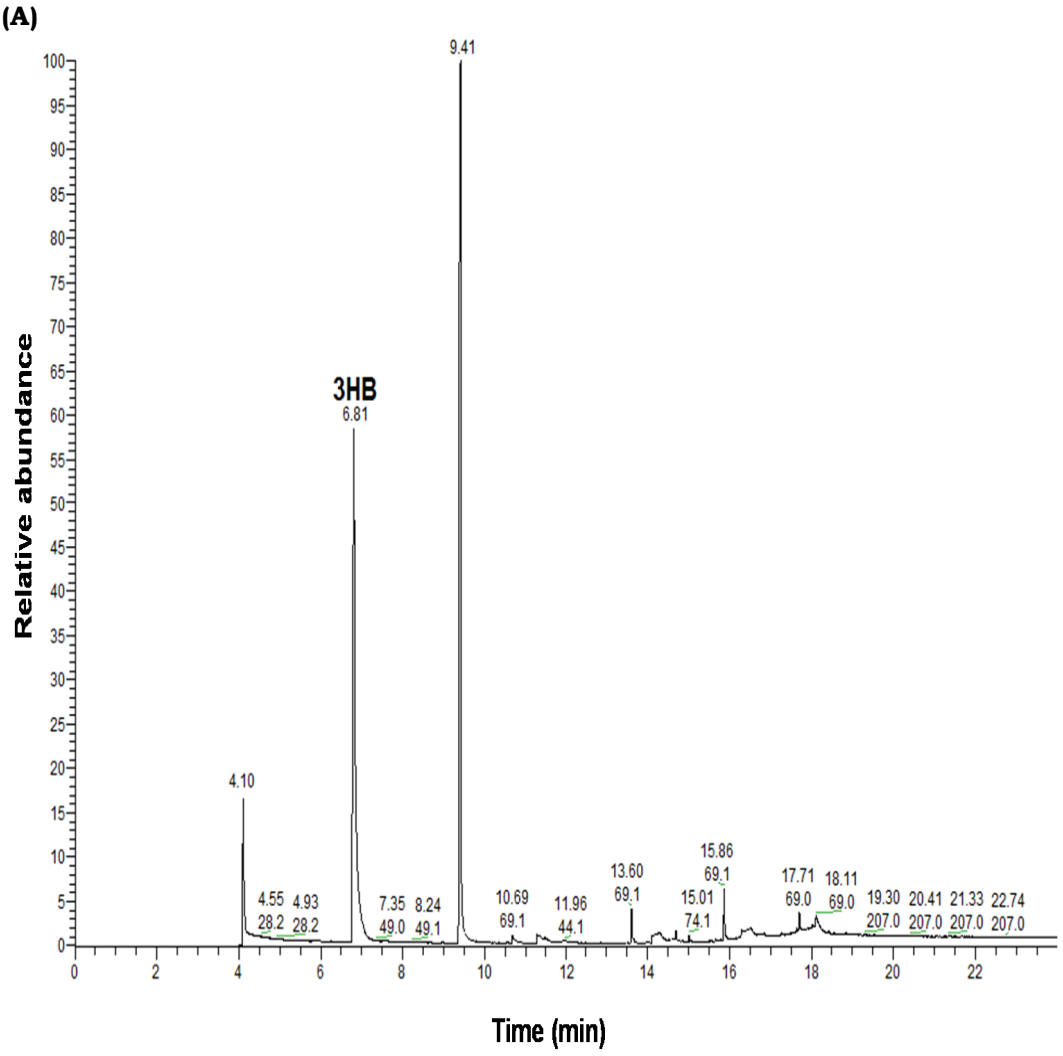

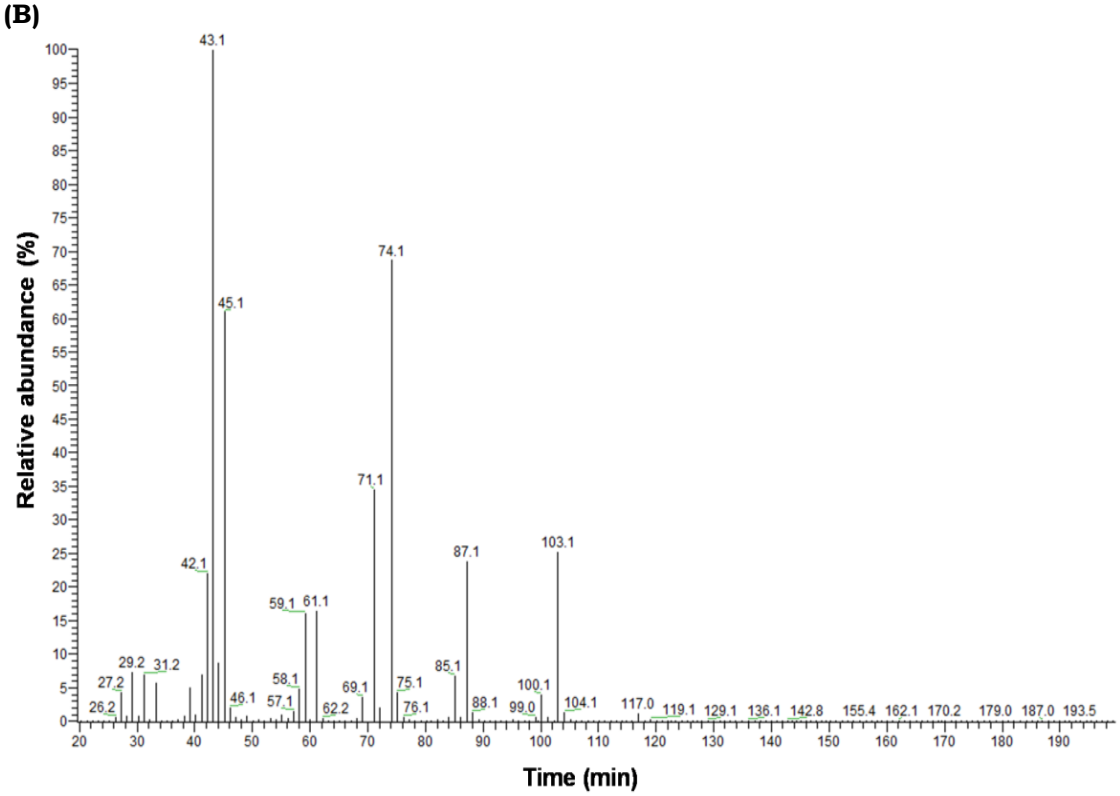

Figure 3.9: GC-MS analysis of the polymer produced when *B. cereus* SPV was grown under sulphur limitation: (A) Total ion chromatogram for the methanolysis products of the PHA produced under this condition with methyl benzoate added as an internal standard. (B) Mass spectra of the monomer methyl-3-hydroxybutyric acid produced under sulphur limiting condition.

3.2.4. PHA production under phosphate limitation

Bacillus cereus SPV when grown in the phosphate deficient medium, showed poor growth in the medium compared to the other nutrient limiting conditions with a maximum dry cell weight of 0.19 g/L achieved after 48 hrs (**Table 3.1: Figure 3.10**). However, a maximum P(3HB) yield was observed at 72 hrs (33.33 % dcw). This observation is consistent with a previous study where P(3HB) production was found to increase in the late stationary phase in *Azotobacter vinelandii* UWD, under phosphate limitation (Page and Knosp, 1989).

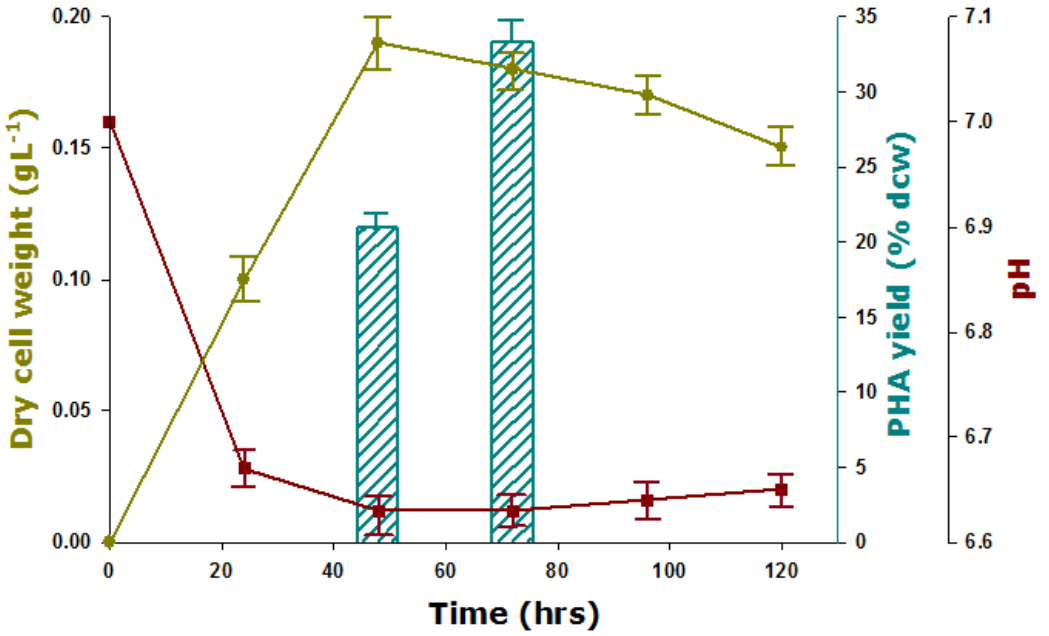

Figure 3.10: Fermentation profile for P(3HB) production from *B. cereus* SPV in phosphate limiting conditions in the shaken flask. [Dry cell weight (●), pH of the medium (♦), PHA yield (▨)]

Preliminary FTIR analysis confirmed the presence of the signature bands of scl-PHAs in the FTIR spectrum of the polymer as shown in **Figure 3.2**. **Figure 3.11(A)** shows the total ion current chromatogram for the polymer and the mass spectrum of the peak at R_t 6.87, showing excellent similarity to the mass spectra for methyl-3-hydroxybutyrate in the MS (NIST) library. Here too, similar fragmentation pattern was seen as that observed for the P(3HB) produced under the previous nutrient limiting conditions.

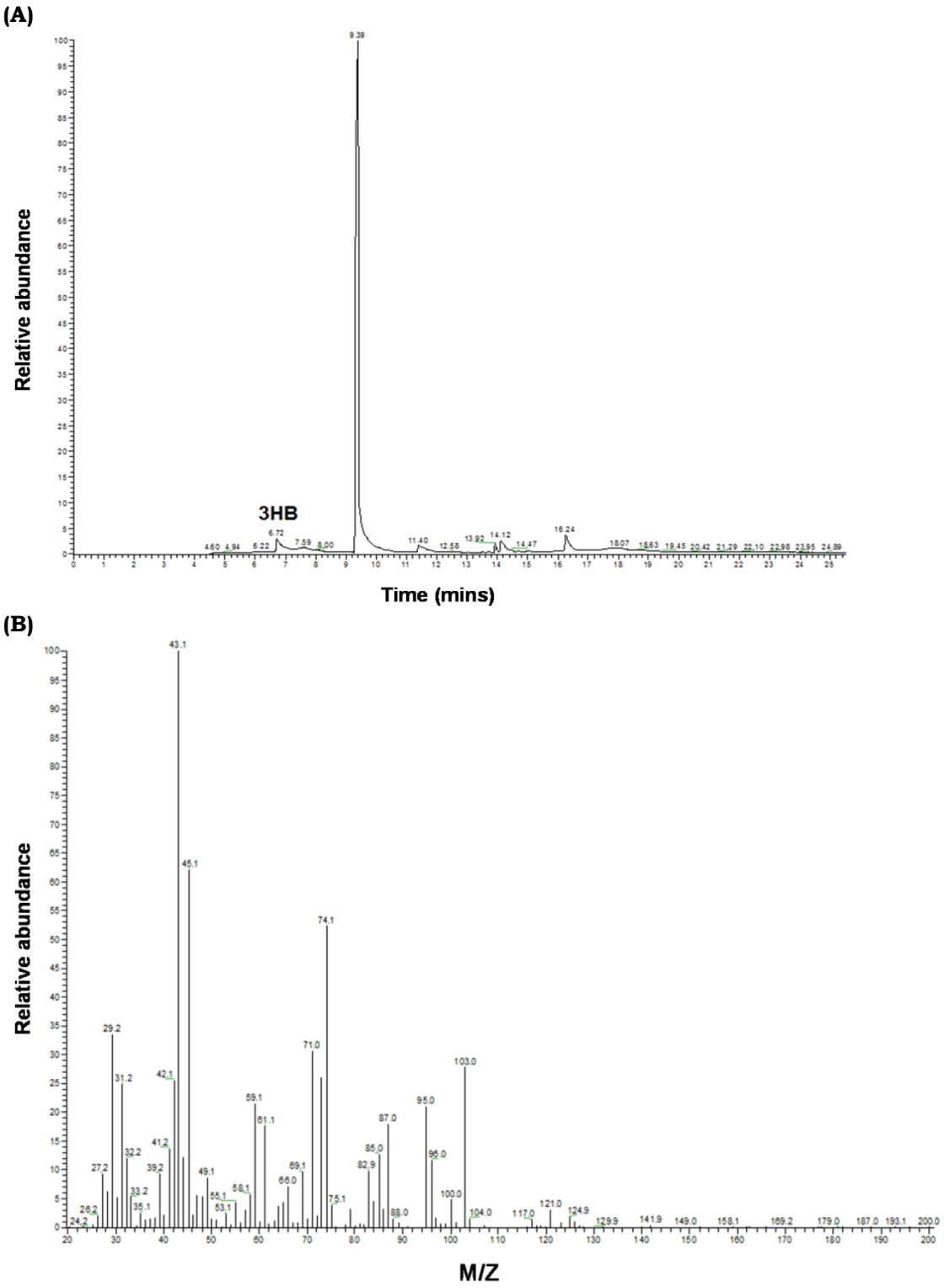

Figure 3.11: GC-MS analysis of the polymer produced when *B. cereus* SPV was grown under phosphate limitation: (A) The total ion chromatogram for the methanolysis products of the isolated PHA produced under this condition with methyl benzoate added as an internal standard. (B) Mass spectra of the methyl ester of 3-hydroxybutyric acid, the monomer produced under this limiting condition.

3.3. Discussion

In this study the effect of a single nutrient limitation such as nitrogen, potassium, sulphur, and phosphate, on the accumulation of PHAs by *B. cereus* SPV was studied for the first time. The organism was grown in different nutrient limiting media with glucose (20 g/L) as the carbon source in all the studies. The organism accumulated mainly P(3HB) in all the limiting conditions with the exception of P(3HB-co-3HV) in the potassium limiting condition.

An earlier study of P(3HB) production by *Bacillus cereus* SPV under nitrogen limiting conditions showed that low pH conditions of the culture during maximal P(3HB) production resulted in a complete lack of P(3HB) degradation (Valappil *et al.,* 2006). Hence, the P(3HB) produced was not degraded in order to be utilized for sporulation in contrast to the previous report (Wu *et al.,* 2001). Low pH conditions have been found to inhibit utilization of the polymer as well as spore formation in *Bacillus cereus* SPV (Valappil *et al.,* 2007). This observation could be the turning point of the utilization of *Bacillus* sp. for the production of PHAs. A similar observation was made in all other nutrient limiting conditions used in this study except for phosphate limitation where lack of low pH conditions might have caused degradation of the P(3HB). In this work the initial pH of the different nutrient limiting media used was maintained at 7.0. With the progression of the culture the pH of the culture was found to become quite acidic (~ 5.0), hence preventing PHA degradation. The acid resistance of *Bacillus cereus* is known to be dependent on its growth phase i.e., the log phase cells are more sensitive to acid stress and then become increasingly resistant as the culture enters stationary phase (Browne and Dowds, 2002). Hence, the intial pH of the culture media facilitated good log phase growth of *B.cereus* SPV, which then became acidic to further improve the yield of PHA by inhibiting potential

degradation of the already accumulated PHA. This prevention of PHA degradation by low culture pH in *B. cereus* SPV was confirmed by the studies carried out by Philip *et al*. (2009). P(3HB) degradation leads the formation of 3-hydroxybutyric acid and therefore, due to the law of mass action, under low pH conditions the degradation of the polymer is inhibited. A similar finding was made by Kominek and Halvorson in 1965. They found that polymer degradation and spore formation were inhibited in *Bacillus cereus* T by a low pH environment (Kominek and Halvorson, 1965).

Wakisaga *et al*. (1982) found that the potassium deficient medium was not only good to depress sporulation of *B. cereus* IFO 3466 but also useful in improving P(3HB) granule accumulation in two asporogenous mutants, *B. thuringiensis* subsp. kurstaki strain B-43-D-e and *B. thuringiensis* subsp. aizawai strain B-106-4-4 (Wakisaga *et al.,* 1982). In another study, potassium sulphate was found to be the limiting nutrient leading to PHA formation in *Bacillus thuringiensis* (Kim and Lenz, 2001). In the present study by limiting potassium we obtained maximum cellular growth (1.71 g/L) and PHA accumulation (13.4 % dcw) by 48 hrs. The production of P(3HB-co-3HV) copolymer under the potassium limiting condition, using glucose as the carbon source is a significant finding. The production of such copolymers using structurally unrelated carbon sources will allow industrial production of these copolymers using cheap carbon sources. Reddy *et al. (*2009) also observed the production of P(3HB-co-3HV) by *Bacillus* sp. 88D using glucose and glycerol as carbon feed. However, they had used E medium for the study which is a nitrogen limiting medium. These observations confirm that PHA production is dependent on the organism used, the culture conditions and the carbon feed used (Reddy *et al.*, 2009).

Wakisaga *et al.* (1982) also observed that phosphate ions at a concentration greater than 120 μg/mL was found to stimulate P(3HB) production in the

Bacillus strain 290-1 (polymer yield not quoted). In the present study however, phosphate was limiting, cell growth was found to be very low (0.18 g/L) although the P(3HB) yield was better (33.33 % dcw) compared to potassium (13.4 % dcw) or sulphur (13.15 % dcw) limitation. This result was consistent with the previous results obtained by Wu *et al. (*2001) where a P(3HB) yield of 30 % dcw was obtained under phosphate limiting conditions. Also, in this study, growth in the phosphate deficient medium did not lead to an acidic pH during stationary phase. Hence, PHA degradation was not impaired as in other cases. Hence, maintenance of low pH during the stationary phase, under phosphate limiting conditions, could further increase the PHA yield.

The nitrogen deficient medium used in the study was by far the best medium in terms of both the cellular growth (2 g/L) and PHA accumulation (38 % dcw) (Table 3.1). Based on the results obtained in the present study, although nitrogen, sulphur and phosphate deficient media are preferred for P(3HB) production potassium limitation need to be considered for the production of the PHA copolymer with 3HB and 3HV monomers.

Chapter 4: Production and Characterisation of Medium Chain Length, mcl-PHAs

4.1. Introduction

Medium chain length polyhydroxyalkanoates, mcl-PHAs were first discovered in 1983 when *P. oleovorans* was grown in octane (de Smet *et al.*, 1983). Since then *Pseudomonas* sp. belonging to the rRNA homology group I, have been mainly used for its production. Mcl-PHAs are characterised by the presence of 6 to 14 carbon atoms in their carbon backbone. The organisms accumulate these mcl-PHA inclusions by polymerising precursor substrates produced via the fatty acid β-oxidation and fatty acid synthesis pathway. The organisms are able to do so when subjected to different nutrient(s) limiting conditions, in the presence of excess carbon source. The PHA synthase present in these organisms are able to polymerise wide ranging substrates for mcl-PHA production, hence diverse range of mcl PHAs are known; in fact till date more than 150 different types of mcl monomers have been reported. Once extracted, these mcl PHAs exhibit flexible elastomeric properties unlike the short chain length, scl-PHAs that are brittle and stiff. Hence, mcl-PHAs are being studied for a number of industrial, agricultural and medical applications where more flexible polymers are required (Zinn *et al.*, 2001; Chen and Qiong, 2005).

This chapter reports the work that was carried out with an objective of biosynthesizing mcl-PHAs using different *Pseudomonas* sp. To begin with five different *Pseudomonas* sp. were studied for mcl-PHA production. The organisms studied were *P. aeruginosa*, *P. putida* , *P. fluorescens*, *P. oleovorans* and *P. mendocina.* The organisms were grown in different mcl PHA production media (media compositions described in section 2.3.3). However, after the initial screening of these organisms, *P. mendocina* was mainly focussed on for the production of mcl-PHAs.

P. mendocina is a Gram negative bacteria also belonging to the rRNA homology group I. It was first isolated by N.J. Paleroni from soil and water samples collected from the province of Mendoza, Argentina (Palleroni *et al.*, 1970). Like other *Pseudomonas* sp. it is also able to accumulate mcl-PHAs under nutrient limiting conditions, hence is a "growth limited producer". However, not many studies have been carried out on this organism for PHA production, hence it remains a relatively unexplored organism. Also, in depth studies on the polymers produced by this organism or the use of the polymers as biomaterials for medical applications have not been carried out previously. Therefore, during this research, *P. mendocina* was the main focus for the production of mcl-PHAs. The organism was grown on both structurally related and unrelated carbon sources to explore, if it could accumulate PHAs using both types of carbon feed. The structurally related carbon feed used were fatty acids such as hexanoate, heptanoate, octanoate and nonanoate at 20 mM. The structurally unrelated carbon feed used were carbohydrates such as glucose, sucrose and fructose at 20 g/L.

Downstream processing parameters like the kind of extraction methods used and polymer purification steps employed have an effect on the yield, molecular weight, thermal properties and lipopolysaccharide (LPS) content of the polymer extracted. LPS is a natural component of the Gram negative bacterial cell wall and is a pyrogen. Therefore downstream processing parameters must ensure that the presence of such contaminating LPS in the polymer is mitigated. Solvent extraction of mcl-PHAs have been carried out frequently, also as mcl-PHAs, unlike scl-PHAs, are soluble in a wider range of solvents therefore cheaper and less toxic solvents may be used. Studies were therefore carried out using different extraction methodologies employing different solvents, such as: extraction using dispersion of $CHCl_3$ and NaOCl, temperature dependent extraction using hexane, acetone extraction, extraction using soxhlet and $CHCl_3$ extraction (described in section 2.5) to see

their effects on the yield, molecular weight, thermal properties and LPS content of the polymer.

Studies were also carried out to find the optimum conditions for polymer production. These conditions were generated using the partial factorial design as described in section 2.4.1.2.

Therefore, this chapter describes the studies that were carried out with an objective of producing mcl-PHAs from the different *Pseudomonas* sp. assessing the effects of downstream processing on the polymer extraction and finding optimum conditions for polymer production.

4.2. Results

4.2.1. Selection of mcl-PHA production media

The particular PHA produced depends on the organism used, the culture conditions and the carbon sources provided (Haywood *et al.*, 1990; Timm and Steinbuchel, 1990; Jendrossek *et al.*, 1995). Also, it is essential that the PHA production medium, in addition to stimulating PHA production should also support the organism's growth since PHA is an intracellular product. Initial studies were therefore carried out to select appropriate PHA production media that would support the growth of the organisms as well accumulation of PHA inclusions. *P. putida* and *P. aeruginosa* grew in the E2 medium and ME2 medium but *P. putida* produced the polymers only in the E2 medium and *P. aeruginosa* in the ME2 medium; In E medium however, *P. putida* and *P. aeruginosa* did not grow at all. *P. oleovorans* grew and produced polymers in both E and E2 media, but higher yield was obtained in E2 medium. *P. fluorescencs* was not able to produce polymer when grown in either fatty acids or glucose using E, E2 and ME2 media. *P. mendocina* grew and

produced polymers using both the structurally related and unrelated carbon sources in MSM medium.

4.2.2. Screening of *Pseudomonas* sp. for mcl-PHA Production

Studies were carried out to obtain the production of mcl-PHAs from *P. putida* and *P. aeruginosa*, using both structurally related and unrelated carbon sources. When grown on a structurally related carbon source, octanoate, both *P. putida* and *P. aeruginosa* were able to produce the polymer. *P. putida* accumulated polymer to a maximum of 11.60 % dcw in 48 hrs. *P. aeruginosa* on the other hand accumulated polymer to a maximum of 11.40 % dcw in 48 hrs **(Table 4.1)**. When hexanoate was used as a carbon source, it did not support the growth of *P. putida; P. aeruginosa* grew using hexanoate as a carbon source but no polymer was produced. When grown on structurally unrelated carbon sources such as glucose, fructose and glycerol, both *P. putida* and *P. aeruginosa* grew well but no polymer production was observed.

Characterisation of the polymer accumulated by these organisms was done using GC-MS and NMR as described in section 2.9.1. Interestingly *P. aeruginosa* accumulated a copolymer containing 3-hydroxyoctanoate, (3HO) and 2-hydroxydodecanoate (2HDD) as revealed by GC-MS. 3HO constituted 60 mol % of the polymer and 2HDD constituted 40 mol %. **Figure 4.1** shows the total ion current chromatogram (TIC) for the methanolysis products of the isolated PHA. 3HO had a retention time (R_t) of 10.51 minutes, molecular weight, M_w = 174 and 2HDD had retention time of 13.01 minutes and its M_w = 230. The internal standard used was methyl benzoate which had a R_t of 9.2 minutes. The fragmentation pattern of 3HO, **Figure 4.1(B)**, showed the m/z peak at 74.1. This peak originates from the carbonyl end of the molecule due

to the cleavage between C_3 and C_4 carbon atoms following McLafferty rearrangement (McLafferty, 1956). The peak at m/z 103.1 represented the hydroxyl end of the molecule which occurred due to the cleavage at bonds between C_3 and C_4; the alkyl end of this cleavage resulted in the peak at m/z 71.1. The peak at m/z 43.2 occurred due to the alkyl end of the molecule following the cleavage between C_5 and C_6 carbon atoms. The fragmentation pattern for 2HDD, **Figure 4.1(C)**, showed the m/z peak at 90.1 which originated from the carbonyl end of the molecule. This was due to the cleavage between C_2 and C_3 carbon atoms following McLafferty rearrangement. The peaks at m/z 43.2 occurred due to the alkyl end of the molecule following cleavage between C_9 and C_{10} carbon atoms. Structures of these mcl-PHA monomers are given in **Figure 4.2**.

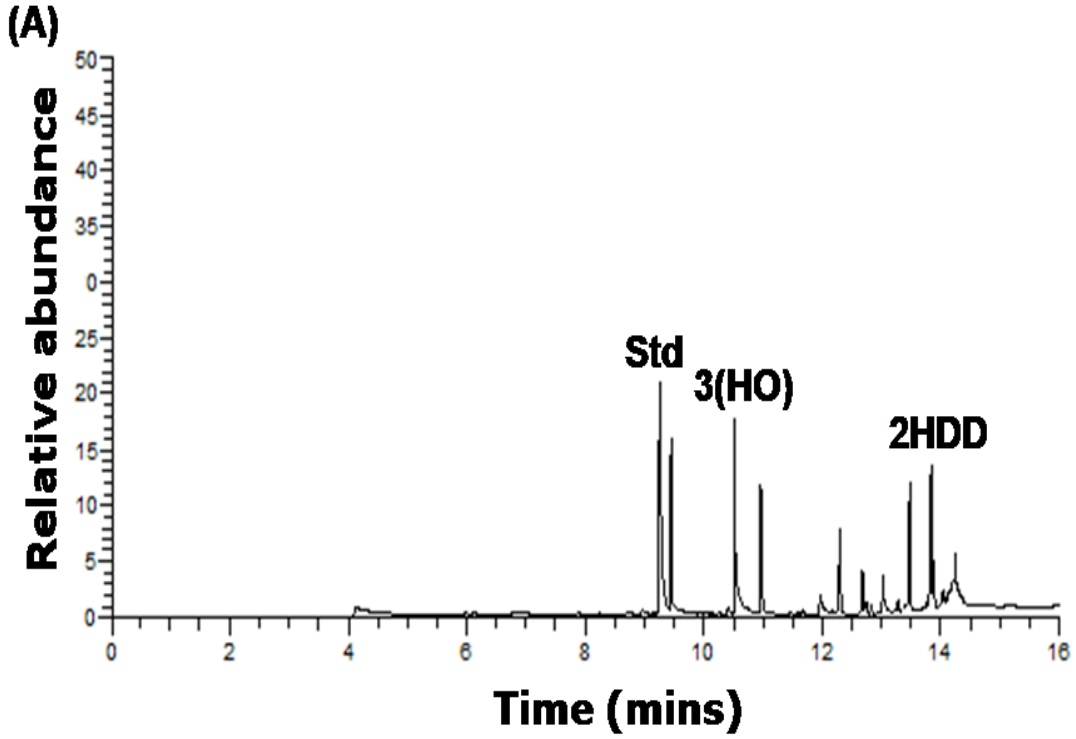

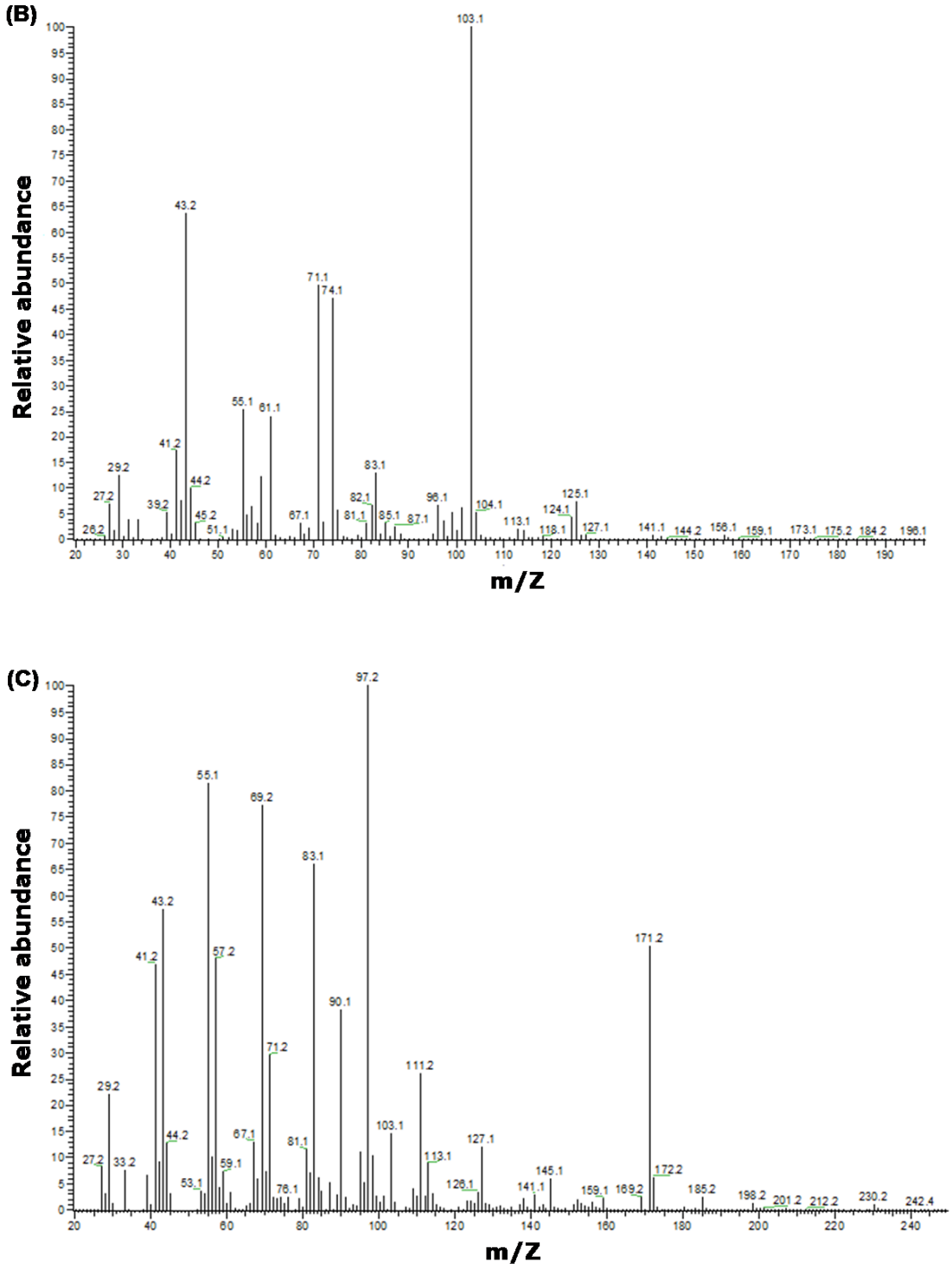

Figure 4.1: GC-MS analysis of the polymer produced when *P. aeruginosa* was grown in octanoate in ME2 medium: (A) Total ion chromatogram for the methanolysis products of the polymer produced under this condition.(B) Mass spectra of the monomer methyl ester of 3-hydroxyoctanoic acid and (C) methyl ester of 2-hydroxydodecanoic acid.

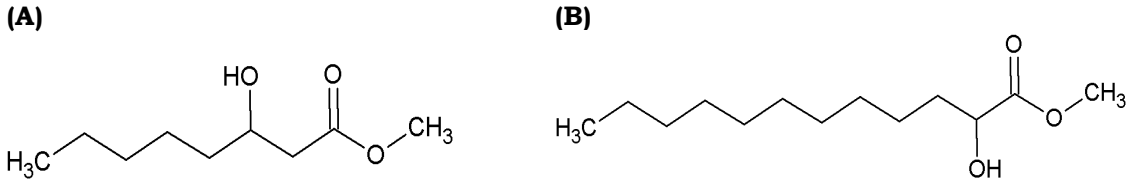

Figure 4.2: Structure of (A) Methyl-3-hydroxyoctanoic acid and (B) Methyl-2-hydroxydodecanoic acid.

^{1}H NMR analyses of these PHAs were also carried out. The ^{1}H-NMR spectrum with the assignment of the corresponding PHAs is shown in **Figure 4.3**. The assignment of the polymer type obtained using GC-MS was further confirmed. In the ^{1}H NMR spectrum, five peaks were obtained. This is because there were five different environments for the hydrogens in the P(3HO) molecule. The ^{1}H NMR analysis showed the presence of protons bonded to C_3 (-CH group) at 5.2 ppm, C_2 (-CH_2 group) at 2.5 ppm, C_4 (-CH_2 group) at 1.6 ppm, other (-CH_2 group) at 1.2 ppm, and the end methyl group (CH_3) i.e. C_8 for P(3HO) and C_{12} for P(2HDD) at 0.8 ppm.

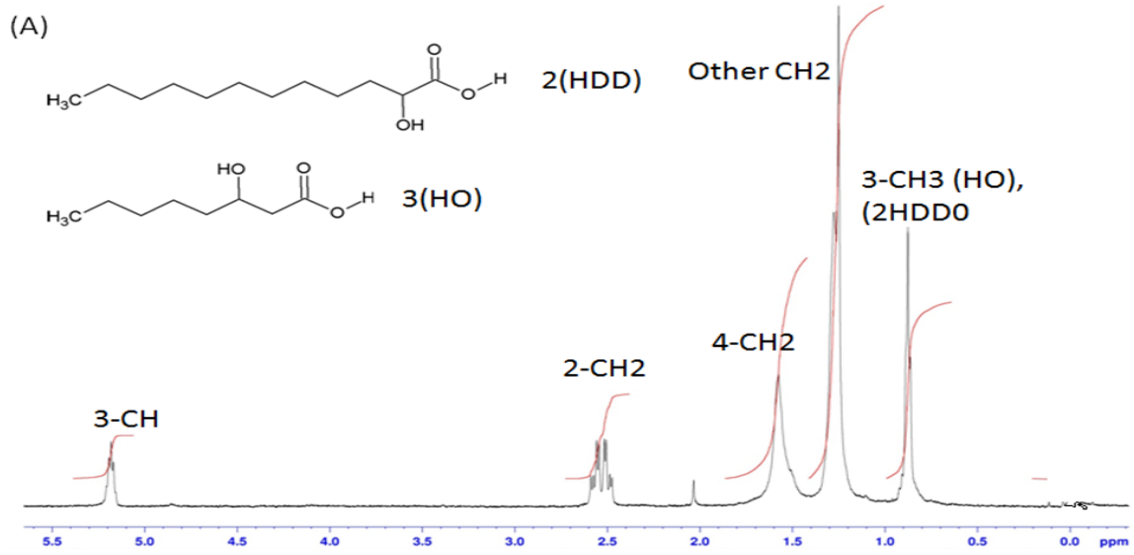

Figure 4.3: ^{1}H NMR spectrum of the polymer produced from *P. aeruginosa* when grown in octanoate.

P. oleovorans was grown on the structurally related carbon source, octanoate, in order to assess the accumulation of mcl-PHA using E and E2 media. The organism showed good growth until 24 hrs. 2.4g dcw/L was obtained in E2 medium and 1.7g dcw/L was obtained in E medium. By 72 hrs the growth had relatively decreased with the dry cell weight being reduced to 1.30 g dcw/L and 1.50 g dcw/L for E2 and E medium respectively (**Table 1**). The highest yield of PHA achieved was 29.20 % dcw at 29 hrs in the E2 medium as opposed to 15.50 % dcw at 24 hrs in the E medium.

Characterisation of the polymer produced was carried out using GC-MS and NMR (^{1}H and ^{13}C NMR). **Figure 4.4** shows the total ion chromatogram of the polymer accumulated by the organism. The peak at R_t of 10.53 minutes was identified as the methyl ester of 3-hydroxyoctanoic acid. Here again the standard methyl benzoate occurred at 9.2 minutes. The occurrence of peaks due to the fragmentation of the molecular ion was the same as that described for the methyl ester of 3HO produced from *P. aeruginosa,* when grown in octanoate (**Figure 4.1 B**).

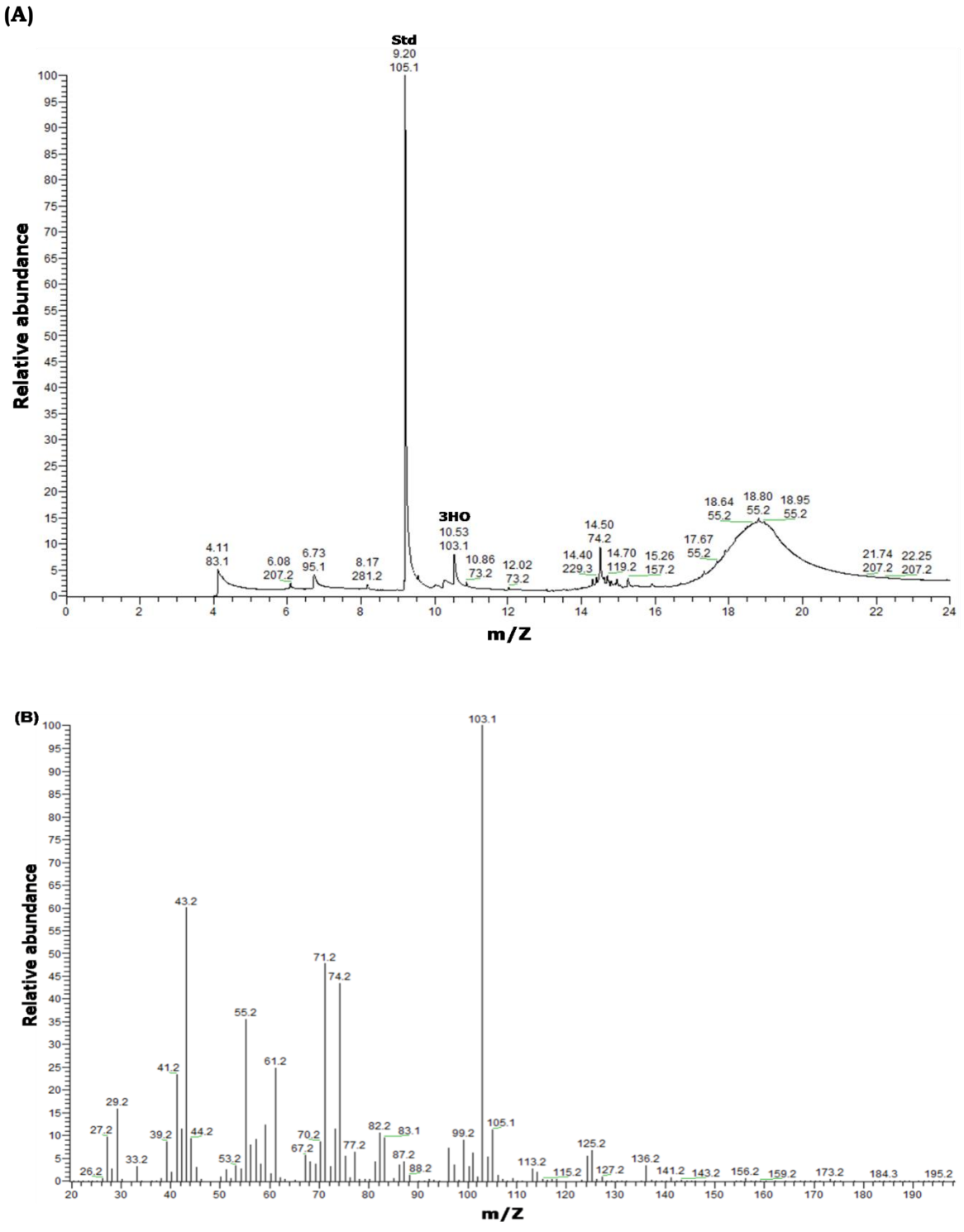

Figure 4.4: GC-MS analysis of the polymer produced when *P. oleovorans* was grown in octanoate: (A) Total ion chromatogram of the methanolysis products of the PHA isolated under this condition: (B) Mass spectra of the methyl ester of the monomer, 3-hydroxyoctanoic acid.

The polymer was also subjected to ^{1}H and ^{13}NMR analysis, the spectra for which are shown in **Figure 4.5**. In the ^{1}H NMR **(Figure 4.5(A))** spectrum, five peaks were obtained. This is because there were five different environments for the hydrogens in P(3HO) molecule. The ^{1}H NMR analysis showed the presence of the peak at 5.2 ppm corresponding to protons bonded to C_3 (-CH group), 2.5 ppm to C_2 (-CH_2 group), 1.6 ppm to C_4 (-CH_2 group), 1.2 ppm to C_5, C_6 and C_7 (-CH_2 groups of 3HO) and C_5(-CH_2 group of 3HHx) and 0.8 ppm to C_8 (-CH_3 of 3HO) and C_6 (CH_3 of 3HHx). In the ^{13}C NMR nine different peaks were obtained corresponding to the nine different environments for the carbon in the molecule. The chemical shift at 169.07 ppm corresponded to the C_1 (C=O group), 70.01 ppm to C_3 (–CH group), 39.07 to C_2 (-CH_2 group), 34 ppm to C_4 (-CH_2 group), 32 ppm to C_5 (-CH_2 group of 3HHx), 30 ppm to C_5 (-CH_2 group of 3HO), 25 ppm to C6 (-CH_2 group of 3HO), 22.5 ppm to C_7 (-CH_2 group of 3HO) and 14 ppm to C_8 (-CH_2 group of 3HO) and C_6 (-CH_2 group of 3HHx). Thus the monomers present in the polymer were 3HHx and 3HO.

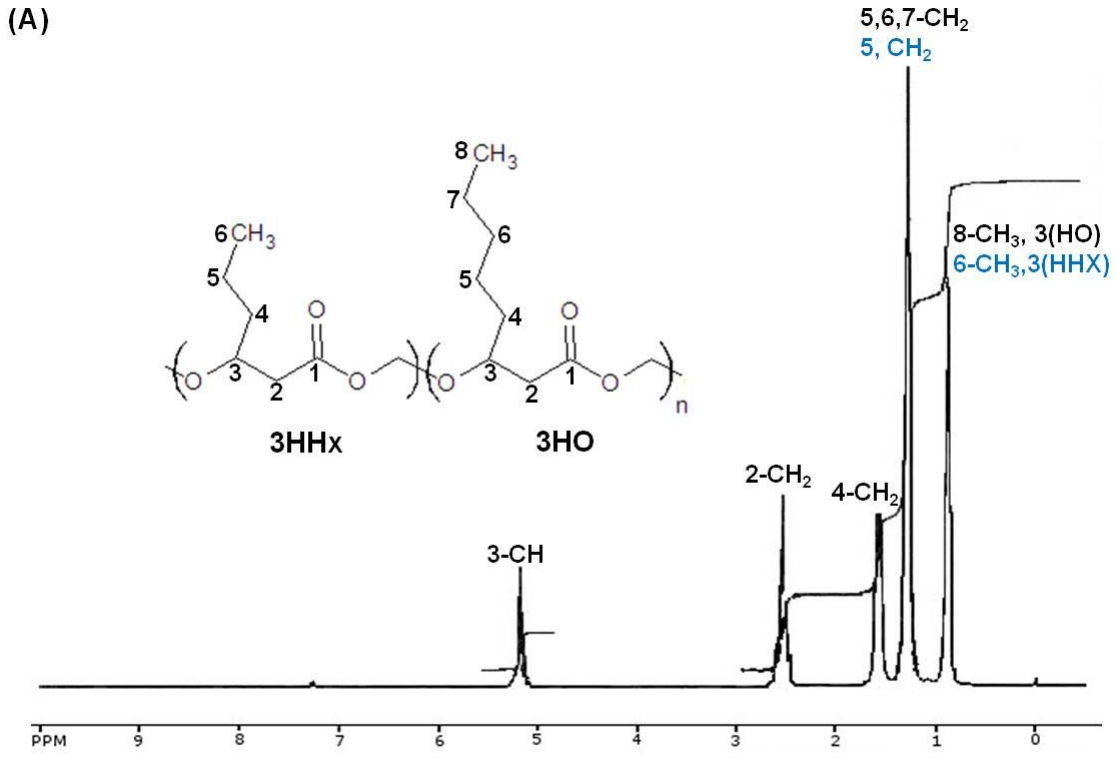

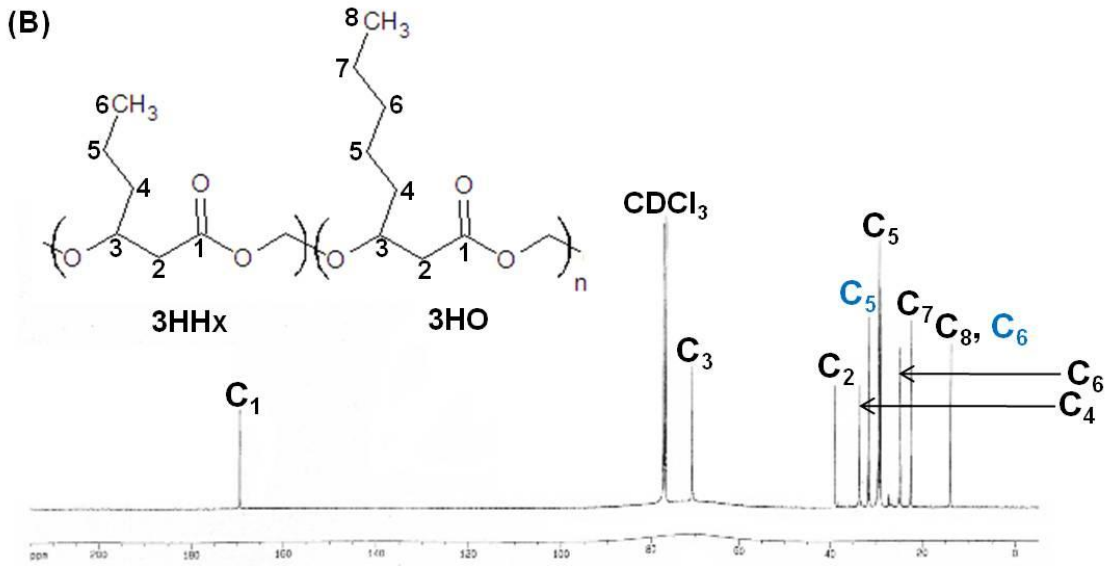

Figure 4.5: NMR analysis of the polymer produced when *P. oleovorans* was grown in octanoate: (A) ^{13}C NMR spectra and (B) ^{1}H NMR spectra of the polymer recorded in $CDCl_3$.

The main findings from this initial screening of the microorganisms are compiled in **Table 4.1.**

Organism	Carbon	C/N (g/g)	Time (hrs)	Growth parameters			PHA	Media
				Dry cell weight (g/L)	PHA yield (% dcw)	pH		
P. oleovorans	Octanoate	8.70	29	1.10	15.50	7.18	3HO	E
P. oleovorans	Octanoate	8.70	24	2.40	29.20	7.28	3HO, 3HHx	E2
P. putida	Octanoate	8.70	48	1.80	11.60	7.32	3HO	E2
P. aeruginosa	Octanoate	16.67	48	0.93	11.40	7.30	3HO 2HDD	ME2

Table 4.1: The production of mcl-PHAs and its copolymers using *Pseudomonas* strains

4.2.3. Production of mcl-PHAs from *P. mendocina*

P. mendocina was studied extensively for the production of mcl-PHAs. The organism was grown individually on structurally related carbon sources, hexanoate, heptanoate, octanoate and nonanoate at 20 mM and structurally non related carbon sources, glucose, sucrose and fructose at 20 g/L.

P. mendocina was initially grown in octanoate as the sole carbon source and the results obtained are shown in **Figure 4.6**. The dry cell weights achieved was between 0.36 and 0.87g dcw/L. The dcw increased steadily up to 36 hrs at which highest dry cell weight of 0.87 g/L was reached after which it decreased to about 0.64g dcw/L at 54 hrs. The organism had already started to accumulate PHA by 24 hrs, however the highest accumulation of polymer which was 31.3 % dcw was observed at 48 hrs. The PHA yield also decreased to about 22.5 % dcw at 54 hrs. At the beginning of the fermentation the C/N ratio of the culture medium was 20:1, however the amount of carbon decreased steadily in the media as the fermentation progressed and by 48 hrs had dropped from the initial value of 1.9 g/L to 0.14 g/L. At this time point the amount of nitrogen in the medium was 0.25 mg/L. The pH of the culture broth increased as the fermentation progressed and by 54 hrs the pH had reached 7.82.

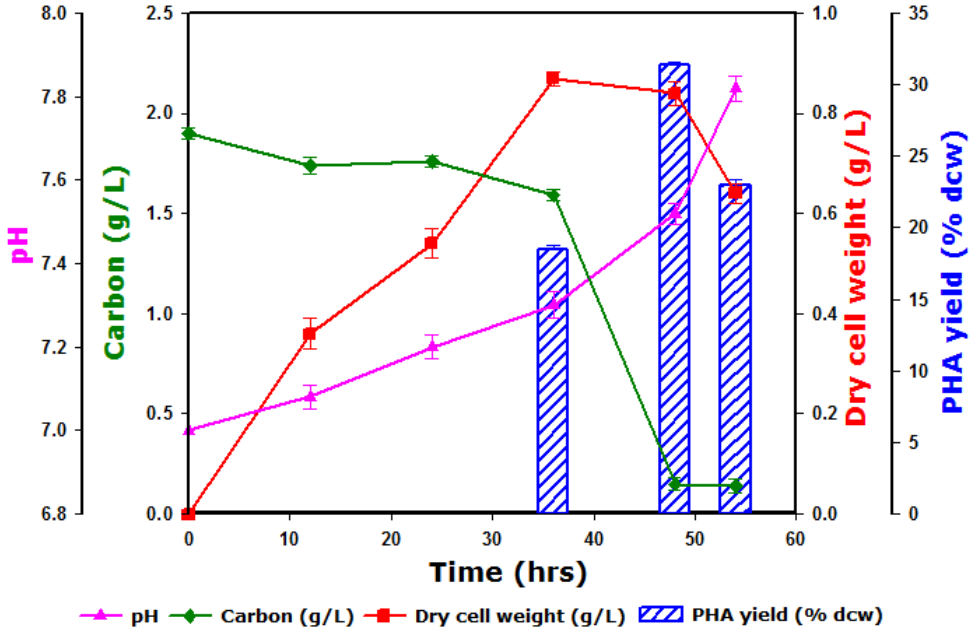

Figure 4.6: Fermentation profile for mcl-PHA production by *P. mendocina* using octanoate as the carbon source.

P. mendocina was next grown in heptanoate as the sole carbon source and the results obtained are shown in **Figure 4.7**. At the beginning of the fermentation, the C/N ratio of the culture medium was 23. By 24 hrs the organism had entered the stationary phase. The dry cell weights observed for the organism ranged between 0.25 to 0.80 g dcw/L. At 36 hrs the highest dcw of 0.80 g dcw/L was achieved after which a decrease was observed. In fact by, 54 hrs, the dcw had decreased to about 0.62 g dcw/L. The polymer accumulated by the organism ranged between 12 to 16.33% of the dcw. At 24 hrs polymer production was observed but not in sufficient quantifiable amounts. The polymer was accumulated to a maximum of 16.33 % dcw at 48 hrs, at which point, the amount of carbon in the medium was 0.36 g/L and nitrogen was 0.16 µg/mL. At the beginning of the fermentation the pH was set at 7, however the pH increased as the fermentation progressed and reached 7.72 at the end of fermentation.

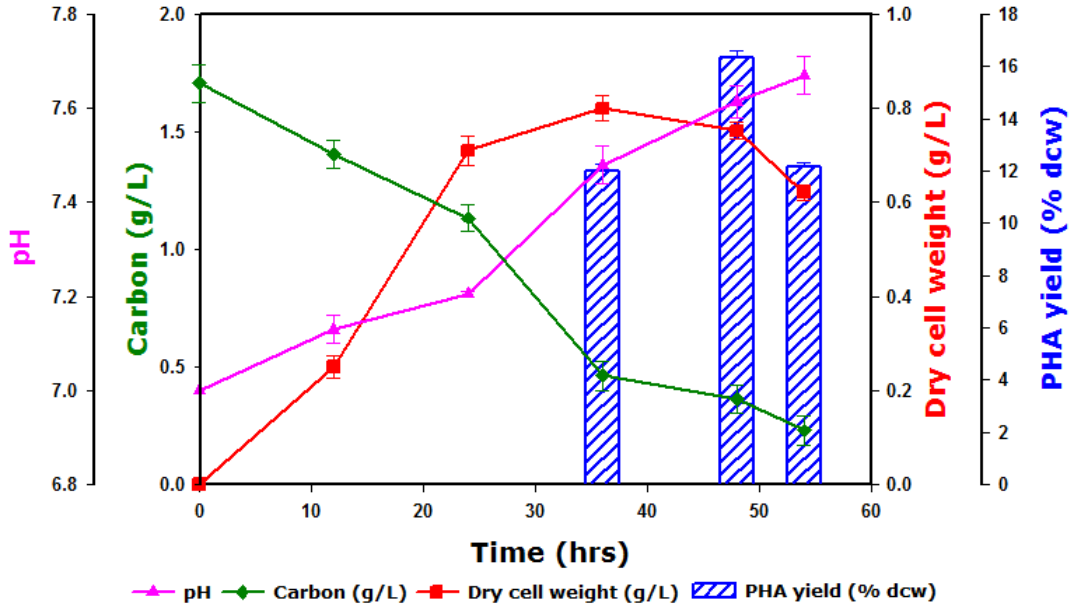

Figure 4.7: Fermentation profile for mcl-PHA production by *P. mendocina* using heptanoate as the carbon source.

Nonanoate was chosen as the next carbon source for the growth and polymer production using *P. mendocina*. The results obtained are shown in **Figure 4.8**. The C/N ratio of the culture medium at the beginning of the fermentation was 15.54. The organism entered the stationary phase by 24 hrs which lasted till about 48 hrs. The dry cell weights obtained ranged between 0.08 to 0.12g dcw/L. Polymer production was only observed after 36 hrs. The polymer accumulation of the organism ranged between 15 to 27.27 % of the dcw. Here too the highest yield, 27.27 % dcw was achieved at 48 hrs after which it decreased to 15 % dcw at 54 hrs. As the fermentation progressed the organism started to utilise the carbon source. Hence, the level of carbon started to decrease in the medium as shown in the carbon profile (**Figure 4.8**). By 54 hrs the amount of carbon in the medium had dropped to 0.11 g/L and the amount of nitrogen in the medium was 0.32 µg/mL. During fermentation the pH of the culture medium increased and reached a value of 7.35 by the end of the fermentation.

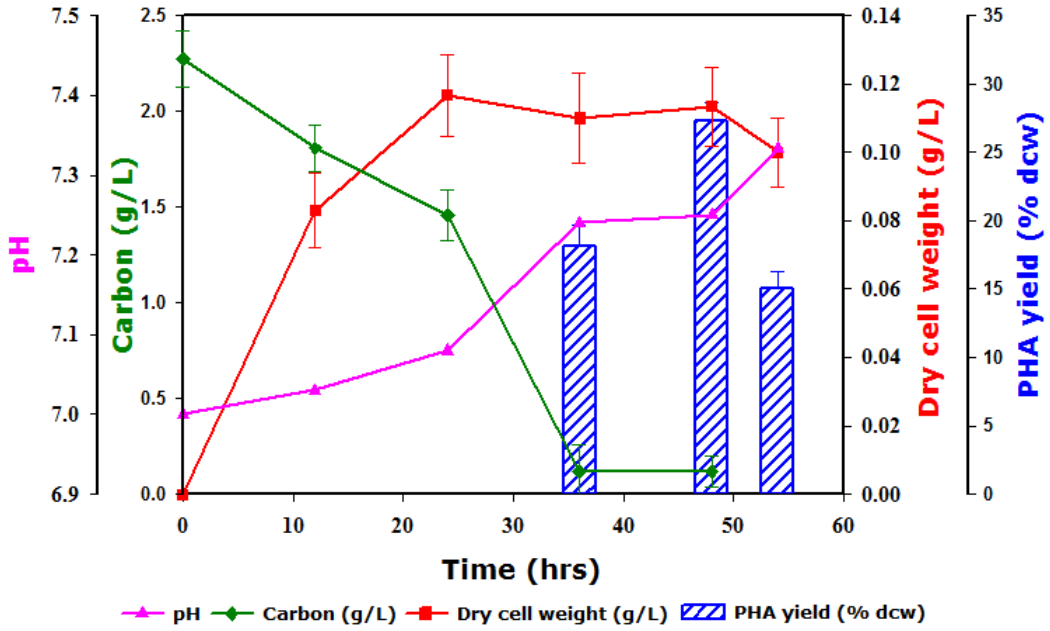

Figure 4.8: Fermentation profile for mcl-PHA production by *P. mendocina* using nonanoate as the carbon source.

The next step forward was the use of structurally unrelated carbon sources, the first to be used was glucose. The results obtained with the growth of *P. mendocina* using glucose as the sole carbon source are shown in **Figure 4.9**. The C/N ratio of the culture medium at the start of the fermentation was 58. The dry cell weights of the organism ranged between 0.3 to 1.3 g dcw/L. The highest dry cell weight (1.3 g dcw/L) was observed at 36 hrs, by 54 hrs the dcw had decreased to about 0.93 g dcw/L. The PHA produced by the organism ranged between 2.4 to 16.12 % dcw. The polymer yield increased up to 48 hrs with the highest PHA accumulation of 16.12 % dcw after which the yield decreased to 11.11 % dcw by the 54th hr. Carbon utilisation by the organism led to a decrease in the carbon concentration from the initial value of 7.72 g/L to that of 4.78 g/L at 48 hrs. The level of nitrogen also decreased from the initial value of 0.13 g/L to that of 0.06 mg/L at 24 hrs, after which it could not be detected in the media. As the fermentation progressed, the pH of the culture medium, which was initially set to 7 had decreased and dropped to a minimum of 6.61 by 54 hrs.

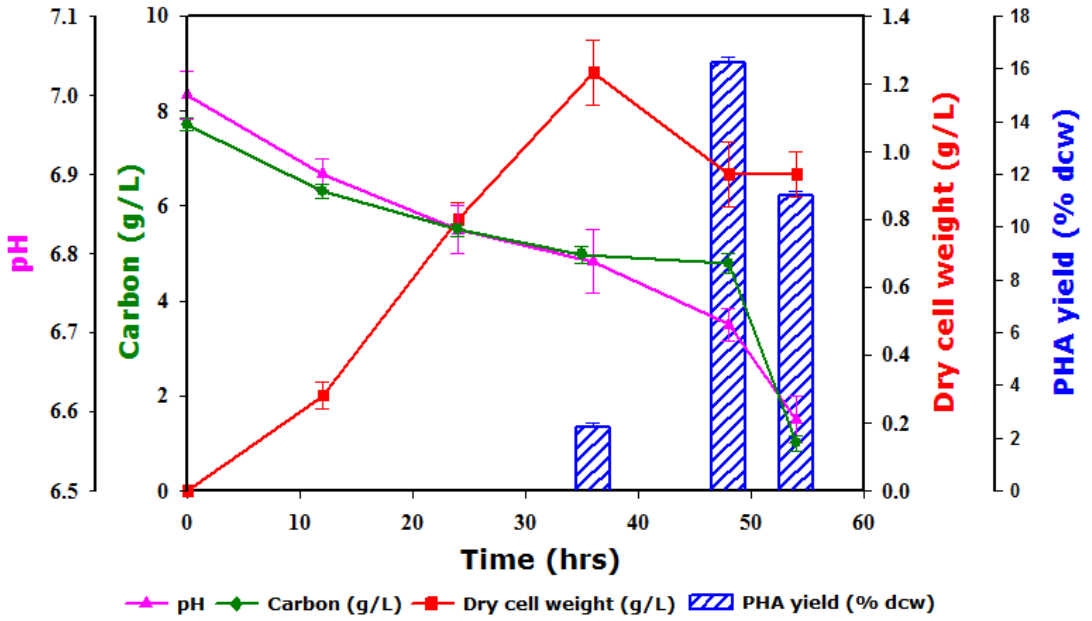

Figure 4.9: Fermentation profile for mcl-PHA production by *P. mendocina* using glucose as the carbon source.

The next structurally unrelated carbon substrate used was sucrose. **Figure 4.10** shows a typical fermentation run for the organism when grown in sucrose as the sole carbon source. The C/N ratio of the culture medium at the beginning of the fermentation was 67. The organism had entered the stationary phase by 36 hrs. The dry cell weights of the organism ranged between 0.28 to 1.30 g/L. The organism had maximum accumulation of the polymer at 48 hrs which was 23% of the dcw. Both the carbon and the nitrogen amounts in the media decreased as the fermentation progressed. At 48 hrs when the highest yield of the polymer was achieved, the level of carbon present in the medium was 6.69 g/L. At this time point the level of nitrogen present in the medium could not be detected. The pH of the medium which was set at 7, at the beginning of the fermentation decreased and reached 6.76 by 54 hrs.

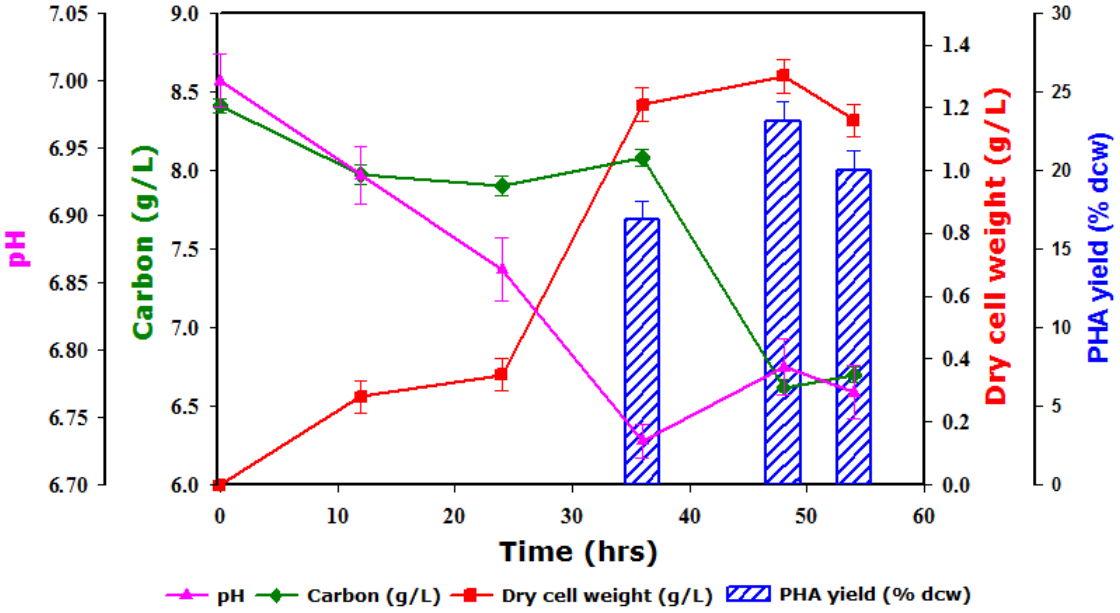

Figure 4.10: Fermentation profile for mcl-PHA production from *P. mendocina* using sucrose as the carbon source.

The final structurally unrelated substrate used for polymer production using *P. mendocina* was fructose. **Figure 4.11** describes a typical fermentation run for the organism when grown in fructose as the sole carbon source. The carbon to nitrogen ratio at the beginning of the fermentation was set at 53.22 (g/g). The organism entered stationary phase after 36 hrs of fermentation and this phase lasted until 54 hrs of the fermentation. The dry cell weights of the organism ranged between 0.05 to 1.03 g dcw/L. By 24 hrs polymer accumulation had taken place because of the polymer precipitation observed during its extraction; however the amount extracted was not quantifiable. The maximum amount of polymer accumulated in the organism (4.6 % dcw) was observed at 48 hrs. The carbon profile as shown in **Figure 4.11** showed that the C content had decreased from 8.6 g/L to the level of 5.6 g/L by 54 hrs. The amount of nitrogen present in the media at 24 hrs was 0.019 mg/L after which it could not be detected. The pH of the medium which was set at 7 had fallen as the fermentation progressed and had reached 6.83 by 54 hrs.

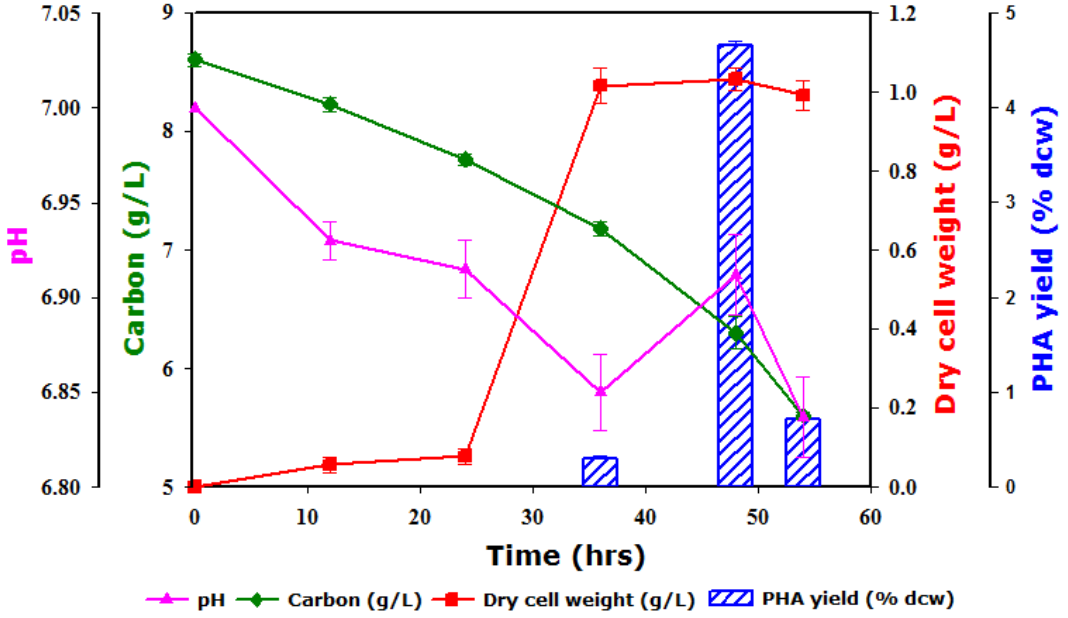

Figure 4.11: Fermentation profile for mcl-PHA production from *P. mendocina* using fructose as the carbon source.

4.2.4. Characterisation of mcl-PHAs

4.2.4.1. Wet stem analysis

Wet stem analysis was carried out to assess the accumulation of the PHA inclusions. **Figure 4.12** shows the accumulated intracellular mcl-PHA inclusions when *P. mendocina* was grown in octanoate at 48 hrs. Most of the cells were found to accumulate about 4 to 5 granules per cell. The size of the accumulated granules ranged between 0.2 to 0.5 µm in diameter.

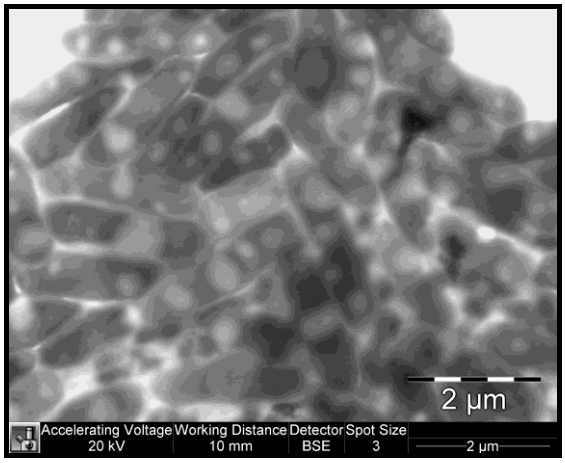

Figure 4.12: *P. mendocina* showing the accumulated mcl-PHA granules when grown in octanoate.

4.2.4.2. Fourier transform infrared spectroscopy

Preliminary confirmation of the polymer produced from *P. mendocina* using different carbon feeds was done using FTIR. **Figure 4.13**, shows the FTIR spectra of these polymers. FTIR analyses of the polymers produced from the different carbon sources used, except sucrose, confirmed the presence of the characteristic marker ester carbonyl band for mcl-PHAs which occurs at 1742 cm^{-1} and the band at 1165 cm^{-1} which occurs due to C-O stretching (Randriamahefa *et al.*, 2003) as shown in **Figure 4.13**. This observation thus indicates that these polymers were of mcl nature. The bands at 2955, 2925 and 2856 cm^{-1} correspond to the aliphatic C-H group of the polymer backbone (Sánchez *et al.*, 2003). For sucrose, in addition to the band at 1742 cm^{-1}, the other band at 1185 cm^{-1} which occurs due to C-O stretching and the band at 1282 cm^{-1} corresponding to the –CH group characteristic of poly(3-hydroxybutyrate), P(3HB), an scl-PHA was observed. The FTIR data thus indicated that the polymer extracted from sucrose contained both scl and mcl monomers.

(A)

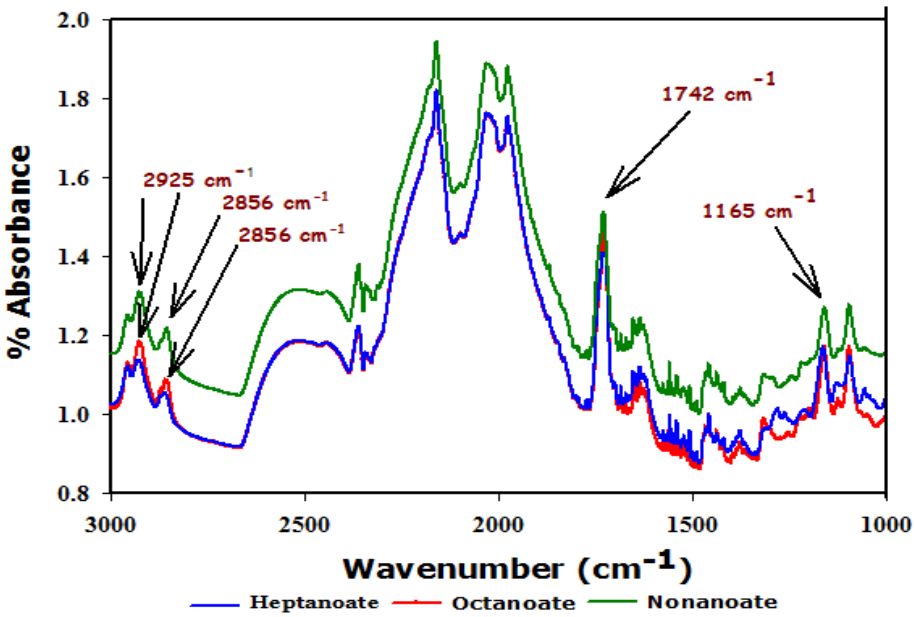

(B)

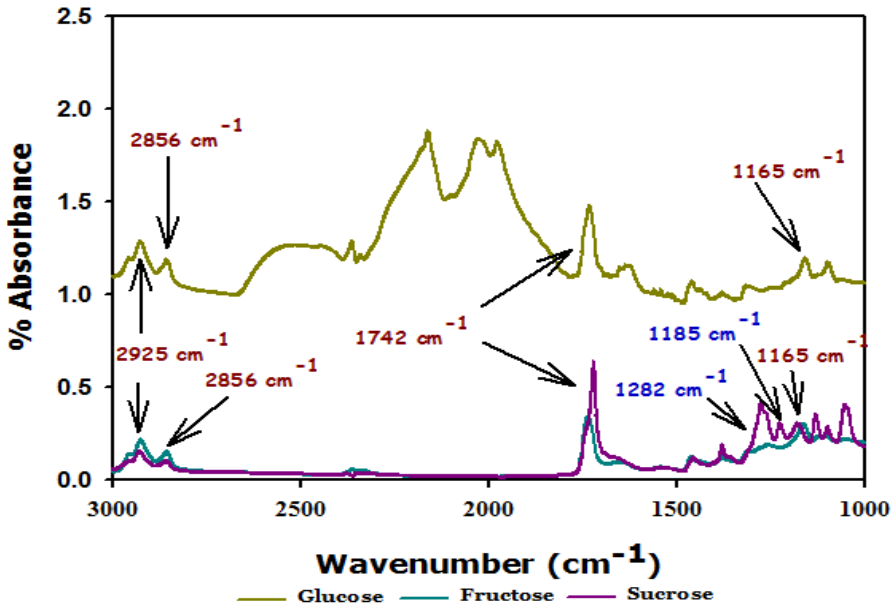

Figure 4.13: Combined ATR-FTIR spectra of the mcl-PHAs produced by *P. mendocina* using the different carbon sources: (A) different fatty acids and (B) different carbohydrates

The bands at 1170 and 1743 cm^{-1} are characteristic of the amorphous phase in mcl-PHA and that at 1728 cm^{-1} is characteristic of the crystalline phase

(Ouyang *et al.*, 2007). The band at 1453 cm^{-1} is a reference band and is insensitive to the degree of crystallinity and copolymer composition of PHA, whereas that at 1230 cm^{-1} has the largest difference between the crystalline and the amorphous states. Therefore, a crystallinity index (CI) can be defined as the ratios of the band's intensities at 1230 cm^{-1} to that of 1453 cm^{-1}. In this study, the polymer extracted from octanoate, heptanoate and nonanoate feed had a CI value of 1.02, 1.03 and 1.00 respectively. Structurally unrelated carbon sources such as glucose, fructose and sucrose led to the production of polymer with a CI value of 0.87, 1.5 and 2.47.

4.2.4.3. Gas chromatography mass spectroscopy analysis

FTIR analysis confirmed the mcl nature of the polymers produced using the different carbon sources except sucrose in which both the scl and mcl monomers were present. Further detailed structural characterisation of the kind of monomers present in the extracted PHAs was done using GC-MS. For this the polymer extracted was first subjected to methanolysis as discussed in section 2.9.1.2 followed by GCMS analysis.

The polymer extracted from lyophilised cells grown in octanoate was subjected to methanolysis and the total ion current chromatogram for the methanolysed product can be seen in **Figure 4.14**. The mass spectrum of the molecular ion related mass fragment peak at an R_t of 10.63 minutes, showed excellent similarity to that of the mass spectrum of the methyl ester of 3-hydroxyoctanoate (M_w = 174) in the MS (NIST) library. The occurrence of peaks due to the fragmentation of the molecular ion is the same as that for the methyl ester of 3HO, as discussed previously produced from *P. aeruginosa* (refer to section 4.2.2) The internal standard 2-ethyl-2-hydroxybytyric acid had a R_t of 7.86 minutes. The structure of this 3HO monomer is shown in **Figure 4.2.**

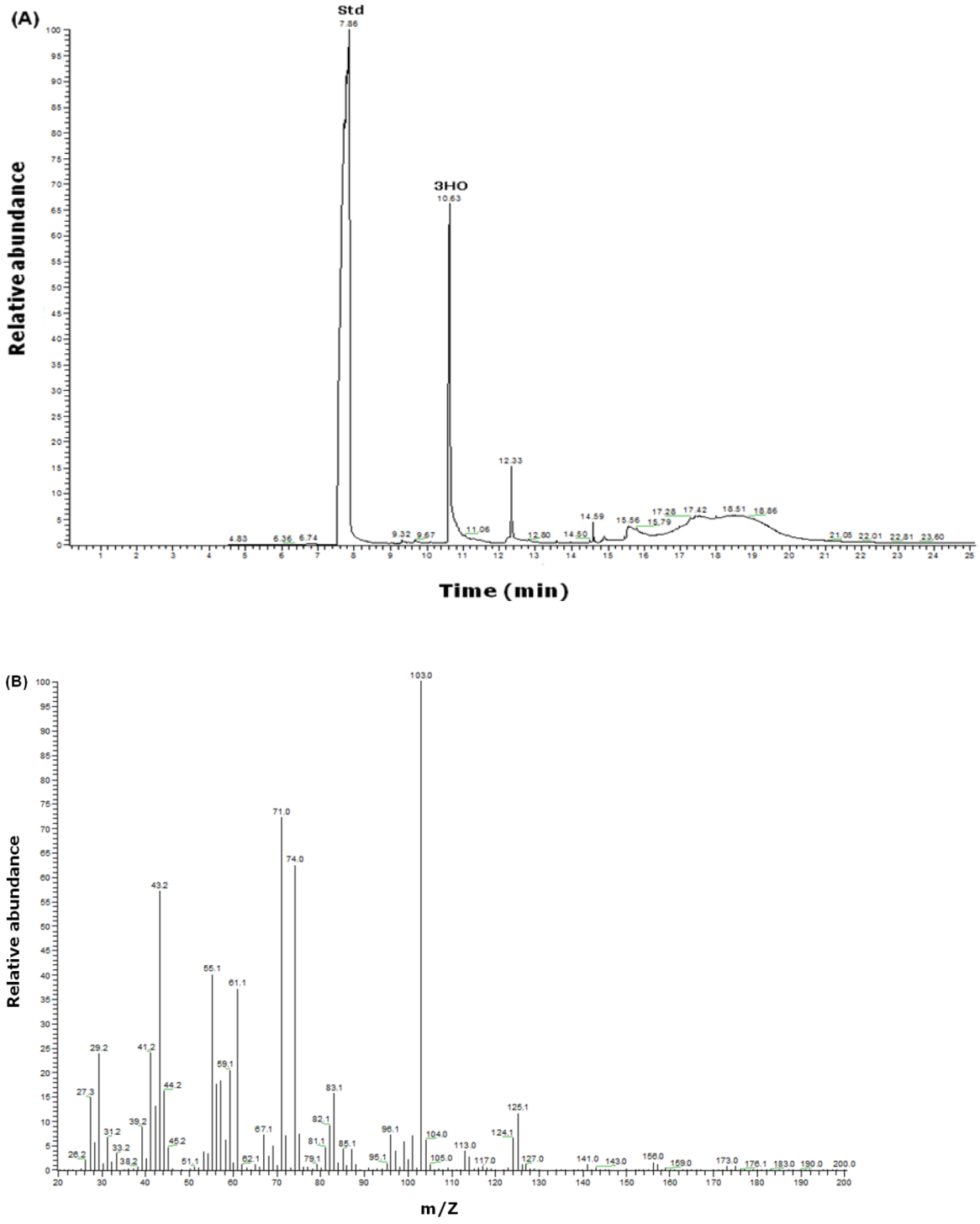

Figure 4.14: GC-MS analysis of the polymer produced when *P. oleovorans* was grown in octanoate: (A) Total ion gas chromatogram of the PHA produced from octanoate obtained prior to mass spectrometric analysis. (B) The mass spectrum of the GC peak at R_t of 10.63 minutes, showed the molecular ion-related mass fragments due to methyl esters of 3-hydroxyoctanoate having a molecular weight, M_w = 174.

The polymer extracted from glucose was also analysed using GCMS. The analysis confirmed the presence of two different monomers in the methanolysed PHA. The total ion current chromatogram for the methanolysis product of the polymer is shown in **Figure 4.15.** The molecular ion related mass fragment peak at R_t of 10.58 minutes, due to the methyl ester of 3HO was observed again. The peak at R_t of 12.01 minutes showed excellent similarity to the mass spectrum of methyl esters of 3-hydroxydecanoate. The molecular weights (M_w) of the methyl esters of these monomers were 174 for 3HO and 202 for 3HD. 3HD was the major monomer present in this copolymer at 66 mol% and 3HO was the minor constituent at 34 mol%. The internal standard, 2-ethyl-2-hydroxybytyric acid had a R_t of 7.71 minutes. For 3HO the occurrence of peaks due to the fragmentation of the molecular ion is the same as that described in section 4.2.2.

The fragmentation pattern of 3HD showed a peak at m/z 74.1, which originates from the carbonyl end of the molecule due to the cleavage between C_3 and C_4 carbon atoms following McLafferty rearrangement. The peak at m/z 102.9 occurred due to the fragmentation ion of the hydroxyl end of the molecule following the cleavage between C_3 and C_4 carbon atoms; similarly the alkyl end of this cleavage resulted in the peak at m/z 71.1. The peak at m/z 43.1 occurred due to the alkyl end of the molecule following the cleavage between C_7 and C_8 carbon atoms. The structure of this monomer methyl-3-hydroxyoctanoic acid is shown in **Figure 4.2** and methyl-3-hydroxydecanoic acid in **Figure 4.16**. The peaks between R_t = 12.36 and 19 minutes corresponded to that of lipids.

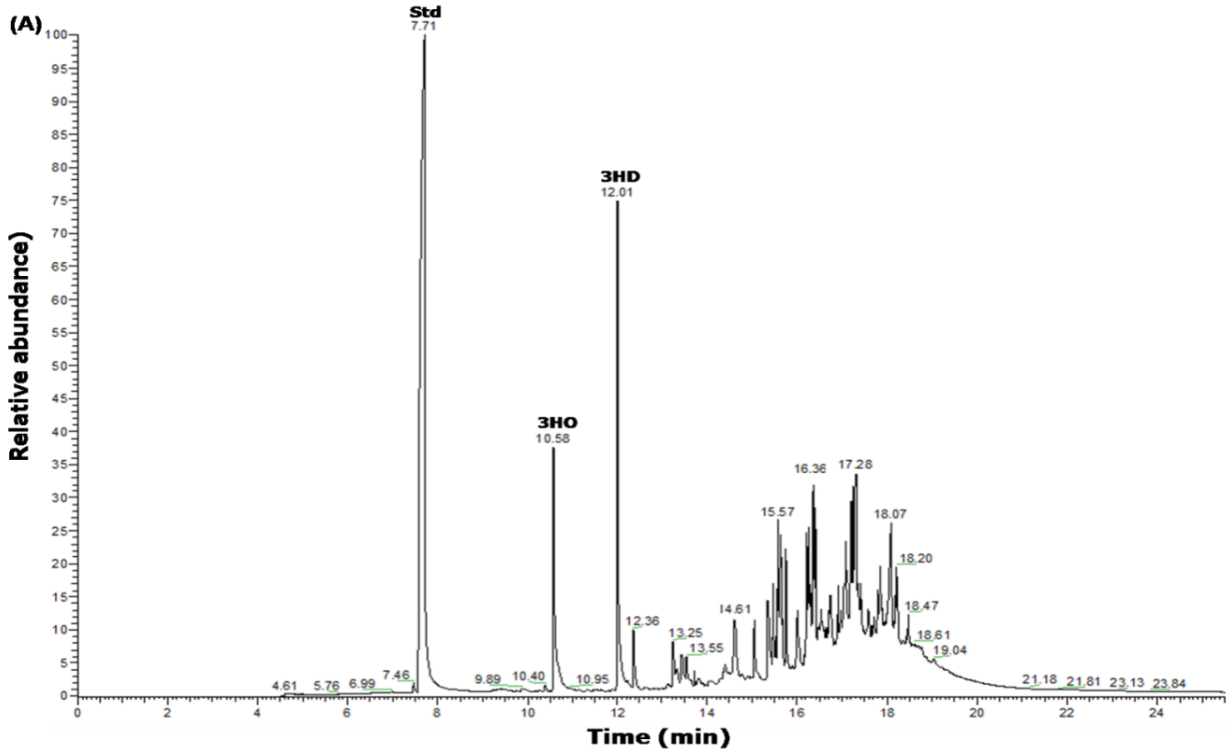
(A)
Std
7.71
3HD
12.01
3HO
10.58
Relative abundance
Time (min)
4.61
5.76
6.99
7.46
9.89
10.40
10.95
12.36
13.25
13.55
14.61
15.57
16.36
17.28
18.07
18.20
18.47
18.61
19.04
21.18
21.81
23.13
23.84

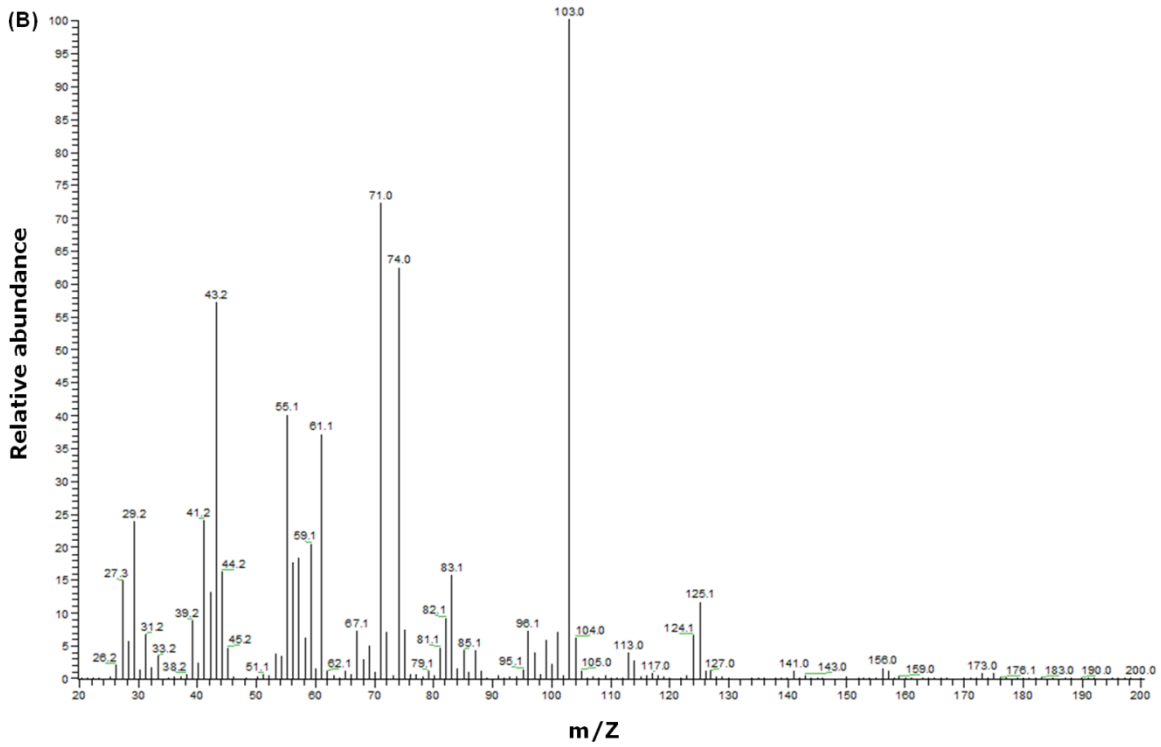
(B)
Relative abundance
m/Z
103.0
71.0
74.0
43.2
55.1
61.1
29.2
41.2
59.1
44.2
27.3
83.1
39.2
82.1
125.1
31.2
67.1
96.1
124.1
45.2
81.1
85.1
104.0
113.0
33.2
26.2
38.2
51.1
62.1
79.1
95.1
105.0
117.0
127.0
141.0
143.0
156.0
159.0
173.0
176.1
183.0
190.0
200.0

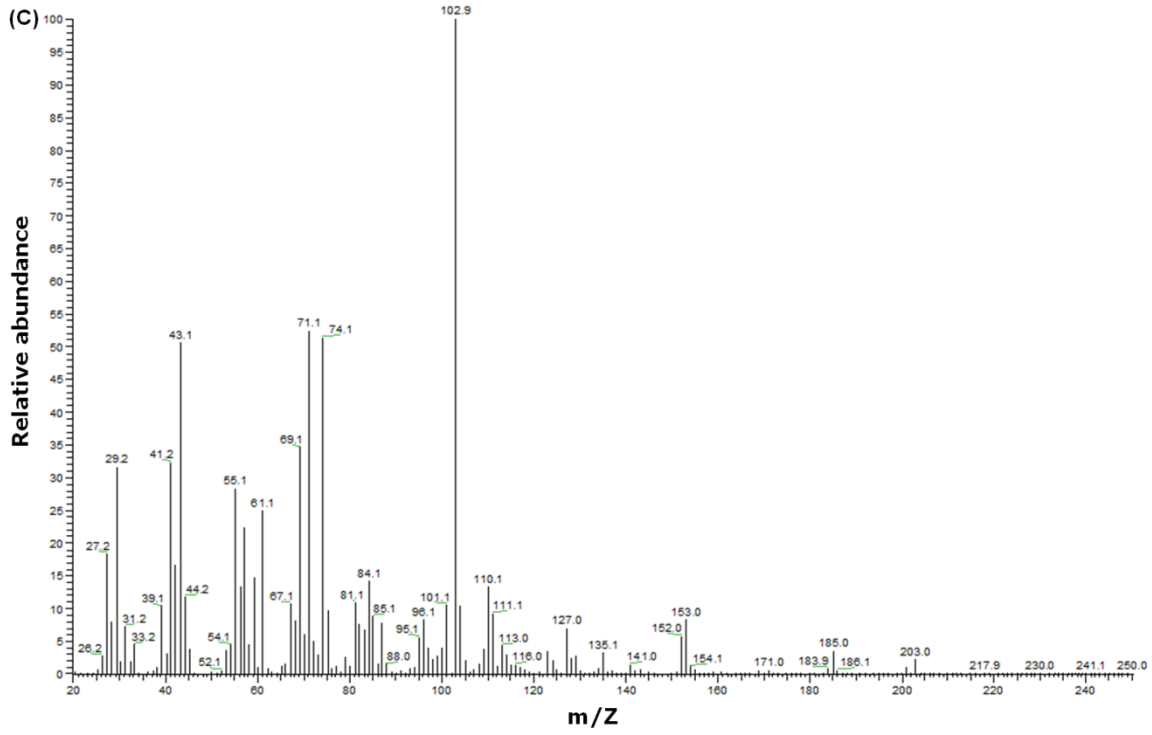

Figure 4.15: GC-MS analysis of the polymer produced when *P. mendocina* was grown in glucose: (A) Total ion chromatogram of the methanolysis products of the PHA produced on glucose feed. (B) Mass spectrum of the monomer of methyl ester of 3-hydroxyoctanoic acid with a R_t of 10.69 minutes and (C) Mass spectrum of the monomer of methyl ester of 3-hydroxydecanoic acid with a R_t of 12.01 minutes.

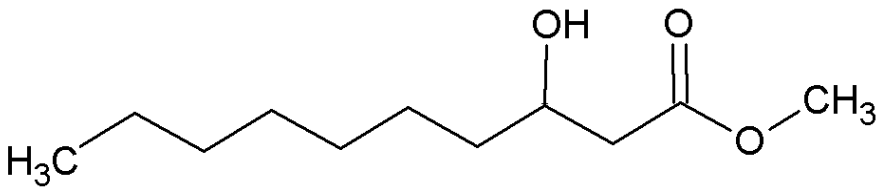

Figure 4.16: Structure of methyl-3-hydroxydecanoate

GC-MS analysis confirmed the presence of a short chain length monomer 3HB and medium chain length monomer 3HO when *P. mendocina* was grown on structurally unrelated carbon source sucrose. The monomers, 3HB and 3HO were present in almost equal amounts, 3HB (49.2 mol %) and 3HO (50.8 mol %). **Figure 4.17(A)** shows the total ion current chromatogram (TIC) for the methanolysis products of the isolated PHA with peak at 7.32 minutes being the methyl ester of 3HB (M_w = 118) and peak at retention time (R_t)

10.66 (M_w = 174) identified as the methyl ester of 3HO. The occurrence of peaks due to the fragmentation of the molecular ion is the same for 3HB as that described in section 3.2.1. The peak at m/z 100.8 occurs due to the loss of the water molecule from the molecular ion. The occurrence of peaks due to the fragmentation of the molecular ion is the same for 3HO as that described in section 4.2.2. The structures of these molecules have been shown previously in **Figure 4.2** for the methyl esters of 3-hydroxyoctanoic acid and **Figure 3.7(A)** for the methyl ester of 3-hydroxybutyric acid. The peaks after R_t = 11.5 minutes corresponded to that of lipids.

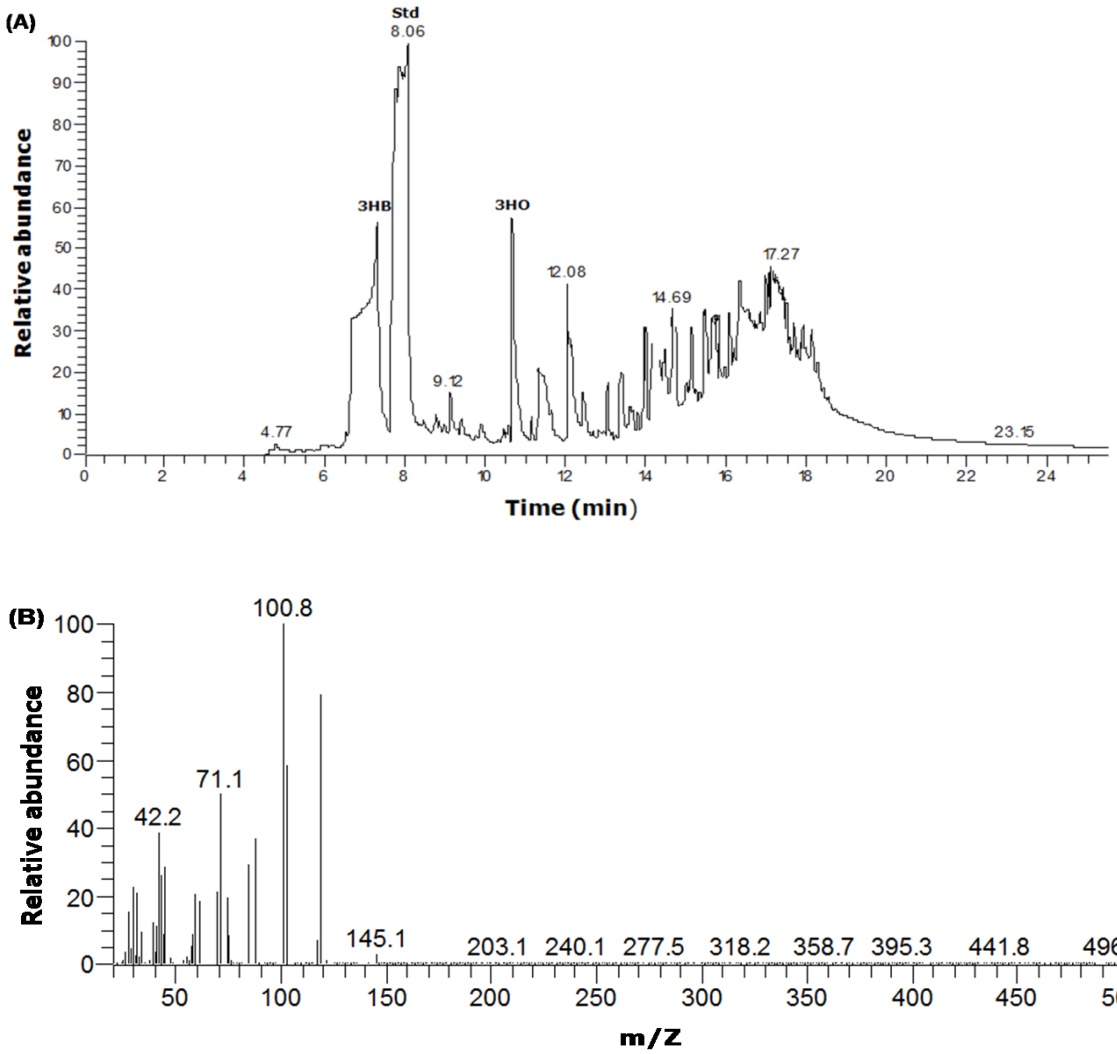

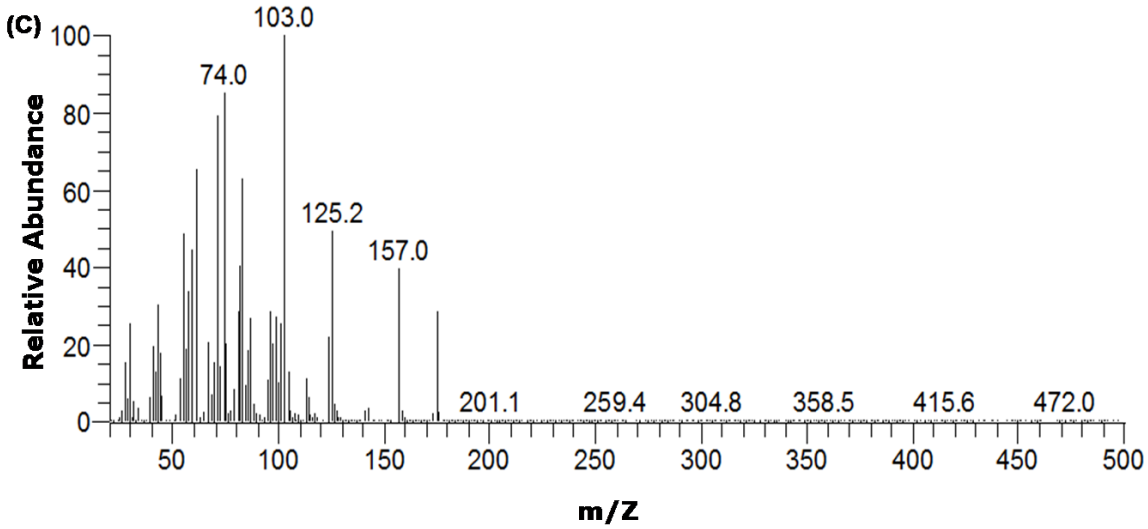

Figure 4.17: GC-MS analysis of the polymer when *P. mendocina* was grown in sucrose: (A) Total ion chromatogram of the methanolysis product of PHA, (B) Mass spectrum of the methylester of 3-hydroxybutyric acid with a R_t of 7.32 minutes and (C) Mass spectrum of methylester of 3-hydroxyoctanoic acid with a R_t of 10.66 minutes.

The polymer extracted from fructose feed was also subjected to methanolysis and then analysed using GCMS. **Figure 4.18** shows the total ion current chromatogram for this methanolysis product of the polymer. The molecular ion related mass fragment at a peak with R_t of 12.41 minutes showed excellent similarity to the mass spectrum of methyl esters of 3-hydroxydecanoate with M_w of 202. The occurrence of peaks due to the fragmentation of the molecular ion is the same for 3HD as that described previously for the polymer extracted from glucose feed. The structure of the monomer is also given in **Figure 4.16.** The peaks between R_t of 13.5 and 17.34 corresponded to lipids.

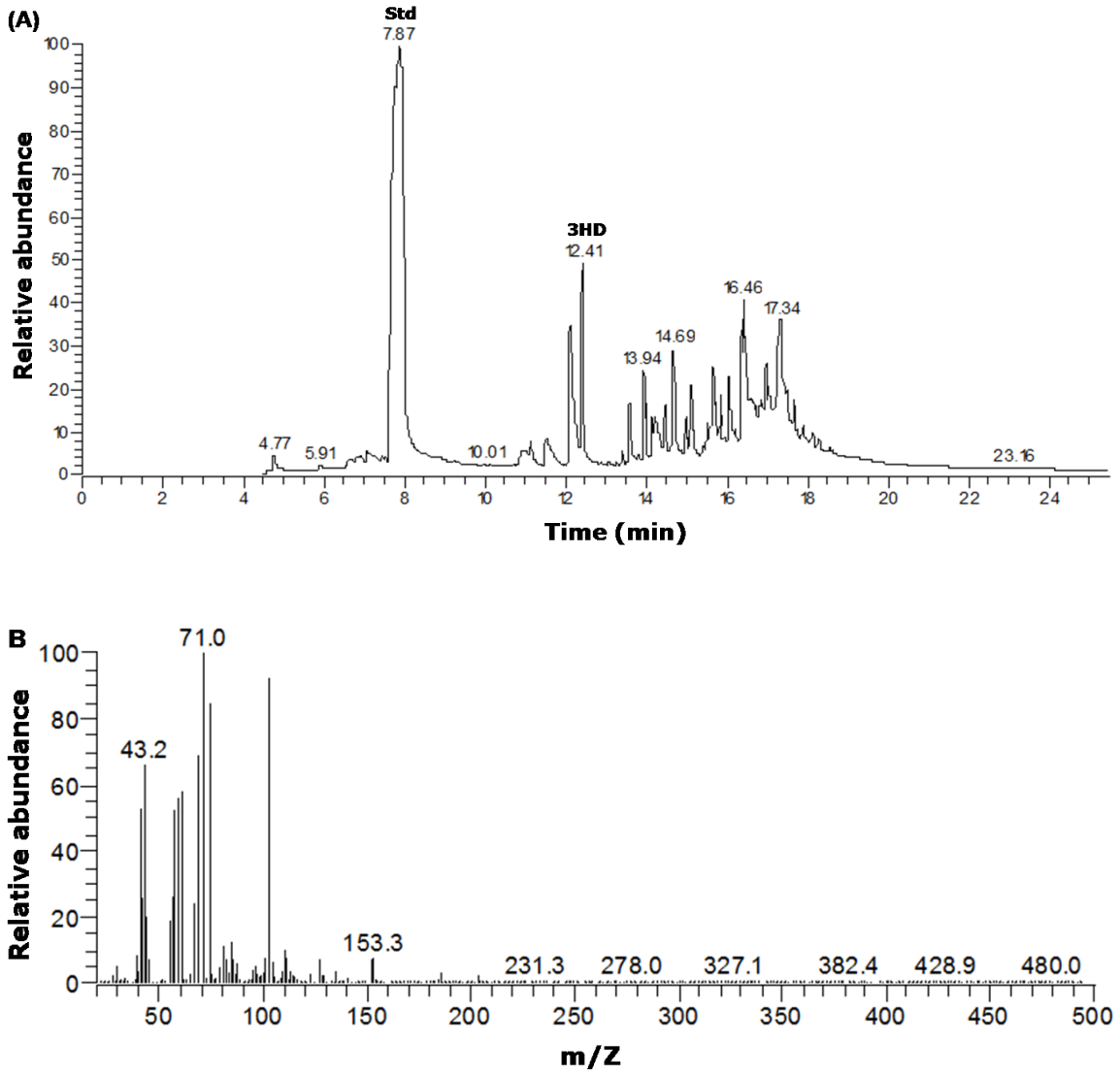

Figure 4.18: GCMS analysis of the polymer produced from sucrose: (A) Total ion gas chromatogram of the methanolysed product of the PHA, (B) The mass spectrum of the GC peak at R_t of 12.41 minutes, showed the molecular ion-related mass fragment due to methyl ester of 3-hydroxydecanoate having a molecular weight, M_w = 202.

4.2.4.4. Nuclear magnetic resonance spectroscopy

The polymers produced from *P. mendocina* using different carbon sources were also subjected to NMR analysis. For these spectral measurements purified polymer was used, the analysis was done as described in section 2.9.1.3.

The polymer produced from *P. mendocina* when grown in octanoate was analysed using ^{1}H, ^{13}C and heteronuclear single quantum coherence NMR, HSQC NMR. **Figure 4.19(A)** and **(B)** shows the ^{1}H and ^{13} NMR spectra of the polymer. In the ^{1}H NMR spectrum, five peaks were obtained as there are five different environments for the proton in the molecule. The ^{1}H NMR analysis showed the presence of protons bonded to C_2 (-CH_2 group), C_3 (-CH group), C_4 (-CH_2 group), C_5, C_6, C_7 (-CH_2 group) and C_8 (-CH_3 group) with chemical shifts of 2.5, 5.2, 1.6, 1.2 and 0.8 ppm respectively. In the ^{13}C NMR eight different peaks were obtained corresponding to the eight different environments for the carbon in the molecule. The chemical shift at 169.38 ppm corresponded to C_1 (C=O group), 70.82 ppm to C_3 (–CH group), 39.08 to C_2 (-CH_2 group), 23 - 35 ppm to C_4, C_5, C_6, C_7 (-CH_2 group) and 13.95 ppm to C_8 (-CH_3). In **Figure 4.19(C)**, the HSQC NMR, shows the presence of protons in a particular carbon environment. Spot A, corresponds to hydrogens at 5.2 ppm that comes from the carbon environment at 72 ppm which corresponds to C_3 (-CH group). Spot B, corresponds to hydrogens at 2.5 ppm which resides on the carbon at 40 ppm corresponding to C_2 (-CH_2 group). Spot C, corresponds to the hydrogens at 1.5 ppm that comes from the carbon environment at 35 ppm which corresponds to C_4 (-CH_2 group). Spots D and E is due to the hydrogens at 1.2 ppm which occurs due to the carbon environment of C_5, C_6, C_7 (-CH_2 group). Spot F shows the hydrogens at 0.8 ppm which is linked to the carbon environment at 14 ppm corresponding to C_8 (-CH_3). ^{1}H, ^{13}C and HSQC NMR thus confirmed the presence of a homopolymer of P(3HO) in the polymer extracted octanoate feed.

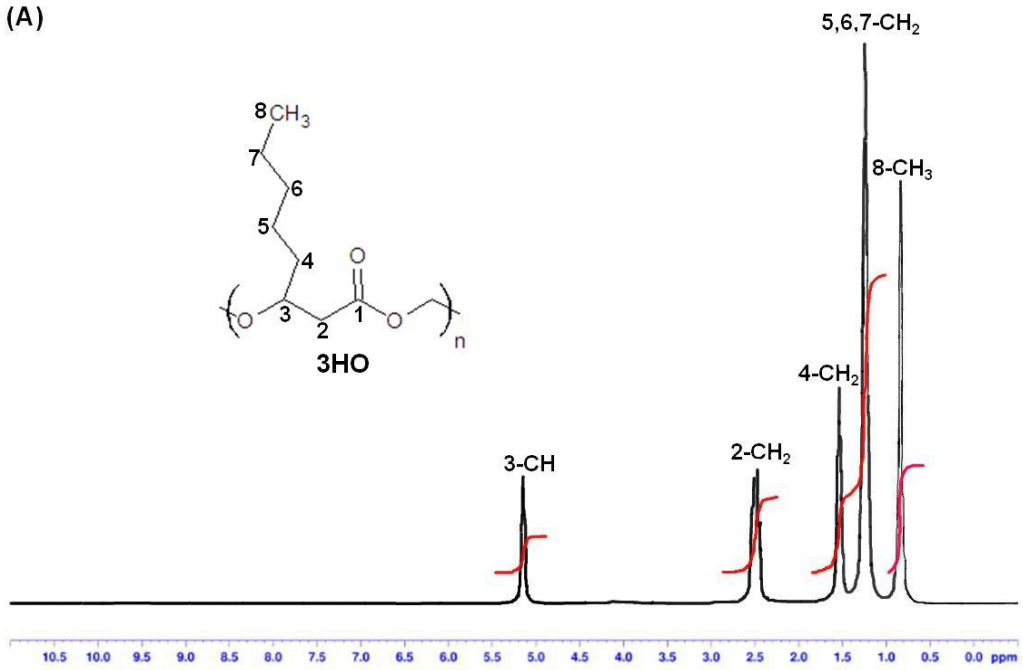
(A)
5,6,7-CH2
8-CH3
4-CH2
2-CH2
3-CH
3HO
10.5 10.0 9.5 9.0 8.5 8.0 7.5 7.0 6.5 6.0 5.5 5.0 4.5 4.0 3.5 3.0 2.5 2.0 1.5 1.0 0.5 0.0 ppm

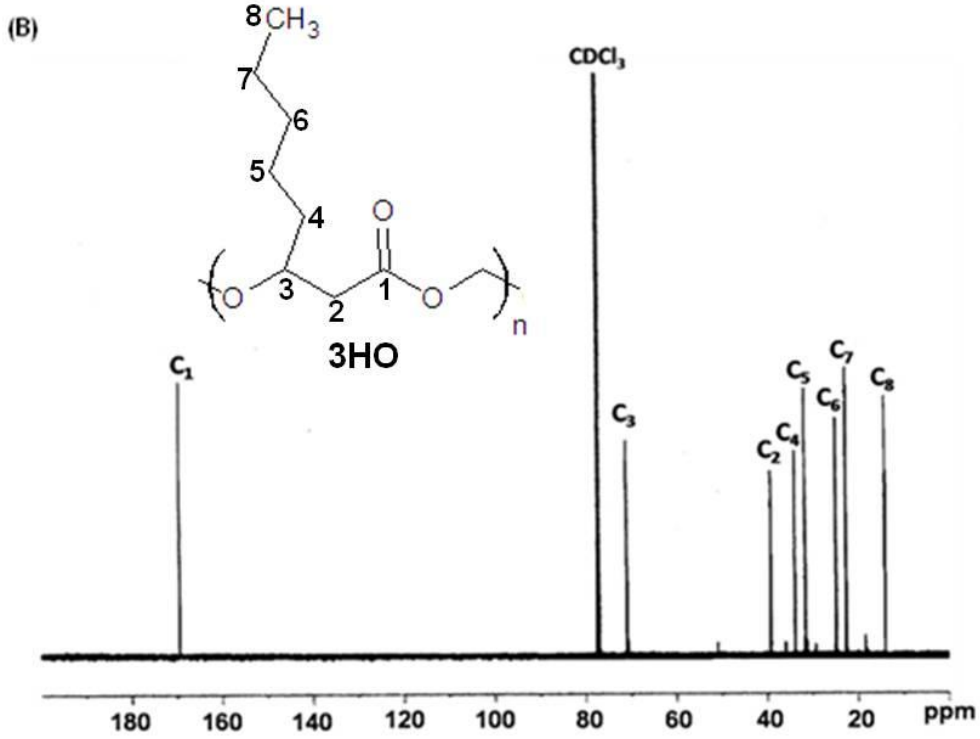
(B)
CDCl3
C1
C3
C2
C4
C5
C6
C7
C8
3HO
180 160 140 120 100 80 60 40 20 ppm

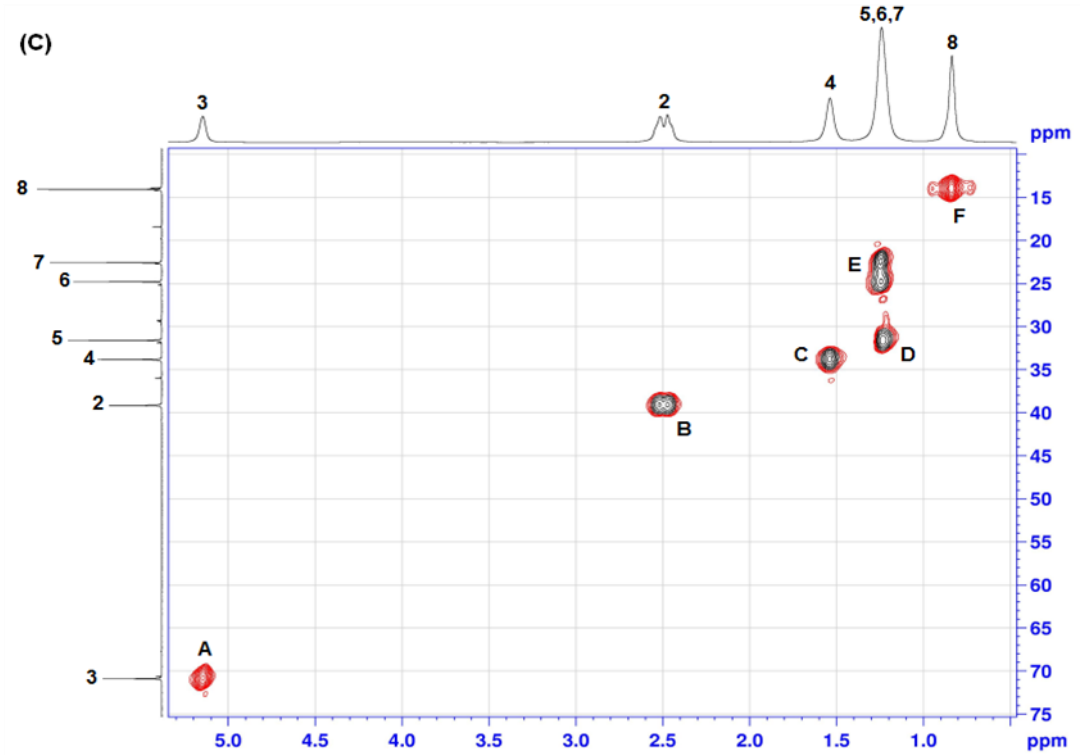

Figure 4.19: NMR spectra of the extracted homopolymer of P(3HO) produced from *P. mendocina* when grown in octanoate: (A) ^{1}H NMR spectrum, (B) ^{13}C NMR and (C) HSQC NMR.

The polymer extracted from heptanoate was analysed using the ^{1}H and ^{13}C NMR. The assignments of these spectra are shown in **Figure 4.20**. The ^{1}H spectrum **Figure 4.20(A)** shows that there were five different environments for the protons, and hence the five peaks. The ^{1}H NMR analysis showed the presence of the peak at 5.2 ppm corresponding to protons bonded to C_3 (-CH group), 2.5 ppm to C_2 (-CH_2 group), 1.6 ppm to C_4 (-CH_2 group), 1.2 ppm to C_5 and C_6 (-CH_2 group of 3HP), C_5,C_6,C_7, and C_8 (-CH_2 group of 3HN) and 0.8 ppm to C_5 (-CH_3 group of 3HV), C_7 (-CH_3 group of 3HP) and C_9 (-CH_3 group of 3HN). The ^{13}C spectrum shows that there were 13 peaks observed, indicating 13 different environments for the carbon in the polymer extracted. These 13 different carbon environments came from 3 different types of monomers present in the polymer. These different monomers present were 3-hydroxyvalerate, 3HV, 3-hydroxyheptanoate, 3HP and 3-hydroxynonanoate, 3HN. The chemical shift at 169.07 ppm corresponded to the C_1 (C=O group),

71.01 ppm to C_3 (–CH group), 57 to C_2 (-CH_2 group), 41 ppm to C_4, (-CH_2 group of 3HP and 3HN), 39 ppm to C_4 (-CH_2 group of 3HV), 34 ppm to C_5 (-CH_2 group of 3HP and 3HN, 30 ppm to C_6 (-CH_2 group of 3HP), 27 ppm to C_6 (-CH_2 group of 3HN, 22.5 ppm to C_7 (-CH_2 group of 3HN), 20 ppm to C_8 (-CH_2 group of 3HN) and 14 ppm to C_5 (-CH_3 group of 3HV), C_7 (-CH_3 group of 3HN) and C_9(-CH_3 group of 3HN). The monomers thus present in the polymer were 3HV, 3HP and 3HN.

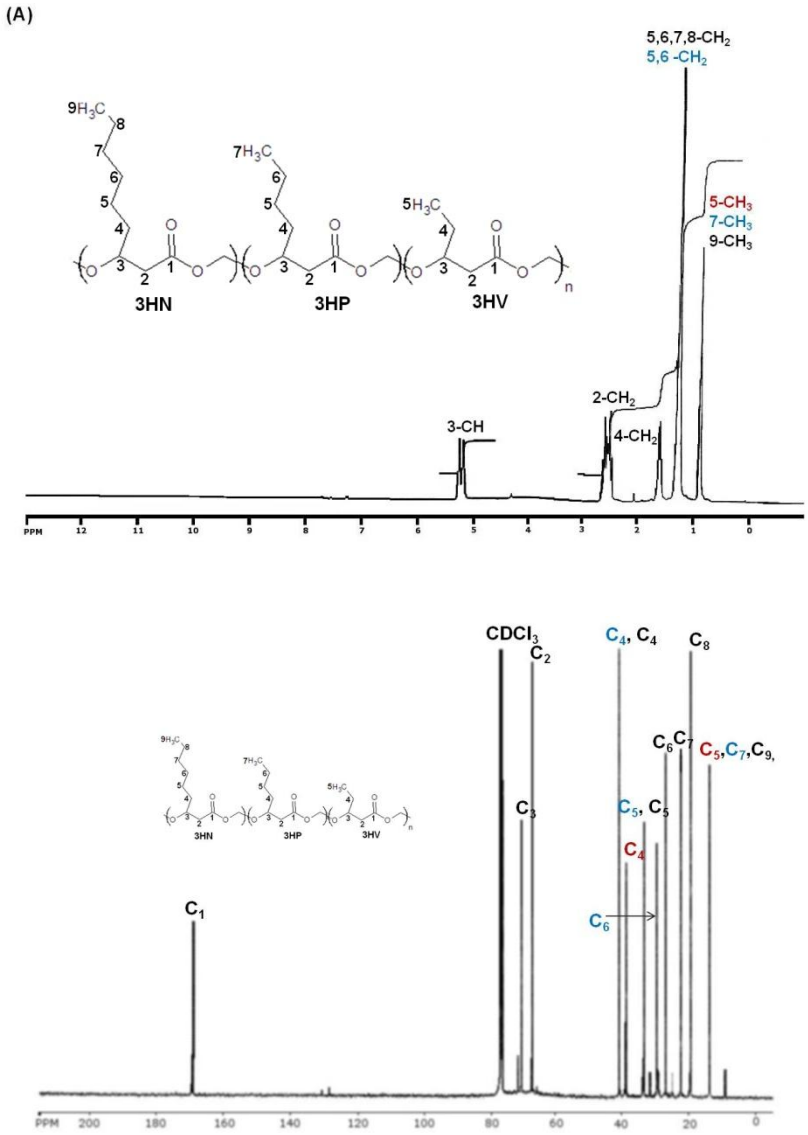

Figure 4.20: NMR spectra of the polymer produced from *P. mendocina* when grown in heptanoate: (A) ^{1}H NMR spectrum and (B) ^{13}C NMR of the polymer recorded in $CDCl_3$.

The polymer extracted from the freeze dried cells of *P. mendocina* grown in nonanoate was also analysed using the ^{1}H and ^{13}C NMR. The assignments of these spectra are given in **Figure 4.21**. The proton spectrum shows five different environments for the hydrogen in the polymer as shown in the **Figure 4.21(A).** The peak at 5.2 ppm was corresponding to protons bonded to C_3 (-CH group), 2.5 ppm to C_2 (-CH_2 group), 1.6 ppm to C_4 (-CH_2 group), 1.2 ppm to C_5 and C_6 (-CH_2 group of 3HP), C_5, C_6, C_7, and C_8 (-CH_2 group of 3HN) and 0.8 ppm to C_7 (-CH_3 group of 3HP) and C_9 (-CH_3 group of 3HN). The ^{13}C spectrum, **Figure 4.21(B)** shows 10 peaks, corresponding to 10 different environments for the carbon in the extracted polymer. The chemical shift at 169.07 ppm corresponded to the C_1 (C=O group), 71.01 ppm to C_3 (–CH group), 39 to C_2 (-CH_2 group), 33.5 to C_4 (-CH_2 group), 32 ppm to C_5, (-CH_2 group) 28.9 ppm to C_6 (-CH_2 group of 3HP), 27 ppm to C_6 (-CH_2 group of 3HN), 25 ppm to C_7 (-CH_2 group of 3HN), 22.5 ppm to C_8 (-CH_2 group of 3HN), 13.5 ppm to C_7 (-CH_3 group of 3HP) and C_9 (-CH_3 group of 3HN). The monomers thus present in the polymer were 3-hydroxyheptanoate and 3-hydroxynonanoate.

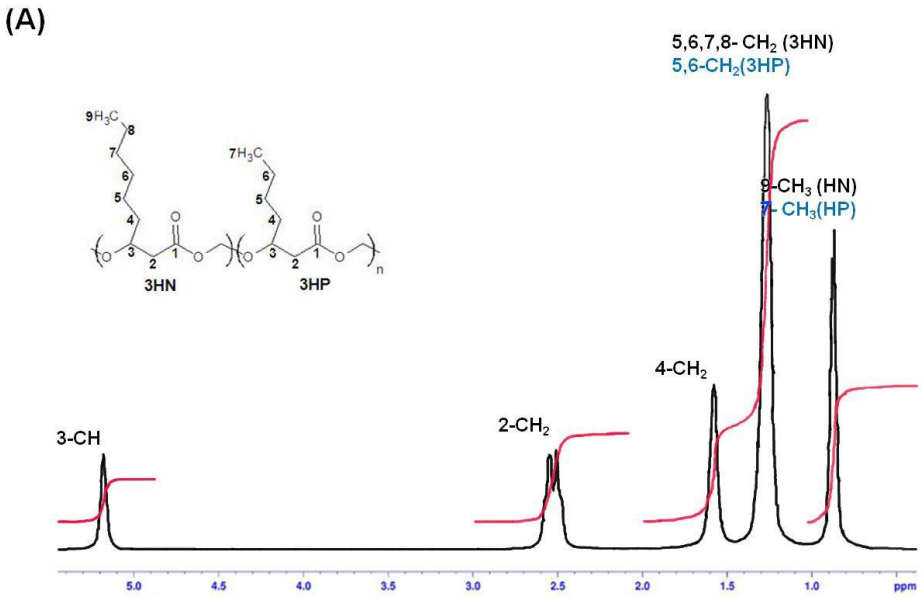

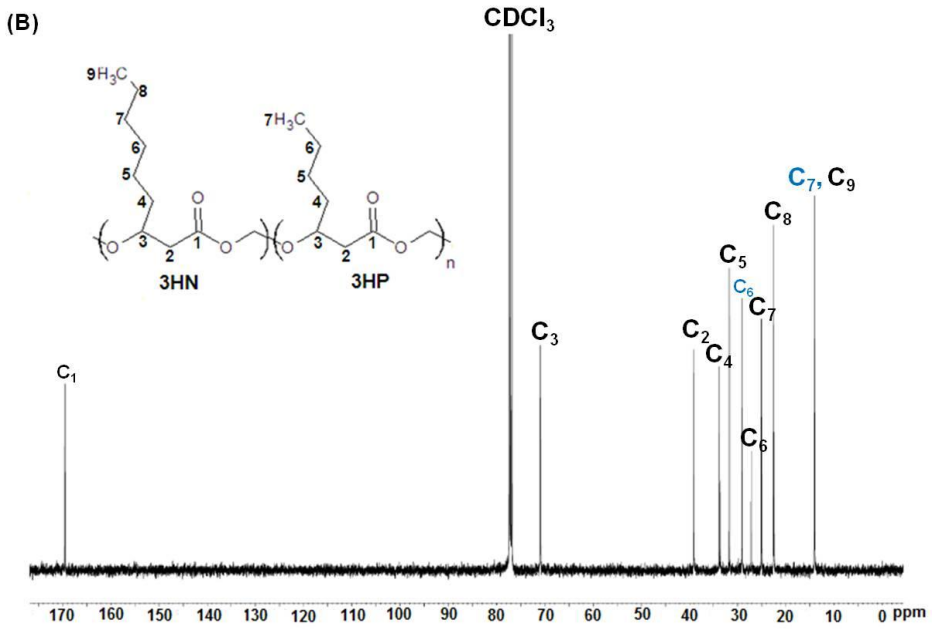

Figure 4.21: NMR analysis of the polymer produced when *P. mendocina* was grown in nonanoate: (A) ^{1}H NMR spectrum and (B) ^{13}C NMR of the polymer recorded in $CDCL_3$.

The polymer produced when *P. mendocina* was grown in glucose was also analysed using the ^{1}H NMR and ^{13}C NMR as shown in **Figure 4.22**. In this case, the ^{13}C NMR was not of good quality and hence has not been used in the characterisation. The ^{1}H spectrum shows five different environments for the hydrogen in the polymer. The peak at 5.2 ppm corresponded to protons bonded to C_3 (-CH group), 2.5 ppm to C_2 (-CH_2 group), 1.6 ppm to C_4 (-CH_2 group), 1.2 ppm to C_5,C_6 and C_7, (-CH_2 group) and 0.8 ppm to C_8 (-CH_3 group of 3HO). The monomer thus present in the polymer was 3-hydroxydecanoic acid.

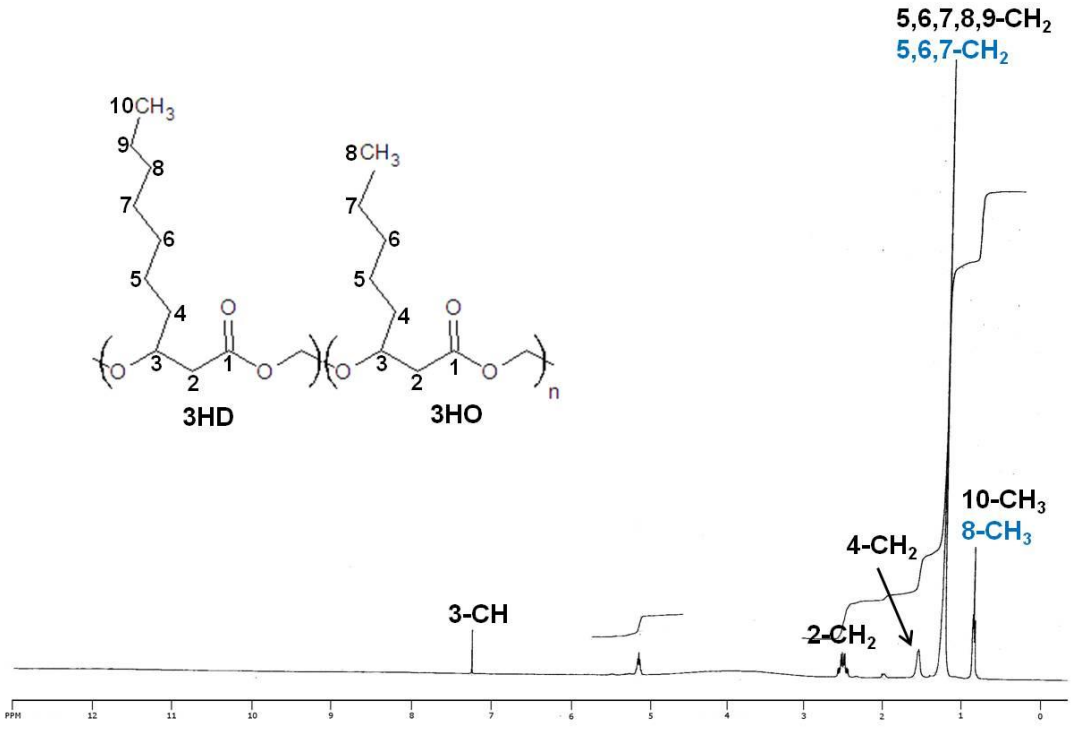

Figure 4.22: ^{1}H NMR spectrum of the polymer produced from *P. mendocina* when grown in glucose

The polymer extracted when *Pseudomonas mendocina* was grown in sucrose was also analysed using the ^{1}H and ^{13}C NMR. The occurrence and assignments of these peaks are given in **Figure 4.23**. The presence of the peak at 5.2 ppm corresponding to protons bonded to C_3 (-CH group), 2.5 ppm to C_2 (-CH_2 group), 1.6 ppm to C_4 (-CH_2 group), 1.2 ppm to C_5,C_6, and C_7 (-CH_2 group of 3(HO)) and 0.8 ppm to C_4 (-CH_3 group of 3HB) and C_8 (-CH_3 group of 3HO). In the ^{13}C NMR, 11 different peaks were observed for the 11 different environments of C in the molecule. The chemical shift at 169.07ppm corresponded to the C_1 (C=O group), 71.01 ppm to C_3 (–CH group of 3HB), 67.5 ppm to C_3 (-CH group of 3HO), 41 ppm to C_2 (-CH_2 group), 33.5 ppm to C_4 (-CH_2 group) 31.5 ppm to C_5 (-CH_2 group) 29.5 ppm to C_6 (-CH_2 group) 27 ppm to C_7 (-CH_2 group) and 19.5 ppm to C_4 (-CH_3 group of 3HB) and C_8 (-CH_3 group of 3HO). The monomers thus present in the polymer were 3HB and 3HO.

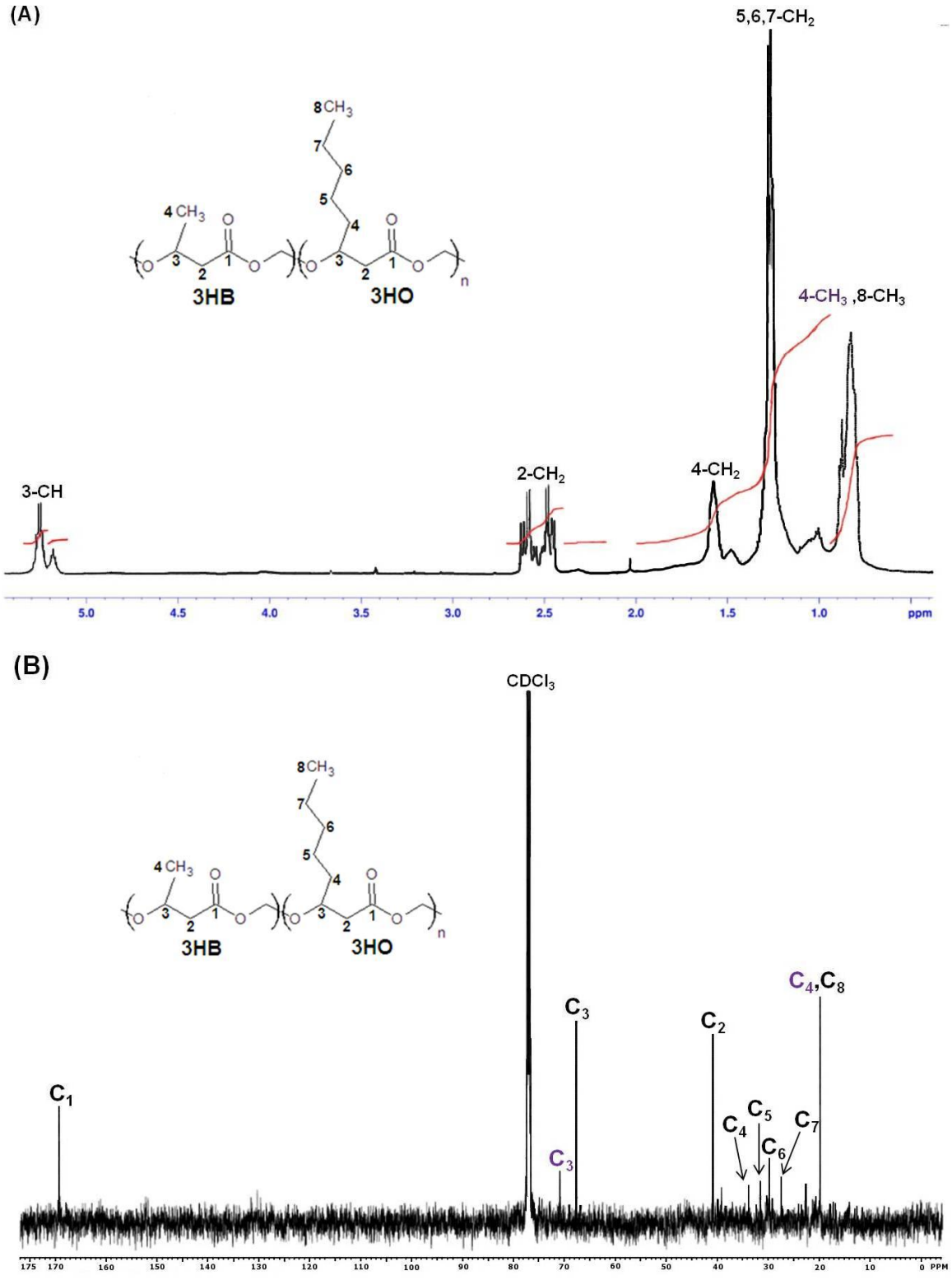

Figure 4.23: NMR analysis of the polymer produced when *P. mendocina* was grown in sucrose: (A) ^{1}H NMR spectrum and (B) ^{13}C NMR spectrum of the polymer recorded in $CDCl_3$.

All the results from these studies of growing the organism in the various carbon sources have been compiled in **Table 4.2**

Carbon source	Carbon/ Nitrogen (g/g)	Time (hrs)	DCW (g/L)	PHA yield (%dcw)	pH	Type of PHA
Heptanoate	23.00	48	0.80	16.33	7.61	3HN, 3HP, 3HV
Octanoate	20.00	48	0.84	31.38	7.52	3HO
Nonanoate	16.00	48	0.11	27.27	7.27	3HN, 3HP
Glucose	58.00	48	0.93	16.12	6.71	3HO, 3HD
Sucrose	67.00	48	1.30	23.00	6.78	3HO, 3HB
Fructose	53.00	48	1.03	4.60	6.91	3HD

Table 4.2: Compilation of different results obtained for *P. mendocina* when grown under different carbon sources.

4.2.4.4. Thermal characterisation

PHAs are partially crystalline polymers and therefore their thermal properties are usually expressed in terms of the glass to rubber transition temperature (T_g) of the amorphous phase and the melting temperature (T_m) of the crystalline phase. In PHAs, particularly scl-PHAs, at some point the polymer chains are found to arrange themselves in some sort of ordered structures i.e. crystalline form. This is called crystallisation temperature, (T_c). Studies were carried out to study the thermal properties of the polymer, extracted from the lyophilized *P. mendocina* cells grown on different carbon feeds. About 6 to 8 mg of the polymer was encapsulated in standard aluminium pans and subjected to thermal analysis using differential scanning calorimetry, (DSC), using a temperature range between -50 to 80^{o}C. The thermal properties of the polymer are quoted from the first heat run and have been compiled in **Table 4.3.**

Carbon source	T_g (°C)	T_m (°C)	ΔH_f (J/g)	T_c (°C)
Heptanoate	-27.24	-	-	-
Octanoate	-36.05	45.00	9.30	-
Nonanoate	-37.53	36.16	8.96	-
Glucose	-35.21	37.56	3.82	-
Fructose	-35.13	46.46	5.31	-
Sucrose	-	167.07	26.95	94.88

Table 4.3: Compilation of the thermal properties of the polymer produced from the different carbon sources: T_g = glass transition temperature, T_m= melting temperature, ΔH_f = heat of fusion and T_c = crystallisation temperature and (-) = not observed.

Interestingly no melting peak was observed for the polymer produced from heptanoate. Growing *P. mendocina* in sucrose had resulted in the accumulation of a copolymer containing an scl-monomer, P(3HB) and a mcl-monomer P(3HO). This copolymer exhibited an interesting thermal property, a very high T_m peak of 167.07°C and absence of T_g peak when compared to polymers produced from other carbon sources. Typically, a crystallisation peak was also observed for the polymer which is characteristic of the hard and brittle scl-PHA family (**Figure 4.24**).

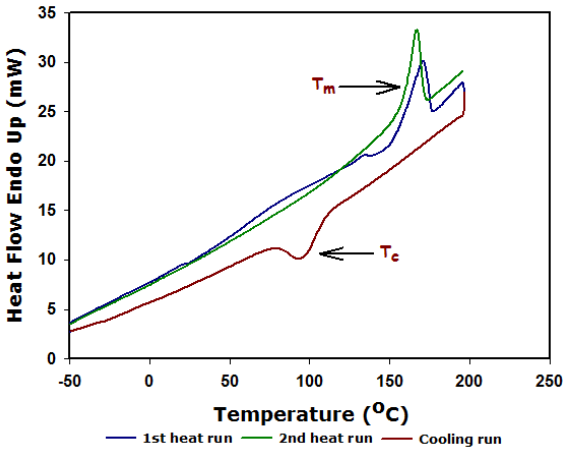

Figure 4.24: Thermal profile of the polymer extracted from lyophilised *P. mendocina* cells grown in sucrose. The figure shows the normalised DSC heating curve showing the peak for glass transition temperature, T_g = -61°C, the peak for the melting temperature, T_m = 167.07°C and peak for crystallisation, T_c = 94.88°C

4.2.5. Detailed characterisation of P(3HO)

4.2.5.1. Downstream processing study

Fermentation conditions and downstream processing such as biomass pre-treatment, extraction method employed and subsequent steps of polymer purification all have a combined effect on the yield of the extracted polymer, molecular weight and processability of the extracted polymer (Sudesh *et al.*, 2000; Furrer *et al.*, 2007). Therefore, different extraction methods such as extraction using dispersion of $CHCl_3$ and NaOCl (Hahn *et al.*, 1993; Hahn *et al.*, 1994; Hahn *et al.*, 1995), soxhlet extraction (Ramsay *et al.*, 1994), extraction using acetone (Jiang *et al.*, 2006) and temperature dependent extraction using hexane (Furrer *et al.*, 2007) were studied for their effects on the polymer P(3HO) produced from *P. mendocina* using octanoate feed. Detailed description of these extraction methods are given in section 2.5.

Extraction of the polymer using the dispersion of NaOCl and $CHCl_3$ gave the highest yield of polymer which was 31.38 % dcw. The yield obtained from other extraction methods were found to be, using $CHCl_3$, 23.04 % dcw; using acetone, 21.38 % dcw; soxhlet extraction, 12.64 % dcw and temperature dependent extraction using hexane, 8.83 % dcw **(Table4.4).**

Extraction Method	Yield(% dcw)	Mn	Mw	PDI	T_g (^oC)	T_m (^oC)	ΔH_f (J/g)	Endotoxicity (EU/ml)
Soxhlet	12.64	266000	469000	1.76	-36.18	48.31	7.44	1.11
Dispersion	31.38	122000	225000	1.84	-35.46	48.45	12.10	4.3
Acetone	21.38	283000	585000	2.06	-34.51	49.46	16.59	3.57
Chloroform	23.04	210000	463000	2.20	-35.81	39.21	9.77	2.38
Hexane	8.83	264000	598000	2.26	nd	47.99	6.62	3.43

Table 4.4: Compilation of the yields, endotoxicity, molecular weights and thermal properties of P(3HO) extracted using different extraction techniques. Where, Mw = Weight average molecular weight; M_n= Number average molecular weight; PDI= Poly dispersity index (M_w/M_n); T_g= Glass transition temperature; T_m= Melting temperature; ΔH_f = Heat of fusion; dcw = dry cell weight; nd = not determined.

4.2.5.1.1. Molecular weight analysis:

GPC analysis confirmed that the extraction method has a significant effect on the molecular weights of the extracted polymer. The molecular weight and the polydispersity index value of the extracted polymer using different techniques are compiled in **Table 4.4**. PDI is a measure of the distribution of the molecular masses in a given polymer sample. The PDI value of P(3HO) was found to be between 1.76 to 2.26. The P(3HO) extracted using hexane was found to have the highest molecular weight, M_w of 5.98 x 10^5, M_n of 2.64 x 10^5, with a PDI value of 2.26. On the other hand P(3HO) extracted using a dispersion of $CHCl_3$ and NaOCl, had the lowest M_w value of 2.25 x 10^5, M_n of 1.22 x 10^5 with a PDI value of 1.84. Also the PDI values for polymer extracted using the dispersion (1.84) and the soxhlet extraction methods (1.76) were low in comparison to the PDI values of polymer extracted from other methods. Polymer extracted using acetone had a M_w of 5.85 x 10^5 and a M_n of 2.83 x 10^5 with a PDI value of 2.06.

4.2.5.1.2. Thermal properties:

The thermal properties of the polymer are crucial for its processability. Therefore, detailed studies were carried out to see the effect of different extraction methods on the thermal properties T_m, ΔH_f and T_g for P(3HO) as shown in **Table 4.4.** Thermal studies show that the extraction method employed does influence the thermal properties of the polymer. The T_g value of P(3HO) extracted using different methodologies differed but were much lower than room temperature, ranging between -34.51 to -36.18^{o}C. The melting temperature of the polymer also differed and was between 39.21 to 49.46^{o}C. The ΔH_f was highest for P(3HO) obtained from acetone (16.59 J/g) and lowest for that extracted from hexane (6.62 J/g). The highest value of ΔH_f observed was for the acetone extracted P(3HO) in accordance with the fact that the highest T_m observed was also for the acetone extracted P(3HO)

(**Table 4.4**). An interesting observation was that no T_g was observed for P(3HO) extracted using hexane.

4.2.5.1.3. Endotoxin study:

The polymers extracted were not subjected to any additional steps of polymer purification. The endotoxin level in these extracted polymers was quantified using the FDA approved Limulus Amebocyte Lysate (LAL) test as described in section 2.8.4.3. The polymer extracted using dispersion of $CHCl_3$ and NaOCl had the highest level of endotoxin, 4.8 EU/mL. In the acetone extraction method the endotoxin level was lower than that extracted from the dispersion method (3.57 EU/mL), but was comparable to that extracted using hexane (3.43 EU/mL). For $CHCl_3$ extraction, the polymer's endotoxin content was 2.38 EU/mL, which was lower than that extracted using dispersion, acetone and hexane but was higher than that extracted using soxhlet method. The polymer extracted using the soxhlet method had lowest endotoxin level, 1.11 (EU/ml).

The polymer extraction using the dispersion of hypochlorite and chloroform was further optimised as described in section 2.5.1. The polymer extracted using this optimised method was then subjected to sequential repeated steps of polymer purification as described in section 2.6. The endotoxin level in the purified polymer was then quantified using the Limulus Amebocyte Lysate (LAL) test (section 2.8.4.3). The endotoxin level in the purified P(3HO) was found to be 0.35 EU/mL. Thus, the purification steps had efficiently removed the coprecipitated LPS. Thermal analysis on this polymer was also carried out. The T_m of the polymer was found to be 45°C with ΔH_f = 9.30 J/g. The glass transition temperature T_g was -36.05°C. Molecular weight analysis of the polymer (**Figure 4.25**) showed that the M_n value of the polymer was 1.43 x 10^5, M_w was 3.12 x 10^5 with a PDI index of 2.17.

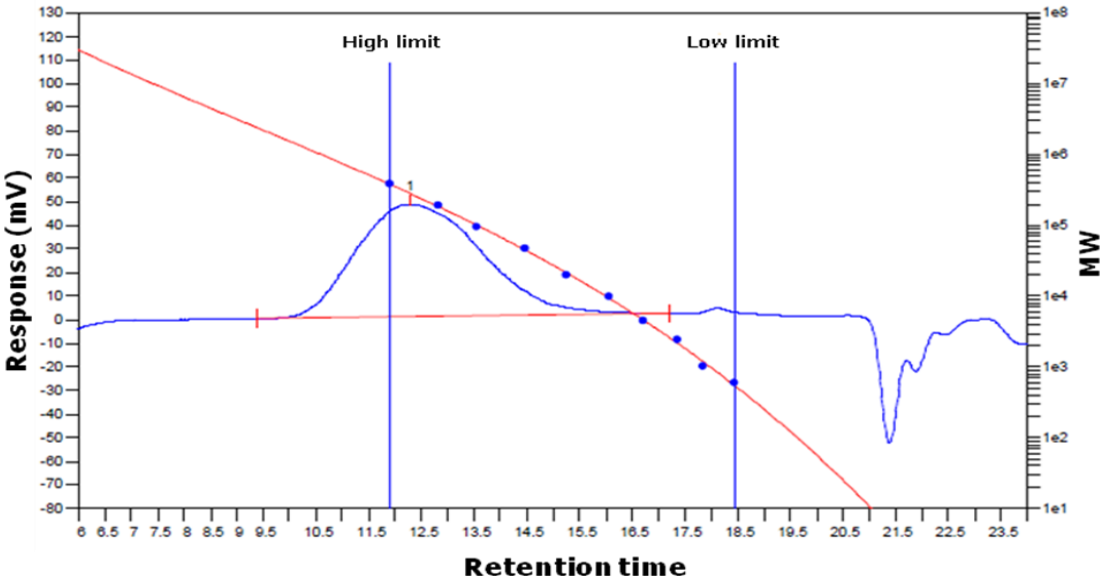

Figure 4. 25: GPC spectrum of the purified P(3HO) produced from *P. mendocina* when grown in octanoate.

Hence, the downstream processing study showed that the kind of extraction method employed has a significant effect on the yield, thermal properties, molecular weight and LPS content of the polymer.

4.2.5.2. Mechanical properties

The extracted P(3HO) produced from *P. mendocina* using octanoate was subjected to static mechanical tests. P(3HO) strips of 10mm length, 4mm width and 0.63 to 0.70 mm depth was prepared from cutting films made using the compression technique (see section 2.12.1). The stress strain curve of the polymer obtained from static tensile test study was typical of those observed for elastomeric polymers. No yield stress or knee i.e. the point of discontinuity appeared in the slope of the stress strain curve as shown in **Figure 4.26**. The Young's modulus (E) value of the polymer was 11.4 MPa which was calculated from the slope of the stress-strain curve.

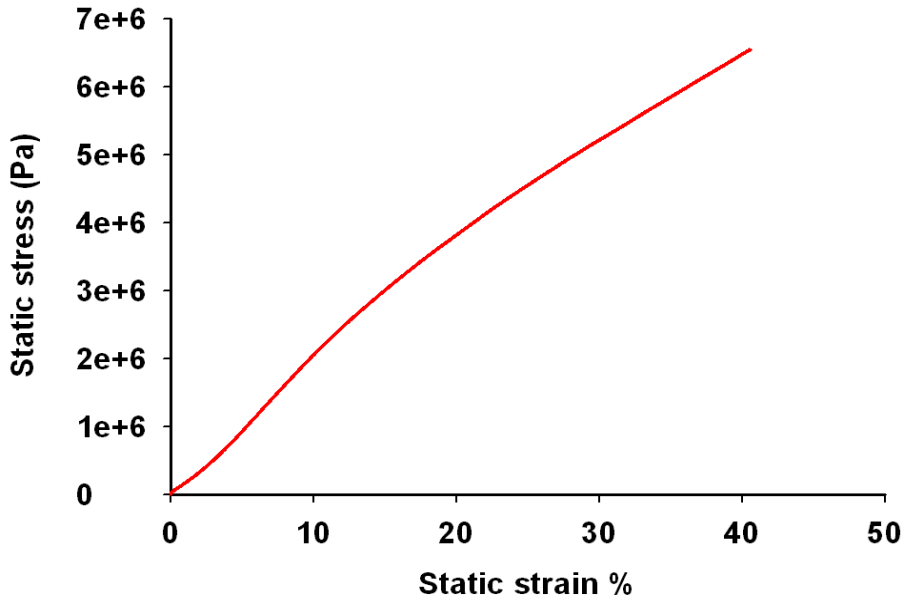

Figure 4.26: Stress strain curve for P(3HO) produced using the compression technique.

Dynamic mechanical analysis of the polymer was also carried out to study the viscoelastic properties of the polymer, loss modulus and storage modulus as a function of temperature. P(3HO) being a polymer stores mechanical energy without dissipation (storage modulus) which represents the elastic portion of the polymer. It also dissipates energy on deformation (loss modulus) which represents the viscous portion of the polymer. The internal friction between the polymer chains can be quantified by tan δ, which is the ratio of the loss modulus to that of storage modulus. **Figure 4.27** shows the strain response (loss modulus) to applied stress (storage modulus) of the extracted P(3HO). The temperature range used for the study was -50 to 80^{o}C. Detailed data for the viscoelastic properties of the polymer at different temperature is shown in **Table 5.** The storage modulus and loss modulus both showed a decrease in their values with increasing temperature.

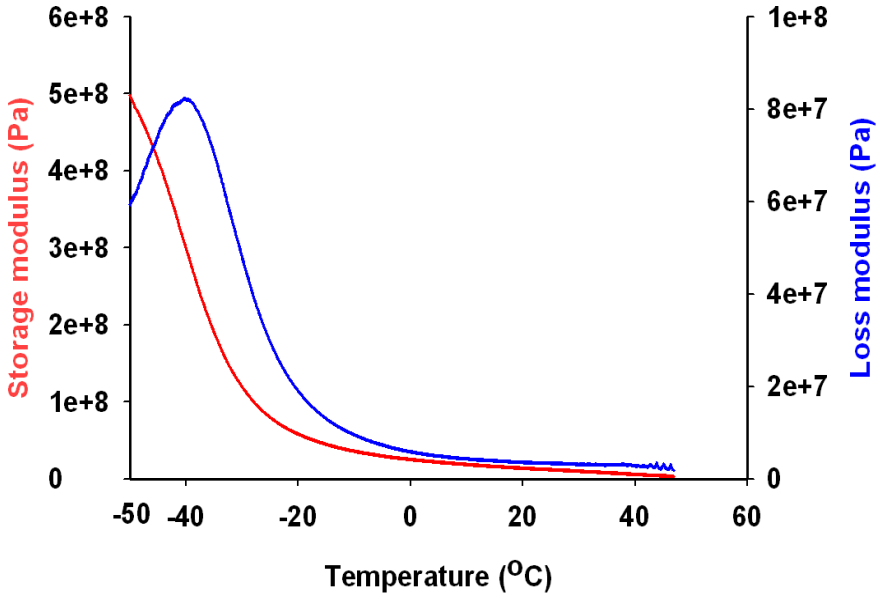

Figure 4.27: The viscoelastic properties of P(3HO) as a function of temperature. Storage modulus and loss modulus was measured between -50 and 60°C.

Temperature (°C)	-50	-20	0	20	40
Storage modulus (Pa)	5.1 X 10^8	6.0 X 10^7	2.4 X 10^7	1.3 X 10^7	5.1 X 10^6
Loss modulus (Pa)	6.0 X 10^7	2.0 X 10^7	6.0 X 10^6	3.4 X 10^6	2.7 X 10^6
Tan δ	0.12	0.33	0.25	0.26	0.52

Table 4. 5: Compilations of the changes in storage modulus, loss modulus and tan δ at different temperatures.

4.2.5.3. Crystallinity

The crystallinity % of P(3HO) was determined using X-ray diffraction patterns of P(3HO) films (prepared using compression technique as described in section 2.8.3) with different levels of ageing. **Figure 4.28(A)** corresponds to the diffractogram of P(3HO) without ageing and **Figure 4.28(B)** corresponds to the diffractogram of P(3HO) which was aged for four weeks at room temperature so that it could achieve maximum crystallinity. The %

crystallinity for the polymer was found to be 37.2 % after ageing using both Lorentzian and Gauss models.

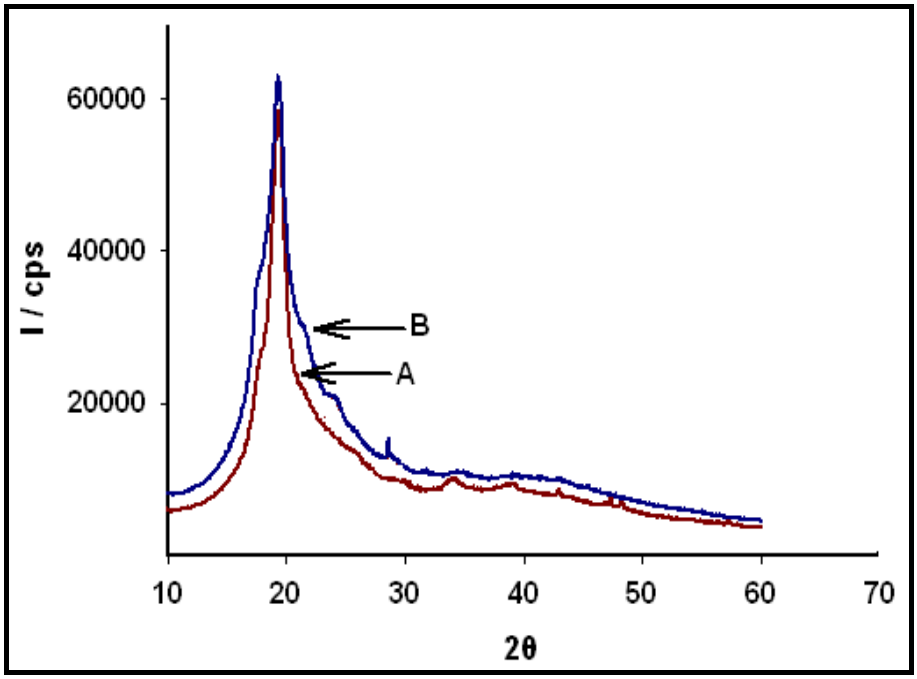

Figure 4.28: X-ray diffractograms of (A) the unaged P(3HO) film and (B) the aged film.

4.2.6. Optimisation of P(3HO) production

Studies were carried out to optimise the yield of the P(3HO) produced from *P. mendocina* using octanoate as feed. The optimal condition for P(3HO) production was investigated using conditions dictated by an appropriate partial factorial design (refer section 2.4.1.2). Four different fermentation conditions were generated from the partial factorial design using variations in agitation speed of the stirrer, (rpm), carbon to nitrogen ratio (C/N) in g/g and pH of the medium. The fermentation conditions generated are tabulated in **Table 2.11** (refer section 2.4.1.2).

The fermentation profile for *P.mendocina* when grown under condition 1, pH stat of 6.8, the initial C/N ratio of the medium, 10:1 (g/g) and the rpm set at

150 is shown in **Figure 4.29**. As the organism started to grow it began to utilise the carbon source provided, as reflected in the decreasing carbon profile. The nitrogen source provided to the organism also started to decrease as the fermentation progressed (data not shown). Within 3 hrs of fermentation there was a sharp decrease observed in the oxygen concentration in the medium which again started to increase after 33 hrs into the fermentation. The dry cell weight of the organism ranged between 0.86 to 1.70 g dcw/L. It increased steadily upto 36 hrs (1.70 g dcw/L) after which it decreased. The organism had started to accumulate polymer within 12 hrs of fermentation but the amount produced was too low to be quantified. The maximum yield of P(3HO) accumulation was achieved at 36 hrs, at which point the cells had accumulated polymer upto 18.18 % of its dcw.

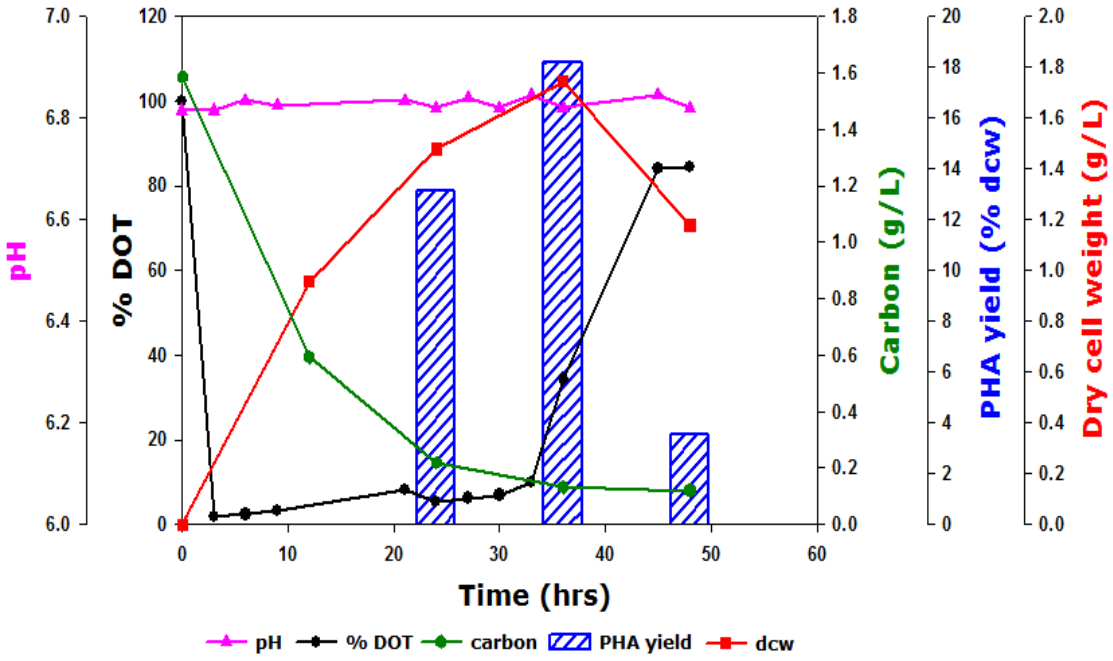

Figure 4.29: Growth and accumulation of P(3HO) by *P. mendocina* when grown under conditions of rpm = 150, C/N = 10:1 and pH = 6.8.

The fermentation profile for *P. mendocina* grown under condition 2, i.e. a constant rpm of 250, pH stat of 7.5 and an initial C/N ratio of 10:1 (g/g) is shown in Figure 4.3**0**. Under these conditions the organism grew well, with

dry cell weights varying between 1.05 to 2.86 g dcw/L. These conditions also led to the maximum production of P(3HO), when compared to all other conditions with yield reaching upto 35% of the dcw. At this time point of 36 hrs the amount of carbon present in the medium was 0.13 g/L and nitrogen was 22.3 µg/L. As the fermentation progressed the oxygen concentration decreased, within 3 hrs the amount had dropped to 20 % and again started to increase after 36 hrs of fermentation.

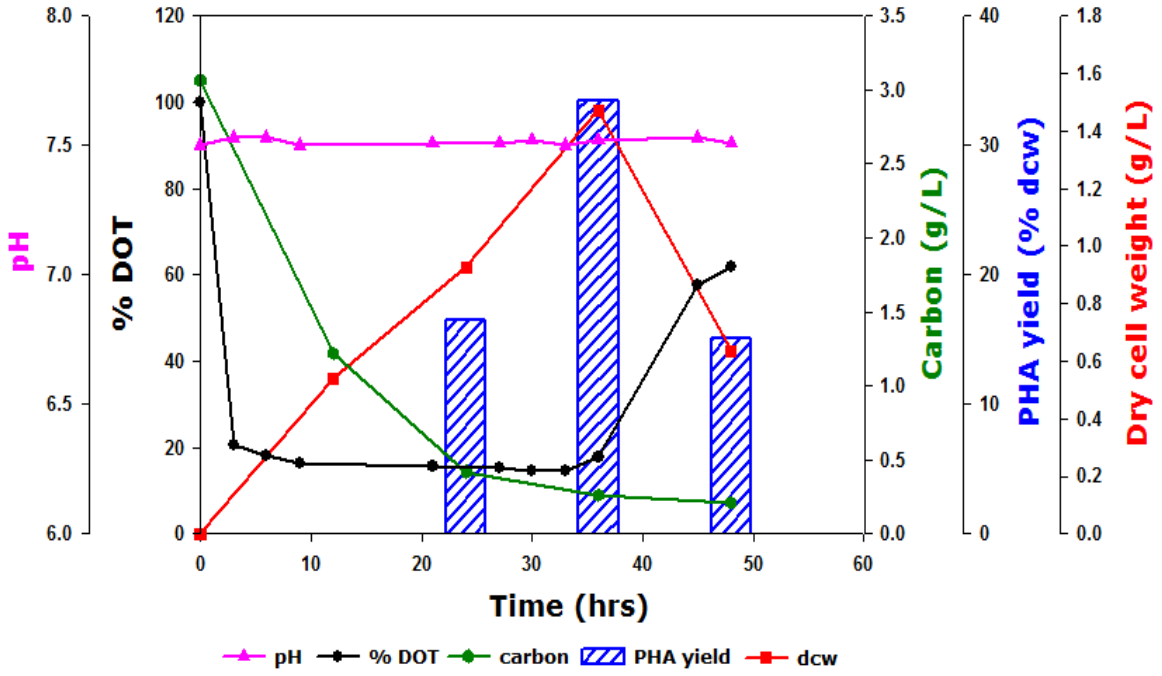

Figure 4.30: Growth and accumulation of P(3HO) by *P. mendocina* when grown under conditions of rpm = 250, C/N = 10:1 and pH = 7.5.

The fermentation profile for *P. mendocina* when grown under condition 3, constant rpm of 150, pH set to and maintained at 7.5 throughout the run and an initial C/N ratio of 20:1(g/g) is shown in **Figure 4.31.** The % DOT had dropped from 100 to about 1% within 3 hrs of the fermentation. The drop in oxygen continued till about 20 hrs and had reached 8% after which it started to increase. The amount of carbon had also dropped from an initial value of 1.5 g/L and reached 0.26 g/L within 48 hrs. Similarly, the levels of nitrogen also decreased as the fermentation progressed. At 48 hrs the level had

dropped from 82.45 mg/L to 2.6 mg/L. The dry cell weight achieved under this condition was between 0.75 to 1.40 g dcw/L and the polymer yield achieved ranged between 5.60 to 13.80 % dcw. The highest dry cell weight (1.40 g dcw/L) and polymer yield (13.80 % dcw) was observed at 36 hrs, after which both dry cell weight and the polymer yield decreased. The organism had begun to accumulate polymer by 12 hrs but not in sufficient quantifiable amounts.

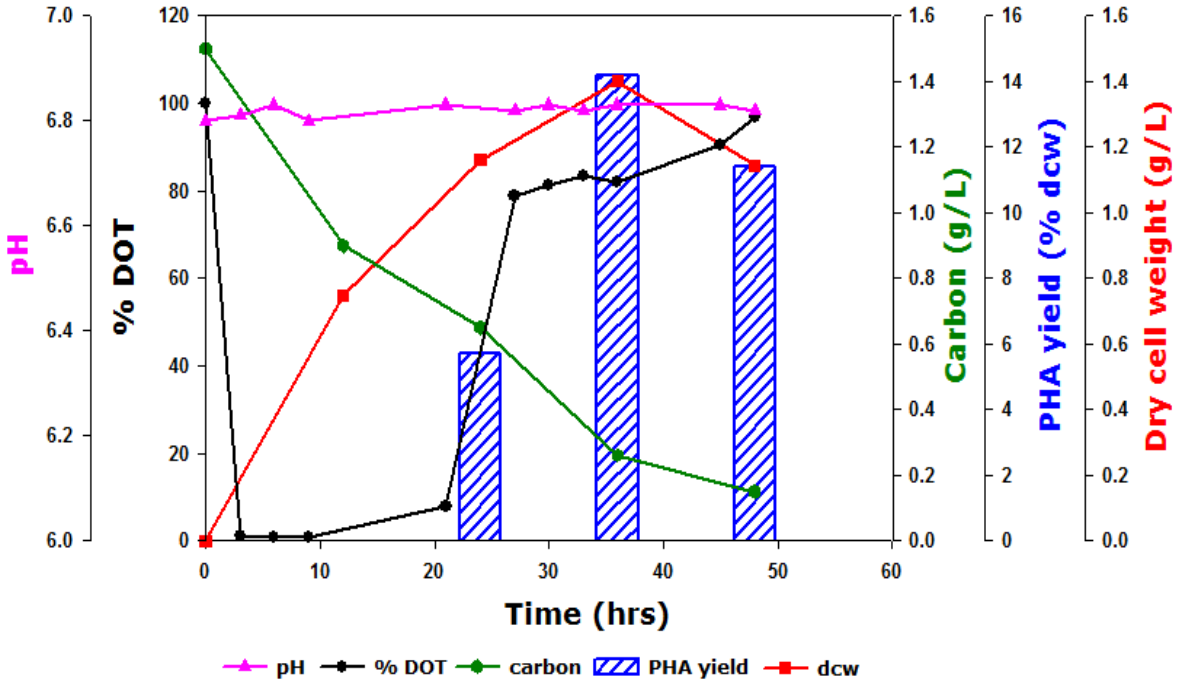

Figure 4.31: Growth and accumulation of P(3HO) by *P. mendocina* when grown under conditions of rpm = 150, C/N = 20:1 and pH = 6.8

Finally, the fermentation profile for *P. mendocina* when grown under condition 4, a pH stat of 7.5, the stirrer speed maintained at a constant rpm of 250 and an initial C/N ratio of 20:1(g/g) for the final media is shown in **Figure 4.32.** With the growth of the organism both the amounts of carbon and nitrogen present in the media decreased. Within 3 hrs of fermentation a sharp decrease in the amounts of oxygen was observed, the amount had dropped from 100% to reaching low levels of 2%. However, after 20 hrs of fermentation the level of oxygen started to increase. The dry cell weights of

the organism ranged between 0.98 to 1.55 g dcw/L. It increased steadily upto 36 hrs (1.55 g dcw/L) after which it decreased. The organism had started to accumulate polymer within 12 hrs of fermentation but the amount produced was too low to be quantified. The polymer had accumulated to a maximum of 14.80 % of the dcw at 36 hrs. By 48 hrs the yield had decreased to 12.30 % dcw.

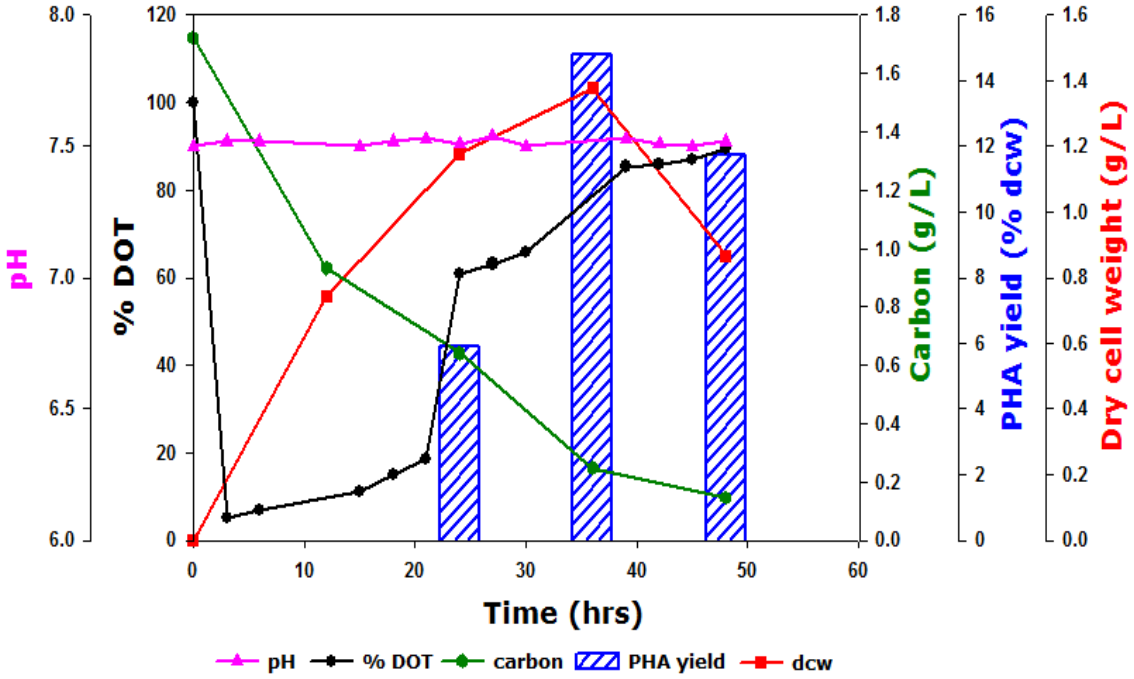

Figure 4.32: Growth and accumulation of P(3HO) by *P. mendocina* when grown under conditions of rpm = 250, C/N = 20:1 and pH = 7.5

4.3. Discussion

4.3.1. Selection of mcl-PHA production media

During this study the *Pseudomonas* sp. were grown in different PHA production media to see if the organisms had selective media preference for growth and accumulation of PHAs. Media selection is important because the media composition and in particular the carbon source play an important role

of supporting both the organism's growth and the accumulation of PHAs. It was found that the organisms under study did have selective preference for media to support its growth and PHA accumulation. *P. putida* preferred E2 medium and *P. aeruginosa* the ME2 medium for PHA accumulation. *P. oleovorans* accumulated higher yields of polymer in E2 medium. MSM medium was preferred for both growth and PHA accumulation by *P. mendocina*.

This preference of a particular media for PHA production shown by the various organisms is possibly due to the regulation of the expression of the PHA biosynthetic genes by environmental signals, in this case nutrient composition. It has been seen that PHA accumulation occurs in most bacteria in response to nutrient limitation (nitrogen in all our study). Thus, in all the media used for the study, the amount of nitrogen 'N' was much less than the amount of carbon, 'C' leading to high C/N ratio (**Table 4.2**); the C/N ratio of the media used in this study was calculated in g/g, all the C/N values reported in literature have also been calculated in g/g. In nitrogen deficient E2 media the carbon to nitrogen ratio of 1 was conducive for *P. putida* and *P. oleovorans* to produce PHAs. *P. aeruginosa* grew but did not produce polymer in this E2 medium, however it grew and produced polymer in ME2 medium which had a higher C/N ratio of 17. Thus *P. aeruginosa* required a much higher C/N ratio to accumulate PHAs. The highest yield of PHA, i.e. 31.38 % dcw, was obtained when *P. mendocina* was grown in octanoate at a C/N ratio of 20 (**Table 4.2**). When grown in heptanoate, the starting C/N ratio was 23 and under this condition the highest accumulation of PHA achieved was 16.33 % dcw. Similarly for production using nonanoate, the starting C/N ratio was 15.54 and under this condition the organism was able to accumulate the polymer upto a maximum yield of 27.27 % of the dry cell weight. However, when grown in carbohydrates (20 g/L each) the starting C/N ratio was 58 for glucose, 67 for sucrose and 53 for fructose. Studies carried out by He *et al.*

(1988) using *P. stutzeri* 1317, showed that the organism when fed on glucose and ammonium sulphate at a C/N ratio of 39 accumulated mcl-PHAs upto 52% of its dry cell weight (He *et al.*, 1998). A recombinant strain of *P. putida* KT2440 was grown on various carbon sources with ammonium chloride as the nitrogen source to study mcl-PHA accumulation. The C/N ratio in the feed were 2.89, 3.46, 5.99 and 5.55 for octanoate, decanoate, glucose and gluconic acid respectively. Under all these conditions the organism accumulated mcl-PHAs with yield ranging between 25 to 27.6 % dcw (Shin *et al.*, 2002). In yet another study *P. putida* KT2442 accumulated mcl-PHA upto 38.1% dcw when grown on decanoate and $NaNH_4HPO_4$ at a C/N ratio of 143 (Huijberts and Eggink, 1996). Studies carried out on *P. citronellois* showed that the organism when grown on octanoate and ammonium sulphate at a C/N ratio of 25 accumulated mcl-PHA upto 36.2 % dcw (Choi and Yoon, 1994).

Hence the range of C/N ratios used in this study was between 9 to 67. Under this range of C/N used, the PHA yields obtained varied between 4.60 to 31.38 % dcw. When compared to literature, for C/N ratios varying between 2.89 to 39 the PHA yield obtained under this range was 25 to 52 %. Thus, the kind of PHA production medium used i.e. its chemical composition and the C/N ratio used as in the case of nitrogen limitation play a very important role in the growth and PHA accumulation of microorganism.

4.3.2. Screening of *Pseudomonas* sp. for mcl-PHA production

P. oleovorans was able to grow and accumulate polymer when grown on both E and E2 media using octanoate feed. Maximum accumulation of the polymer was 29.2 % dcw at 24 hrs in the E2 medium and 15.50 % dcw at 29 hrs in the E medium after which the yield decreased. Similarly *P. putida* and *P. aeruginosa* accumulated maximum amounts of PHA, 11.60 % dcw and

11.40 % dcw, at 48 hrs, in E2 and ME2 media. After maximum accumulation, the yield were observed to decrease. This decrease in the PHAs observed could be possibly because the organisms start utilising these accumulated PHAs as an energy resource to support its growth. Therefore, to achieve a high yield of PHA production this further utilisation of the accumulated PHAs by the organism needs to be eliminated. One such approach is to carry out a two step fermentation, whereby a high cell concentration is achieved in the first step followed by limiting the organism growth in the second step in order to induce maximum PHA accumulation. For example Kim *et al*., 1997 carried out a two step fed batch cultivation of *P. putida* by combining the use of glucose and octanoate. They first grew the organism in glucose which is a good carbon source for cell growth, to obtain a high cell concentration. Next, the organism was grown on octanoate for the PHA accumulation. Using this approach a PHA yield of up to 40 % dcw were achieved. High yields of PHAs have also been observed for pH stat fermentation, in which the pH is maintained by a feed containing carbon and nitrogen in a defined ratio. For example, *P. oleovorans* was able to accumulate PHAs upto 62 to 75 % of its dcw when pH stat fermentation was carried out with a feed containing carbon and nitrogen source in a ratio of 10, 20 and 100. Maximum accumulation of 75 % dcw was achieved when the C/N feed of 10:1 was used. Continuous cultivation have also been proposed which allows growth of an organism under a defined limitation under prolong periods of time (Durner *et al*., 2000).

NMR analysis confirmed that the polymer extracted when *P. oleovorans* was grown on E2 medium, using octanoate, contained 3-hydroxyoctanoic acid, 3HO and 3-hydroxyhexanoic acid, 3HHx. However, the GCMS analysis only showed the presence of 3HO. This could be because the amount of the 3HHx monomer present in the polymer was too low to be detected during GC-MS analysis. Alternatively, the 3HHx structure may not be present in the GC-MS

(NIST) library, hence, the monomer could not be matched in the library and hence not detected.

The monomers 3HHx and 3HO identified in the extracted polymer in this present study was also observed by Durner *et al.* (2000). They found that *P. oleovorans* when grown on dual carbon and nitrogen limitations in E medium using octanoate feed, accumulated 3-hydroxyoctanoate (88 mol %) and 3-hydroxyhexanoate (12 mol %) (Durner *et al.*, 2000). However, in a recent study by (Elbahloul and Steinbüchel, 2009) it was found that *P. putida GP01 (P. oleovorans)* accumulated PHA compolymer with 3HO as the predominant monomer (96 mol %) along with minor constituents of 3HHx, 2.8 mol % and 3HD, 0.9 mol % when grown on octanoate using MSM medium. In this study, a fed batch fermentation at pH stat of 7 was carried out. Thus, from this present study and from what has been reported in literature, *P. oleovorans* when grown in octanoate accumulates 3HO as the major monomer; also the cultivation conditions and media composition used have an effect on the PHA monomers accumulated and also on the yield of the polymer. This observation is in allighnment with the observations that PHA production is affected by the organism used, the culture conditions and the carbon source provided (Anderson and Dawes, 1990; Lee *et al.*, 1995).

P. oleovorans when fed on octanoic acid, utilizes the fatty acid oxidation pathway of the organism for the conversion of the octanoic acid to the corresponding 3-hydroxyacyl-CoA. These 3-hydroxyacyl-CoA substrates are then polymerised by the PHA synthase into the corresponding PHAs (Durner *et al.*, 2000). Accumulation of P(3HO) as a major monomer is also consistent with the fact that 3HO is most common monomer produced when most *Pseudomonas* sp. are grown on even numbered carbon sources (Kim *et al.*, 2007). In this present study the presence of 3HHx monomer in the polymer could also be explained by the fact that when grown of fatty acids of 6-12 carbon atoms; the organisms usually accumulate monomers of the same chain

length as the carbon source provided and monomers shortened by two, four or six carbon atoms due to the fatty acid ß-oxidation pathway (Huisman *et al.*, 1989; Ballistreri *et al.*, 2001).

Interestingly, GC-MS and ^{1}H NMR analysis, showed that *P. aeruginosa* accumulated a copolymer containing 3HO and 2HDD when grown in octanoate. The formation of the 2-hydroxydodecanoyl-CoA required for the synthesis of this copolymer could be due to the elongation of octanoyl-CoA by condensation of two acetyl-CoA moieties generated via the fatty acid *de novo* biosynthetic pathway during the utilisation of octanoate. However, the presence of the hydroxyl group at the 2 position rather than the normal 3 position is unusual and indicates the presence of a unique metabolic pathway or enzyme in this particular strain of *P. aeruginosa.* Thus, possibly as the PHA monomers are being produced, a water molecule is lost resulting in the formation of a C_2=C_3 double bond. Following this, a rehydration reaction possibly results in the addition of an -OH group onto the C_2 position.

P. putida was also able to accumulate PHA when grown in octanoate. Similar observation of mcl-PHA accumulation has been made when *P. putida* was grown in octanoate (Kim *et al.*, 2000; Lee *et al.*, 2000). These results therefore show that both *P. putida* and *P. aeruginosa* can accumulate mcl-PHAs when grown on the structurally related carbon source, octanoate. Though, production of mcl-PHAs from structurally unrelated carbon sources have been reported in other strains of *P. aeruginosa* and *P. putida* e.g. *P. putida* KT2442 (Huijberts *et al.*, 1992), *Pseudomonas* sp. strain NCIMB 40135 (Haywood *et al.*, 1990), this was not the case with the strains used in this work. When grown using structurally unrelated carbon sources such as glucose, the organism must first be able to metabolise the substrate into acetyl-CoA which would then enter the fatty acid *de novo* biosynthetic pathway for the production of the mcl-PHAs. Here the enzyme acyl-CoA-ACP transferase (encoded by *phaG*) links fatty acids *de novo* synthesis with mcl-

PHA production, as shown in **Figure 1.4**. Therefore, the inability of the organisms to produce mcl-PHAs could be ascribed to the lack of this transferase activity.

4.3.3. Production and characterisation of mcl-PHAs from *P. mendocina*

P. mendocina was the main focus for the production of mcl-PHAs during this study. The organism was grown in both structurally related and unrelated carbon feed using a two stage seed culture preparation. The second stage seed culture which was carried out in the PHA production media was used to facilitate improved acclimatisation of the organism in the media. Such acclimatisation would enable better growth and adaptation by the organism in the final PHA production media. When grown in the MSM media with excess of carbohydrates such as glucose, sucrose and fructose (20 g/L) and fatty acids such as hexanoate, heptanoate, octanoate and nonanoate (20 mM) as individual carbon and energy source, the organism was able to grow and accumulate a range of different PHAs with varying yields. These observations could be because of the culture conditions in particular the amount of carbon and nitrogen present in the final production medium at the beginning of fermentation and also the type of carbon feed provided. For instance, in this present study at C/N ratios of 58, 67 and 53, the maximum PHA accumulated by the *P. mendocina* cells were 16.12 % dcw, 23 % dcw and 4.6 % dcw for glucose, sucrose and fructose respectively. Similar studies carried out on the biosynthesis of PHAs, have reported varying yields of PHAs for varying C/N ratios with different carbon feeds. Studies carried out by Haywood *et al.* (1990) showed that *Pseudomonas* sp NCIMB 40135 when grown on carbohydrates such as glucose and fructose were found to accumulate polymer up to 8 and 16 % dcw respectively as opposed to 16.12 and 4.6 % dcw from glucose and fructose observed in this present study. These differences in the

yields obtained could be because in the studies carried out by Haywood *et al*, (1990) a continuous fermentation was carried out hence, a constant nutrient limited condition was maintained with simultaneous supply of excess carbon source. On the other hand, *P. putida* KT2442, when grown in ME2 medium using glucose and fructose at a C/N ratio of 46, each accumulated polymer up to 16.9 % dcw and 24.5 % dcw respectively (Huijberts *et al.*, 1992). Thus the polymer yield obtained for glucose by Huijberts *et al.* (1992) was comparable with the present study (16.12 % dcw) but was six times higher for polymer produced from fructose (4.60 % dcw). One of the major reasons for this difference in the yield of the polymer produced from fructose is possibly due to the C/N ratio; in this present study the C/N ratio for fructose feed was 53, however Huijberts *et al.*(1992) had used a C/N ratio of 46. Therefore, it could be that a C/N ratio of 46 is relatively more favourable over 53 for PHA accumulation using fructose. Sánchez *et al.* (2003) observed PHA accumulation of up to 40 % dcw for *P. putida* IPT046 when grown on carbohydrates, glucose and fructose (Sánchez *et al.*, 2003). However, this high yield of the PHA obtained could be attributed to the fed batch mode of fermentation.

P. mendocina when grown using hexanoate, grew well but no polymer was produced. A similar observation was also made by Tian *et al.* using *P. mendocina* strain 0806 (Tian *et al.*, 2000). *P. oleovorans* was also not able to accumulate PHAs during batch growth in hexanoate (Durner *et al.*, 2000). This indicates that hexanoate possibly led to the induction of the fatty acid β-oxidation related enzymes, but not the related PHA biosynthetic enzymes. Hence, this could be utilised as a carbon source for growth but not for polymer production. The maximum yield of the polymer in this present study was 31.38 % dcw for octanoate feed (C/N = 20), 16.33 % dcw for heptanoate feed (C/N = 23) and 27.27 % dcw for nonanoate feed (C/N = 26). When, *P. putida* GPO1 was observed to accumulate polymer up to 37 % dcw when grown in

octanoate, a chemostat fermentation was carried out with a constant C/N ratio of 15. Therefore, an optimal nutrient condition was available for the organism throughout the fermentation in terms of carbon and nitrogen source. *P. nitroreducens* when grown on octanoate at a C/N ratio of 2 was observed to accumulate polymers of up to 34.3% of its dry cell weight (Yao *et al.*, 1999).

These results showed that *P. mendocina* was able to grow and accumulate PHAs when grown on both structurally related and unrelated carbon sources, however the yields of the PHAs was better in the structurally related carbon source as opposed to the structurally unrelated carbon sources. Similar observations of higher polymer yield from structurally related as opposed to unrelated carbon sources was observed for *Pseudomonas* sp NCIMB 40135 (Haywood *et al.*, 1990) and *P. putida* (Huijberts *et al.*, 1992). One reason for this observation of higher yield for fatty acids as opposed to carbohydrates, could be because of the ease of the utilisation of structurally related carbon sources. These do not need as many modifications as the structurally unrelated carbon sources. Hence, the pressure on the biosynthetic machinery is relatively less leading to a higher yield. Another difference that might have led to the differences in the yields could have been the pH of the media. When grown in fatty acids the pH of the medium which was set at 7 at the start of fermentation increased progressively reaching values of 7.82, 7.72 and 7.35 for octanoate, heptanoate and nonanoate respectively. On the other hand for carbohydrates, the pH of the medium which was also set at 7 showed a slight drop in its values and had reached 6.61, 6.76 and 6.83 for glucose, sucrose and fructose respectively. Kim, 2002 have shown that for *Pseudomonas* sp, pH stat fermentations at 7, led to an increase in the yield of mcl-PHA production when compared to non pH stat study. In this present study the highest yield of the polymer from both fatty acids and carbohydrates was achieved at 48 hrs into the fermentation at which stage the organism was in the stationary

phase. By this time point both the levels of carbon and nitrogen present in the media had really reduced. After 48 hrs of fermentation the polymer yield dropped for all the carbon sources possibly due to the utilisation of PHA for growth under carbon deficient conditions. As PHAs are accumulated as energy resources, therefore it is seen that under carbon limiting conditions the organism starts to utilise the accumulated PHAs to sustain its growth. This utilization of accumulated PHAs by the organisms have been well established (Anderson and Dawes, 1990; Huijberts and Eggink, 1996). All the fermentations carried out were batch fermentations. Since in batch fermentation the media is not replenished therefore the organism has higher possibility of utilizing the accumulated PHA granules when faced with nutrient(s) constrains. Therefore, to prevent this usage of accumulated PHAs, various fermentation strategies have been reported as discussed previously in section 4.3.2.

Once extracted, preliminary characterisation of the polymer was done using ATR-FTIR analysis. The spectrum of the isolated PHAs extracted from all the carbon conditions except sucrose confirmed the presence of polymers of mcl nature (**Figure 4.13).** However, for the polymer extracted from sucrose feed, the ATR-FTIR analysis indicated the presence of both scl and mcl monomers. FTIR analysis was similarly used to confirm the presence of P(3HB) in the polymer extracted from *P. pseudoalcaligenes* LMG 1225 (Randriamahefa *et al.*, 2003). In this present study it was found that the CI values for the polymers produced from carbohydrates (ranging between 1.5 to 2.47) were comparatively higher than the CI values for polymers produced from fatty acids (ranging between 1 to 1.03) except glucose which had a low CI value of 0.87. These results therefore suggest that the polymers produced using carbohydrates have higher crystallinity when compared to polymers produce from fatty acid except glucose. Similarly a low CI value of 0.41 was observed for polymer (78-92 mol-% 3(HO)-co-4-17mol% 3-hydroxycaproate (HC)-co- 2-11

mol-% 3(HD)) produced from *Pseudomonas* sp. Gpo1 105816, also grown on octanoate (Randriamahefa *et al.*, 2003). Ouyang *et al.* (2007) found that on increasing the 3-hydroxydodecanoate 3HDD fraction in the copolymer, P(3HHx-co-3HO-co-3HD-co-3HDD) from 15 to 30 mol % the CI value increased from 0.23 to 0.46, it was still however lower than CI values reported for polymers from carbohydrates (Ouyang *et al.*, 2007). The CI value of P(3HB) has also been reported using FTIR, 1.75 (Valappil *et al.*, 2007). Thus CI value for P(3HB) an scl-PHA is higher compared to the mcl-PHAs and its copolymers reported in this present study and that in literature. This is expected as scl-PHAs are found to have higher crystallinity than mcl-PHAs.

It has been described in literature that *Pseudomonas* sp. uses the fatty acid β-oxidation pathway when grown in structurally related carbon sources and the *de novo* fatty acid synthesis pathway when grown in structurally unrelated carbon sources. As *P. mendocina* is able to accumulate PHAs using both fatty acids and carbohydrates, therefore, one can conclude that the organism is able to utilise both the fatty acid β-oxidation pathway and the *de novo* biosynthetic pathway to metabolise these carbon feeds respectively to produce the medium chain length hydroxyacyl CoA substrates, mcl-HACoAs. These mcl-HACoAs are then polymerised by the PHA synthase to mcl-PHAs.

In depth ^{1}H, ^{13}C and HSQC NMR analysis of the polymer produced from octanoate has further confirmed the results of the GC-MS analysis and established without any doubt that the polymer produced by *P. mendocina* using octanoate as the sole carbon source is the homopolymer poly(3-hydroxyoctanoate), P(3HO). This is a very unusual finding since in all other known cases a copolymer of P(3HO) containing other monomers have been obtained. Tian *et al.* (2000) have observed the production of a copolymer of P(3HO) and poly(3-hydroxydecanoate) using *P. mendocina* 0806 grown on octanoate (Tian *et al.*, 2000). The most well studied *Pseudomonas* sp. like

P. putida GPO1 or *P. oleovorans* (Preusting *et al.*, 1990; Durner *et al.*, 2000; Hartmann *et al.*, 2006; Elbahloul and Steinbüchel, 2009), *P. aeruginosa* (Ballistreri *et al.*, 2001) and others like *P. putida* IPT046 (Sánchez *et al.*, 2003), *Pseudomonas*. sp 61-3 (Kato, 1996) *P. resinovorans*, *P. citronellolis* (Cromwick *et al.*, 1996), *P. stutzeri* (He *et al.*, 1998) have all been reported to accumulate P(3HO) with varying degrees of other monomeric units present when grown on a range of carbon sources.

^{1}H and ^{13}C NMR analysis confirmed the presence of 3HV, 3HP and 3HN monomers in the polymer extracted from heptanoate. When grown on nonanoate feed NMR analysis confirmed the presence of 3HP and 3HN monomers in the accumulated polymer chains. Similar observations were made when *P. oleovorans* was grown in nonanoate. The organism had accumulated approximately 40 mol % of 3HP and 60 mol % of 3HN (Durner *et al.*, 2000). In yet another study carried out on *P. oleovorans* grown on nonanoate, the organism was able to accumulate monomers of only 3HP and 3HN (Huisman *et al.*, 1989). *P. putida* KT2440 was also reported to accumulate monomers of 3HP and 3HN when grown on nonanoic acid (Sun *et al.*, 2007). As mentiond above the organism used the ß-oxidation pathway to biosynthesize the polymer; During the process the 3-ketoacyl-CoA formed via the ß-oxidation of the fatty acids is cleaved by the ß-ketothiolase to form acetyl-CoA and an acyl-CoA comprising of two less carbons atoms as compared to the acyl-CoA that entered the first cycle. Therefore, the heptanoate substrate resulted in the formation of hydroxyacyl-CoA containing seven and five carbon atoms which eventually gets polymerised into polymer contsining 3HV and 3HP. The accumulation of 3HN could be because of the addition of one acetyl-CoA molecules to the hydroxyacyl-CoA containing seven carbon atoms. Similarly the accumulation of 3HN and 3HP, monomers with nonanoate feed occurred because of the formation of acyl-CoA moeities with nine and two less carbon atoms after the first cycle of ß-oxidation of

nonanoate. These substrates were finally polymerised into polymer containing 3HN and 3HP.

This ability of *P. mendocina* to accumulate monomers from structurally related monomers has been a common observation for *Pseudomonas* sp and have been reported widely (Witholt and Kessler, 1999; Zinn *et al.*, 2001; Kim *et al.*, 2007). The presence of 3HO as the major monomer in the PHA extracted from even chain fatty acids is also consistent with previous published reports of (Lageveen *et al.*, 1988; Durner *et al.*, 2000; Ballistreri *et al.*, 2001).

When grown in glucose, GCMS analysis confirmed the presence of 3HO and 3HD monomers in the extracted polymer. In the GC-MS spectrum, peaks for lipids were also observed, this is because the polymer was not subjected to extensive purification steps like the polymer obtained from octanoate feed. The results of the GC-MS analysis was also confirmed by the ^{1}H proton NMR. For the ^{1}H NMR, however purified polymer was used. It has also been observed that the *Pseudomonas* sp. Strain NCIMB 40135 produced mcl-PHA containing monomers of 3HO and 3HD when grown on glucose (Haywood *et al.*, 1990). Similarly, *P. putida* KT2440 also accumulated monomers of only 3HO and 3HD when grown in glucose (Sun *et al.*, 2007). *P. putida* IPTO46 was also observed to accumulate monomers of 3HO and 3HD when grown on glucose and fructose (Sánchez *et al.*, 2003). When *P. mendocina* was grown on fructose GC-MS analysis indicated the presence of themonomer 3HD. However, when Haywood *et al.* (1990) grew *Pseudomonas* sp. NCIMB 40135 in fructose the organism was reported to accumulate monomers of 3HO and 3HD. *P. mendocina*, used in this study was however unable to produce polymer containing 3HO using fructose indicating a fundamental difference in the metabolic pathway used. Therefore, in this present study, accumulation of these monomers, 3HO, 3HD using glucose, and 3HD using fructose was possibly due to the generation of these substrates via the fatty acid *de novo*

biosynthesis pathway. Interestingly *P. mendocina* accumulated P(3HB-co-3HO) when grown in sucrose as confirmed by GC-MS, ^{1}H and ^{13}C NMR analysis. Accumulation of such copolymers containing both scl and mcl monomers are quite rare. Such production of hybrid copolymers has been described in literature owing to the broad substrate specificity of this class of PHA synthases in some organisms. For example *Pseudomonas* sp. 61-3 accumulated copolymers of 3HB and mcl-monomers when grown in glucanoate as well as alkanoic acids (Kato, 1996). Similarly *Pseudomonas* sp. A33 was able to accumulate the copolymers containing 3(HB) and nine other mcl monomers like 3-hydroxyhexadecanoate, 3(HHD), 3-hydroxydodecenoate, 3(HDDE), 3-hydroxytetradecenoate, 3(HTDE) and 3-hydroxyhexadecenoate, 3(HHDE) when grown using both fatty acid and glucose (Lee *et al.*, 1995). *P. nitroreducens* AS 1.2343 on the other hand was reported to accumulate only P(3HB) when grown on octanoic acid (Yao *et al.*, 1999).

In this present study the monomer 3-hydroxydecanoate was found to be present in all the polymers extracted from the structurally unrelated carbon sources. This observation is in agreement with the observation that several *Pseudomonas* strains when grown on structurally unrelated carbon sources accumulate PHAs consisting predominantly of the 3-hydroxydecanoate monomer unit (Haywood *et al.*, 1990; Huijberts *et al.*, 1992).

Thus, variation was observed in the growth, polymer yields and types of monomers accumulated by the organism *P. mendocina* in this present study and that reported in literature. Broadly culture conditions, carbon source provided and the organism used have an effect on the PHA accumulation, however these factors have a combined and simultaneous effects on PHA production which are complex and not easy to elucidate. PHA metabolism is a complex process that involves regulation at different levels: (I) Activation of *pha* gene expression due to specific environmental signals, such as nutrient starvation; (II) activation of the PHA biosynthetic enzymes by specific cell

components or metabolic intermediates; (III) inhibition of metabolic enzymes of competing pathways and therefore enrichment of required intermediates for PHA synthesis; or (IV) a combination of these (Kessler and Witholt, 2001). Diversity in the PHA biosynthesis capability of *Pseudomonas* could also be attributed to the difference in substrate specificity of the two *pha* genes coding for the PHA synthase in these organisms. *P. mendocina* like other *Pseudomonas* have two *phaC* genes encoding for the PHA synthase. Hein *et al*. (2002) found that *phaC1* codes for the major synthase in *P. mendocina* for PHA production and that *phaC2* encodes an enzyme with a minor role in the accumulation of mcl monomers from structurally unrelated carbon sources. Similarly, in the studies carried out by Conte *et al*. (2006), it was found that in *P. corrugate*, *phaC1* activation occured with any carbon sources but *phaC2* gene expression occurred only in the presence of glucose or sodium octanoate (Conte *et al.*, 2006).

The thermal properties of these polymers were also studied using the differential scanning calorimetry analysis (**Table 4.3**). When grown in fatty acids the highest value for the endothermic transition due to the melting of the crystalline phase, $T_{m,}$ owas observed at 45°C with a ΔH_f = 9.30 J/g for octanoate. For nonanoate the T_m value was 36.16°C with a ΔH_f = 8.96 J/g. Since higher T_m values correspond to higher crystallinity therefore, the polymer obtained using octanoate as the carbon source had the highest crystallinity. Mcl-PHAs crystallise very slowly and for some copolymers no T_m value is observed because the copolymers do not crystallise at all. For example mcl-PHAs bearing phenoxy substituents like poly(3-hydroxy-5-phenylvalerate) are completely amorphous and hence do not have a T_m peak (Kim *et al.*, 1996). No melting peak was observed in the polymer obtained using heptanoate as the carbon source when *P. citronellois* (Choi and Yoon, 1994) and *P. oleovorans* (Gross *et al.*, 1989) were grown on it. The absence of

any T_m peak for the polymer produced using heptanoate indicates the lack of a crystalline phase.

The glass transition due to the amorphous phase occurred at -36.05°C, -27.24°C and -37.53°C for the polymers extracted from octanoate, heptanoate and nonanoate respectively. All these values for the thermal transitions were taken from the first heat scan. For polymers produced from carbohydrates, the T_m and ΔH_f values observed were 37.56°C and 3.82 J/g for glucose, 167.07°C and 126.95 J/g for sucrose and 46.46°C and 5.31 J/g for fructose. The thermal profile of the copolymer P(3HB-co-3HO) produced from sucrose was interesting with a very low T_g and a high T_m values. The high T_m value for the copolymer could be due to the P(3HB) component for the polymer. P(3HB) is known to have a high T_m of 169°C (Misra *et al.*, 2007). Such a high T_m also corresponds to high crystallinity of the polymer which explains the presence of the crystalline peak in the thermogram (**Figure 4.24**). Interestingly during the cooling run the melted disordered polymer chains of the crystalline phase, were able to rearrange themselves in ordered structures. Therefore, during the second heating run the heat supplied was again utilized by the polymer chains to again melt hence a melting peak, T_m was observed.

The T_g value of the mcl-PHA is found to decrease with the increase in the average length of the pendant group caused by the increased mobility of the polymer chains (van der Walle *et al.*, 2001). When *P. oleovorans* was grown on a range of n-alkanoates ranging from C_6 to C_{10} in carbon chain length, a relative decrease in T_g of the PHA produced using hexanoate (T_g = -25°C) to that produced using decanoate (T_g = -40°C), was observed, corresponding to an increase in the average length of the predominant side-chain (Gross *et al.*, 1989). A similar observation was made with a decrease of T_g value of almost 18°C for mcl-PHAs produced from coconut fatty acid (-43.7°C) to that produced from linseed oil fatty acid with a T_g value of -61.7°C (van der Walle *et al.*, 2001). Similarly when *P. mendocina* was grown in the fatty acids, a

decrease in Tg values from -27.24°C for hexanoate to that of -37.53 °C for nonanoate was observed.

The polymers produced from fatty acids have lower values for melting temperature as opposed to polymers produced from carbohydrates. Higher the crystallinity higher is the melting temperature (Philip *et al.*, 2007); thus implying that, the polymers from structurally related carbon sources are less crystalline than those produced from structurally unrelated carbon sources. These results can also be correlated with the crystallinity index for the polymers where by low CI values of around 1 for fatty acids based polymers was obtained as oppose to 1.5 to 2.47 for carbohydrates based polymer except in the case of glucose (0.87). A CI index of 1.03 was observed for the polymer produced from heptanoate however, thermal analysis did not reveal any T_m peak for the polymer. This could be because as mentioned earlier CI index is not an absolute measure of crystallinity.

4.3.4. In depth characterisation of P(3HO)

4.3.4.1. Downstream processing study

PHAs are accumulated by various organisms as water insoluble inclusions. Therefore, extraction of these PHAs is a crucial step in the whole PHA production cycle. This is because the extraction methods employed have a severe bearing on the yield of the extracted PHAs, its molecular weight, thermal processability and on the pharmacological purity of the polymer. Lipopolysaccharide (LPS) is a major component of the Gram negative bacterial cell wall that gets coextracted with the PHAs. LPS is pyrogenic in nature and therefore the extraction methods employed must remove this contaminating LPS in addition to extracting the PHAs. When studies were carried out on the effects of different extraction methods (as describe in section 2.5) on the yield, molecular weights, thermal properties and LPS level

of P(3HO) produced from *P. mendocina* using octanoate it was found that the extraction method does have an effect on these parameters. Extraction of polymer using the dispersion of NaOCl and $CHCl_3$ gave the highest yield of polymer which was 31.38 % dcw. This could be because in this method the cells gets disrupted by the hypochlorite which then provides better access of the accumulated intracellular granules to the chloroform in which it get dissolved. In $CHCl_3$ extraction the yield was 23.04 % dcw and acetone was 21.40 % dcw. This low yields as opposed to the dispersion method could be because in this case, intact cells are incubated with the solvents, so that the solvent can penetrate the cells and dissolve its intracellular PHAs. Therefore, the penetration of the cells by the solvents may not be efficient because of which less PHA granules get dissolved in the extracting solvent, hence less polymer gets extracted leading to lower yields. The low yield during soxhlet extraction, 12.64 % dcw could be because of (i) degradation of polymer by incubating it with hypochlorite; Hypochlorite have been known to degrade polymer (Furrer *et al.*, 2007) and (ii) loss of polymer during repeated washing of the cells following hypochlorite treatment. Mcl-PHAs are soluble in acetone, since one of the solvent used for cell washing was acetone therefore; polymer could have been lost in the process. Temperature dependent extraction using hexane gave yield of only 8.83 % dcw. This method is based on the solubility of the polymer at two different temperatures. Like acetone and chloroform extraction, here too the polymer was incubated only in hexane at temperature of 60^{o}C to extract the intracellular polymer. Therefore, the low yield could be because the solvent was not efficient in penetrating the cell and hence unable to dissolve the polymer, secondly the temperature at 60^{o}C was not optimum to dissolve the intracellular polymer. The extracted polymer was precipitated by lowering the temperature of the hexane polymer solution to 5^{o}C. The lowering of temperature to 5^{o}C may not be sufficient in precipitating all the polymer.

Extraction methods can also affect the molecular weights of the polymer by causing scissions in the polymer chains. This was confirmed when GPC analysis of the polymer extracted using different extraction methods. The PDI value of P(3HO) which was between 1.76 to 2.26, was within the range of what has been obtained previously for mcl-PHA from octanoate. P(3HO) extracted using the dispersion of $CHCl_3$ and NaOCl had the lowest M_w value of 2.25×10^5, M_n of 1.22×10^5 with a PDI value of 1.84. This could be because the NaOCl used had introduced chain scissions in the polymer. Therefore, although the dispersion method resulted in the highest yield of the polymer (31.38 % dcw), hypochlorite has caused some degradation which explains its low molecular weight. In fact sodium hypochlorite has been found to cause severe degradation of the polymer, with up to 50 % reduction in the molecular weight (Lee *et al.*, 1995; Yasotha *et al.*, 2006). However, the extent of this degradation varies considerably between organisms. For example, within Gram-negative organisms, the amount of P(3HB) degraded to a lower molecular weight compound in *A. eutrophus* (75 % reduction in the M_n) during the recovery process, was significantly higher compared to that in recombinant *E. coli* (15 % reduction in M_n). On the other hand extraction of P(3HO) using the temperature dependent extraction of hexane and extraction using acetone were able to efficiently extract high molecular weight long chains of the P(3HO) as compared to other extraction techniques. This could be because of the lack of chain scissions occurring in the polymer because of the absence of NaOCl in these extraction methods. The PDI values of the polymer extracted using soxhlet extraction (1.76) and dispersion (1.84) was the lowest compared to other extractions. Thus, suggesting that the polymer chains extracted using the dispersion and soxhlet extraction methods had uniform distribution of the molecular masses as opposed to other extraction methods.

The molecular weight values thus observed for the extracted polymer in this study were higer than the range that has been observed for mcl-PHAs. The M_w values quoted in literature for mcl-PHAs with both saturated and unsaturated pendant groups lie between the range of 60,000 and 412,000 and M_n between 40,000 and 231,000.

Thermal properties:

The thermal properties of the polymer are really crucial for its processing. Therefore, studies were carried out to see if different extraction methods induced morphological differences in the extracted P(3HO) resulting in different thermal properties. The T_g and T_m values varied for P(3HO) extracted using different methodologies and ranged between -35.04 to -36.18^oC and 39.21 to 49.46^oC. The ΔH_f was highest for P(3HO) obtained from acetone (16.59 J/g) and lowest for that extracted from hexane 6.62 J/g. The highest value of ΔH_f observed for acetone extracted P(3HO) was in accordance with the fact that the highest T_m observed was also for the acetone extracted P(3HO). Since T_m increases with increasing crystallinity, therefore P(3HO) extracted using acetone amongst all the other extraction methods enables maximum close packing of the polymer chains in a regular three dimensional fashion to form crystalline array (crystalline structure). On the other hand P(3HO) extracted using $CHCl_3$ enables minimum close packing of the polymer chain, and hence has the lowest T_m value. An interesting observation was that no T_g was observed for P(3HO) extracted using hexane. As T_g measurement depend on a crystalline transition of the amorphous region, therefore hexane extraction may have allowed some, if not all polymer chains to have a crystalline arrangement, hence the P(3HO) being largely or totally amorphous in nature, may not have or readily exhibited a T_g. In this study, both the T_g and T_m, values observed were lower then what has been reported for mcl-PHAs produced from *P. oleovorans* (T_g = -31^oC, T_m = 56^oC) and *P. aeruginosa*

(T_g = -37°C, T_m = 58°C) using octanoate. This combination of T_g below room temperature and a low degree of crystallinity imparts elastomeric behaviour to this polymer. In fact mcl-PHAs are the only microbially produced biopolymers which exhibit properties of thermoplastic elastomers and resemble natural rubbers produced by *H. brasiliensis* (Steinbüchel and Eversloh, 2003).

The polymer extracted using dispersion of $CHCl_3$ and NaOCl had the highest level of endotoxin, 4.8 EU/mL. This shows that the digestion of the cells by NaOCl released more of the contaminating LPS molecules directly to the $CHCl_3$ containing the dissolved polymer. Since the LPS were also soluble in $CHCl_3$, non solvent precipitation of the polymer in chilled methanol resulted in coprecipitation of the LPS. In the acetone method as the biomass was incubated with acetone into which the polymer dissolved and then precipitated in chilled ethanol. Therefore, the cell wall was quite intact when compared to the dispersion method and hence less LPS may have come in contact with the polymer. Here the endotoxin content was lower than that extracted using the dispersion method but was comparable to that extracted using hexane. In hexane extraction too the cells were not digested by hypochlorite treatment and therefore less endotoxin i.e. LPS coprecipitated with the polymer. In addition it could be possible that LPS did not precipitate out at 5°C. In $CHCl_3$ extraction the dried bacterial biomass is incubated in $CHCl_3$ which is used both as an extractant and as a solvent for the intracellular PHA. The polymer was ultimately precipitated in chilled methanol. Here, the polymer's endotoxin content was 2.38 EU/ml, which was lower than that extracted using dispersion, acetone and hexane but was higher than that extracted using soxhlet method. The polymer extracted using soxhlet method had the lowest endtoxin level, 1.11 (EU/ml). This is due to the rigorous sequential washing of the hypochlorite treated dried biomass with solvents (HPLC water, acetone, ethanol and diethylether) which removes

the LPS and the physical separation of the extract from the cellular debris in the soxhlet extraction method. In this study the polymers extracted were not subjected to any additional steps of purification. It is seen that with subsequent steps of purification the endotoxin content of the polymer decreases. For example when Furrer *et al*. (2007) carried out an additional step of redissolution in 2-propanol at 45°C and precipitation at 10°C for the polymer, a purity close to 100% (w/w) was obtained. The endotoxicity had decreased by 5 times but polydispersity had also decreased from 2.0 to 1.5 (Furrer *et al.*, 2007).

The extraction method using the dispersion of chloroform and hypochlorite was used throughout the study for polymer extraction. This is because amongst all the other methods of extraction, dispersion of hypochlorite and chloroform was very efficient in extracting the polymer. Highest yield of extracted polymer (31.38 % dcw) was achieved using this method. However, as discussed above the polymer had high levels of LPS present (4.5 EU/mL) and also low molecular weight with a low PDI value of 1.84, due to degradation of the polymer by the hypochlorite. Therefore, this method was optimised to extract polymer with higher yields, prevent degradation and reduce the LPS content as described in section 2.5.1. Polymer yield play a very important role for its cost effective production. Also as the polymer P(3HO) produced was to be studied as a potential biomaterial for medical applications (discussed in chapter 5) obtaining a good yield, reducing its degradation and LPS content became very important. In the improved extraction method, the hypochlorite concentration was increased from 30 to 80%, this provided better access to the polymer however to prevent the degradation of the extracted polymer, the amount of chloroform was increased. The hypochlorite to chloroform ratio was increased from 1:1 to 1:4. Chloroform performs a dual function of both extracting the polymer as well as providing protection to the polymer from NaOCl. The incubation time was

also reduced from two and a half hours to 2 hours to reduce the exposure of the polymer to the NaOCl and to reduce its contact with the LPS.

The polymer was also repeatedly purified (refer section 2.6) to remove the contaminating LPS. The polymer in the first step was precepitated using a chilled mixture of 1:1 (vol/vol) of 70% each of methanol and ethanol. Using this precipitation mixture Elbahloul and Steinbüchel, (2009) achieved the polymer extraction of up to 95 % (wt/wt) of polymers in the dried cells. The purity of the polymer was also reported to be 99% ±0.2 % (Elbahloul and Steinbüchel, 2009). The polymer was then subjected to repeated purification by dissolving it in acetone and precipitating in the methanol/ethanol mixture. Acetone was used because it has been reported to have higher solubility for polymer as opposed to LPS thus leading to pure polymers (Jiang *et al.*, 2006). With this improved method of polymer extraction, yield of the polymer achieved was (32 % dcw). This method had definitely increased the efficiency of polymer extraction as the yield obtained (32 %) is after repeated purification of the polymer and in each purification step, polymer is lost. On the other hand the unoptimised method of polymer extraction using the dispersion method had resulted in a yield of 31.38% without the polymer being subjected to any kind of purification. Hence, the yield would have been expected to decrease with further purification of the polymer. GPC analysis of the polymer confirmed that the M_w value for the polymer was 3.12 x 10^5, M_n was 1.43 x 10^5 and the PDI index was 2.17. Thus the molecular weight of the polymer extracted using the optimised method was higher, than the unoptimised dispersion method (M_w = 2.25 x 10^5), thus suggesting that increasing the amount of chloroform had certainly provided increased protection from the degradation effects of hypochlorite. The endotoxin levels in the polymer was found to be 0.35 EU/mL. This complies with the endotoxin requirements of the FDA for biomedical applications such as implants and drug delivery systems (U.S. Department of Health and Human Services,

1997). Thermal analysis on this polymer was also carried out. The melting temperature of the polymer was found to be 45°C as compared to 48.45°C (unoptimised method). The glass transition temperature, Tg was -36.05°C. As higher melting temperature indicates high degree of crystallinity therefore, this low value of the T_m for the polymer implies that the crystallinity of the extracted polymer had reduced. This reduction in the crystallinity of the polymer could be because in the polymer extracted using the unoptimised method, impurities could have been coextracted with the polymer which added to its crystallinity and hence higher melting temperature.

4.3.4.2. Mechanical properties

The stress strain curve of the polymer obtained from the static tensile test study was typical of those observed for elastomeric polymers. No yield stress or knee appeared in the curve as shown in **Figure 4.26**. The Young's modulus (E) value of the polymer was 11.4 MPa which was calculated from the slope of the stress-strain curve. However, in an earlier study carried out by Marchessault *et al.* (1990) the 'E' value for P(3HO) was reported to be 17 MPa (Marchessault *et al.,* 1990). In yet another study carried out by Gagnon *et al.* (1992) the mcl-PHA which had 86% of HO and minor quantities of 3-hydroxydecanoate and 3-hydroxyhexanoate, the 'E' value of the polymer was 7.6 ± 0.5 MPa (Gagnon *et al.,* 1992). Dynamic mechanical analysis of the polymer was also carried out to study the viscoelastic properties of the polymer, loss modulus and storage modulus as a function of temperature. **Figure 4.27** shows the strain response (loss modulus) to applied stress (storage modulus) of the extracted P(3HO). The storage modulus and loss modulus both showed a decrease in their values with the increasing temperature. This could be because under dynamic force with increasing temperature the movement of the polymer chains (viscous flow) decreases, resulting in the decrease of the loss modulus as expected. Similarly the ability of the polymer chains to return to its original shape (elastic behaviour) at the

end of each cycle decreases; hence the ability of the polymer chains to store energy without dissipation also decreases. When studies were carried out on the viscoelastic properties of P(3HB), a similar observation of decreasing storage modulus and loss modulus was obtained within the studied temperature range of -20 to 50^{o}C (Misra *et al.,* 2007)

4.3.4. 3. Crystallinity

The crystallinity % for the P(3HO) was found to be 37.2 % using both Lorentzian and Gauss models. This relatively low crystallinity of the polymer is because of the large pendant side group which makes it difficult to have a close packing in a regular three dimensional fashion to form a crystalline array. Since axial geometry in a chain is a major factor in determining the ability of a chain to form crystallites, therefore the crystalline contribution is probably due to isotactic and syndiotactic structure sequences (Preusting *et al.*, 1990; Sánchez *et al.*, 2003). In fact, saturated mcl-PHAs which are able to crystallise due to their isotactic configuration, are also seen to crystallise with alkyl side chains in an extended conformation to form ordered sheets and are therefore much less crystalline than P(3HB) or P(3HB-co-3HV) owing to low crystallisation rates. Therefore, this explains the low crytallinity of P(3HO), 37.2 % when compared to P(3HB) 46 % (Misra *et al.*, 2007)

4.3.5. Optimisation of P(3HO) production

Production of a homopolymer of P(3HO) has never been reported in literature previously. In this work we have made attempts to find the optimum conditions for P(3HO) production by using initially a design of experiments generated using partial factorial design**.** The fermentation parameters selected and the fermentation conditions generated are discussed in section 2.4.1.2.

As PHAs are accumulated intracellularly by organisms, therefore good growth of the organism is of paramount importance as good healthy bacteria can accumulate these intracellular PHAs. However, as PHA accumulation in organisms is triggered by stressful conditions of nutrient(s) limitations therefore providing an organism with rich medium may lead to good growth of the bacteria without any PHA accumulation. Therefore, a balance must be achieved in providing growth conditions which are able to support growth reasonably the organism but also simultaneously be stressful enough to drive bacteria to accumulate the PHAs. It was because of these reasons that the optimization was carried by using a two stage seed culture preparation. In the first stage, the organism was grown in growth media (nutrient broth) to achieve good growth of the organism. Following this the organism was grown for the second seed culture preparation in the PHA production medium with a C/N ratio of 20. This second seed culture facilitated improved acclimatisation of the organism in the media. Such acclimatisation would enable better growth and adaptation by the organism in the final PHA production media.

The parameters of C/N, pH of the medium and impeller speed have been reported to play an important role in PHA accumulation by microorganisms (Huisman *et al.*, 1989; Philip *et al.*, 2009). Therefore in the final PHA production medium these parameters were considered to be varied as discussed in section 2.4.1.2 to find optimum condition for the production of P(3HO). Under condition 1 the amounts of oxygen between 3-30 hrs of fermentation was very low, ranging between 2-8%. This low level of oxygen would have hindered the growth of the organism resulting in low dry cells weights (3.51 to 18.20g dcw/L) and maximum polymer yield of 18.20 % dcw was achieved. However under condition 2 when pH of the medium was changed to 7.5 and the rpm to 250 highest level of dry cell weights ranging between 1.05 to 2.86 g dcw/L and polymer accumulation of 35 % of dcw by the organism was achieved. Since in both the conditions the amounts of nutrients

provided in the medium was the same with a C/N ratio of 10 therefore, the increased growth and production of P(3HO) under conditions 2, must be due to the changes in the pH and the rpm which has led to changes in the cells metabolism which may have in turn effected its grown and thus its polymer accumulation. Also in condition 2, the amounts of dissolved oxygen remained at 20 % upto 36 hrs of the fermentation. Therefore, the level of oxygen in the medium was sufficient to support good growth of the organism, ultimately leading to an increased P(3HO) yield.

pH of culture medium seem to have an important effect on the accumulation and degradation of PHAs. For example when studies were carried out by Philip *et al*. (2009), on the effects of pH on P(3HB) accumulation by *B. cereus* SPV they found that amongst the three pH stat fermentations at, 3, 6.8 and 10 maximum accumulation of PHAs, 23 % of dcw polymer yield, was observed at a pH stat of 6.8 (Philip *et al.*, 2009). Numerous studies have been carried out on the production of mcl-PHAs by *Pseudomonas* sp. at a constant pH of 7; these studies have also reported an increase in the accumulation of the accumulated mcl-PHAs when compared to non pH stat runs (Huisman *et al.*, 1991; Elbahloul and Steinbüchel, 2009). However no studies on the accumulation of PHAs by *Pseudomonas* sp. at pH values higher than 7 have been carried out. From the results of fermentation conditions 1 and 2, we can assume that a higher pH of 7.5 was preferred by the organism for growth and organism. However, the good growth and polymer yield achieved under condition 2 could be also due to the combined effect of impeller speed and pH of the medium. Under all these conditions the air flow rate used was 1 vvm. Therefore the poor growth and low accumulation of PHAs observed under condition 1 could also be because the impeller speed of 150 rpm was unable to disperse the incoming air more efficiently than that of 250 rpm because of which low oxygen transfer rates may have been achieved. Hence, less oxygen was available for organism to support its growth. This problem is compounded

by the fact that mcl-PHA producers like *Pseudomonas* sp. have high oxygen demand (Kim *et al.*, 1997). The effect of impeller speed on PHA production has also been found to be dependent on the media used. When *Azotobacter chroococcum* was grown in $NH4^+$ medium with 60% alpecin, PHA production was found to increase with an increase in impeller speeds. However, when the organism was grown in the medium devoid of alpecin, PHA production decreased with increasing impeller speed. This is because in the former case, PHA production was stimulated because of nitrogen limitation, however when grown in a medium devoid of alpecin PHA accumulation was due to simultaneous limitations of nitrogen and oxygen. Hence, increase in impeller speed resulted in better mixing of oxygen in the medium, which presented decreased oxygen stressful conditions to trigger PHA accumulation in the organism (Pozo *et al.*, 2002)

When conditions of the fermentations were changed to a C/N ratio of 20:1, pH 6.8 and rpm of 150 (condition 3) a low dry cell weight ranging between 0.75 to 1.40 g dcw/L was obtained. The organism had also accumulated the polymer to a maximum of 13.80 %dcw. Similarly under condition 4, when all the parameters were set at the upper limit, pH at 7.5, rpm at 250 and starting C/N of the medium at 20 poor cell growth and polymer yield was achieved. The major parameter value different in conditions 2 and 3 as opposed to conditions 1 and 2 was the starting C/N ratio of the culture medium. The C/N ratio for conditions 3 and 4 was increased to 20 as oppose to 10 for conditions 1 and 2. The amounts of nitrogen was varied instead of carbon, this is because fatty acids at concentration higher then 20mM are known to be toxic to the bacteria, in fact fatty acids even at lower concentrations are found to be mildly toxic to the bacteria. Decreasing the amount of octanoate further was not considered as decreasing the amounts would have reduced the carbon available for the organism and this would have effected the organisms growth and PHA accumulation; particularly because microorganisms accumulated

PHAs under nutrient stress in the presence of excess carbon source. Therefore, the C/N ratio was varied by varying the amounts of nitrogen, thus amount of nitrogen available to the organism under conditions 3 and 4 was reduced when compared to conditions 1 and 2. These, reduction in the levels of nitrogen could have resulted in poor cell growth and therefore on a decrease P(3HO) accumulation for the organism under these conditions. Thus, amongst all the four conditions studied, condition 2 with an rpm of 250, pH of 7.5 and C/N of 10:1 increased the yield of the polymer P(3HO) by 10% as compared to polymer produced at shaken flask level as discussed in section 4.3.3. Another observation was that unlike the shaken flask production of P(3HO), where the highest yield (31.38 % dcw) was achieved at 48 hrs, here maximum yield of the polymer under all the four conditions was obtained at 36 hrs.

This study therefore resulted in the production of some novel mcl-PHAs and its copolymers like P(3HO-co-2HDD) from *P. aeruginosa*. The P(3HB-co-3HO) copolymer from *P. mendocina* when grown in sucrose and most importantly the homopolymer of P(3HO) which has never been reported in literature previously. The downstream processing studies showed, how the kind of extraction method employed have an effect on the yield, thermal properties, molecular weight and LPS content of the polymer. Partial factorial studies have been used to study certain specific condition which has led to an increase in the yield from 31.3 % of dcw to 35 % dcw.

Chapter 5: Applications of poly(3-hydroxyoctanoate)

5.1. Introduction

Once extracted, PHAs exhibit properties ranging from hard brittle to flexible and elastomeric in nature. Biocompatibility and biodegradibilty of PHAs are also well established. It is because of these reasons that PHAs have been gaining increasing interest as for a number of agricultural, industrial and particularly for medical applications. However, before using PHAs for possible applications one must consider the properties of the PHA in question. This is because the physical properties of PHAs greatly affect their possible medical applications. For instance short chain length PHAs like P(3HB), are hard and brittle in nature and hence, are more suitable for hard tissue engineering. In contrast, for soft tissue engineering, more elastomeric and flexible materials are needed and hence mcl-PHAs and its copolymers are more suitable for biomedical applications such as heart valves, other vascular applications, for skin tissue engineering, wound healing applications and controlled drug delivery. In addition, the fact that mcl-PHAs are more structurally diverse than scl-PHAs, this structural diversity provides more flexibility in tailoring the physical and mechanical properties of these mcl-PHAs to meet the requirement of the engineered tissue. Because of these important properties, mcl-PHAs such as P(3HHx) and copolymers like P(3HB-co-3HHx), P(3HO-co-3HHx) are being increasingly studied to develop osteosynthetic materials, surgical sutures, stents, scaffolds for tissue engineering and matrices for drug delivery (Tim *et al.,* 1999; Stock *et al.,* 2001; Wang *et al.,* 2003).

This chapter describes the work that was done with an objective to study the novel homopolymer poly(3-hydroxyoctanoate), P(3HO), produced from *P. mendocina* using the octanoate feed, as a possible biomaterial for medical application. The polymer was fabricated into two dimensional films using the solvent casting method as described in section 2.12.2. The fabrication was done using the polymer i.e. neat P(3HO) and by combining the polymer with

bioactive particles 45S5 Bioglass® nanosize (composition of these bioglass particles is described in section 2.12) to produce a P(3HO)/n-BG 45S5® composite films. These fabricated neat and composite films were then studied for the following proposed applications: (i) P(3HO) neat film as biomaterial for pericardial patch and (ii) P(3HO)/n-BG composite films for multifunctional wound dressing.

5.1.1. The neat P(3HO) film as a potential biomaterial for a pericardial patch

Myocardial infarction is one of the most common causes of heart disease and the common end point of cardiac disease is congestive heart failure (CHF). CHF is a condition in which the heart cannot pump sufficient amount of blood to the body. Thus heart transplantation becomes a final treatment option for this end stage heart failure (Chen *et al.,* 2008). However, lack of organ donors is one major limitation for this solution. Therefore, scientists have been constantly working on an alternative solution to repair the damaged heart. Pioneering experiments have now been carried out confirming that the diseased myocardium can be restored by the transplantation of functional cardiac myocytes into the heart (Koh *et al.,* 1993; Etzion *et al.,* 2001; Ehmsen *et al.,* 2002; Chen *et al.,* 2008). An alternative approach is to deliver the cardiac cells to the heart by using a tissue engineering strategy, in which a biodegradable patch is populated *in vitro* with cardiac cells and implanted onto the infarct region. Therefore, in this present study the P(3HO) neat film is proposed to be used as a pericardial patch material as shown in **Figure 5.1**

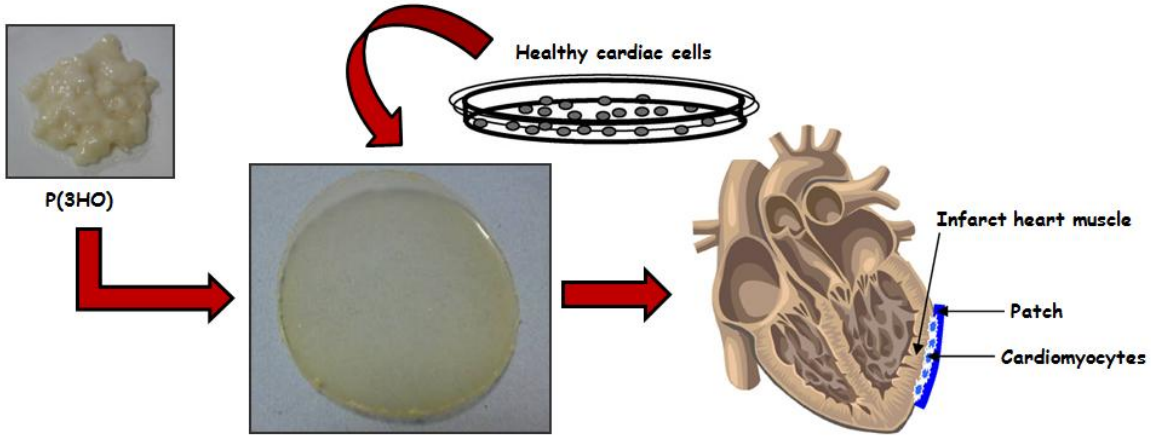

Figure 5.1: Illustration of a P(3HO) pericardial patch. The pericardial patch will be seeded with healthy cardiac cells *in vitro*, the cells allowed to proliferate and then sutured onto the infarct region.

The pericardial patch will serve two functions:

1. Delivery of healthy cardiac cells into the infarct region.
2. Provide left ventricular restraint.

From previous work it has been concluded that the addition of a sheet material to a damaged left ventricular wall (injected inside or sutured outside) could have important effects on cardiac mechanics, with potentially beneficial reduction of elevated myofibril stresses (Flachskampf *et al.,* 2000; Wall *et al.,* 2006; Fujimoto *et al.,* 2007; Chen *et al.,* 2008).

Many studies have been carried out using both synthetic and naturally occurring polymers for application in myocardial tissue engineering. Copolymers of P(3HO) have been previously studied for soft tissue engineering of vascular tissue and heart valves as discussed in section 1.10.2. Studies were therefore carried out for the first time to assess P(3HO) neat films as possible material for a pericardial patch.

5.1.2. P(3HO)/ 45S5 Bioglass® composite film as a multifunctional wound dressing film

The human skin is the largest organ of the body and protects the body from external environment by maintaining temperature and haemostasis in addition to performing sensory detection (Nair and Laurencin, 2006). It consists of two main layers, the upper epidermal barrier layer and the lower, much thicker, dermis. Keratinocytes are the most common cell type in the epidermis and form the surface barrier layer. Melanocytes are found in the lower layer of the epidermis and provide skin colour. Fibroblasts form the lower dermal layer. The dermis contains the blood vessels, nerves, sweat glands, hair follicles, and oil glands. The dermis consists mainly of connective tissue, which is largely made up of a protein called collagen. Collagen gives the skin its flexibility and provides structural support. The fibroblasts that make collagen are the main type of cells in the dermis (Nair and Laurencin, 2006). Skin tissue engineering is very important as it is needed to provide skin grafts to permanently replace damaged or missing skin or to provide a temporary wound covering to burn victims, also for non healing wounds such as diabetic ulcers, venous ulcers and cosmetic surgery. A damaged skin or a non healing wound could compromise the health of an individual.

Much research has been carried out on the development and clinical use of tissue engineered skin. Skin cells have been seeded and populated into suitable films. The cell film construct is then grafted to the wound; cells then proliferate from the film to the wound bed forming cell clusters and ultimately the normal epidermis. The film in addition to supplying healthy cells also provides protection to the wound until it is degraded or absorbed (Terskiih and Vasiliev, 1999; Peschel *et al.*, 2007). To this end scaffolds such as chitosan (CH)/gelatin/hyaluronic acid (Ha) or collagen/ Ha scaffolds, which could be populated with skin cells, cultivated and then transferred to the wound have been studied (Bello *et al.,* 2001; Ng *et al.,* 2005; Peschel *et al.,* 2007). Research

has also been carried out with PHA scaffolds such as poly (3HB-co-5mol%-3HHx), poly(3HB-co-7mol%-4HB) and poly(3HB-co-97mol%-4HB) (Tang *et al.,* 2008) P(3HB) and P(4HB) blended with hyaluronic acid and chitosan (Peschel *et al.,* 2007)and P(3HB-co-3HV-co-3HX) (Ji *et al.,* 2008) for skin tissue engineering.

In this present study bioactive nano sized 45S5 Bioglass® were incorporated into the P(3HO) matrix and fabricated into a 2D composite film. Bioactive glass particles have been shown to form tenacious bonds to both hard and soft tissues; bonding is enabled by the formation of a hydroxyapatite (similar to biological apatite) layer on the glass surface on exposure to biological fluids (Misra *et al.*, 2006; Chen, 2008). By incorporating such bioactive glass particles as coatings or fillers into bioresorbable polymer, scaffolds of tailored biological and mechanical properties can be produced for potential application in tissue engineering (Misra *et al.,* 2006; Misra *et al.,* 2007). Composites of poly(3-hydroxybutyrate) and n-BG have been developed and studied for bone tissue engineering (Misra *et al.,* 2006; Misra *et al.,* 2007; Misra *et al.,* 2008; Misra *et al.,* 2009). However, the haemostatic effect of n-BG has not been explored much. Silicate bioactive glasses have been studied for its haemostatic effect by Ostomel *et al.* (2006) although the glass used by them was of different composition to the n-BG used in this work (Ostomel *et al.,* 2006). Therefore, a composite film of P(3HO) and n-BG (**Figure 5.2**) was developed for the first time as a material with the potential to be used as a multifunctional wound dressing, which will act as both a film for skin regeneration and also accelerate wound haemostasis thus potentially reducing blood loss following tissue injury. Thus, the P(3HO)/n-BG composite film will act as a film for skin tissue regeneration and also provide a haemostatic effect.

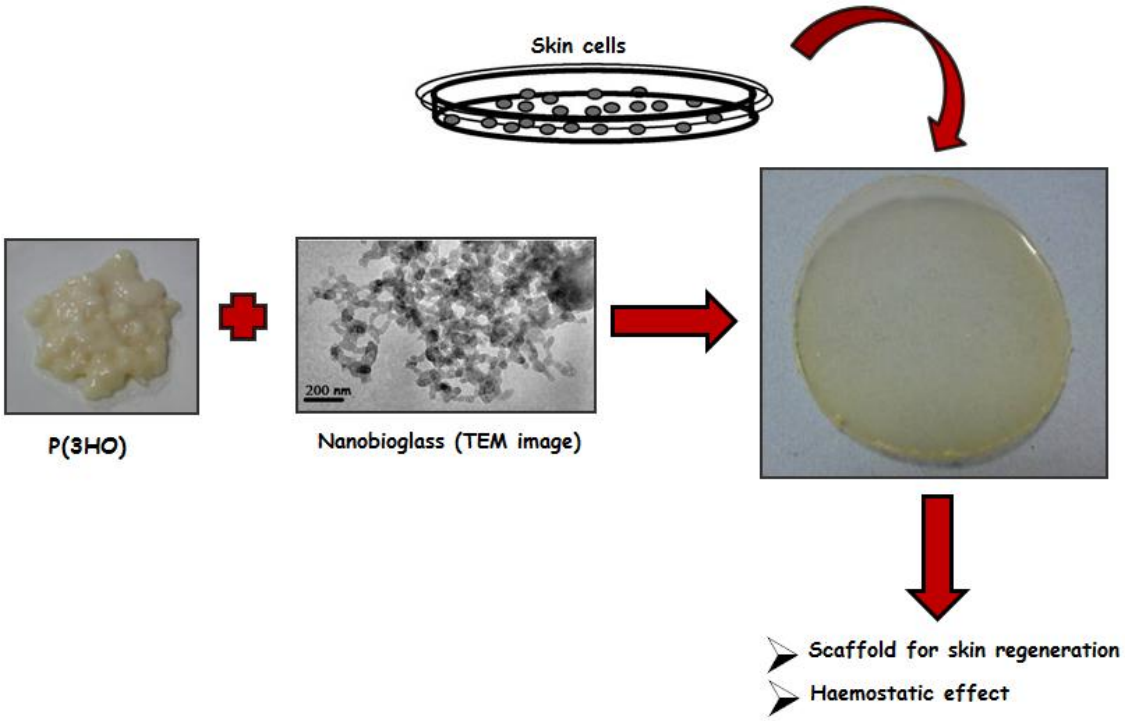

Figure 5.2: Illustration of a P(3HO)/n-BG multifunctional wound dressing.

Therefore, to evaluate these proposed potential applications, the fabricated films were subjected to an in depth investigation to study their physical and chemical properties, *in vitro* degradation behaviour and biocompatibility.

5.2. Results

5.2.1. Fabrication of P(3HO) into two dimensional neat and composite films.

The fabrication was done using neat P(3HO) and by combining the polymer with a bioactive nanosize 45S5 Bioglass® (n-BG) to produce a P(3HO) neat 2D film and a P(3HO)/n-BG 2D composite films **(Figure 5.3).** Detailed fabrication and nomenclature of these films are described in section 2.12. The thickness of the fabricated films were: 5 wt% composite = 0.26 mm, 5 wt%

neat film = 0.15 mm, 10 wt% composite film = 0.50 mm and 10 wt% neat = 0.40 mm.

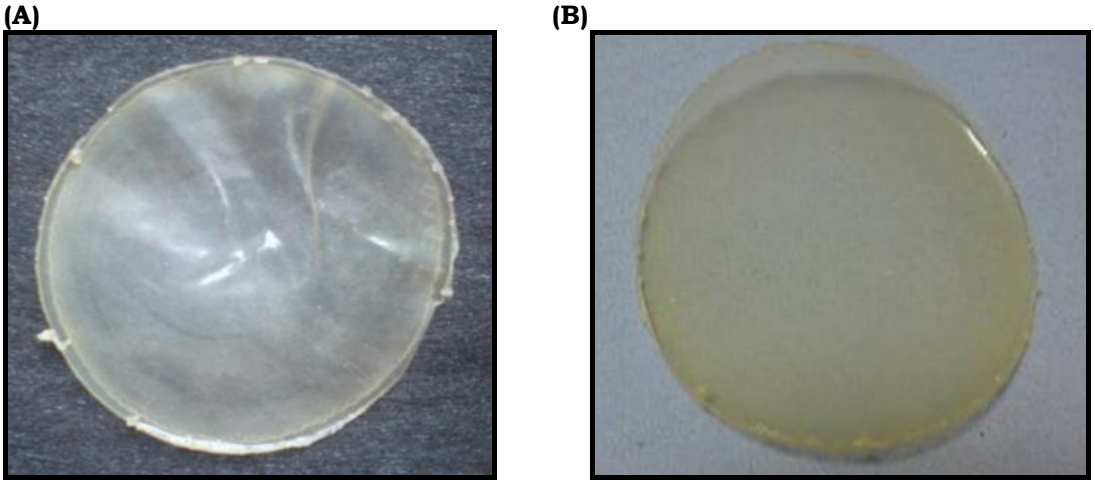

Figure 5.3: Fabricated (A) P(3HO) neat and P(3HO)/n-BG composite films using the solvent casting method.

5.2.2. Microstructural studies

Surface and microstructural features of a biomaterial can have important implications on its biocompatibility and hence its applications. Therefore, to evaluate these microstructural properties and understand its impact on the biocompatibility, the fabricated films were subjected to a series of tests using scanning electron microscopy, SEM, white light interferometry using a ZYGO® and contact angle study. The surface morphology and microstructure of these films were observed by SEM. The SEM images of the neat P(3HO) films (**Figures 5.4 (A) and (B)**) revealed smooth surface properties. However for the P(3HO)/n-BG composite films the incorporation of the n-BG changed the surface morphology by introducing a rough topography to the surface. The n-BG was embedded both in the polymer matrix and on the surface of the polymer as shown in the SEM analysis of the transverse section and planar surface of the composite film (**Figures 5.4 (C) and (D)**)

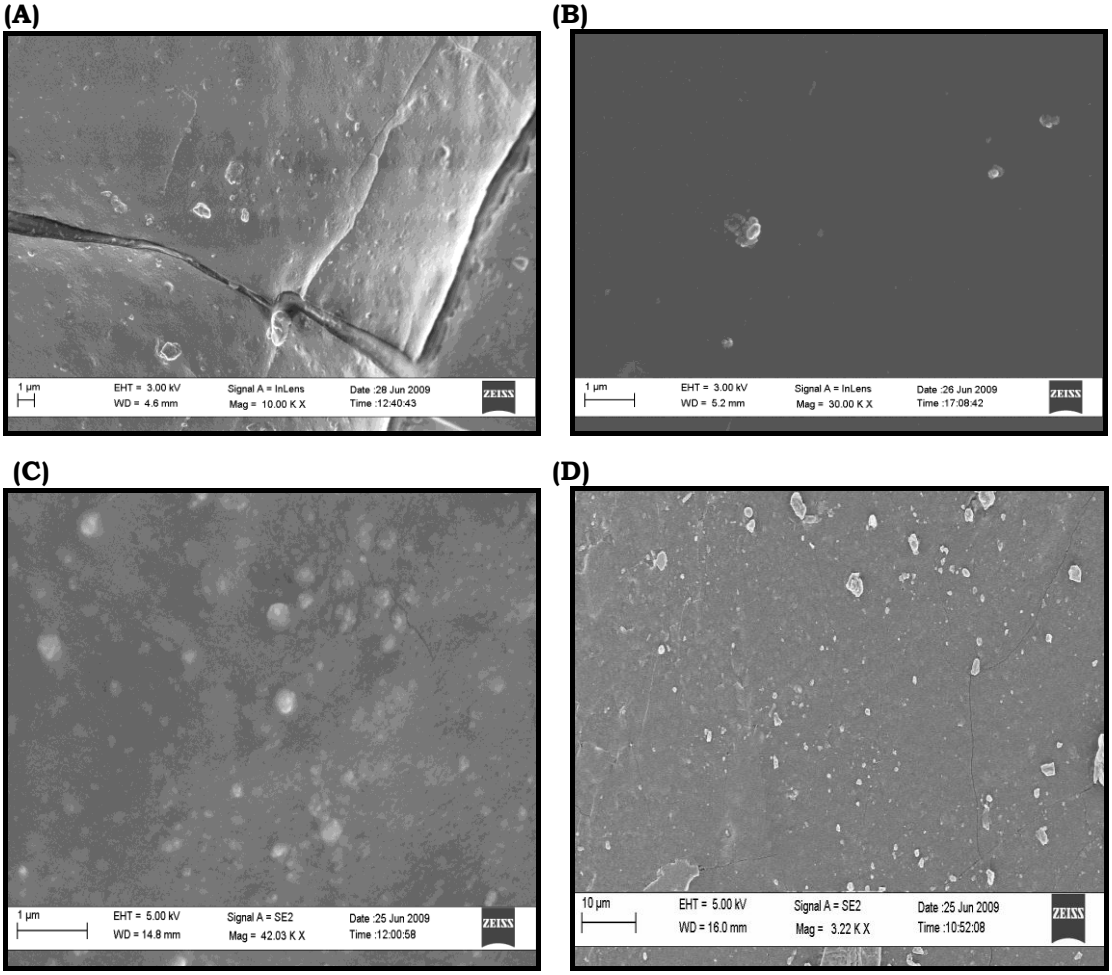

Figure 5.4: SEM images of the P(3HO) neat and P(3HO)/n-BG composite films: (A) cross section and (B) planar surface of a P(3HO) neat film revealing a smooth surface. (C) cross section and (D) planar surface of a P(3HO)/n-BG composite film revealing a rough surface

Surface analysis of the films was also carried out using white light interferometry using ZYGO® to visualise the topography of the films as shown in the surface scans in **Figure 5.5**. Incorporation of the n-BG into the polymer matrix had increased the roughness of the composite film. This was confirmed by the white light interferometry analysis, whereby a typical root-mean-square-average (RMS) value of 0.440 µm was observed for the 5 wt% composite film as opposed to 0.238 µm for the 5 wt% neat film. Only the roughness of the 5 wt% neat and 5 wt% composite films was analysed.

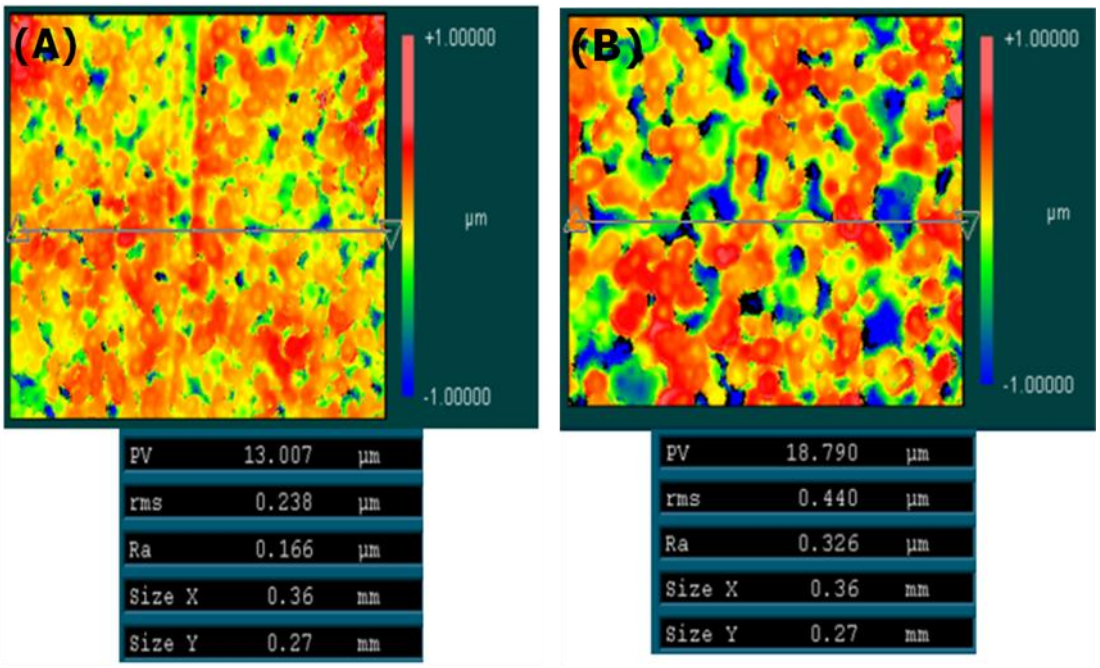

Figure 5.5: White light interferometry analysis of the surface topography of the fabricated films: (A) P(3HO) neat (5 wt%) and (B) P(3HO)/n-BG composite (5wt%) films.

Water contact angle measurements were carried out on both the surfaces of the P(3HO) neat film and the P(3HO)/n-BG composite films to assess their wettability. The water contact angle (θH2O) is a measure of the hydrophilcity or hydrophobicity of a material surface. Surfaces with θH2O less than 70^{o} is considered to be hydrophilic and θH2O greater than 70^{o} is considered to be hydrophobic (Peschel *et al.,* 2007). Static contact angle measurements of the fabricated films are given in **Figure 5.6.**

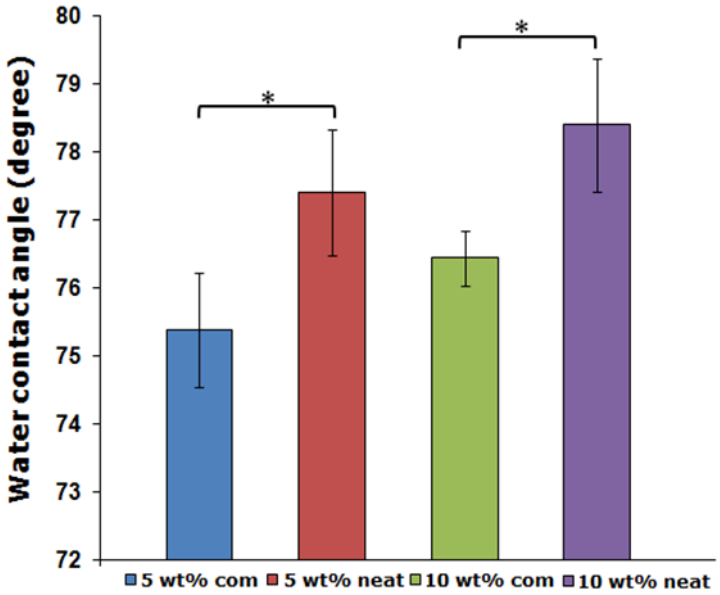

Figure 5.6: Contact angle measurement for the neat P(3HO) and P(3HO)/n-BG composite films. The data (n=4; error bars = ±SD) were compared using the Student's t-test and differences were considered significant when *p<0.05: 5 wt% com, 5 wt% neat, 10 wt% com and 10 wt% neat.

θH_2O value obtained were, 5 wt% composite film = 75.43^{o}±0.83; 5 wt% neat film = 77.3^{o}±1; 10 wt% composite film = 76.63^{o}±0.4 and 10 wt% neat film = $78\ ^{o}$±1. The surfaces of the fabricated neat and composite films were therefore relatively hydrophobic. However, the composite films wettability had increased (n=4, *p<0.05).

5.2.3. Mechanical characterisation

Static tests were carried out on the fabricated polymer neat and composite films to understand their mechanical properties. The tensile tests were carried out on thin strips of the films; six repeats per sample. The initial load was set to 1 mN and then increased to 6000 mN at the rate of 200 mN min^{-1}. The stress strain curves of the films are shown in **Figure 5.7(A-D)**.

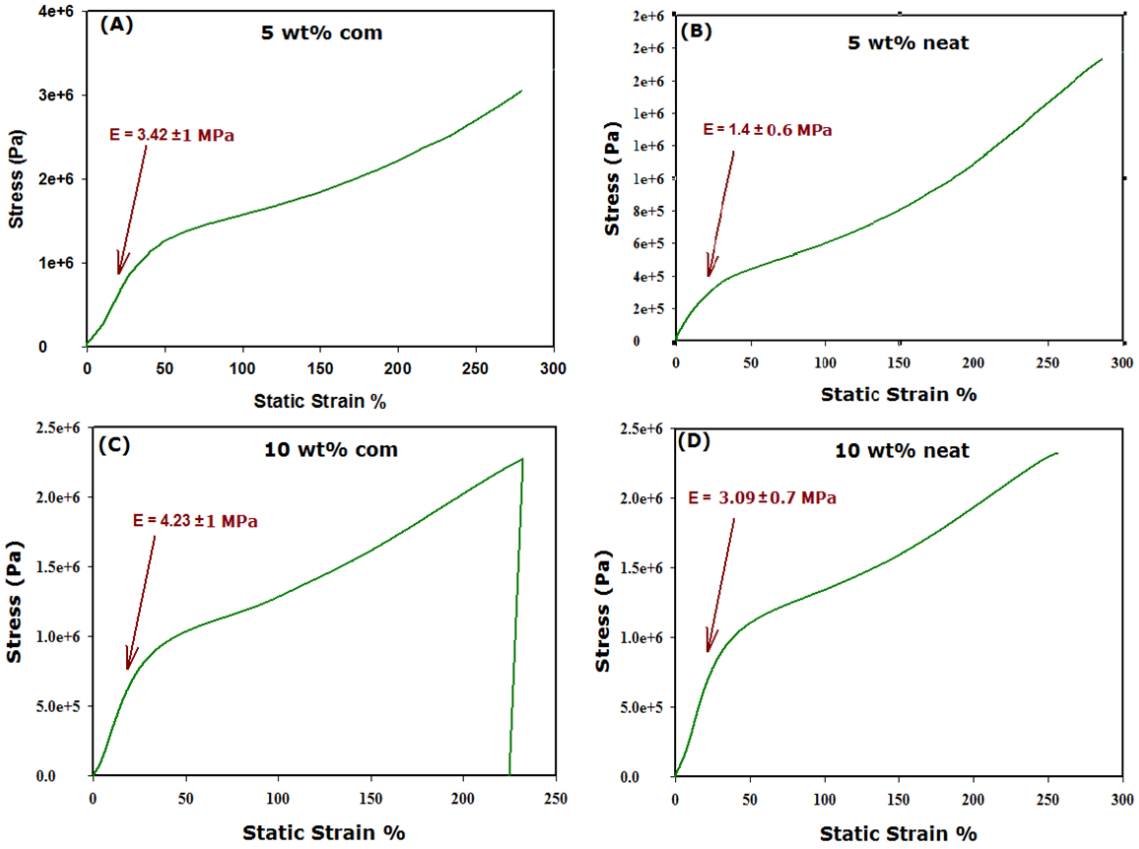

Figure 5.7: Stress strain profile of the fabricated films: (A): 5 wt% composite film (B): 5 wt% neat film (C): 10 wt% composite film (D): 10 wt% neat film. The films were subjected to a load between 200 to 6000 mN which was increasing at the rate of 200N min^{-1}.

The stress strain curve observed for all the samples resembled that of elastomers. No "knee" i.e., the point of discontinuity in the slope of the stress strain curve (Nocolais and Mashelkar, 1977) appeared in any of the curves (**Figure 5.7**) in this present study. The Young's modulus value calculated from the slope of the curves was as follows: 5 wt% composite film = 3.42 ± 1 MPa, 5 wt% neat film = 1.4 ± 0.6 MPa, 10 wt% composite film = 4.23 ±1 MPa and 10 wt% neat film = 3.09 ± 0.7 MPa. These results show that the addition of the n-BG particles increases the Young's modulus value of the composites. Under the experimental conditions of our study as described in section 2.9.2, the 5 wt% composite and 5 wt% neat films failed during the test; the tensile strength for the 5 wt% composite film was 3.3 MPa and 5 wt %neat film was 1.8 MPa. Ultimate strength or % elongation of these films was: 5 wt%

composite film = 236.75% ± 10 and 5 wt% neat film = 278% ± 10. The composite and the neat 10 wt% film did not fail under this experimental condition (section 2.9.2). The % elongation at the end of the test for these films were, 10 wt% com film = 222.5 ± 6% and 10 wt% neat film = 256.34 ± 9.

5.2.3. Thermal characterisation

Thermal characteristics of a material are an important property that defines the stability of a material as a function of temperature. This may have an important implication on the materials processability and end goal application. Two different thermal analyses of the fabricated films were carried out; First using the differential scanning calorimetry, DSC, to characterise the thermal transitions corresponding to the melting, glass transition and crystallisation temperatures. The second analysis was done using the thermogravimetric, TGA analyzer to determine the thermal stability in terms of weight loss of the polymer as a function of temperature.

For the DSC analysis, 6 to 8 mg of the fabricated neat and P(3HO)/n-BG composite films were encapsulated in standard aluminium pans and subjected to DSC analysis with a sequential programme of heating/cooling/heating at a heating rate of 20^{o}C within a temperature range between -50 to 80^{o}C. **Figures 5.8 (A-D)** show the thermal profiles of the first and second heat scans of the fabricated films.

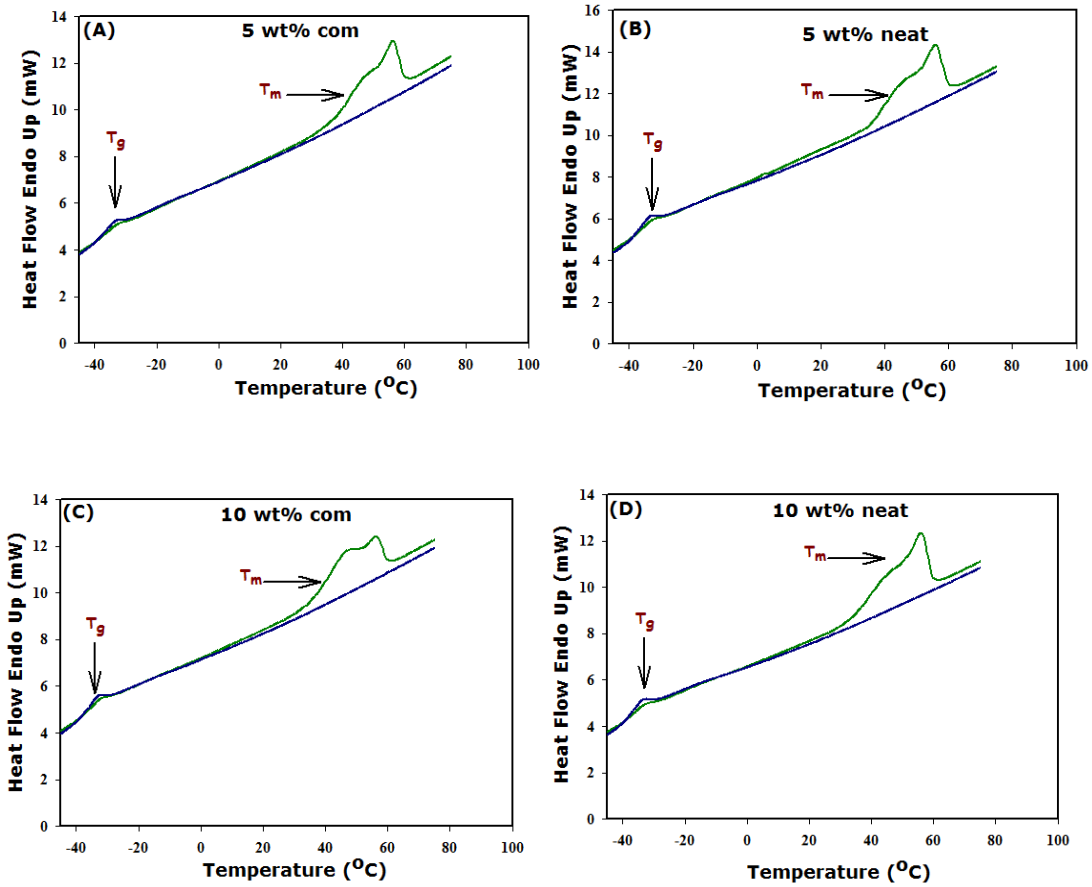

Figure 5.8: Thermal profile of the fabricated films (A) 5 wt% composite film, (B) 5wt% neat film, (C) 10 wt% composite film and (D) 10 wt% neat film.

All the fabricated films showed the endothermic transition of the amorphous phase from the glassy to the rubbery state (T_g) and the transiton due to the melting of the crystalline phase (T_m) during the first heat scan. In the second heat scan only a T_g peak was observed. The results of the analyses are summarised in **Table 5.1**.

Samples	First heat run			Second heat run
	T_g (°C)	T_m (°C)	ΔH_f (J/g)	T_g (°C)
5 wt% com	-34.86	45.62	15.47	-34.65
5 wt%neat	-35.55	46.60	17.42	-35.91
10 wt% com	-34.37	45.56	14.04	34.83
10 wt% neat	-34.80	47.43	18.05	-35.42

Table 5.1: Compilation of the thermal properties of the fabricated P(3HO) neat and P3(HO)/n-BG composite films.

Thermogravimetric analysis (TGA) scans of the fabricated films are shown in **Figure 5.9**.

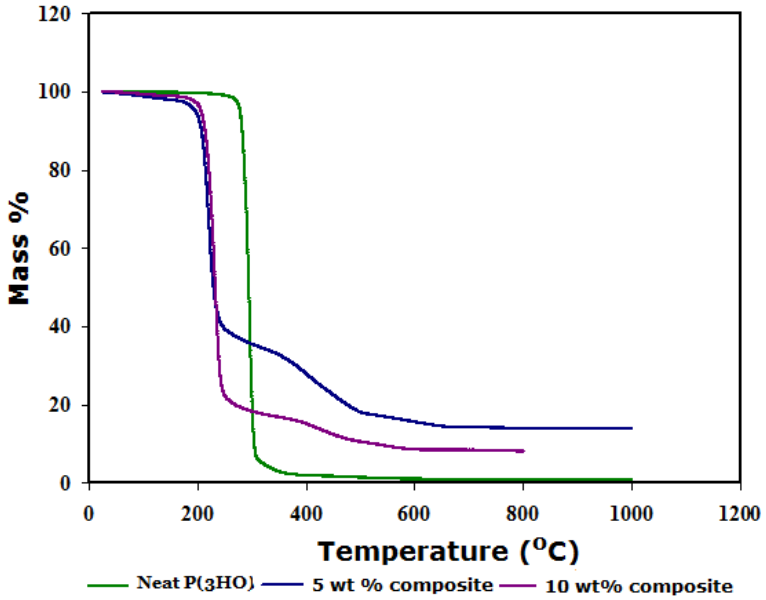

Figure 5.9: Thermogravimetric profile of the fabricated films. Scan showing the changes in the mass of the (a) P(3HO) neat film (b) 5 wt% composite film and (c) 10wt % composite film as a function of temperature.

At a temperature of 300°C the onset of the degradation of the P(3HO) neat film commenced. However, the composite films were less thermally stable compared to the neat films since their degradation commenced at 195°C for the 5 wt% composite film and 200°C for the 10 wt% composite film.

5.2.4. *In vitro* degradation study

A detailed study on the *in vitro* degradation behaviour of the fabricated neat and composite films were carried out by thermostatically incubating the fabricated films at 37°C in different media i.e. physiological phosphate buffer saline, (PBS), Dulbecco's modified eagles medium, (DMEM) and Dulbecco's modified eagles medium knock out, DMEM^{KT}. The reasons for using these media are described in section 2.13. Physical and chemical properties of the

films were monitored to assess any changes that take place whilst undergoing degradation.

5.2.4.1. Weight loss and water absorbed by the scaffolds during the degradation

The weight lost, (WL), during degradation of the films was calculated as a percentage of weight loss from the original weight of the film. The % of water absorbed, (WA) was calculated as a percentage of weight gain from the dried films at the end of incubation. The WA and WL and weight loss by the films are depicted in **Figure 5.10** and **Figure 5.11.** The results of these studies can be summarised as follows: (i) The water absorption for the films increased on prolonged immersion in all the three media. (ii) At the end of 4 months the water absorption was higher for the composite films as opposed to the neat films. For instance in the PBS medium the WA on the 5 wt% composite film and 10 wt% composite films were 22.74% and 20.60% higher than the comparable neat films; in DMEM medium the WA on the 5 wt% composite film and 10 wt% composite films were 18.94% and 25.65% higher than the comparable neat films; In $DMEM^{KT}$ medium the WA was 5.65 and 10.93% higher for the 5 and 10 wt% composite films as oppose to the comparable neat films (iii) The weight lost by the films also increased progressively with incubation time. (iv) The weight lost by the composite films was more than that of the comparable neat films. For instance in the PBS medium the WL was 8.08 and 10.35 % higher for the 5 and 10 wt% composite films respectively as opposed to the comparable neat films; in DMEM medium the WL for the 5 wt% composite film and 10 wt% composite films were 8.49 % and 8.47 % higher than the comparable neat films; In $DMEM^{KT}$ medium the WL was 9.93 and 13.64% higher for the 5 and 10 wt% composite films as opposed to the comparable neat films.

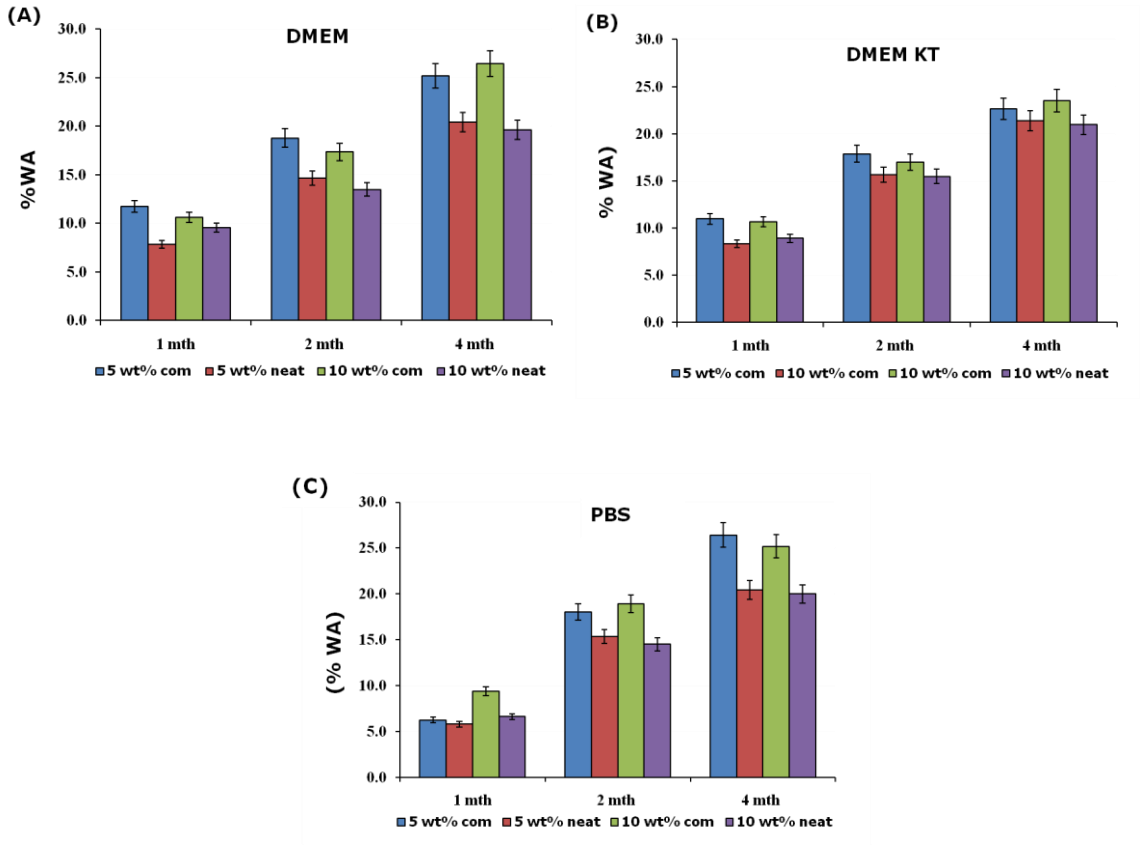

Figure 5.10: Water absorption by the degrading P(3HO) neat and P(3HO)/n-BG composite films during the *in vitro* degradation study in (A) DMEM , (B) DMEM^{KT} and (C) physiological buffer phosphate buffer saline, media. The WA of the films were monitored for a period of 1, 2 and 4 months during this study: 5 wt% com, 5wt %neat, 10 wt% com and 10 wt% neat.

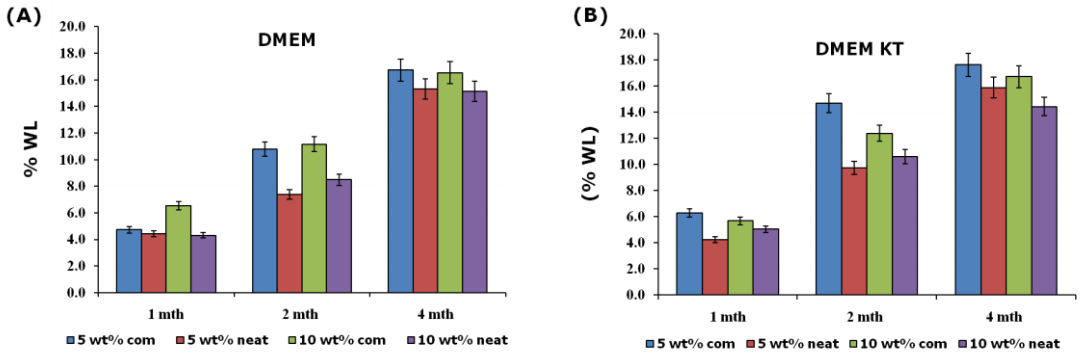

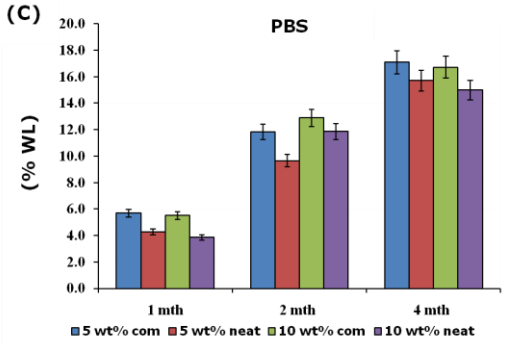

Figure 5.11: Weight loss by the degrading P(3HO) neat and P(3HO)/n-BG composite films during the *in vitro* degradation study in (A) DMEM , (B) DMEM^{KT} and (C) physiological buffer phosphate buffer saline, media. The WL of the films were monitored for a period of 1, 2 and 4 months during this study: ■ 5 wt% com, ■ 5 wt %neat, ■ 10 wt% com and ■ 10 wt% neat

5.2.4.2. Static mechanical test of the degrading films

Static mechanical tests were carried out on the fabricated films at the end of 1, 2 and 4 months of incubation. The Young's modulus value of the films was calculated, the results of which are depicted in **Figure 5.12**. The results of these studies are summarised as follows: (i) The Young's modulus or stiffness of the fabricated films had increased by 6 to 9 % in all the three media until two months of incubation. (ii) After two months of incubation the stiffness of the fabricated films decreased by 2 to 9 % in PBS and DMEM^{KT} media and by 2 to 4.20 % in DMEM medium as shown by the reduction in the Young's modulus value at the end of 4 months incubation study. (iii) The Young's modulus value for the composite films were higher than the comparable neat films, n = 4 where *$p<0.05$; The Young's modulus for the films at 4 months of incubation was 9.13 MPa, 8.30 MPa, 12.5 MP and 8.73 MPa for 5 wt% composite, 5 wt% neat, 10 wt% composite and P(3HO): 10 neat films respectively in PBS medium. Similarly in DMEM medium the Young's modulus values were 7.78 MPa, 6.80 MPa, 10.40 MPa and 7.94 MPa for the 5 wt% composite, 5 wt% neat, 10 wt% composite and 10 wt% neat films respectively. The values in the DMEM^{KT} medium were 11.20 MPa, 7.26 MPa,

12.0 MPa and 7.94 MPa for the 5 wt% composite, 5 wt% neat, 10 wt% composite and 10 wt% neat films

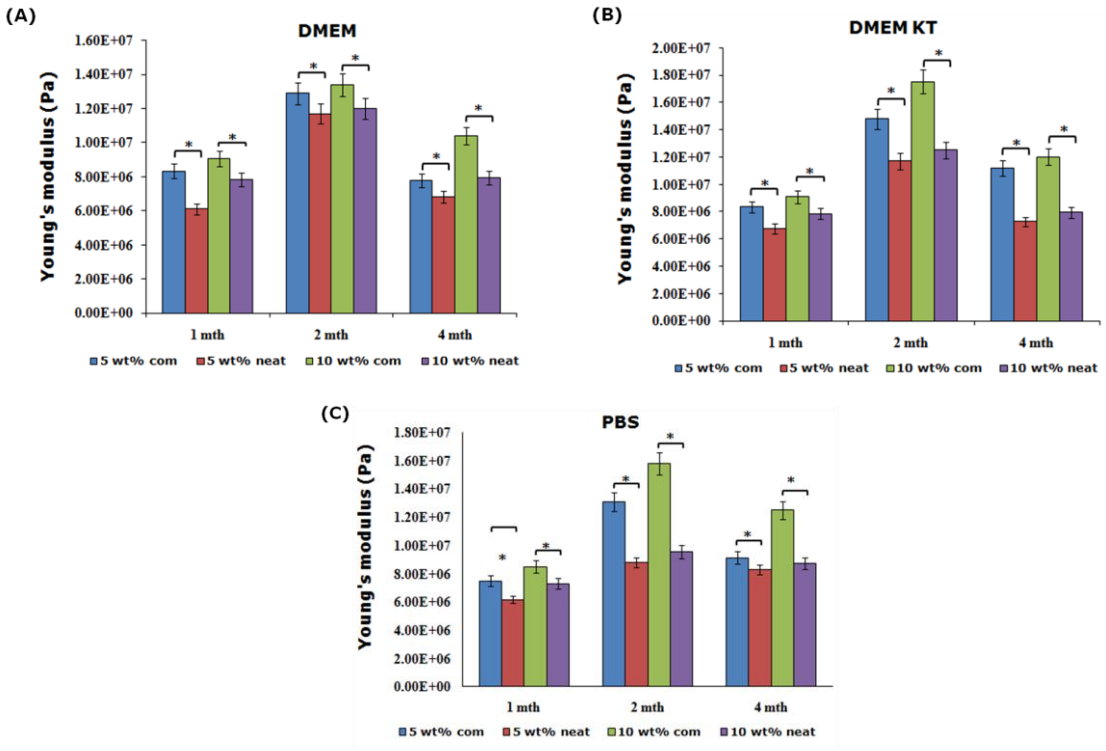

Figure 5.12: Young's modulus of the degraded samples during the *in vitro* degradation study. The samples were thermostatically incubated in (A) DMEM, (B) DMEM^{KT} and (C) PBS media for a period of 1, 2 and 4 months. The data (n=4; error bars = ±SD) were compared using the Student's t-test and differences were considered significant when *p<0.05: ■ 5 wt% com, ■ 5 wt%neat, ■ 10 wt% com and ■ 10 wt% neat.

5.2.4.3. Thermal properties of the degrading films

The thermal properties of the fabricated films were also monitored to analyse thermal changes incurred during degradation. The results of this analysis are depicted in **Figure 5.13** These degradation results can be summarised as follows: (i) A general trend of increase in the melting temperature of the films at 1 month when compared to the T_m values of the films before degradation, followed by a decrease was observed for all the films in PBS and the composite films in DMEM media. For instance for the 5 wt% composite film, the T_m value after 1 month of degradtion was 53°C and before degradation was 45.62°C. The T_m then decreased from 53°C to 49.31°C at 2 months and

48.60°C at 4 months. (ii) The films in DMEM^{KT} medium and the neat films in DMEM medium however showed a general trend of decrease in the T_m value at 1 month when compared to the T_m values of the films before degradation. The T_m value then increased at 2 month following which it again decreased at 4 months. For instance, in DMEM^{KT} medium the T_m of the 5 wt% neat film had decreased from 46.60°C (before degradation) to 44.06°C at 1 month. The value then rose to 49.70°C at 2 months after which it again deceased to 46.71°C at 4 months. An interesting observation was the appearance of two endothermic peaks due to the glass transition of the amorphous phase i.e. the glass transition temperature in the degraded films. **Figure 5.14** shows a typical thermal profile of a degrading film with the distinct melting and glass transition peaks. (v) The first glass transition temperature of the fabricated films ranged between -34 to -38.74°C (vi) The second glass transition occurred between -51 and -57°C. Note: all the values for the T_m, ΔH_f and T_g are taken from the first heat run. In the second heat run no T_m peak appeared, and it was characterised by the presence of two T_g peaks.

(A1)

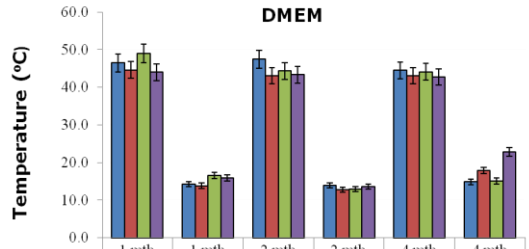

	1 mth (Tm)	1 mth (ΔHf)	2 mth (Tm)	2 mth (ΔHf)	4 mth (Tm)	4 mth (ΔHf)
5 wt% com	46.43	14.27	47.43	13.95	44.49	14.84
5 wt% neat	44.6	13.81	43.05	12.82	43.05	17.87
10 wt% com	48.92	16.47	44.36	12.99	44.09	15.07
10 wt% neat	44	15.92	43.32	13.58	42.78	22.75

(A2)

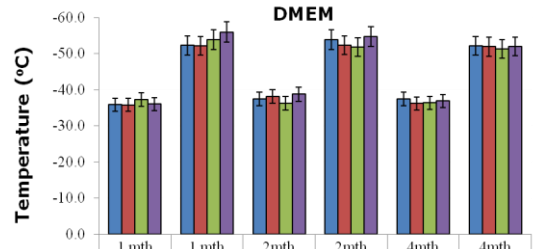

	1 mth (Tg1)	1 mth (Tg2)	2mth (Tg1)	2mth (Tg2)	4mth (Tg1)	4mth (Tg2)
5 wt% com	-35.87	-52.24	-37.46	-53.87	-37.50	-52.15
5 wt% neat	-35.77	-52.18	-38.08	-52.30	-36.21	-51.90
10 wt% com	-37.23	-53.85	-36.25	-51.74	-36.35	-51.30
10 wt% neat	-36.04	-55.94	-38.77	-54.79	-36.88	-51.92

(B1)

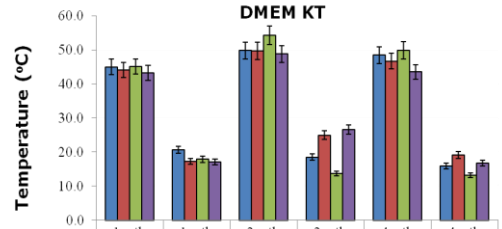

	1 mth (Tm)	1 mth (ΔHf)	2 mth (Tm)	2 mth (ΔHf)	4 mth (Tm)	4 mth (ΔHf)
5 wt% com	44.99	20.68	49.78	18.49	48.42	15.89
5 wt% neat	44.06	17.31	49.70	24.98	46.71	19.15
10 wt% com	45.09	17.89	54.31	13.66	49.84	13.18
10 wt% neat	43.24	17.13	48.80	26.61	43.52	16.72

(B2)

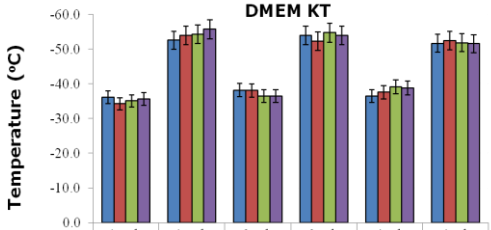

	1 mth (Tg1)	1 mth (Tg2)	2mth (Tg1)	2mth (Tg2)	4mth (Tg1)	4mth (Tg2)
5 wt% com	-36.19	-52.58	-38.16	-53.96	-36.50	-51.65
5 wt% neat	-34.25	-54.01	-38.08	-52.30	-37.58	-52.47
10 wt% com	-35.12	-54.28	-36.55	-54.74	-39.17	-51.88
10 wt% neat	-35.67	-55.75	-36.56	-54.00	-38.82	-51.62

(C1)

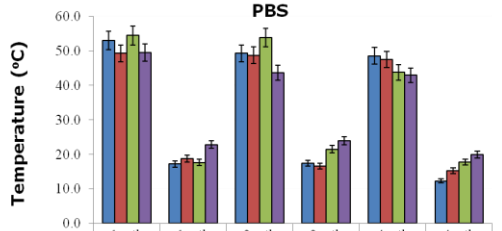

	1 mth (Tm)	1 mth (ΔHf)	2 mth (Tm)	2 mth (ΔHf)	4 mth (Tm)	4 mth (ΔHf)
5 wt% com	53.00	17.19	49.31	17.40	48.60	12.31
5 wt% neat	49.31	18.77	48.75	16.54	47.55	15.25
10 wt% com	54.48	17.65	53.90	21.47	43.76	17.76
10 wt% neat	49.49	22.86	43.62	23.94	42.94	19.92

(C2)

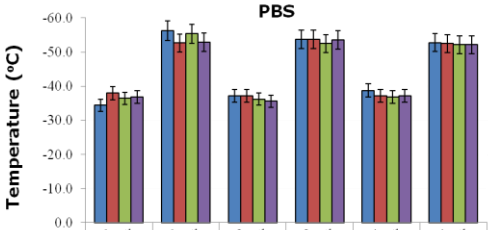

	1 mth (Tg1)	1 mth (Tg2)	2 mth (Tg1)	2 mth (Tg2)	4 mth (Tg1)	4 mth (Tg2)
5 wt% com	-34.41	-56.25	-37.13	-53.70	-38.74	-52.79
5 wt% neat	-37.96	-52.69	-37.13	-53.70	-37.15	-52.54
10 wt% com	-36.41	-55.39	-36.23	-52.47	-36.81	-52.18
10 wt% neat	-36.88	-52.88	-35.60	-53.57	-37.09	-52.17

Figure 5.13: The thermal properties of the P(3HO) neat and P(3HO)/n-BG composite films whilst under going *in vitro* degradation. (A1) DMEM media, Tm and ΔH_f; (A2) DMEM media, Tg; (B1) DMEM^{KT} media, Tm and ΔH_f ; (B2) DMEM^{KT} media, Tg; (C1) PBS media, Tm and ΔH_f and (C2) PBS media, T_g at the end of the incubation time i.e. 1, 2 and 4 months: Melting temperature =T_m, enthalpy of fusion = ΔH_f, glass transition temperature = T_g, first glass transition = T_{g1}, second glass transition = T_{g2}: ■ 5 wt% com, ■ 5 wt% neat, ■ 10 wt% com and ■ 10 wt% neat.

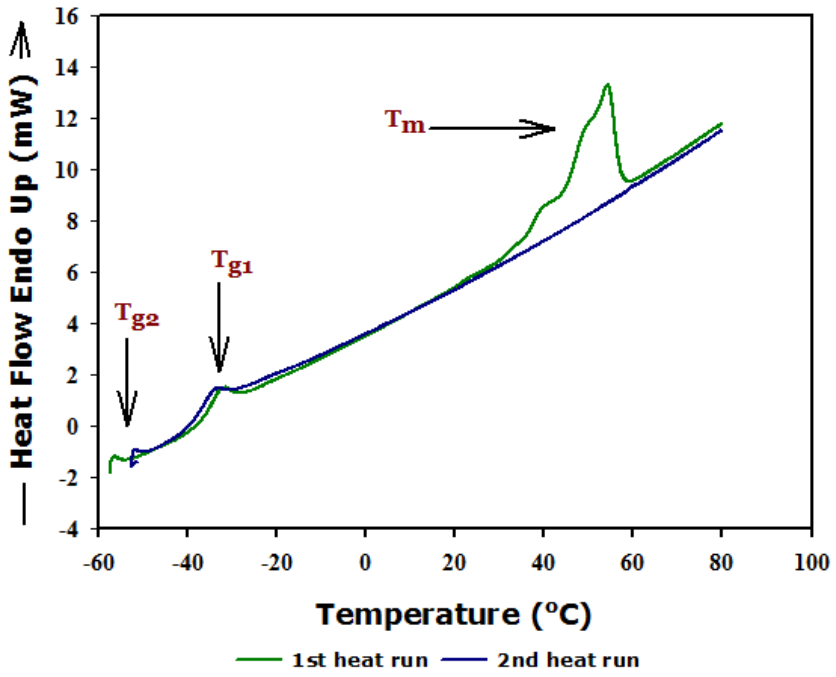

Figure 5.14: Typical thermogram of a degraded P(3HO): 10 neat film in DMEM medium at 4 months of incubation. The first heat run shows the presence of the T_m peak and the and two T_g peaks T_{g1} and T_{g2}. In the second heat run again the two T_g peaks were observed: T_m= Melting temperature, T_{g1} = First glass transition, T_{g2} = Second glass transition.

5.2.4.4. pH studies of the media

The media in which the films were incubated for the degradation were also monitored to analyse any pH changes. The pH of all the three media increased progressively with time reaching values of around 9 in DMEM, 8.2 in DMEM^{KT} and 7.8 in PBS media. The observations of these pH changes are shown in **Figure 5.15**

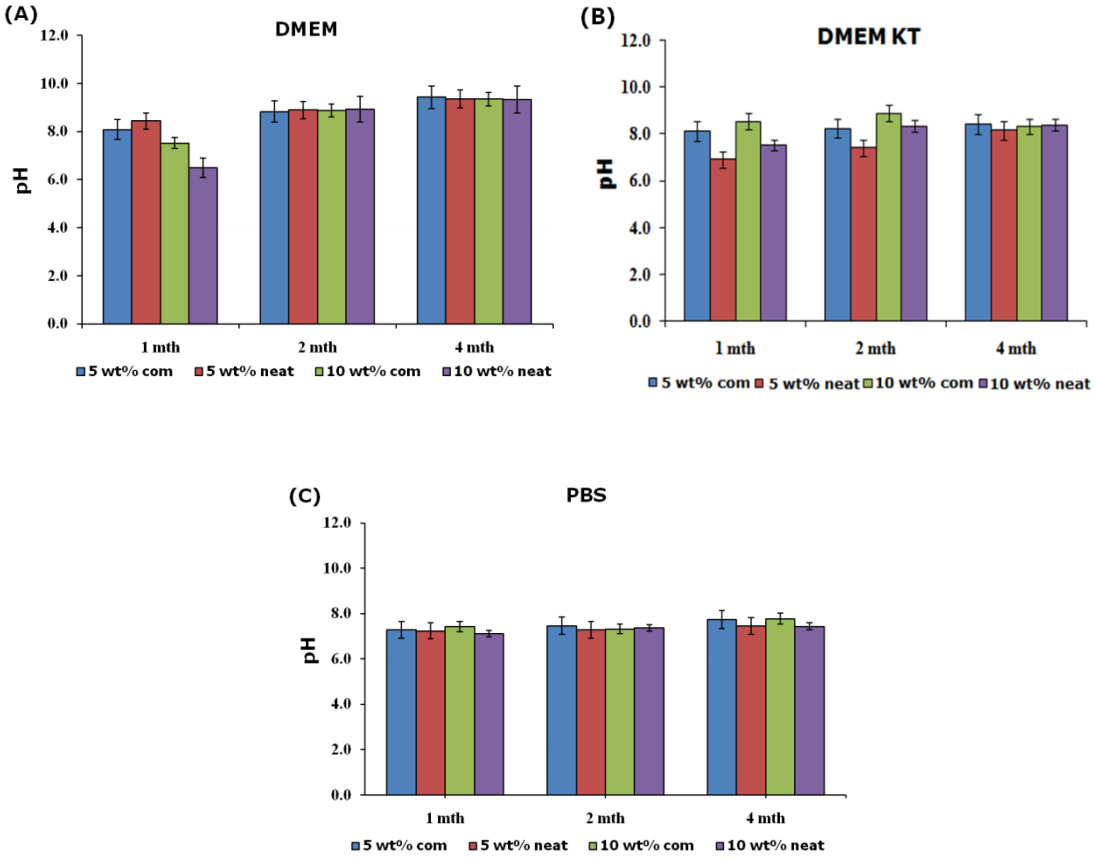

Figure 5.15: Compilation of the pH of the media in which the films were incubated for the *in vitro* degradation study: (A) DMEM, (B) DMEM^{KT}, (C) PBS media. The pH was measured over the four months of incubation. The media was refreshed every 1 week: ■ 5 wt% com, ■ 5 wt%neat, ■ 10 wt% com and ■ 10 wt% neat.

5.2.4.5. Surface studies of the degrading films

At the end of 4 months of incubation the films were rinsed in HPLC water and then subjected to SEM analysis as described in section 2.13.1. SEM analyses of the planar surfaces of the samples were carried out to analyse any changes occurring on the film surface due to degradation. SEM images (**Figures 5.16**) showed loose degraded flakes of polymer present on the surface.

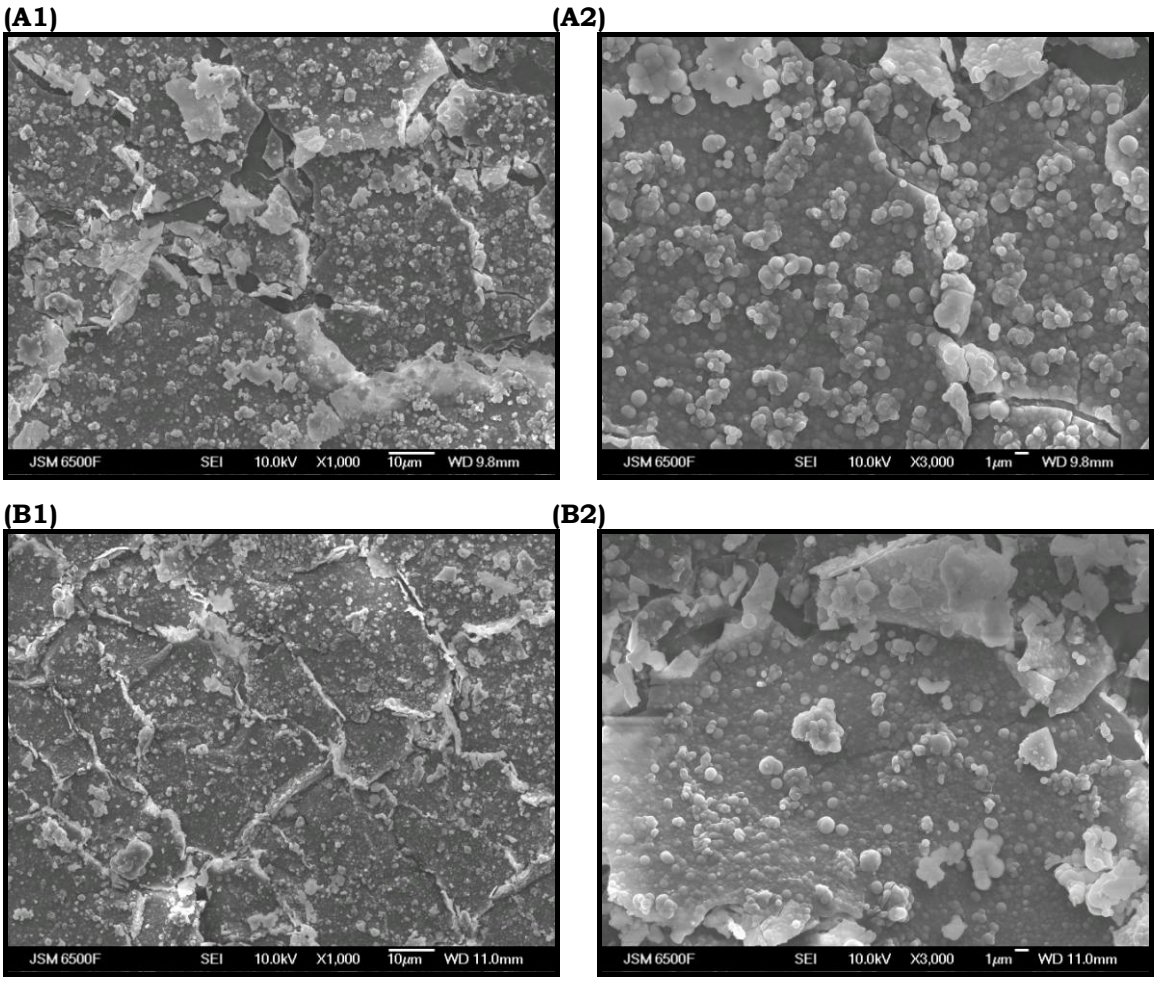

Figure 5.16: SEM images of the degrading films at the end of 4 months of incubation: (A) degrading P(3HO)/n-BG composite film (5 wt% composite) in DMEM medium): (B1) 1000X, (B2) 3000X, (B) degrading P(3HO) neat film (5 wt% neat) in DMEM medium): (A1) 1000x, (A2) 3000X.

5.2.5 Protein adsorption study

Protein adsorption assays are important in evaluating cell adhesion and survival, and therefore essential in evaluating biocompatibility of biomaterials for tissue engineering. Therefore, protein adsorption assays were carried out as described in section 2.14. The typical adsorption profile for the protein is shown in **Figure 5.17**. The amount of protein adsorbed on the films were: 5 wt% composite film = 140 μg/cm^2, 5 wt% neat film = 75 μg/cm^2, 10

wt% composite film = 130.33 μg/cm² and 10 wt% film = 83.17 μg/cm². The protein adsorption was significantly higher (n=4, **p<0.01) on the P(3HO)/n-BG composite films than on the P(3HO) neat films. The adsorption of proteins on the 5 wt% composite film was 46.42 % higher than that on the comparable neat film. Similarly the adsorption on the 10 wt% composite film was 36.18 % more than that of the comparable neat film.

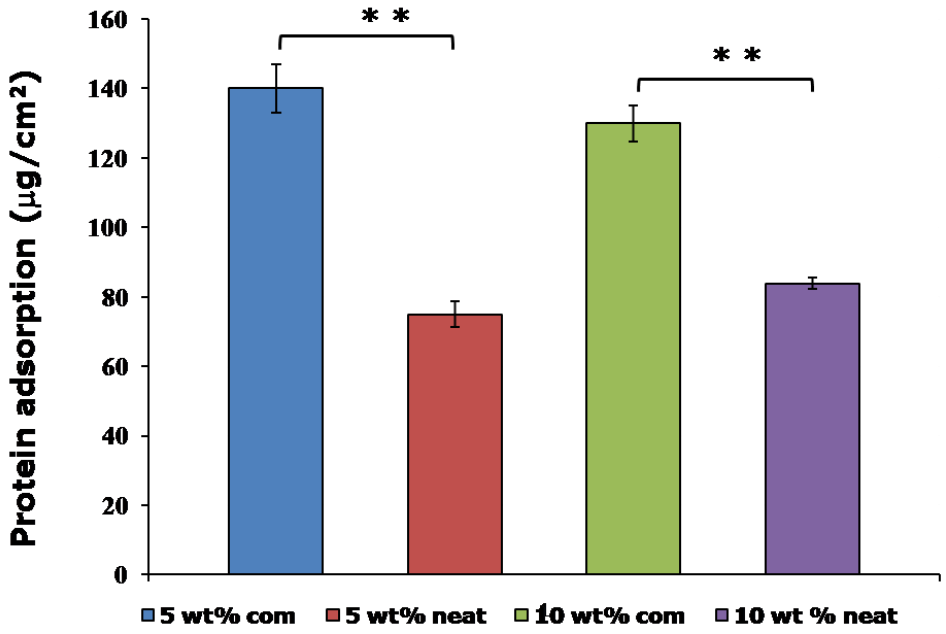

Figure 5.17: Protein adsorption study of the fabricated films. The data (n=4; error bars = ±SD) were compared using the Student's t-test and differences were considered significant when **p<0.01: ■ 5 wt% com, ■ 5 wt% neat, ■ 10 wt% com and ■ 10 wt% neat.

5.2.6. *In vitro* cytocompatibility study

In vitro cytocompatibilty studies were carried out using the keratinocyte cell line HaCaT. Cell attachment and proliferation studies carried out using the neutral red assay (described in section 2.15.2) established the biocompatibility of the films fabricated from P(3HO) produced using *P. mendocina* with octanoate as the carbon source. Proliferations of the HaCaT cells on the fabricated films were studied over a period of 1, 4 and 7 days, the results of

which are summarised in **Figure 5.18.** The proliferation studies were carried out using the standard tissue culture plate as a control, the growth on which was normalised to 100%.

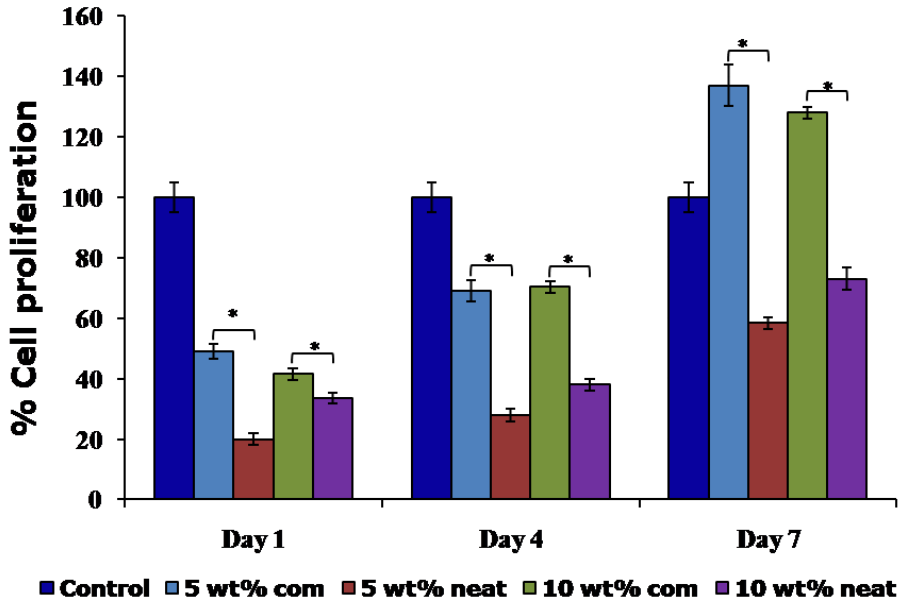

Figure 5.18: Proliferation study of the seeded HaCaT cells on the fabricated P(3HO) neat and P(3HO)/n-BG composite films at day 1, 4 and 7. The data (n=8; error bars = ±SD) were compared using the Student's t-test and differences were considered significant when *p<0.05: ■ Control (TCP), ■ 5 wt% com, ■ 5 wt% neat, ■ 10 wt% com and ■ 10 wt% neat.

The growth of HaCaT cells on all the films increased over the studied time duration. However, compared to the neat films the cells showed better attachment and proliferation on the comparable composite films. At day 7 there was a significant increase in the growth of the cells on the composite films when compared to the neat films and the control (n = 8, **p<0.05). The growth of HaCaT cells on the 5 wt% composite film was 139.8% as opposed to 58.42% on the 5 wt% neat film. Similarly, the growth of the cells on the 10 wt% composite film was 137.83% as oppose to 73.09 % on the 10 wt% neat film.

Keratinocytes have been reported to form four distinct layers and divide and differentiate as they move from the deeper layer to the outermost layers. This arrangement of cell layers from the bottom to the outermost is as follows: (1) stratum basale (basal layer), (2) stratum spinulosum (spiny or prickle cell layer), (3) stratum granulosum (granular layer) and (4) stratum corneum (horn sheet layer) (Yung, 2010). In this study the HaCaT cells seeded onto the fabricated films were also analysed using SEM (described in section 2.15.3) to analyse their morphology and attachment onto the films. The cells were able to attach and proliferate on both the neat and composite films. **Figure 5.19(A1-A2)** shows the attachment and proliferation of the HaCaT cells on the fabricated films.

In both the neat films, 5 and 10 wt%, confluent growth was observed by day 4, however arrangement of the cells into mature coherent sheets occurred only by day 7. **Figure 5.19(B1-B2)** shows the confluent growth of the HaCaT cells on the fabricated neat film on day 4.

In the composite films too, the cells showed good growth and proliferation. The covering of the cell layer with coherent horn sheets (**Figure 5.19(C1-C2))** was already observed by day 4 in both the 5 and 10 wt% composite films. As horn sheets are the outermost and most mature or differentiated stage of the HaCaT cell line, this implies that the cells had successfuly attached, proliferated and grown on the fabricated composite films.

The proliferation of HaCaT cells continued below the horn sheets as indicated by increased cell proliferation data (**Figure 5.18**). These SEM observations show that the HaCaT cells were able to proliferate better on the composite films as opposed to the neat films. These observations correlated well with the proliferation data observed from the neutral red assay.

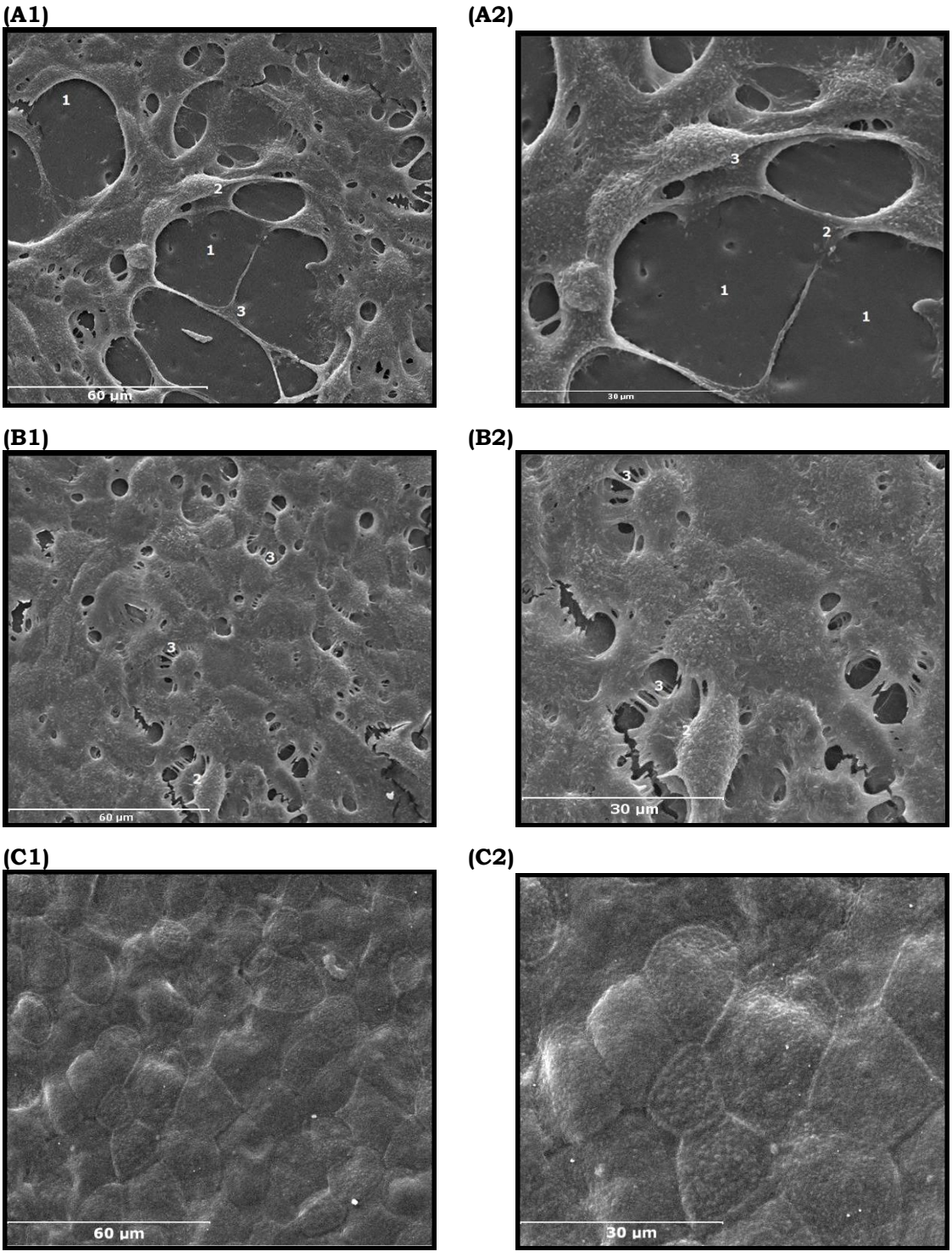

Figure 5.19: SEM images of the seeded HaCaT cells on the fabricated films: (A) Seeded HaCaT cells showing its attachment and proliferation on the film: (A1) Magnification 2000X (A2) Magnification 3000X; (B) Seeded HaCaT cells at day 4, on the neat film, confluent growth of the cells observed: (B1) Magnification 2000X

(B2) Magnification 3000X; (C) Seeded HaCaT cells on day 7 on the composite film, arrangement of cells in horn sheets: (C1) Magnification 2000X (C2) Magnification 3000X: (1) Uncovered polymer matrix, (2) Cell layer and (3) Spreading of the cell.

5.2.7. *In vitro* haemostatic study of the bioactive nanosize 45S5 Bioglass® particles

In vitro study on the haemostatic effect of the bioactive nano size 45S5 Bioglass® was evaluated using the thromboelastograph, TEG® as described in section 2.1.3. Three different amounts of n-BG i.e. 1, 2 and 4 mg were used for the study, in order to look for dose-related changes. The TEG® profiles and the tabulated clotting parameters are listed in **Figure 5.20** and **Table 2** respectively. The n-BG was found to be haemostaticaly active and increasing amounts of n-BG accelerated the initiation of clotting (R time), although rate of clotting (alpha angle) was not altered in a clearly dose-related manner and clot strength (maximum amplitude) was slightly reduced.

Sample	R (min)	Alpha (degree)	Maximum Amplitude (mm)
4 mg nBG (Profile 1)	3.80	61.40	57.30
2 mg nBG (Profile 2)	5.60	50.70	57.95
1 mg nBG (Profile 3)	6.25	52.50	60.90
Control (Profile 4)	9.70	60.20	66.10

Table 5.2: *In vitro TEG*® clotting parameters

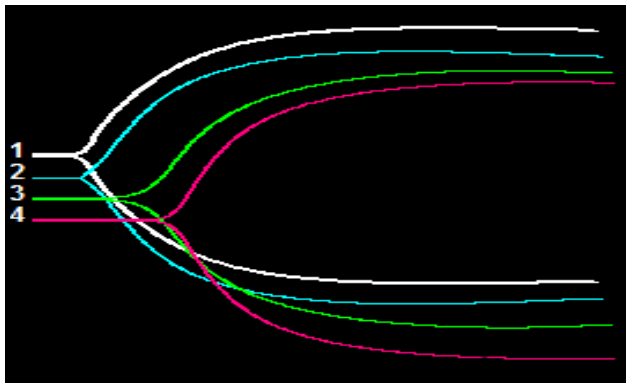

Figure 5.20: Profile of TEG analysis of the various amounts of n-BG: Profile 1= 4 mg n-BG, profile 2=2 mg n-BG, profile 3= 1 mg n-BG and profile 4=control.

5.3. Discussion

In this section, the results of the investigation on the films developed in the framework of this project are discussed in relation to microstructural, mechanical, thermal properties, *in vitro* degradation, haemostasis, protein adsorption and cell studies in order to assess if the properties of the films make it suitable for the proposed applications.

5.3.1. Properties of the fabricated films

The fabricated neat P(3HO) and the composite, P(3HO)/n-BG films were subjected to a series of analyses to assess their microstructural properties. This is because microstructural properties such as surface topography, roughness and wettability have been reported to play a pivotal role in the applicability of a potential biomaterial. Surface study of the fabricated films using the SEM (**Figure 5.4**) revealed that the P(3HO) neat films had a smooth surface topography. Incorporation of the bioactive nanosize 45S5 Bioglass® particles into the polymer in case of the composite films has indeed changed the surface morphology by introducing rough topography on the surface of the composite film due to the direct exposure of the nanobioactive glass particles on the surface. SEM images of **Figure 5.4** revealed that the n-BG particles were present both in the matrix as well as on the surface of the polymer. This increased roughness of the composite films was confirmed by the white light interferometry analysis, where by a typical RMS value of 0.440 μm was observed for the composite film as opposed to 0.238 μm for the P(3HO) neat film. In this present study the roughness of the 10 wt% neat and 10 wt% composite films could not be assessed, however similar observation of increase roughness for the 10 wt% composite film as opposed to 10 wt% neat film could be expected due to the incorporation of the n-BG in the 10 wt% composite film. In this present study the the roughness of the 5 wt%

composite film had roughly doubled in contrast to the results of Misra *et al.* (2007) where the roughness of the P(3HB) film had changed only slightly from 2.01 μm to 2.05 μm for the P(3HB)/45S5 Bioglass® (microsize) composite film. The authors had attributed this low roughness value due to the fact that the bioglass particles were embedded in the polymer matrix (Misra *et al.*, 2007). However, incorporation of TiO_2 as a filler in PDLLA composite was found to increase the roughness of the PDLLA film from 2.71 μm to 4.70 μm for a PDLLA/ TiO_2 composite film (Boccaccini *et al.*, 2005). Hence, the increase in the surface roughness is also governed by the method of fabrication and differences in density of polymer and glass.

Water contact angle studies of the fabricated films were also carried out to assess their wettability i.e. hydrophilicity. Surfaces with θH2O less than 70^o is considered to be hydrophilic and θH2O greater than 70^o is considered to be hydrophobic (Peschel *et al.,* 2007). The studies showed that incorporation of the n-BG particles into the polymer matrix also had an effect on the hydrophilicity of the composite films. The incorporated n-BG are known to be hydrophilic in nature and therefore, its incorporation into the polymer matrix was expected to increase the hydrophilicity of the composite. The composite films indeed showed increased hydrophilicity as opposed to the neat films. Also, the 5 wt% composite film was more hydrophilic (θH2O = 75.43^o±2) than the 10 wt% composite film (θH2O = $76.63±3^o$). This could be because for both the 5 and 10 wt% composite films, equal amount of n-BG particles 1 wt% (w/v) were added, hence more n-BG particles per gram of the polymer was present for the 5 wt% polymer as opposed to the 10 wt% polymer. This could have therefore resulted in the presence of more n-BG on the surface of the 5 wt% polymer composite films as opposed to the 10 wt% composite films.

This, increase in the wettability of the composite films were consistent with the observations made by Misra *et al.*, 2008. They found that the wettability of the poly-3-hydroxybutyrate, P(3HB) composite had increased by the

incorporation of the n-BG. The θH_2O value for the neat P(3HB) film was found to be 87±9°. In comparison the P(3HB)/n-BG composite film containing 10 wt%, 20 wt% and 30 wt% n-BG, has θH_2O was reduced to 68±9°, 55±1° and 62±2° respectively (Misra *et al.,* 2008). These results therefore show that wettability can be increased by increasing the amounts of the incorporated filler, in this case n-BG in the polymer matrix.

The contact angle values reported for other PHAs in literature are , θH_2O = 73.8° for P(3HO) (containing 84.5 mol% C_8, 6 mol% C_6 and 4.3 mol% C_{10}) (Marcal *et al.,* 2008); θH_2O= 98°± 5 for poly(3-hydroxyoctanoate-co-3-hydroxy-10-undecenoate, P(3HO-co-3HU) (Furrer *et al.,* 2006); θH_2O = 85° for poly(3-hydroxybutyrate-co-3-hydroxyhexanoate), P(3HB-co3HHx) (Ji *et al.,* 2008); θH_2O = 90° for poly(3-hydroxybutyrate-co-3-hydroxyvalerate), P(3HB-co-3HHx)(Ji *et al.,* 2008); θH_2O = 87° for P(3HB) (Misra *et al.,* 2008) . Therefore, in this study the fabricated neat P(3HO) with θH_2O = 77.3° ± 1 (5 wt% neat) and θH_2O = 78° ± 1 were found to be more hydrophilic than most of the reported PHAs except for P(3HO) (containing 84.5 mol% C_8, 6 mol% C_6 and 4.3 mol% C_{10}) which had a θH_2O = 73.8° (Marcal *et al.,* 2008).

Static tensile studies showed that the fabricated films like other mcl-PHAs reported in literature exhibited an elastomeric nature. Marchessault *et al.* (1990) found the Young's modulus 'E' value for P(3HO) to be 17 MPa and the % elongation values ranging between 250-350% (Marchessault *et al.,* 1990). For mcl-PHA containing 86% of 3HO and minor quantities of 3-hydroxydecanoate and 3-hydroxyhexanoate the 'E' value of the polymer film (1.6 mm thickness) was 7.6 ± 0.5 MPa and % elongation to break of 380% (Gagnon *et al.,* 1992). Similarly Asrar *et al.* (2002) observed Young's modulus values ranging from 155 to 600 MPa and elongation to break % ranging between 6.5 to 43 for P(3HO) thermally processed films (micrometer thick,

values not given) containing 2.5 to 9.5 mol % of 3-hydroxyhexanoate, (3HHx) (Asrar *et al.,* 2002). In studies carried out by Ouyang *et al.* (2007) mcl-PHA solvent casted films (100 μm thick) containing different mol% of 3-hydoxydecanoate, 3(HDD) i.e. 15, 28 and 39 had Young's modulus value of 3.6, 6.0 and 11.5 MPa respectively (Ouyang *et al.,* 2007). Thus, the Young's modulus values of the fabricated films in this present study (refer to **Figure 5.7**; thickness quoted in section 5.2.1) was comparatively low when compared to other values reported in literature. Thus, implicating that the films fabricated in this present study were less stiff and more flexible and elastic in nature.

The tensile test also showed that the incorporation of the n-BG contributed to increasing the Young's modulus (measure of stiffness) of the composites as previously observed in the case of P(3HB/n-BG composites (Misra *et al.,* 2008) and nanoscale tricalcium phosphate/PLGA composite (Loher *et al.,* 2006). This increased stiffness of the composites by the incorporation of n-BG could be attributed to two factors, first the nanoparticles efficiently infiltrates the pores of the polymer matrix thereby sealing it and in the process strengthens the whole composite structure. Second, the incorporation of the n-BG into the polymer matrix provides a higher interfacial surface area which enhances the load transfer between the polymer matrix and the stiff n-BG inclusions.

Thermal studies of the fabricated films were also carried out as thermal stability has an important implication on the material's processability and end goal application. The thermal properties of the films are depicted in **Figure 5.9** and summarised in **Table 1**.

During the first heat scan the polymer chains in the crystalline phase of the polymer melts and fall out of their ordered crystalline structures. This absorption of energy for the melting of the polymer chains in the crystalline phase is reflected as the T_m peak. Once melted the polymer chains are unable

to rearrange themselves into ordered structures again during the cooling run that follows the first heating run. This inability of the melted polymer chains to rearrange themselves into ordered crystalline lattices led to the absence of a T_m peak for the transition of the crystalline phase into the amorphous state during the second heat scan. Incorporation of n-BG particles in the polymer matrix resulted in the reduction of the melting temperature, thus corresponding to a decrease in the crystallinity of the composite as shown in **Figure 5.9** and **Table 1.** These observations were consistent with the observation made by Misra *et al*. (2007) whereby the crystallinity and T_m of the composites of poly-3-hydroxybutyrate, P(3HB) and 45S5 Bioglass® (microsize) was lower as opposed to that of neat P(3HB) films (Misra *et al.,* 2007). A decrease in the T_m was also observed when n-BG 45S5 was incorporated into the polymer P(3HB) matrix. The melting temperature had reduced from 172°C for P(3HB) neat film to 156°C, 157°C and 155°C for P(3HB) containing 10, 20 and 30 wt% of n-BG respectively (Misra *et al.,* 2008). This decrease in the T_m could be because of the decrease in the crystallinity of the P(3HO)/n-BG composites due to the incorporation of the filler n-BG in the crystalline portion of the polymer matrix, thereby decreasing the ordered arrangement in the composite. Therefore, as the crystallinity of the composite system gets reduced the polymer chains requires less energy to fall out of their ordered structure. Hence, a decrease in the T_m is observed.

Thermogravimetric analysis of the fabricated films showed that the neat films were more stable than the composite films. This is because incorporation of n-BG had reduced the degradation temperature of the P(3HO) neat film from 300°C to 195°C for the 5 wt% composite and 200°C for the 10 wt% composite film. However, at 300°C the polymer lost all its weight, similar observations was also made by Xi *et al*. (2008). They found that during the TGA analysis, with the temperature increasing to about 300°C the P(3HB-co-3HHx) films

lost nearly all its weight. For the 5 wt % and 10 wt% composite films the initial reduction in mass could be because of the loss of water which was incorporated in the 45S5 Bioglass ® mass as described elsewhere in (Clupper and Hench, 2003). Also for the composites (**Figure 5.9**) the weight loss was rapid upto 250^{o}C but remained constant after about 500^{o}C, implying that at this point the entire polymer was lost and only the n-BG was left. This accelerated degradation of the composites have been hypothesized to occur due to the inclusion of Bioglass® into the polymer matrix which at elevated temperature leads to a reaction at the filler–matrix interface that may degrade the polymer (Blaker *et al.*, 2010)

5.3.2. *In vitro* degradation study

The degradation behaviour of films are of paramount importance and greatly affect its potential as a biomaterial. *In vitro* degradation of the films was carried out to understand, how these films degrade and how its physical and chemical properties change with degradation.

Water absorption and weight loss behaviour of the films were studied over the incubation time period of 4 months. The results (**Section 5.2.4.1, Figure 5.10 and 5.11**) show that the films did absorb water and lost weight during the incubation period thus indicating that the films were undergoing degradation. Both the water absorption and the weight loss increased progressively with time in all the three media. Also, the water absorbed and weight loss was higher for the P(3HO)/n-BG composite films as opposed to the neat P(3HO) films. Similar results of increased water absorption and weight loss have been described in literature due to the incorporation n-BG into the polymer P(3HB) matrix (Misra *et al.,* 2007; Misra *et al.,* 2008). In a study carried out on the degradation of poly(3-hydroxybutyrate-co-3-hydroxyvalerate), P(3HB-co-3HV), Holland *et al*. (1987) observed water absorption in polymers during a 120-day

experiment and found that increased water absorption was associated with progressive degradation of the samples (Holland *et al.,* 1987).

As the films in this study were only incubated in enzyme free media, hence the degradation of the films must have occurred due to abiotic non enzymatic hydrolysis. The water molecules react with the polymer cleaving the ester bond and thus exposing the carboxylic acid group and the hydroxyl group. Hydrolytic degradation of PHAs is multiphasic. In the first stage spanning a few weeks, the amorphous phase of the polymer begins to degrade. This is because the crystalline regions of the polymer are impermeable to water, hydrolysis is therefore restricted to the amorphous regions of the polymer and to the fringes of the crystalline region (Scott and Gilead, 1995). Next, the crystalline part of the polymer begins to degrade resulting in the formation of monomers, dimers and tetramers, simultaneously the molecular mass also decreases. Progressively with time the degradation process develops and the polymer looses its mass (Volova, 2004). Such hydrolytic degradation of PHAs have been previously described in literature and is known to be a slow process when compared to the enzymatic hydrolysis of PHAs (Marois *et al.,* 2000). This is because of the high crystallinity of PHAs, as higher crystallinity means more impermeability of water into the crystalline regions to water (Scott and Gilead, 1995) and also due to the hydrophobic nature of long alkyl pendant chains (Renard *et al.,* 2004).

This slow hydrolytic degradation could be a reason why the fabricated films had lost only 15% of the weight for the P(3HO) neat films and 18% of weight for the P(3HO)/n-BG composite films after 4 months of incubation. However, the water absorption and weight loss observed in this study for the neat films was higher than those observed for other PHAs also studied for hydrolytic degradation. For instance no significant weight loss was observed when P(3HB), P(3HB-co-3HV) samples were incubated for 180 days at 37°C in aqueous media (Doi *et al.,* 1989; Doi *et al.,* 1990). Marios *et al.* (2000) studied

the *in vitro* degradation of the P(3HO) film containing 3 mol% 3HHx in water and phosphate buffer saline. The films showed negligible mass loss of less than 1% after 24 months of incubation (Marois *et al.,* 2000).

Numerous factors affect the biodegradability of PHAs such as stereoregularity, molecular mass, monomeric composition and crystallinity of the polymer. Studies carried out by Mochizuki, (1997) and Tokiwa *et al.* (2004) showed that biodegradation of PHAs is influenced by the chemical structure: like the presence of functional groups in the polymer chain, hydrophilicity / hydrophobicity balance and presence of ordered structure: like crystallinity, orientation and morphological properties (Mochizuki and Hirami, 1997; Tokiwa and Calabia, 2004). Usually the degradation of the polymer decreases with the increase of highly ordered structure i.e. increasing crystallinity. Since more crystalline structures, also have higher melting temperature for the crystalline phase of the polymer, hence for PHAs, degradation rate also decreases with increasing T_m. Therefore, as the films fabricated in this present study has low T_m, and hence low crystallinity therefore the films were more degradable than P(3HB), P(3HB-co-3HV) described in literature (Doi *et al.,* 1989; Doi *et al.,* 1990).

In this present study the pH of all the three media, PBS, DMEM and $DMEM^{KT}$ in which the neat and composite films were incubated increased progressively with time. The degradation of the UV P(3HO) neat films would result in the production of 3-hydroxyoctanoate or 3-hydroxyoctanoic acid depending on the pH of the media. If hydroxyoctanoic acid is denoted as HA, then its dissociation upon release after degradation can be represented as:

$$HA\ (aq) \rightleftharpoons H^+\ (aq) + A^-\ (aq)$$

The pKa for 3-hydroxyoctanoic acid is 4.89. As the pH of all the three media is 7.4 which is greater than the pKa of the acid (4.89), therefore most of the acid molecule would exist in the form of 3-hydroxyoctanoate, a base, leading to an increase in the pH of the media in which the neat UV films are incubated. The increase in the pH of the three media in case of the composite films could also be due to the leaching of the alkaline Na and Ca ions from the incorporated n-BG particles.

When thermal analysis of the degraded samples was carried out using DSC an interesting observation was the appearance of a second transition corresponding to the glass transition temperature that occurred between -51^{o}C and -57^{o}C. Appearance of a second T_g peak indicated that the amorphous region of the samples was undergoing an additional secondary crystallisation. Also, when mechanical testing of the degraded films was carried out it was found that the Young's modulus of the polymer had increased after two months of incubation and again showed a reduction of the modulus at 4 months of incubation (**Figure 5.12**). Although the Young's modulus had decreased at 4 months the value was still higher than that observed for the undegraded films. This appearance of an additional T_g peak in the amorphous region and increase in the Young's modulus of the films after degradation could be due to the ageing of the polymer (Hutchinson, 1995). The ageing in PHA materials occurs due to the secondary crystallisation of the PHAs which involves the development of the interlamellar secondary crystallisation in the amorphous region of the semi crystalline polymer. The small crystallites produced restricts the motion of the polymer chains in the amorphous regions, thereby reducing the mobility of the polymer chain segments; thus raising the modulus and increasing the brittle nature of the material (Biddlestone *et al.,* 1996).

Many PHAs have been reported to show ageing behaviour (Biddlestone *et al.*, 1996; Asrar *et al.*, 2002; Alata *et al.*, 2007; Parulekar and Mohanty, 2007). For

example when Asrar *et al.* (2002) aged the copolymer P(3HB-co-8.1 mol% 3HHx) for 11 day at room temperature, the Young's modulus increased from 18.8 MPa to 22.8 MPa. Alata *et al.* (2007) studied the ageing effect on the mechanical properties of P(3HB-co-3HHx) containing different mol % of 3HHx, ranging from 5 to 18 mol%. After 60 days of ageing they found that the % elongation to break had decreased and the tensile strength had increased for all the copolymers. Similar observations were made for P(3HB) and copolymer of P(3HB-co-3HV).

In tissue engineering, it is important that the cellular behaviour affected by the degradation products be considered for a comprehensive biocompatibility evaluation of the implant polymers. Studies were carried out by Sun and his group in 2007, on the cellular responses of mouse fibroblast cell line L929 to the PHA degradation products, oligo-hydroxyalkanoates (OHAs), oligo(3-hydroxybutyrate), O3HB, M_n 2000, oligo(3-hydroxybutyrate-co-4-hydroxybutyrate), O3HB-co-4HB, M_n 2100, 6 mol% 4HB, oligo (3-hydroxybutyrate-co-3-hydroxyhexanoate), OHBHHx, M_n 2800, 12mol% 3HHx) and medium-chain-length oligo(3-hydroxyalkanoates) (OmclHAs, M_n 2300, 2 mol% 3-hydroxyhexanoate ,3HHx, 25 mol% 3-hydroxyoctanoate, 71mol% 3-hydroxydecanoate and 3 mol% 3-hydroxydodecanoate). They found that the cytotoxicity of OHA decreased with increasing OHA side chain length thus indicating that medium chain length OHAs containing PHA, such as poly(3-hydroxybutyrate-co-3-hydroxyhexanoate), P(3HB-co-3HHx) and mcl-PHAs are more biocompatible than short chain length hydroxyalkanoates (Sun *et al.,* 2007). Therefore, degradation products of the fabricated neat and composite P(3HO) films in this study can also be expected to have decreased cytotoxic effect on the seeded cells as compared to the scl-PHAS, an important requirement for a biomaterial.

5.3.3. Protein adsorption and *in vitro* cell biocompatibility

Many studies have been carried out to understand the cell and material interfacial relationships, particularly related to protein adsorption. This is because most mammalian cells are anchorage dependent and need a biocompatible, protein rich surface for attachment, differentiation and migration to form new tissue (Webster *et al.*, 2000; Wei and Ma, 2004; Misra *et al.*, 2008). It has been shown that cell adhesion takes place in two different stages. The first stage consists of the adsorption of water and a layer of proteins that selectively adhere onto the biomaterial surface, mediated by the surface properties of the substrate (Navarro *et al.,* 2006). The second stage involves cell adhesion onto the layer of proteins, which is a more complex process, mediated by the extracellular matrix (ECM) proteins, cell membrane proteins, and cytoskeletal proteins (Luthen *et al.,* 2005; Misra *et al.,* 2008). Protein adsorption can thus modulate cell adhesion and survival. Therefore, protein adsorption is important in evaluating a film for tissue engineering. The adsorption of proteins onto the fabricated films, in the present study, was carried out using the whole protein serum. The total proteins adsorbed onto the surface of the P(3HO)/n-BG composite film was greater than that adsorbed on the neat P(3HO) films (**Section 5.2.5, Figure 5.17**). This increased adsorption of proteins on the composite films could be due to the incorporation of the n-BG which had increased the surface roughness and hydrophilicity and also the surface area of the composite exposed to the proteins. This result is in agreement with the increased adsorption of proteins observed on composites of P(3HB)/n-BG (Misra *et al.,* 2008), nanoscale hydroxyapatite/PLLA composite film (Wei and Ma, 2004) and fibrous nanoscale tricalcium phosphate/PLGA composite scaffold (Schneider *et al.,* 2008).

The *in vitro* cell biocompatibility studies of the films were carried out by seeding HaCaT cells onto the films and studying its proliferation over a duration of 1, 4 and 7 days. The results (**Section 5.2.6, Figure 5.19)** show that the cell proliferation increased progressively on all the films. Also the proliferation of the cells was better on the composite films as opposed to the neat films. In fact by day 7 the proliferation of the cells on the composite films was 140% (5 wt% com film) and 137.83% (10 wt% com film) of that of the control. However, for the neat film, at day 7, the proliferation was 58.42% (5 wt% neat film) and 73.09% (P(3HO): 10 neat) of the control.

SEM scans of the cells also confirmed that the polymer matrix was able to support cell growth. SEM analysis of cells also showed that the HaCaT cells had already arranged themselves into horn sheets by day 4 in both the 5 and 10 wt% composite films, however in the neat films the horn sheet arrangement of the films appeared only in day 7. Keratinocytes arrange themselves into four distinct layers. The outermost layer of arrangement is the Horn sheets at which state the HaCaT cells are most mature. Therefore, arrangement of horn sheets in the composite films within day 4 indicates that the HaCaT cells have been able to grow and mature faster in the composite films. On the other hand the appearance of horn sheets only by day 7 in the neat films suggest that the HaCaT cells are growing and maturing comparatively slowly in the neat films as opposed to the composite films.

It has been discussed in literature that a rough and hydrophilic surface provides a better matrix for cell attachment and proliferation (Mei *et al.*, 2006; Xi *et al.*, 2008). Therefore, the increased proliferation of the HaCaTs on the composite films could be due to the incorporation of the n-BG which had introduced rough topography onto the surface of the composite films. This had resulted in an increase in the surface roughness of the composite film and its wettability when compared to the neat films which had a smooth surface and were less hydrophilic than the composite films. Also, the inclusion of the n-BG

had increased the surface area of the composite film thereby increasing the available surface for cell attachment. Similar observation of increased MG-63 osteoblast proliferation was observed for P(3HB)/n-BG composites as opposed to neat P(3HB) scaffolds by Misra *et al*. (2008) and increased proliferation of MC3T3-E1 osteoprogenitor cells on P(3HB-co-3HHx)/ hydroxyapatite scaffolds as oppose to P(3HB-co-3HHx) scaffold (Xi *et al.,* 2008). Their studies also concluded that the increased cell proliferation in the composite scaffold was due to the increase in the hydrophilicity and roughness of the film due to n-BG incorporation in the former and hydroxyapatite in the latter study.

5.3.4. *In vitro* haemostatic study

Normal haemostasis has been defined by Laposata *et al*. (1989) as the capability of the haemostatic system to control the activation of clot formation and clot lysis in order to prevent haemorrhage without causing thrombosis (Laposata *et al.,* 1989). The haemostatic effect of bioactive glass was reported by Ostomel *et al*. (2006). Their findings concluded that the mesoporous bioactive glass microspheres (MBGMs) had accelerated clotting time of the sheep blood and also the clot strength formed was stronger than that of the control (Sheep blood only). They concluded that this haemostatic effect of the MBGM was due to its dual role of supplying calcium ions, which act as cofactors for initiating the blood clotting cascade, and also by providing a negatively charged siliceous oxide as a support for surface dependent thrombotic reactions. The haemostatic effect i.e. clotting time and the clot strength was also found to be affected by the composition of the MBGM. MBGMs with a high silicon (Si) to calcium (Ca) ratio of 80 was more haemostatic than that of Si to Ca ratio of 60 (Ostomel *et al.,* 2006).

In this present study the TEG analysis showed that the n-BG was haemostaticaly active and accelerated the time for blood clot formation. The

haemostatic effect of the n-BG could also be due to its dual of supplying calcium ions and providing the negatively charged siliceous oxide as explained by Ostomel *et al.* (2006). Although the n-BG had accelerated clotting time, however the clot formed was of reduced strength as opposed to the control (whole human blood only). Clot strength is characterized by the strength of the fibrin mesh formed during clotting that entraps blood cells, platelets, and plasma (Carr and Alving, 1995). As seen by Ostomel's work the haemostatic effect of the bioglass was affected by the Si to Ca ratio and in this present study the Si to Ca ratio for the n-BG was 1.69. Therefore, the composition the n-BG used in this study though able to accelerate clotting time, cannot lead to an increased strength of the clot. Thus further investigation needs to be carried out with the composition of the n-BG with an aim to achieve both accelerated clotting time and higher clot strengths.

5.3.5. Properties of films and their suitability for the proposed applications

5.3.5.1. Poly-3-hydroxyoctanoate, P(3HO)/n-BG composite films as a potential multifunctional wound dressing film

The P(3HO)/n-BG composite films was fabricated as a material with the potential to be used as a multifunctional wound dressing, which will act as both a scaffold for skin regeneration and also accelerate wound haemostasis thus potentially reducing blood loss following tissue injury. The static mechanical testing of the P(3HO)/n-BG composite films showed that the Young's modulus value for the 5 wt% composite films was 3.42 ± 0.7 MPa and the 4.23 ±1 MPa for the 10 wt% com film. The thermal properties of the films were: T_m =45.62^{o}C, T_g = -34.86^{o}C for the 5 wt% composite and T_m =45.56^{o}C, T_g = -34.37^{o}C for the 10 wt% composite films film. This low stiffness value and T_m and T_g below room temperature imparts elastomeric behaviour to the films. Therefore the composite films fabricated are flexible and elastomeric

making them suitable for multifunctional wound dressing which would act both as a film for skin regeneration and also provide haemostatic effect. **Table 3** compares the properties of the various biomaterials which have been used for skin tissue tissue engineering.

Polymer	Young's modulus (MPa)	Tensile strength (MPa)	Reference
P(3HB)	1640	12.9	(Peschel *et al.*, 2007)
P(3HB)/Ha	401	3.3	
P(3HB)/CH	334	3.3	
P(3HB)/P(4HB)	214	8.1	
P(4HB)	632	44	
P(4HB)/Ha	11.9	3.4(Yield strength 1.5)	
P(4HB)CH	29.2	4.1(Yield strength 2)	
Chitosan films containing Fucoidan	-	7.1	(Sezer *et al.*, 2007)
5 wt% composite film	3.42	3.3	(present study)
10 wt% composite film	4.23	nd	(present study)

Table 5.3: Investigated or potential biomaterial in skin tissue engineering: poly(3-hydroxybutyrate), P(3HB), poly(4-hydroxybutyrate), P(4HB), Chitosan, (CH), Hyaluronic acid, (Ha), nd = not determined, (-)= value not quoted.

Young's modulus value and tensile strength of human skin ranges between 15 to 150 MPs and 5-30 MPa respectively (Tang *et al.*, 2008). Short chain length PHAs like P(3HB) and its blend with Ha, P(3HB)/Ha and CH, P(3HB)/CH have high Young's modulus value hence are very stiff to be used as scaffolds for skin tissue engineering; on the other hand blends of P(4HB)/Ha and P(4HB)/CH have mechanical properties suitable for human skin(Table 5.3). The flexible nature of the composite film in this present study makes it suitable for applications in difficult contours of the body. However, the mechanical properties, Young's modulus value and tensile strength of the fabricated films were found to be lower when compared to human skin (Tang

et al., 2008). Therefore, one approach of improving the mechanical properties of the films to match values that of human skin would be to blend P(3HO) with other biocompatible materials such as chitosan, collagen, P(4HB) etc (Peschel *et al.*, 2007). *In vitro* degradation studies, revealed that the fabricated composite films undergo ageing. This ageing behaviour caused an increase in the initial stiffness of the film. Such an increase could affect the applicability of the material and therefore, may require addition of hydrophilic polymers or plasticizers which may inhibit polymer ageing. Amorphous or hydrophilic additives lead to higher water absorption and accelerate hydrolysis. For example, the water content was found to be higher in P(3HB)/P(DL-lactic acid) than in PHB/polycaprolactone (Zhang *et al.,* 2003).

Biocompatibility is an important requirement for any tissue engineering film. A biocompatible film provides a good surface for cell attachment and proliferation. The composite films showed very good biocompatibility for the seeded HaCaTs. The HaCaT cells were able to attach, proliferate and mature to form the horn sheet layers. In fact by day 7, the growth of the HaCaTs on the composite was 37% more than the control for the 5 wt% composite film and 28% more than control for the 10 wt% composite film.

The incorporated n-BG provides the haemostatic effect for the composite films. n-BG was found to accelerate the clotting time of the control (whole human blood) however the cloth strength was reduced. But as seen by Ostomel et al., the haemostatic effect of the Bioglass can be controlled by the Si to Ca ratio. Therefore, the composition of the n-BG can be tailored to achieve both accelerated clotting time and higher clot strengths as discussed in section 5.3.4.

The incorporated n-BG have also been reported to have an antibacterial effect which is attributed to high aqueous pH caused by the dissolution of the alkali

ions from the n-BG. The 45S5 Bioglass® have been shown to have an antibacterial effect against *S. aereus* and *S. epidermis* which are found to be present in wound dressing. In 2004, Pratten *et al*. (2004) found that bacterial colonization decreased significantly on surgical sutures with 45S5 coating as compared to that without coating (Pratten. *et al.*, 2004).

In conclusion the composite films fabricated in this study showed excellent biocompatibility for the seeded HaCaT cells thus implicating that it can serve as an excellent film for skin generation. The, incorporated n-BG also accelerated clotting time but with a weak clot formation. The incorporated n-BG is also expected to have an antibacterial effect which is advantageous for any wound dressing material. Overall, thus these composite films seem to be good candidates for the development of multifunctional wound dressing films.

5.3.5.2. Poly-3-hydroxyoctanoate, P(3HO) neat films as a potential biomaterial for pericardial patch

The low stiffness values of the fabricated neat films and thermal values below room temperature imparts flexible and elastomeric nature to the films. This flexible and elastomeric nature makes the neat films suitable as a biomaterial for heart patch application based on its stiffness. **Table 5.4** compares the properties of the various biomaterials which have been used for cardiac tissue engineering.

Polymer	E or T	Young's modulus (or stiffness)	Tensile strength	Reference
PGA	T	7-10 GPa	70 MPa	(Garlotta, 2001; Webb *et al.*, 2004)
PLLA or PDLLA	T	1-4 GPa	30-80 MPa	(Webb *et al.*, 2004)
PHB	T	2-3 GPa	36 MPa	(Ramsay *et al.*, 1993)
PGS	E	0.04-1.2 MPa	0.20.5 MPa	(Wang *et al.*, 2002)
Collagen fibre (Tendon/ cartilage/ ligament/ bone	E	2-46 MPa	1-7 MPa	(Misof *et al.*, 1997; Webb *et al.*, 2004)
Collagen gel (calf skin)	E	0.002-0.022 MPa	1-9 kPa	(Roeder *et al.*, 2002)
Myocardium of rat	E	0.001-0.14 MPa	30-70 kPa	(Bing *et al.*, 1971); (Yin *et al.*, 1980);
Myocardium of human	E	0.02-0.5 MPa	3-14 kPa	(Nakano *et al.*, 1990; Nagueh *et al.*, 2004)
P(3HO) (5 wt% neat film)	E	1.4 MPa	1.8 MPa	Present study

Table 5.4: Investigated or potential biomaterial in heart tissue engineering: T = thermoplastic, E= elastomer. Adapted from (Chen *et al.*, 2008)

Other biomaterials being studied for the application are either too stiff like PGA, PLLA or PDLLA whose Young's modulus value range in GPa or are very soft like collagen gel whose Young's modulus value range in 0.002-0.022 MPa. The stiffness of the fabricated P(3HO) films in particular the 5 wt% is comparable to the higher end stiffness value of polyglycerol sebacate, PGS, which range from 0.04 to 1.2 MPa. An interesting point is that the property of P(3HO) can be tailored by grafting acrylamide and carboxyl ions using plasma treatment (Kim *et al.*, 2002) and by blending it with other biocompatible elastomeric polymers such as collagen, so that its mechanical property can match the stiffness of the heart muscle at the beginning of diastole (stiffness is 10–20 kPa) or the stiffness at the end of diastole (200–500 kPa). It is because of its elastomeric and flexible nature that P(3HO) and other mcl-PHAs and their copolymers have been used for soft tissue engineering like heart valves and vascular grafts (see Section 1.10.2.1).

In vitro degradation studies, showed that the neat films also undergo ageing which could affect its application as a biomaterial for heart patch. Therefore,

like in the case of the composites the ageing of the films can be prevented by incorporating appropriate plasticizers into the polymer matrix. Cell culture studies with HaCaTs have also shown that the films are able to support cell attachment and proliferation, an important requirement for a biomaterial. The cells were also able to mature well and thus form the horn sheets. However, the biocompatibility of the films for cardiac cells needs to be studied.

Therefore, the neat P(3HO) films fabricated and assessed in this work show mechanical properties that make them suitable as a biomaterial for pericardial patch application. The film also showed biocompatibility for the HaCaT cells indicating that potentially cardiac cells would also grow well on them. This will be an essential aspect to be investigated in the future.

Chapter 6: Modifications of the homopolymer P(3HO)

6.1. Introduction

Biocompatibility is an important requirement for any potential tissue engineering scaffold and there are numerous factors that affect and govern a material's biocompatibility. These factors are shape, surface porosity, surface hydrophilicity, surface energy, chemistry of the material, the environment where it is incorporated and its degradation products (Yang *et al.,* 2002; Zhao *et al.,* 2003; Zhao *et al.,* 2003; Sun *et al.,* 2007). Surface properties of the material such as roughness and hydrophilcity become particularly important for any scaffold as most mammalian cells are anchorage dependent; and a more hydrophilic and rough surface aids in better cell attachment and proliferation as opposed to a less hydrophilic and smooth surface. Specific applications may also have a specific hydrophilicity requirement, and hence the hydrophilicity of the scaffold material must be tailored to suit the application.

The PHA family are polyesters of 3-hydroxyacids having a dominant hydrogen and carbon backbone. This family of polymers are relatively hydrophobic and although degradable have very slow degradation rates, particularly when it undergoes hydrolytic degradation. Numerous studies have therefore been carried out to modify the PHAs to increase its hydrophilicity, thus tailoring its degradation and improving its biocompatibility. Such modifications, in addition to increasing the hydrophilicity of the material, can also have an effect on other physical and chemical properties of the material such as chemical organisation (bond cleavage, addition of chemical moieties) mechanical strength and thermal processablity. Modification approaches have involved both chemical and physical methods such as blending, forming composites of the polymer, cross linking, graft copolymerization, coating of the polymer surface and UV treatment. These approaches have been discussed in section 1.11.

This chapter discusses the work that was done with an objective of modifying the homopolymer P(3HO) produced from *P. mendocina* in order to improve its properties, thereby making it more suitable as a biomaterial for medical applications. Three approaches were used for modifying the polymer:

6.1.1. Modification of P(3HO) using UV rays

Ultraviolet (UV) light is an electromagnetic radiation with a wavelength shorter than that of visible light, but longer than X-rays, in the range 10 nm to 400 nm, and energies from 3 eV to 124 eV. Modification of polymers using UV rays have been carried out previously (Shangguan *et al.*, 2006; Koo and Jang, 2008). This method is reasonably quick, economical and also environmentally friendly. The photons produced have sufficient energy to break C-C bonds, cause carbonyl esters bonds to cleave, thereby increasing the amounts of C-OH, COOH bonds and decrease the amounts of C-O-C and C-C bonds on the treated surface. Additionally, the photons can interact with the atmospheric oxygen and incorporate oxygen moieties on the UV treated surfaces to form highly polar groups such as hydroxyl, carbonyl and or carboxyl moieties (Bhurke *et al.*, 2000; Ruiz and Martinez, 2005). Shangguan *et al*. (2006) carried out UV treatment of the copolymer of poly(3-hydroxybutyrate-co-3-hydroxyhexanoate) and observed increased hydrophilicity due to an increase in C-O, C=O bonds and decrease in C-C bonds, which improved the materials biocompatibility with the mouse fibroblast cell line L929. Therefore, a similar approach was used to modify P(3HO) in this work (Shangguan *et al.,* 2006).

6.1.2. Incorporating n-BG into the polymer matrix to form composite films

Numerous studies have been carried out to study the cumulative effect of combining an inorganic phase with the polymer i.e. composite systems. The addition of such inorganic phase has been shown to alter the materials biocompatibility and degradation rate by introducing microstructural changes such as surface topography and roughness. 45S5 Bioglass® is a bioactive glass which is biocompatible, osteoconductive, nontoxic, noninflammatory as well as non immunogenic. Therefore it is very useful as a filler in biopolymer composites. Numerous studies have been carried out with 45S5 Bioglass®, both microsize and nanosize which have shown to improve the mechanical properties, surface wettability, biocompatibility and degradation rate, of the whole bioglass polymer composite system. Therefore, in this present study modification of the films made using UV treated P(3HO) was carried out by further incorporating n-BG to form UV P(3HO)/n-BG composite films. It must also be noted that, the fabrication of such composite films were also carried out and studied in detail, as described in Chapter 5, as a modification of the polymer P(3HO). However, in this case the polymer was not subjected to UV treatment.

6.1.3. Blending of P(3HO) with P(3HB)

P(3HO) (as discussed in Chapter 5) is found to be flexible and elastomeric which makes it suitable for soft tissue engineering. On the other hand, P(3HB) produced from *B. cereus* SPV from previous studies has been found to be brittle and stiff and has been studied for bone tissue engineering (Misra *et al.,* 2007; Misra *et al.,* 2008; Misra *et al.,* 2009). Therefore, studies were carried out to modify the properties of P(3HO) by blending it with P(3HB) and also incorporating n-BG into the blend matrix (**Figure 6.1**). Such blends

would be expected to be neither as hard or brittle as P(3HB) and or soft and flexible like P(3HO) i.e. it would possess intermittent properties of the combining polymers. However, detailed study on this approach of modification could not be carried out due to lack of time.

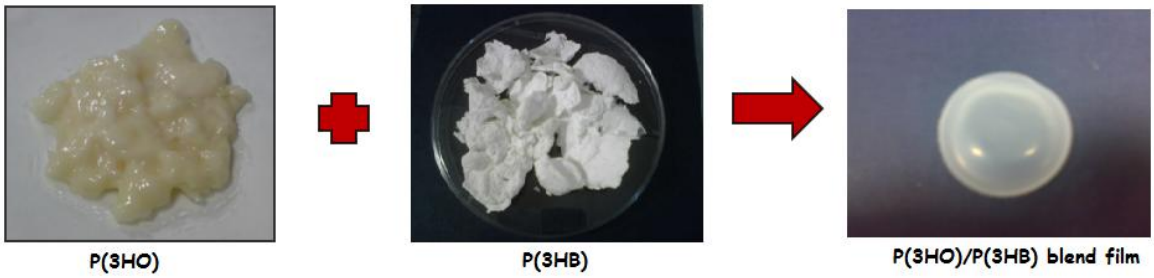

Figure 6.1: Schematic representation of blending of P(3HO) with P(3HB)

6.2. Results

6.2.1. Modification of P(3HO) using UV rays and its effects on the molecular weight of the polymer.

The polymer P(3HO) was subjected to UV rays for 8 hrs. A detailed method of UV treatment is described in section 2.10. UV treatment of the polymer was done such that the UV rays could cause cleavage of the ester bonds of the polymer. However, UV treatment also causes the C-C bonds to break. This breaking of the bonds would cause polymer chain scissions and thus have an effect on the molecular weights i.e. number average molecular weight, (M_n) weight average molecular weight, (M_w) and polydispersity of the polymer (PDI). Therefore, to study this effect, molecular weight analysis of the UV untreated (control) and UV treated polymer was carried out using gel permeation chromatography. UV treatment brought about a slight reduction in the M_w of the polymer from 339142 to 337597. As expected, this reduction in the M_w corresponded to a simultaneous increase in the M_n of the UV treated polymer (180901) as opposed to the control (163350). The PDI value of

the polymer also reduced from 2.07 to 1.87. Thus, exposure to UV rays did cause polymer chain scissions which resulted in the reduction of the polymers $M_{w,}$ increase in M_n and decrease in the PDI value.

6.2.2. Fabrication of the 2D neat P(3HO) (UV treated) and 2D P(3HO) (UV treated)/n-BG composite films

Following UV treatment the polymer was then fabricated into the neat P(3HO) 2D films and the P(3HO)/n-BG composite 2D films. Both the UV neat and the UV composite films were made of the same weight percents as the films made from non UV treated P(3HO) as described in Chapter 2 (section 2.12.3). These fabricated films will be referred to as UV P(3HO) neat film and UV P(3HO)/n-BG composite film; where the weight % have to be mentioned the films will be referred to as UV 5 wt% and UV 10 wt% neat films and UV 5 wt% and UV 10 wt% composite films. The thicknesses of the fabricated films were: UV 5wt% composite = 0.28 mm, UV 5wt% neat = 0.18 mm, UV 5wt% composite = 0.54 mm and UV 10 wt% neat = 0.43 mm. These films were then subjected to an in depth investigation to assess how the UV treatment of the polymer affects its surface, mechanical, thermal, degradation behaviour and biocompatibility.

6.2.2.1. XPS analysis

Surface analysis of the fabricated P(3HO) neat film made from UV treated P(3HO) was analysed using x-ray photon spectroscopy, (XPS). Such a study enables to assess the amount of hydrophilic C-OH, COOH, C=O bonds and the hydrophobic C-C bonds. An increase in the C-OH, COOH, C=O and decrease in the C-C bond content, would therefore indicate modification of the polymer being achieved by UV treatment. The P(3HO) neat film made from non UV treated P(3HO) was used as control.

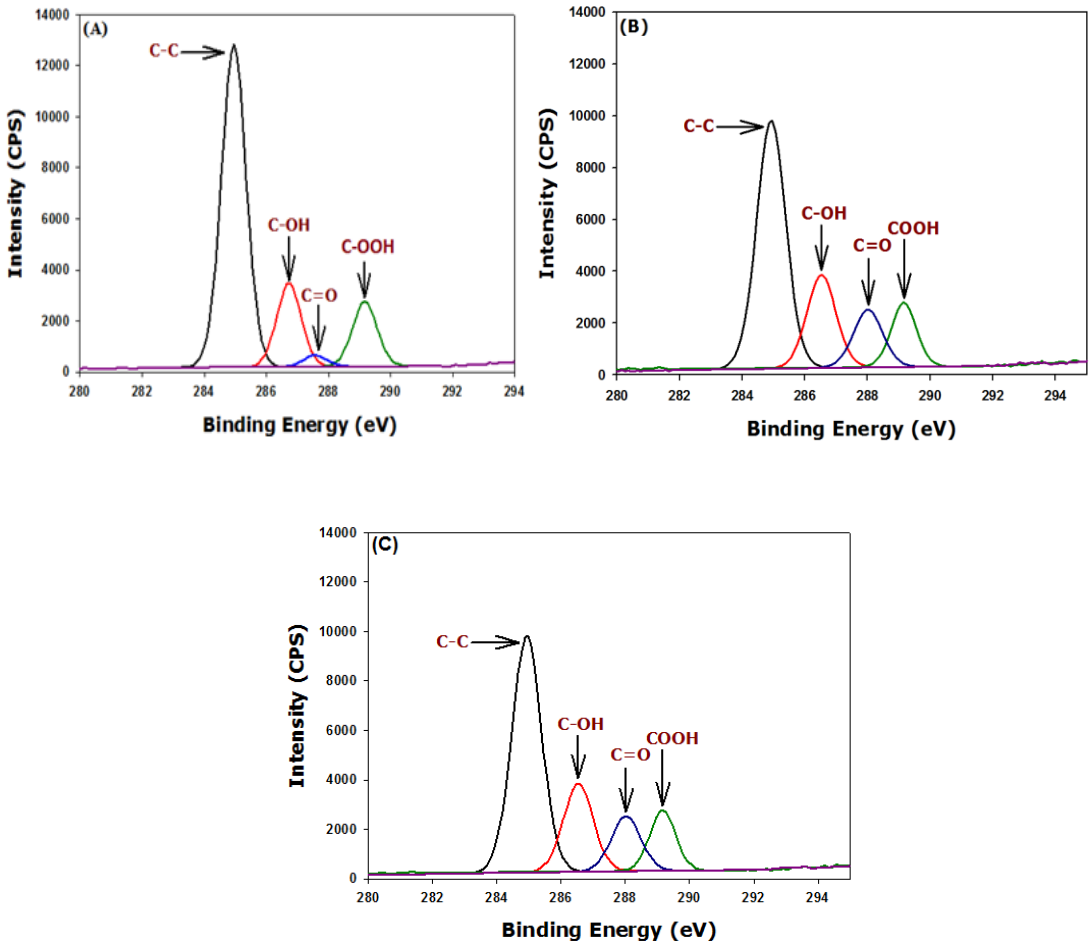

Figure 6.2: XPS carbon spectra of (A) 5 wt% neat film (ctr) and (B) UV 5wt% neat film and UV 5 wt% composite.

Sample	Bonding %			
	C-C	C-OH	COOH	C=O
P(3HO) neat film(control)	70.40	18.52	7.41	3.70
Sample, UV P(3HO) neat film (5 wt%)	51.48	20.02	15.73	12.87
Sample, UV composite film (5 wt%)	51.48	20.02	15.73	12.87

Table 6.1: Compilation of the XPS carbon analysis on the UV fabricated neat and composite and non UV fabricated neat and composite films.

XPS analysis showed that UV treatment increased the proportion of the surface/ hydrophilic bonds and decreased the non polar C-C bonds in the film made from UV treated P(3HO) as shown in **Figure 6.2** and summarised in

Table 6.1. The binding energy (eV) corresponding to typical carbon bonds are 285 (C-C), 286.7 (C-OH), 288 (C=O) and 289.1 (COOH) eV.

6.2.2.2. Microstructural analysis

Modifications of PHAs have been shown to have an effect on the microstructural properties of the polymer which in turn have an important effect on the biocompatibility of a material. Therefore, studies were carried out to assess the effect of UV treatment on the microstructural properties of the fabricated neat and composite films. The surface morphology and microstructure of these films as observed by SEM is shown in **Figures 6.3(A-B).** Here, the P(3HO) neat film appeared to have a rough surface when compared to the non UV treated P(3HO) neat film.

(A1)

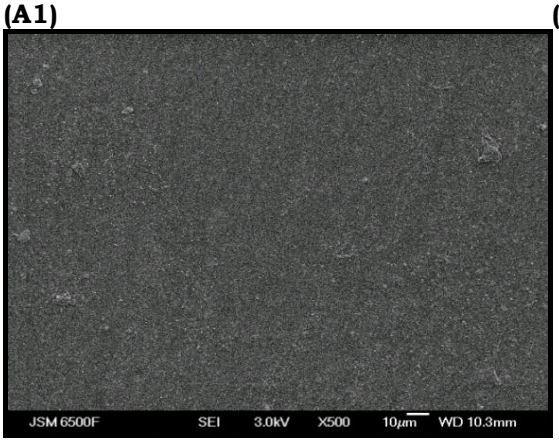

(A2)

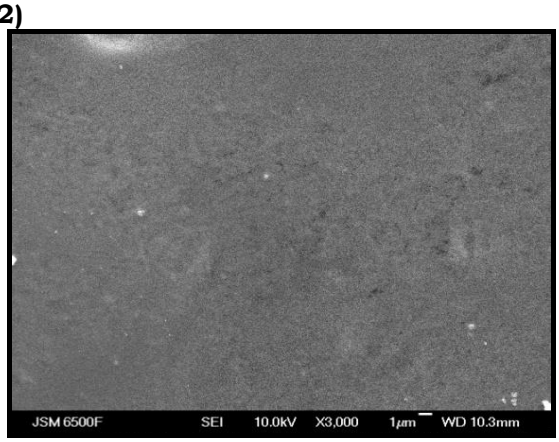

(A3)

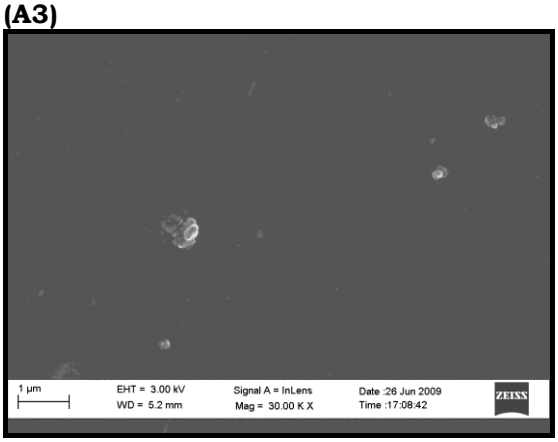

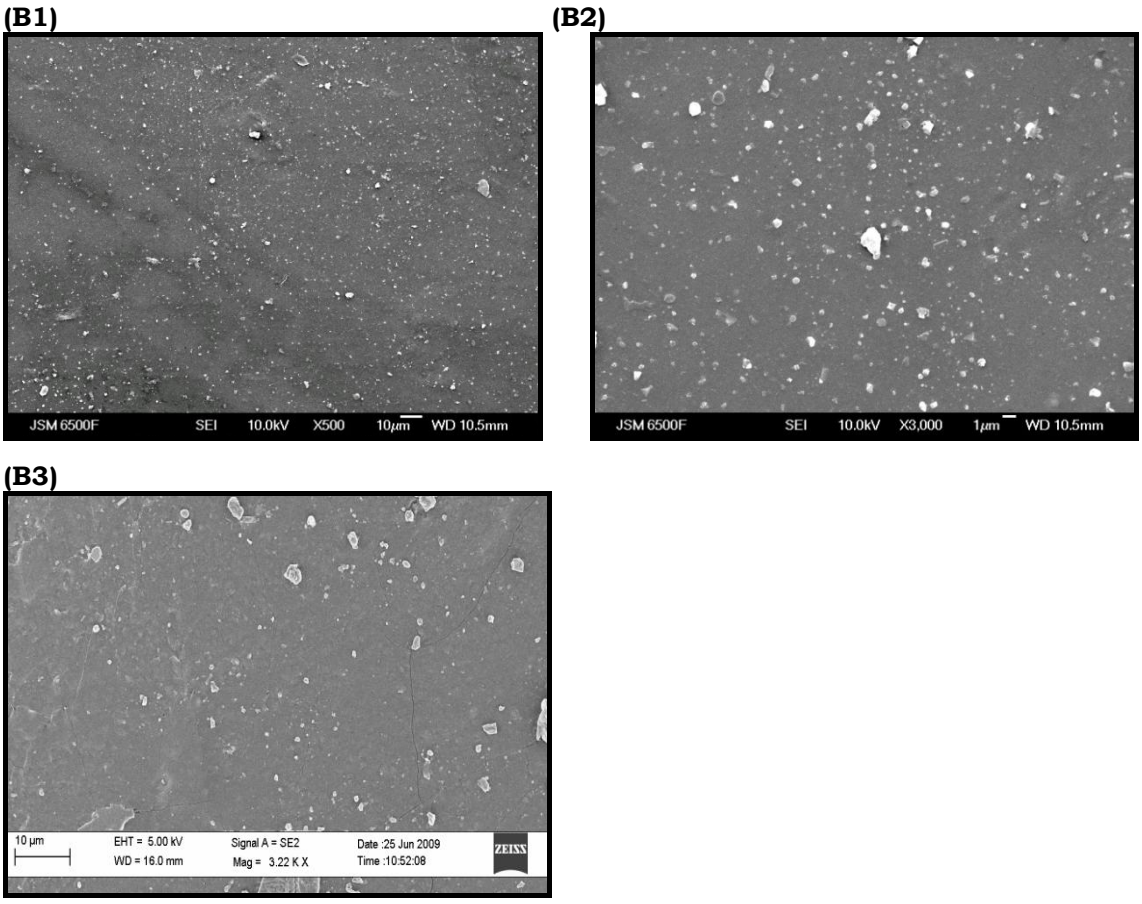

Figure 6.3: SEM images of the UV fabricated films: planar surface of (A) UV P(3HO) neat film:(A1) X1000, (A2) X3000, (A3) non UV treated P(3HO) neat film; SEM images of (B) UV P(3HO)/n-BG composite films: (B1) X1000 and (B2) X3000 and (B3) non UV treated P(3HO)/n-BG composite film.

This increase in the roughness of the UV neat films was also confirmed by the white light interferometry analysis using ZYGO®. The surface scans of these films using ZYGO® (**Figure 6.4)** show that the roughness of the 5 wt% neat film had increased from 0.238 μm (5 wt% neat film made from non UV treated P(3HO), shown previously in **Figure 5.6,** chapter 5) to 0.324 μm for the UV 5 wt% neat film i.e. an increase of 26.54 %.

Similarly, the incorporation of the n-BG into the UV composite film further increased the surface roughness by introducing a rough surface topography on the film surface as shown in the SEM images in **Figure 6.3**. Surface analysis

of the film surface using ZYGO® showed that the roughness value for the UV 5 wt% composite film was 0.578 µm (**Figure 6.4**).

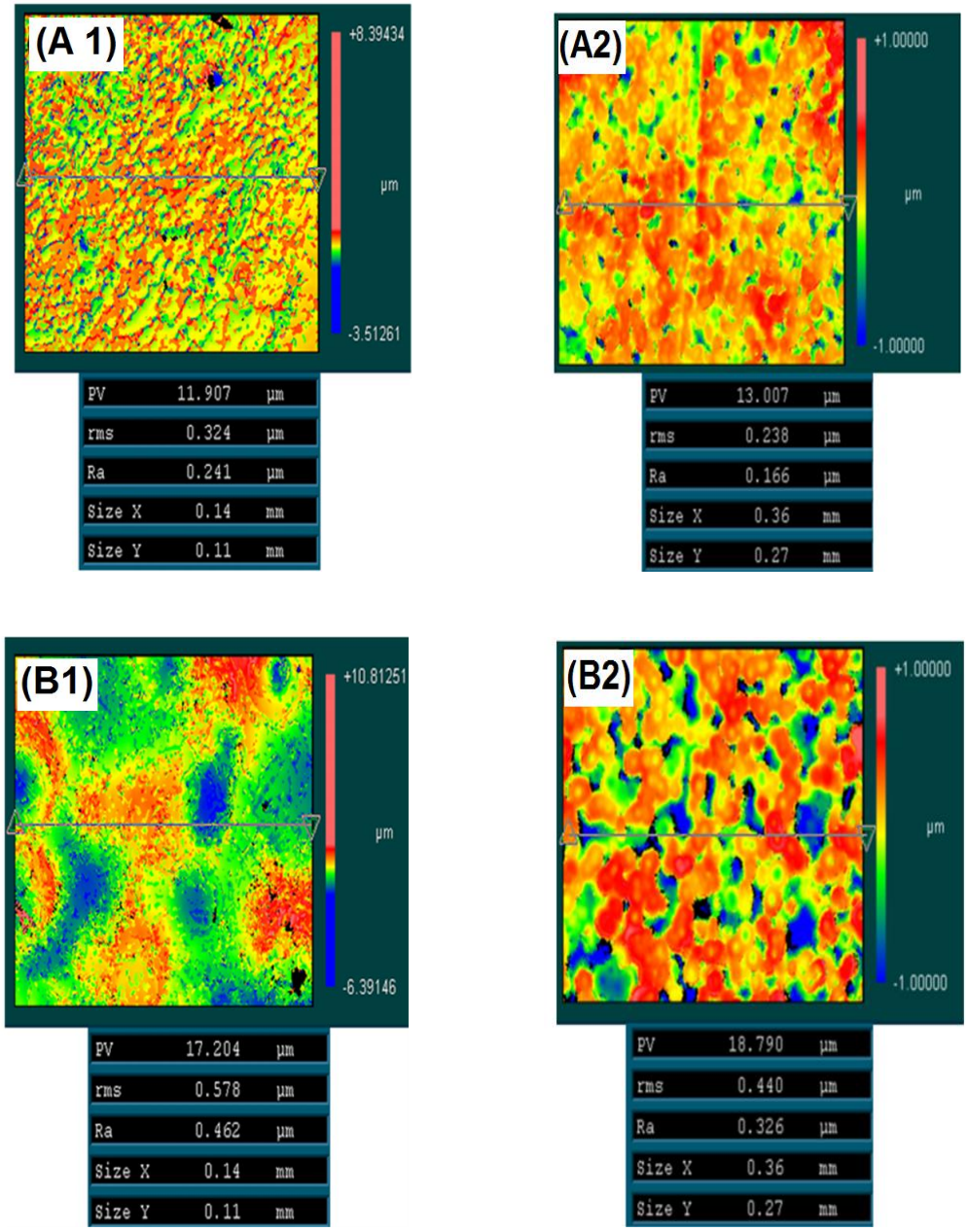

Figure 6.4: White light interferometry analysis of the surface topography of UV treated films: (A1) UV 5wt% neat film, (A2) 5 wt% neat film (control), (B1) UV 5wt% composite film and (B2) 5 wt% composite film (control)

Thus, the surface roughness of the UV composite film had increased by 44% when compared to the UV 5 wt% neat film and by 24% when compared to the 5 wt% composite film made from non UV treated P(3HO). Only UV 5wt % neat and UV 5 wt% compsite films could be assessed for the surface roughness.

Water contact angle measurements, were also carried out on the fabricated films to assess their wettability. Static contact angle measurements of the fabricated films are shown in **Figure 6.5** and compiled in **Table 6.2**.

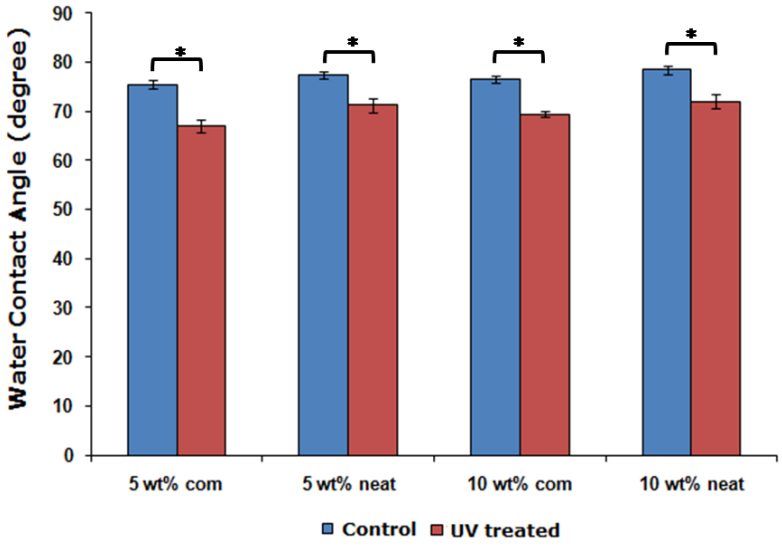

Figure 6.5: Contact angle measurement for the UV P(3HO) neat and UV P(3HO)/n-BG composite films. The data (n=4; error bars = ±SD) were compared using the Student's t-test and differences were considered significant when *p<0.05: ■ control [P(3HO) neat and P(3HO)/n-BG composite films made from non UV treated P(3HO)], ■ test samples prepared from UV treated polymer.

Samples	5 wt% com	5 wt% neat	10 wt% com	10 wt% neat
UV samples	67.00	71.20	69.35	72.00
Control	75.43	77.30	76.63	78.00

Table 6.2: Contact angle measurements of UV P(3HO) neat and UV P(3HO)/n-BG composite films as opposed to the control [P(3HO) neat and P(3HO)/n-BG composite films made from non UV treated P(3HO)]

Thus, the treatment of P(3HO) with the UV rays had reduced the water contact angle on the UV fabricated films (n=4, *p<0.5) as opposed to the films made from the non UV fabricated films. Also, incorporation of n-BG into the polymer matrix has reduced the water contact angle on the UV P(3HO)/n-BG composite films as opposed to the UV P(3HO) neat films. The reduction in the contact angle was 2.42% for the 5 wt% composite film and 1.75 % for the 10 wt% composite film.

6.2.2.3. Mechanical characterisation

The fabricated films made from UV treated polymer were also subjected to static mechanical testing to evaluate if UV treatment had affected the mechanical properties of the polymer. The analysis of the films were carried out using the static test as described in section 2.8.2

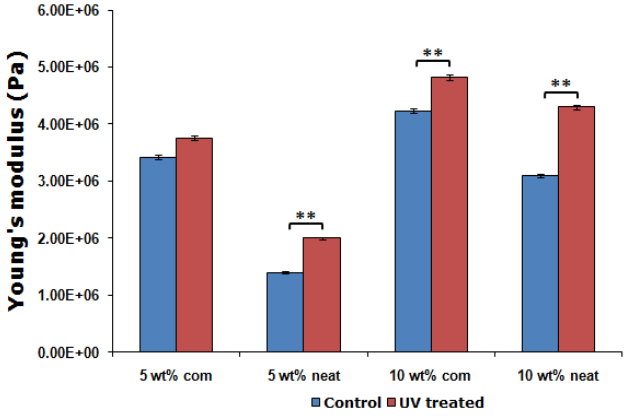

Figure 6.6: Static test of UV P(3HO) neat and UV P(3HO)/n-BG composite films fabricated using UV treated P(3HO). The data (n=4; error bars = ±SD) were compared using the Student's t-test and differences were considered significant when **p<0.01: ■ control [P(3HO) neat and P(3HO)/n-BG composite films made from non UV treated P(3HO)], ■ test samples prepared from UV treated polymer.

The results of the analyses are shown in **Figure 6.6**. There was an increase in the Young's modulus of the films fabricated from the UV treated polymer when compared to films made from non UV treated polymer. Although, the Young's modulus value for the UV P(3HO)/n-BG composite films was greater than that of the UV P(3HO) neat films, however, the % increase in the

stiffness of the UV P(3HO)/n-BG composites was lower than the UV P(3HO) neat films when compared to comparable films made from non UV treated P(3HO). The increase in stiffness with respect to the comparable films made using non UV treated P(3HO) (control) was 9% for the UV 5wt% composite film, 30 % for the UV 5wt% neat film, 12.4% for the UV 10wt% composite film and 28.13% for the UV 10wt% neat film.

6.2.2.4. Thermal characterisation

Thermal anlaysis of a material is crucial in determining its thermal stability as this can have a profound effect on the material's applicability. Thermal analysis of the fabricated films was carried out using differential scanning calorimetry, DSC, to understand if UV treatment had affected the thermal characteristics of amorphous state transition of the glassy state, (T_g) and melting of the crystalline phase, (T_m) (**Figure 6.7**).

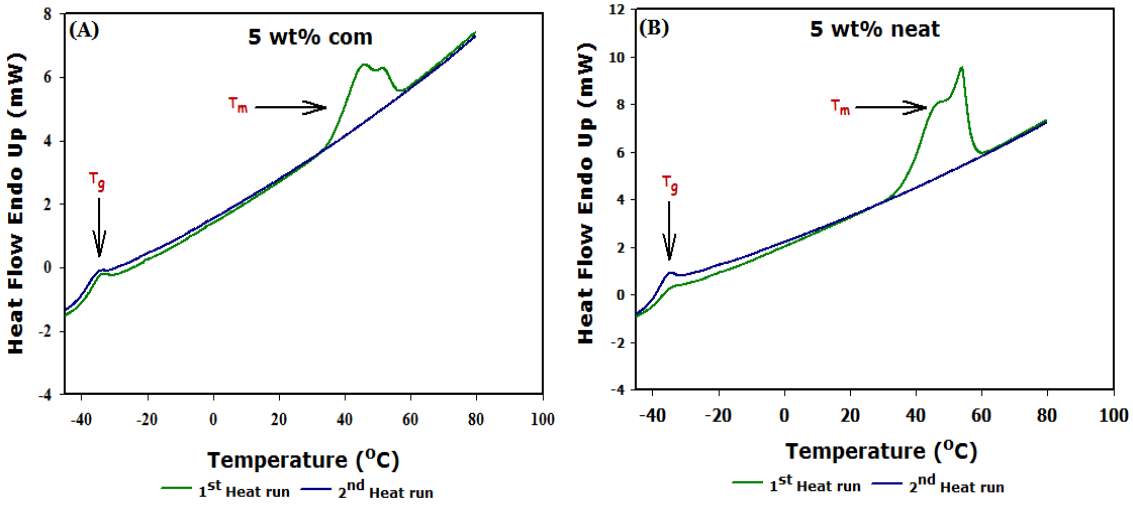

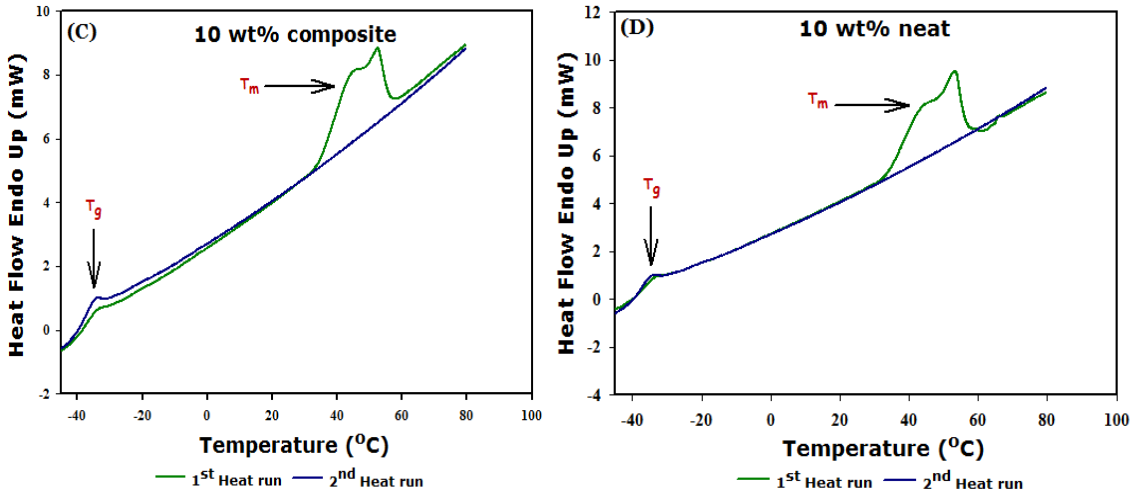

Figure 6.7: Thermal profile of the fabricated films.(A) UV 5 wt% com, (B) UV 5 wt% neat, (C) UV 10 wt% com and (D) UV 10 wt% neat.

All the fabricated films showed the T_g and T_m peaks during the first heat scan. In the second heat scan only a T_g peak was observed. The results of these analyses in comparison with that of the films made from non UV treated P(3HO) are summarised in **Table 6.3**.

Samples	First heat run			Second heat run
	T_g(°C)	T_m (°C)	ΔH_f (J/g)	T_g (°C)
5 wt% com	-36.77	45.38	17.09	-38.68
5 wt % com	-34.38	45.62	15.47	-34.65
5 wt% neat	-37.29	43.72	12.60	-38.09
5 wt% neat	-35.55	46.60	17.42	-35.91
10 wt% com	-36.52	44.70	16.53	-36.80
10 wt% com	-34.37	45.56	14.04	-34.83
10 wt% neat	-36.80	43.76	12.67	-37.08
10 wt% neat	-34.80	47.43	18.05	-35.42

Table 6.3: Compilation of the thermal properties of the fabricated UV P(3HO) neat and UV P(3HO)/n-BG composite films as oppose to control. Colour coded: Black colour (films made from UV treated P(3HO)) and Blue colour (films fabricated from non UV treated P(3HO)).

6.2.2.5. *In vitro* degradation study

The fabricated UV neat and UV composite films were also subjected to *in vitro* degradation by thermostatically incubating the fabricated films at 37°C in

Dulbeccos modified eagles medium, DMEM and DMEM Knock out, DMEM^{KT} media. The physical and chemical properties of the films were monitored to assess any changes that take place whilst undergoing degradation. The reasons for using these media for the degradation study are given in section 2.13.

6.2.2.5.1. Weight loss and water absorbed by the films during the degradation

The % weight loss, (WL) during degradation of the films was calculated as a percentage of weight loss from the original weight of the film. The % of water absorbed, (WA) was calculated as a percentage of weight gain from the dried films at the end of incubation. Both WL and WA by the films are depicted in **Figure 6.8.** The results of these studies can be summarised as follows: (i) The weight loss and water absorption for the UV films increased on prolonged immersion in all the media. For example, the WA for the 5 wt% neat film in DMEM medium was 18.25, 25.42 and 27.77 at 1, 2 and 4 months respectively. Similarly for the 5 wt% neat film in DMEM medium the WL is 1.86, 2.89 and 6.25 for 1, 2 and 4 months of incubation. (ii) The weight loss and water absorption was higher for the UV composite films as opposed to UV neat films. In DMEM medium the WL was 38.05% and 29.84 % higher for the 5wt% and 10 wt% composite films as opposed to the comparable neat films. The WA was 26.14% and 27.83 % higher for the 5wt% and 10 wt% composite films as opposed to the comparable neat films. Similarly in DMEM^{KT} medium the WL was 48.79 and 39.37 % higher on the 5 wt% and 10 wt% composite films as oppose to the comparable neat films. The WA was also 26.54% and 20.69 % higher on the 5 wt% and 10 wt% composite films as opposed to the comparable neat films (iii) For the UV composite films the weight loss was greater in the DMEM^{KT} media as opposed to DMEM media at 4 months. The WL for the 5 wt% composite and 10 wt% composite films in DMEM^{KT} medium were 12.48% and 10.64% as opposed to 10.09% and 8.98% for the comparable composite films in DMEM medium at the end of 4 months of incubation.

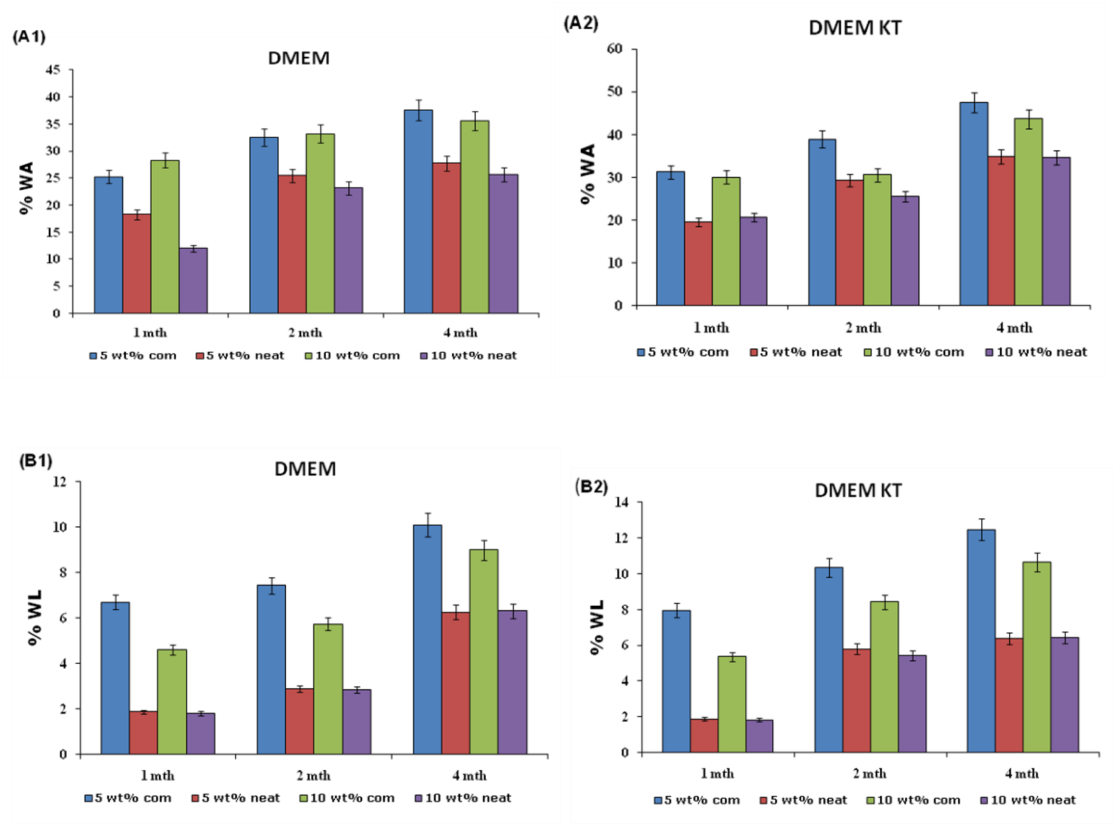

Figure 6.8: Water absorption and weight loss by the degrading UV P(3HO) neat and UV P(3HO)/n-BG composite films during the *in vitro* degradation study in DMEM and DMEM^{KT} media: (A1) WA in DMEM, (A2) WA in DMEM^{KT}, (B1) WL in DMEM, (B2) WL in DMEM^{KT}; control ■ 5 wt% com, ■ 5 wt% neat, ■ 10 wt% com and ■ 10 wt% neat, water absorption = WA and weight loss = WL.

DMEM media							
WL	**1 mth**	**2 mth**	**4 mth**	**WA**	**1 mth**	**2 mth**	**4mth**
UV 5 wt% com	6.69	7.42	10.09	**UV 5 wt% com**	25.23	32.53	37.6
5 wt% com	4.72	10.79	16.73	**5 wt% com**	11.75	18.80	25.19
UV 5 wt% neat	1.86	2.89	6.25	**UV 5 wt% neat**	18.25	25.42	27.77
5 wt% neat	4.42	7.39	15.31	**5 wt% neat**	7.86	14.64	20.42
UV 10 wt% com	4.59	5.73	8.98	**UV 10 wt% com**	28.3	33.21	35.53
10 wt% com	6.53	11.16	16.53	**10 wt% com**	10.65	17.35	26.43
UV 10 wt% neat	1.8	2.82	6.3	**UV 10 wt% neat**	12.03	23.13	25.64
10 wt% neat	4.31	8.48	15.13	**10 wt% neat**	9.56	13.50	19.65
DMEM^{KT} media							
WL	**1 mth**	**2 mth**	**4 mth**	**WA**	**1 mth**	**2 mth**	**4 mth**
UV 5 wt% com	7.96	10.34	12.48	**UV 5 wt% com**	31.23	38.88	47.4
5 wt% com	6.29	14.69	17.63	**5 wt% com**	10.98	17.87	22.64
UV 5 wt% neat	1.88	5.79	6.39	**UV 5 wt% neat**	19.53	29.17	34.82
5 wt% neat	4.24	9.73	15.88	**5 wt% neat**	8.34	15.65	21.36

UV 10 wt% com	5.35	8.42	10.64	**UV 10 wt% com**	30.01	30.56	43.64
10 wt% com	5.67	12.38	16.71	**10 wt% com**	10.67	16.98	23.52
UV 10 wt% neat	1.83	5.43	6.45	**UV 10 wt% neat**	20.57	25.43	34.61
10 wt% neat	5.04	10.59	14.43	**10 wt% neat**	8.91	15.49	20.95

Table 6.4: Compilation of the WL and WA by the degrading films in DMEM and DMEM^{KT} media. Colour coded: black colour (films made from UV treated polymer) and blue colour (films made from non UV treated polymer)

6.2.2.5.2. Static mechanical test of the degrading films

The degraded films at 1, 2 and 4 months of incubation were then subjected to mechanical testing to study any changes occurring in its mechanical properties whilst undergoing degradation. The results of this study are shown in **Figure 6.9**. The results of these studies can be summarised as follows: (i) The Young's modulus, E, of the films increased progressively with time. In DMEM media the E value for UV 5wt% composite was 12.5 MPa, UV5wt% neat was 11.2 MPa, UV10wt% composite was 14.8 MPa and UV10wt% neat was 12.6 MPa after 4 months of incubation. Similarly in DMEM^{KT} media the E value for UV 5wt% composite was 11.6 MPa, UV 5wt% neat was 7.43 MPa, UV10 wt% composite was 12.6 MPa and UV10 wt% neat was 9.4 MPa after 4 months of incubation. (ii) The Young's modulus of the UV composite films was higher than that of the comparable UV neat films at the end of incubation. (iii) The % increase in the stiffness of the fabricated UV neat and UV composite films in both the media after four month incubation, were almost the same ranging between 6-8 %.

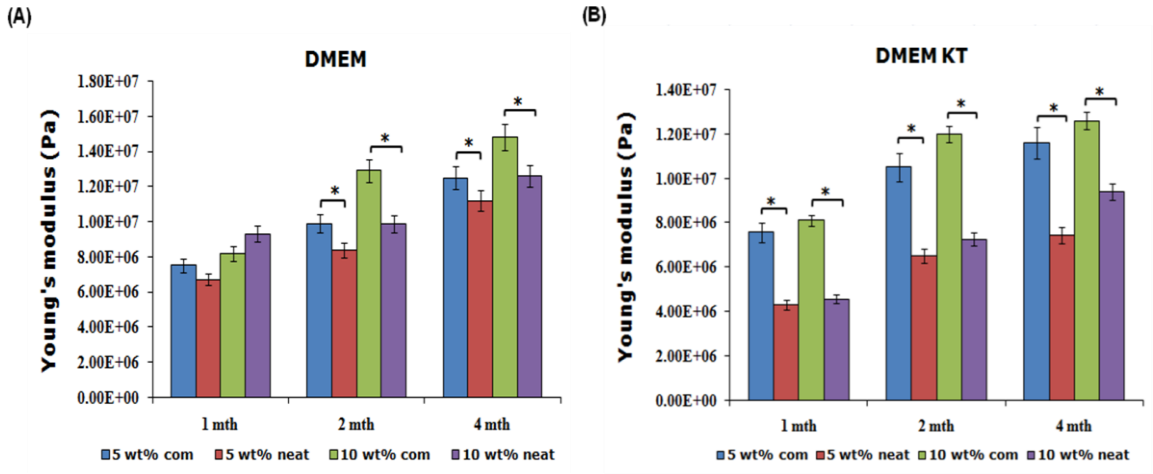

Figure 6.9: Young's modulus of the degraded samples during the *in vitro* degradation study. The samples were thermostatically incubated in (A) DMEM and (B) DMEM^{KT} media for a period of 1, 2 and 4 months. The data (n=4; error bars = ±SD) were compared using the Student's t-test and differences were considered significant when *p<0.05: ■ 5 wt% com, ■ 5 wt% neat, ■ 10 wt% com and ■ 10 wt% neat.

DMEM media	1 mth	2 mth	4 mth
UV 5 wt% com	7.50E+06	9.90E+06	1.25E+07
5 wt% com	8.34E+06	1.29E+07	7.78E+06
UV 5 wt% neat	6.70E+06	8.40E+06	1.12E+07
5 wt% neat	6.10E+06	1.17E+07	6.80E+06
UV 10 wt% com	8.20E+06	1.29E+07	1.48E+07
10 wt% com	9.08E+06	1.34E+07	1.04E+07
UV 10 wt% neat	9.30E+06	9.85E+06	1.26E+07
10 wt% neat	7.85E+06	1.20E+07	7.94E+06

DMEM^{KT} media	1 mth	2 mth	4 mth
UV 5 wt% com	7.56E+06	1.05E+07	1.16E+07
5 wt% com	8.34E+06	1.48E+07	1.12E+07
UV 5 wt% neat	4.30E+06	6.50E+06	7.43E+06
5 wt% neat	6.75E+06	1.17E+07	7.26E+06
UV 10 wt% com	8.10E+06	1.20E+07	1.26E+07
10 wt% com	9.08E+06	1.75E+07	1.20E+07
UV 10 wt% neat	4.57E+06	7.26E+06	9.40E+06
10 wt% neat	7.85E+06	1.25E+07	7.94E+06

Table 6.5: Comparison for the increase in stiffness, E value of the degrading films in DMEM and DMEM^{KT} media. Colour coded: black colour (films made from UV treated polymer) and blue colour (films made from non UV treated polymer)

6.2.2.5.3. Thermal properties of the degrading films

The results of the thermal analysis of the degraded films are depicted in **Figure 6.10.** These, values are taken from the first heat run and can be summarised as follows: (i) The melting temperature of the degrading films showed a general trend of decrease at 1 month of incubation following which it increased progressively with time in the media. For example the 10 wt% composite film had a T_m value of 44.09 (T_m before degradation is 44.7°C) at 1 month of incubation but increased to 45.25 and 49.37°C at 2 and 4 months respectively in DMEM medium. (ii) Two T_g peaks appeared in the degrading films. (iii) The first T_g peak occurred within a range of -35 and -38.62°C in the two media. (iv) The second T_g occurred within a range of -51 and -57°C.

(A1)

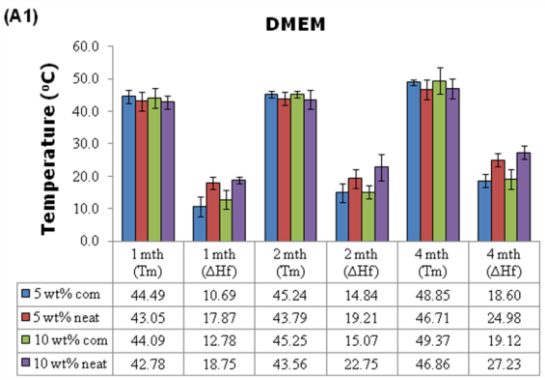

	1 mth (Tm)	1 mth (ΔHf)	2 mth (Tm)	2 mth (ΔHf)	4 mth (Tm)	4 mth (ΔHf)
5 wt% com	44.49	10.69	45.24	14.84	48.85	18.60
5 wt% neat	43.05	17.87	43.79	19.21	46.71	24.98
10 wt% com	44.09	12.78	45.25	15.07	49.37	19.12
10 wt% neat	42.78	18.75	43.56	22.75	46.86	27.23

(A2)

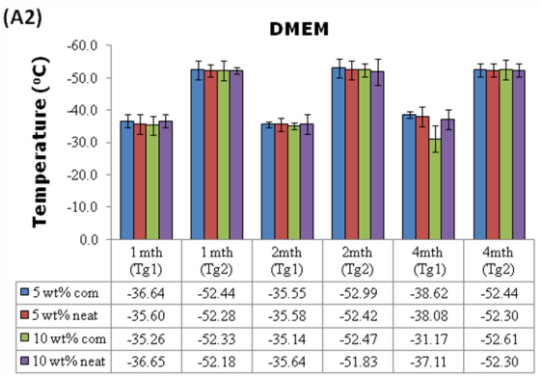

	1 mth (Tg1)	1 mth (Tg2)	2mth (Tg1)	2mth (Tg2)	4mth (Tg1)	4mth (Tg2)
5 wt% com	-36.64	-52.44	-35.55	-52.99	-38.62	-52.44
5 wt% neat	-35.60	-52.28	-35.58	-52.42	-38.08	-52.30
10 wt% com	-35.26	-52.33	-35.14	-52.47	-31.17	-52.61
10 wt% neat	-36.65	-52.18	-35.64	-51.83	-37.11	-52.30

(B1)

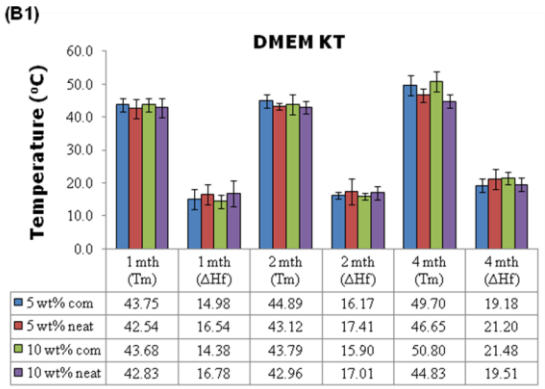

	1 mth (Tm)	1 mth (ΔHf)	2 mth (Tm)	2 mth (ΔHf)	4 mth (Tm)	4 mth (ΔHf)
5 wt% com	43.75	14.98	44.89	16.17	49.70	19.18
5 wt% neat	42.54	16.54	43.12	17.41	46.65	21.20
10 wt% com	43.68	14.38	43.79	15.90	50.80	21.48
10 wt% neat	42.83	16.78	42.96	17.01	44.83	19.51

(B2)

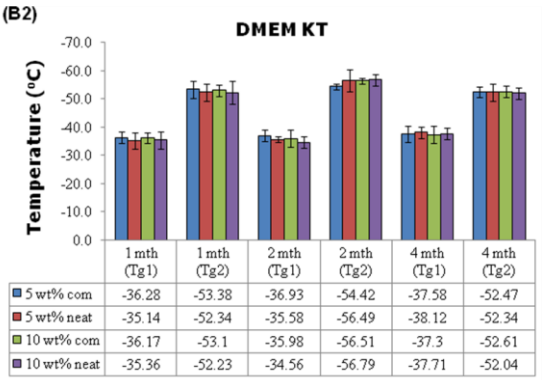

	1 mth (Tg1)	1 mth (Tg2)	2 mth (Tg1)	2 mth (Tg2)	4 mth (Tg1)	4 mth (Tg2)
5 wt% com	-36.28	-53.38	-36.93	-54.42	-37.58	-52.47
5 wt% neat	-35.14	-52.34	-35.58	-56.49	-38.12	-52.34
10 wt% com	-36.17	-53.1	-35.98	-56.51	-37.3	-52.61
10 wt% neat	-35.36	-52.23	-34.56	-56.79	-37.71	-52.04

Figure 6.10: The thermal properties of the UV P(3HO) neat and UV P(3HO)/n-BG composite films whilst under going in vitro degradation. (A1) DMEM media, Tm and ΔH_f; (A2) DMEM media, T_g; (B1) DMEM^{KT} media, T_m and ΔH_f and (B2) DMEM^{KT} media, T_g at the end of the incubation time i.e. 1, 2 and 4 months: Melting temperature =T_m, enthalpy of fusion = ΔH_f, glass transition temperature = Tg, first glass transition = T_{g1}, second glass transition = T_{g2}: ■ 5 wt% com, ■ 5 wt% neat, ■ 10 wt% com and ■ 10 wt% neat

6.2.2.5.4. pH studies of the media

The DMEM and DMEM^{KT} media in which the films were incubated were analysed for any changes in pH due to the degradation products of the films. These pH profiles are shown in **Figure 6.11.** The pH of the media gradually increased with time in both the media, changing from an initial value of 7.4 for both DMEM and DMEM^{KT} to values of over 8 at the end of the 4 month incubation period.

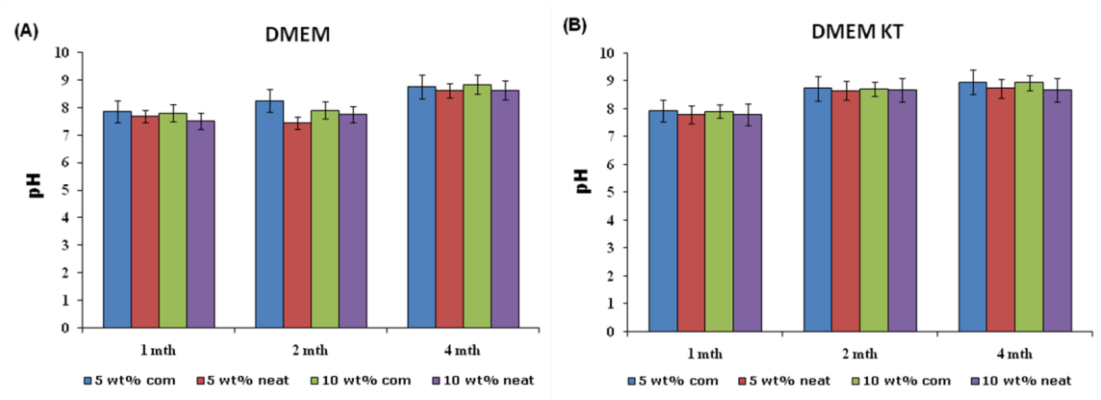

Figure 6.11: Compilation of the pH of the media in which the films were incubated for the *in vitro* degradation study: (A) DMEM and (B) DMEM^{KT} media. The pH was measured over the four months of incubation. The media was refreshed every 1 week: ■ 5 wt% com, ■ 5 wt% neat, ■ 10 wt% com and ■ 10 wt% neat.

6.2.2.5.5. Surface studies of the degrading films

Surface scans of the degrading polymers were carried out using SEM at the end of the 4 months study. The degraded films were washed with HPLC water and then dried prior scanning. Surface scans of the degraded UV neat and UV

composite films are shown in **Figures 6.12.** The films appear to have undergone degradation, with loose degraded polymer flakes appearing on both the surfaces. However, the degradation appeared to be more prominent on the surface of the UV composite films as opposed to the UV neat films.

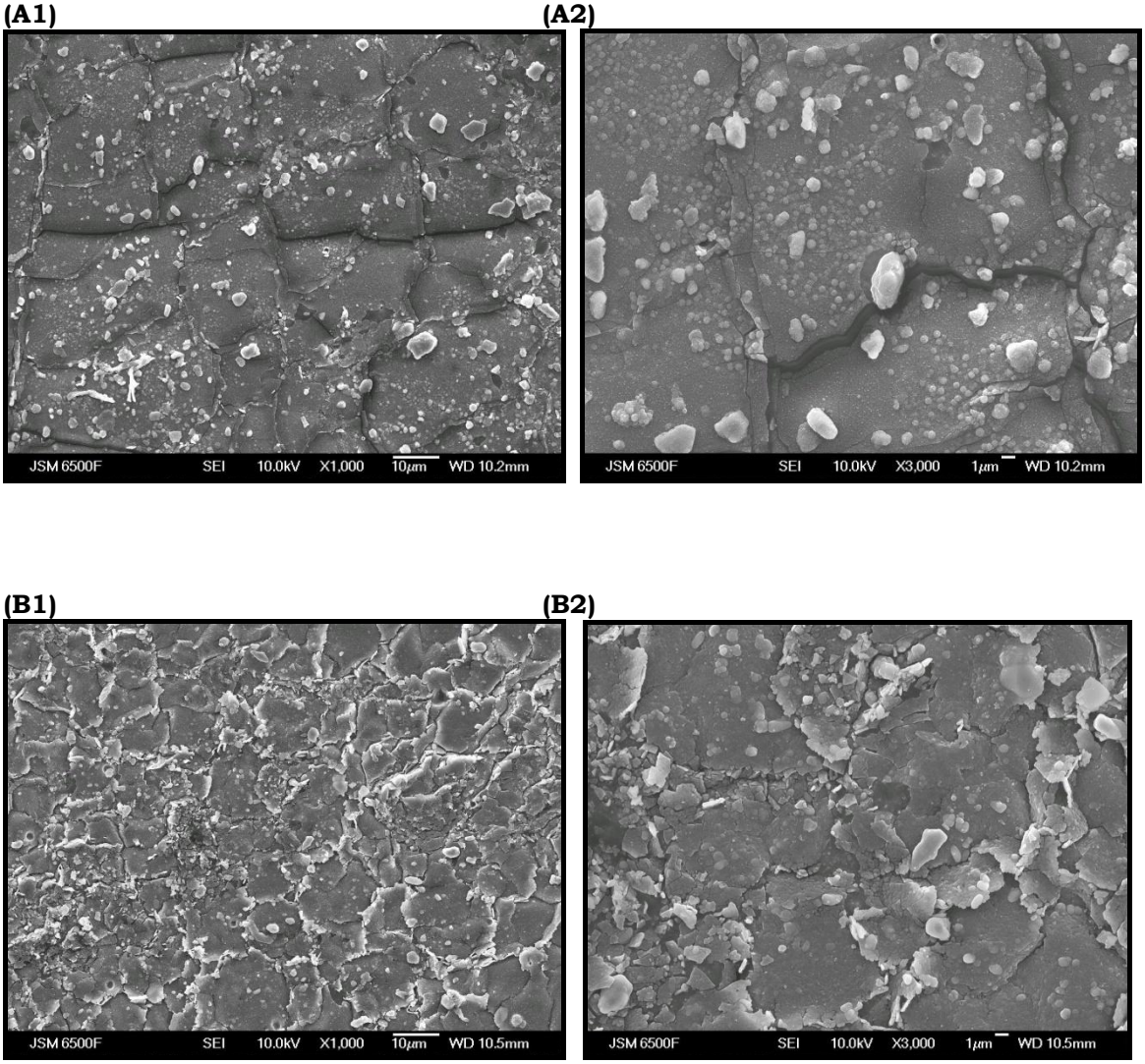

Figure 6.12: SEM images at the end of 4 months of incubation for: (A) degrading UV P(3HO) neat films (UV5 wt% neat in DMEM medium): (A) X1000 and (B) 3000X ; (B) degrading UV P(3HO)/n-BG composite films (UV5 wt% composite in DMEM medium): (A) X1000 and (B) X3000

6.2.2.6. Protein adsorption study

Protein adsorption assays were carried out as described in section 2.11 and the results obtained are shown in **Figure 6.13.** The adsorption of proteins on

the UV fabricated films was significantly higher (n=4, *p<0.01; except UV10wt% neat where *p<0.5) as opposed to that of the control (films made from non UV treated polymer); Protein adsorption was 16.9, 25.26, 17.68 and 10.56% higher for the UV 5wt% composite, UV 5 wt% neat, UV 10 wt% composite and UV 10 wt% neat respectively when compared to the comparable films made from non UV treated P(3HO). Also, the adsorption of proteins was higher on the UV composite films when compared to the UV neat films (n=4, *p<0.01); The protein adsorption on the UV 5 wt% composite film was 168.66 μg/cm^2 as opposed to UV 5 wt% neat (100.33 μg/cm^2), similarly the adsorption on the UV 10 wt% composite film was 158.33 μg/cm^2 as oppose to 93 μg/cm^2 on the UV 10 wt% neat film.

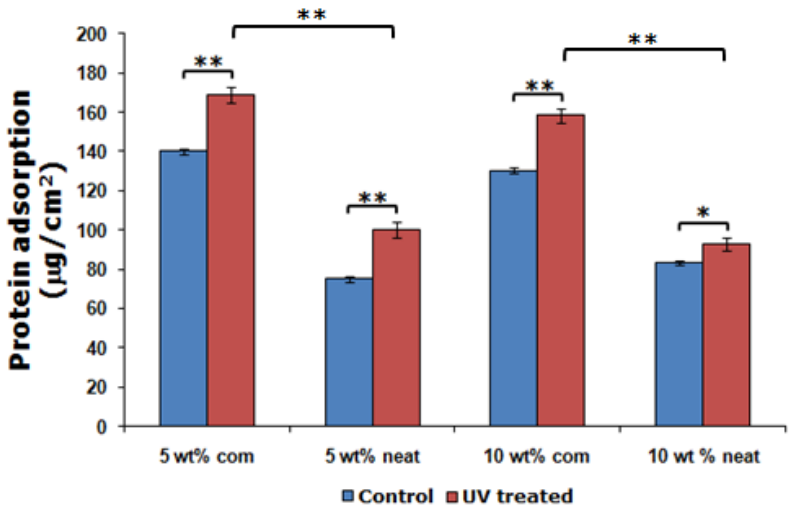

Figure 6.13: Protein adsorption study of the fabricated UV films. The data (n=4; error bars = ±SD) were compared using the Student's t-test and differences were considered significant when *p<,0.5, **p<0.01: ■ control [P(3HO) neat and P(3HO)/n-BG composite films made from non UV treated P(3HO)], ■ test samples prepared from UV treated polymer

XPS analysis of the protein adsorption on the films were also carried out in order to measure the nitrogen content on the films before and after immersion in foetal bovine serum, FBS (**Figure 6.14**).

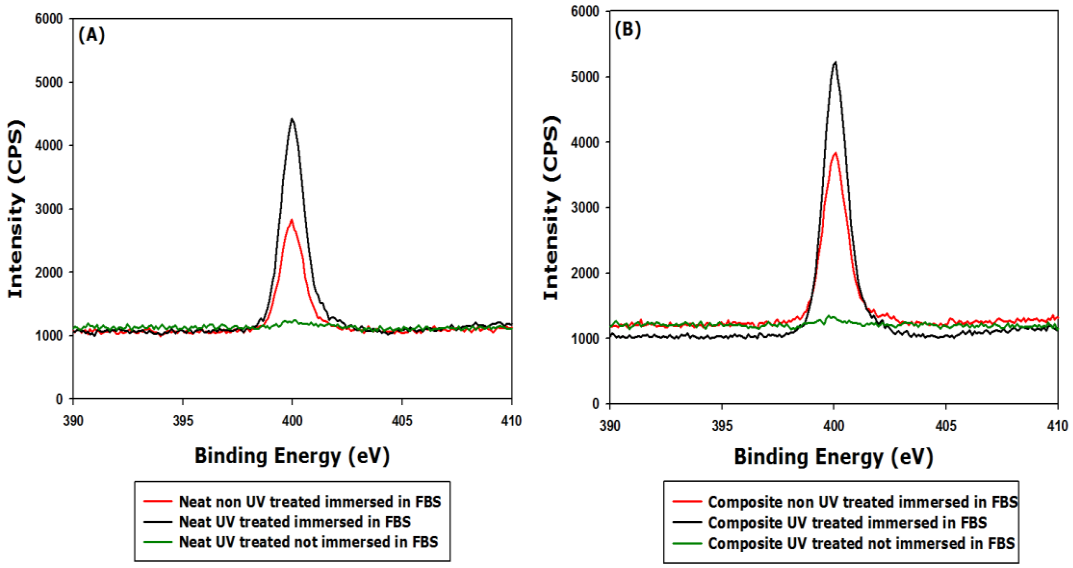

Figure 6.14: Nitrogen (N1s spectra) comparing the absorption of nitrogen in the UV treated neat and composite films before and after immersion in FBS and in comparison to the non UV treated neat and composite films after immersion in FBS.

The presence of nitrogen can be related to protein and thus allows for an indirect evaluation of protein adsorption onto the top surface layer. The adsorption of proteins on the UV neat film was increased by 46.43% when compared to the non UV neat film. Similarly, the adsorption of protein on the UV composite film was increased by 31.22% when compared to the non UV composite film. Thus the films, both neat and composite, made from UV treated polymer showed higher adsorption of proteins when compared to the neat and composite films made from non UV treated polymer.

6.2.2.7. *In vitro* cytocompatibility study

In order to assess the *in vitro* cytocompatibility of the films fabricated using the UV treated polymer, cell culture studies were carried out. The keratinocyte cell line, HaCaT cells, were seeded on these films and their attachment and proliferation studied using the neutral red assay (described in section 2.2.2) over a period of 1, 4 and 7 days. The proliferation studies

were carried out using the standard tissue culture plate, TCP, as a control, the growth on which was normalised to 100%. The results of these studies are depicted in **Figure 6.15** and can be summarised as follows: (i) The growth of the cells on all the films increased with time. (ii) The growth of the HaCaTs on the films made from UV treated P(3HO) was significantly higher than comparable films made from non UV treated P(3HO) (n=4, **p<0.01). For instance, at day 7 the growth of HaCaTs on the UV 5 wt % composite film was 4.5%, UV 5 wt% neat was 39.26%, UV 10 wt% composite was 5.50 and UV 10 wt% neat was 13.29 % higher than the comparable films made from non UV treated P(3HO). (iii) The UV P(3HO)/n-BG composite films also supported better growth than UV P(3HO) neat films: At day 7 the growth on UV 5 wt% composite and UV 10 wt% composite was 146.47 % and 145.86 % as opposed to 96.19 % and 73.09 for the UV 5 wt% and UV 10 wt% neat films respectively. (iv) At day 7 the growth of the cells on the UV P(3HO)/n-BG composite films were also higher than that of the control tissue culture plate, TCP. On the UV 5wt% composite film the % cell proliferation was 46.47% higher than that of the control (TCP) and on the UV 10wt% composite film the % cell proliferation was 37% higher than that of the control, TCP.

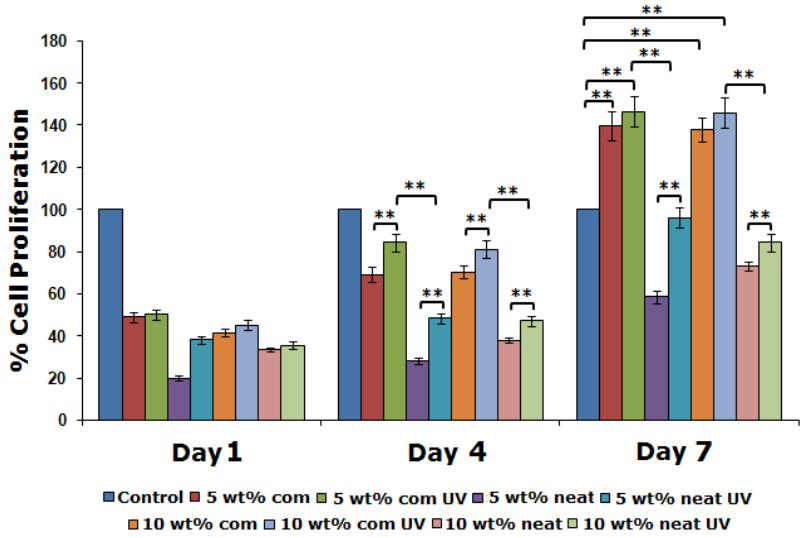

Figure 6.15: Proliferation study of the seeded HaCaTs on the fabricated UV P(3HO) neat and UV P(3HO)/n-BG composite films on day 1, 4 and 7. The UV P(3HO)/n-BG

composites supported better growth than the UV P(3HO) neat. The data (n=8; error bars = ±SD) were compared using the Student's t-test and differences were considered significant when, **p<0.01.

As discussed in Chapter 5, the keratinocytes arrange themselves into four distinct layers. The outer most layer is the horn sheet arrangement of the cells, this is also the layer where the cells are most mature. The SEM images of the seeded HaCaTs show that the cells were able to attach, proliferate and mature on both the UV P(3HO) neat and UV P(3HO)/n-BG composite films.

Figure 6.16 (A1-A2) shows the attachment and proliferation of the seeded HaCaTs on the fabricated films. In the UV P(3HO)/n-BG composites the cells had attached, proliferated and matured to form the horn sheets by day 4. **Figure 6.16 (B1-B2)** shows this arrangement of horn sheets of the HaCaTs on the composite films. In the UV P(3HO) neat films, **Figure 6.16 (C1-C2**), confluent growth of the cells was observed by day 4. Also few arrangements of the HaCaTs into horn sheets were observed.

(A1)

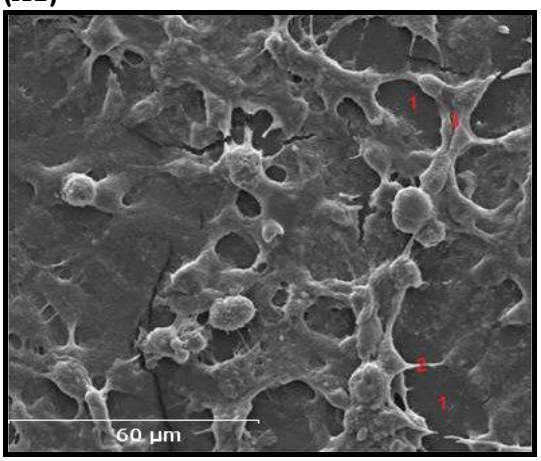

(A2)

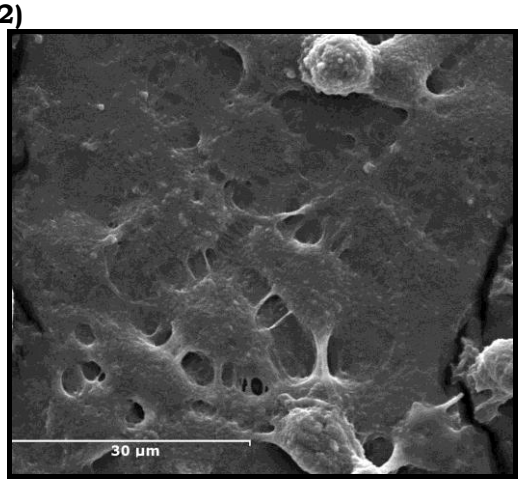

(B1)

(B2)

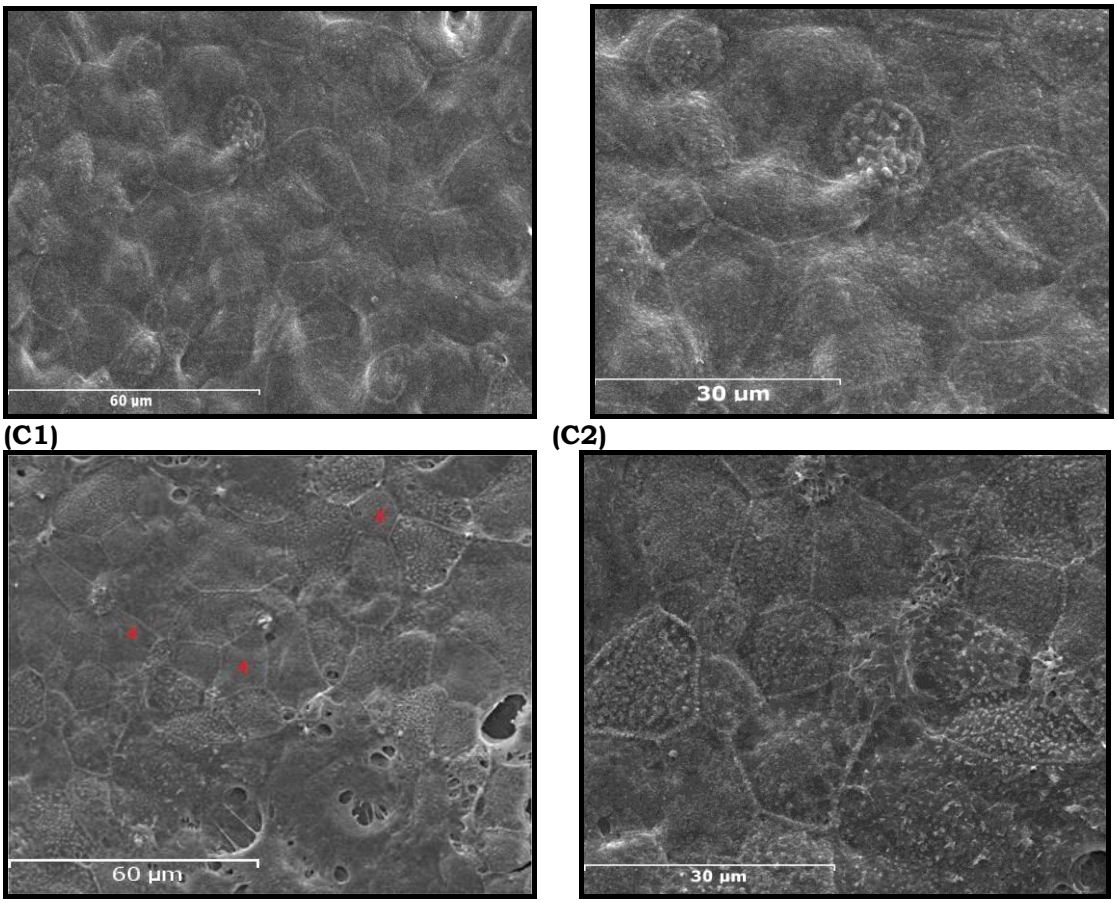

Figure 6.16: SEM images of the seeded HaCaT cells on the UV P(3HO) neat and UV P(3HO)/n-BG composite films: (A) the seeded HaCaT cells showing its attachment and proliferation on the film: (A1) Magnification 2000x (A2) Magnification 3000X; (B) Seeded HaCaT cells at day 7 on the UV composite films, appearance of Horn sheets: (B1) Magnification X2000 (B2) Magnification X3000; (C) Seeded HaCaT cells at day 4 on the neat film. Cells have attached, proliferated and some appearance of horn sheets:(C1) Magnification X2000 (C2) Magnification X3000: (1) Uncovered polymer matrix, (2) Spreading of the cell (3) Cell layer and (4) horn sheets.

6.2.3. Blending of Poly(3-hydroxyoctanoate), P(3HO) and poly(3-hydroxybutyrate), P(3HB)

The blend films were fabricated using P(3HO) produced from *P. mendocina* using the octanoate feed and P(3HB) produced from *B. cereus* SPV using glucose. A detailed method for the fabrication of the films is described in section 2.12.3. The films fabricated were of the following weight %: 5 wt% P(3HB)/1 wt% P(3HO), 5 wt% P(3HO)/1 wt% P(3HB) and 5 wt% P(3HO)/1

wt% P(3HB) containing 1 wt% n-BG i.e., composite 5 wt% P(3HO)/1 wt% P(3HB) film.

6.2.3.1. Microstructural studies.

Microstructural studies of the fabricated films were carried out. SEM scans of the films (**Figure 6.17)** show that the 5 wt% P(3HO)/1 wt% P(3HB) film had a smooth surface. Increasing the weight % of P(3HB) as in the case of 5wt% P(3HB)/1 wt% P(3HO) film showed a rough surface. A rough mash like structure was observed for the composite film with 1 wt% n-BG incorporated as a filler i.e. composite 5 wt% P(3HO)/1 wt% P(3HB) film.

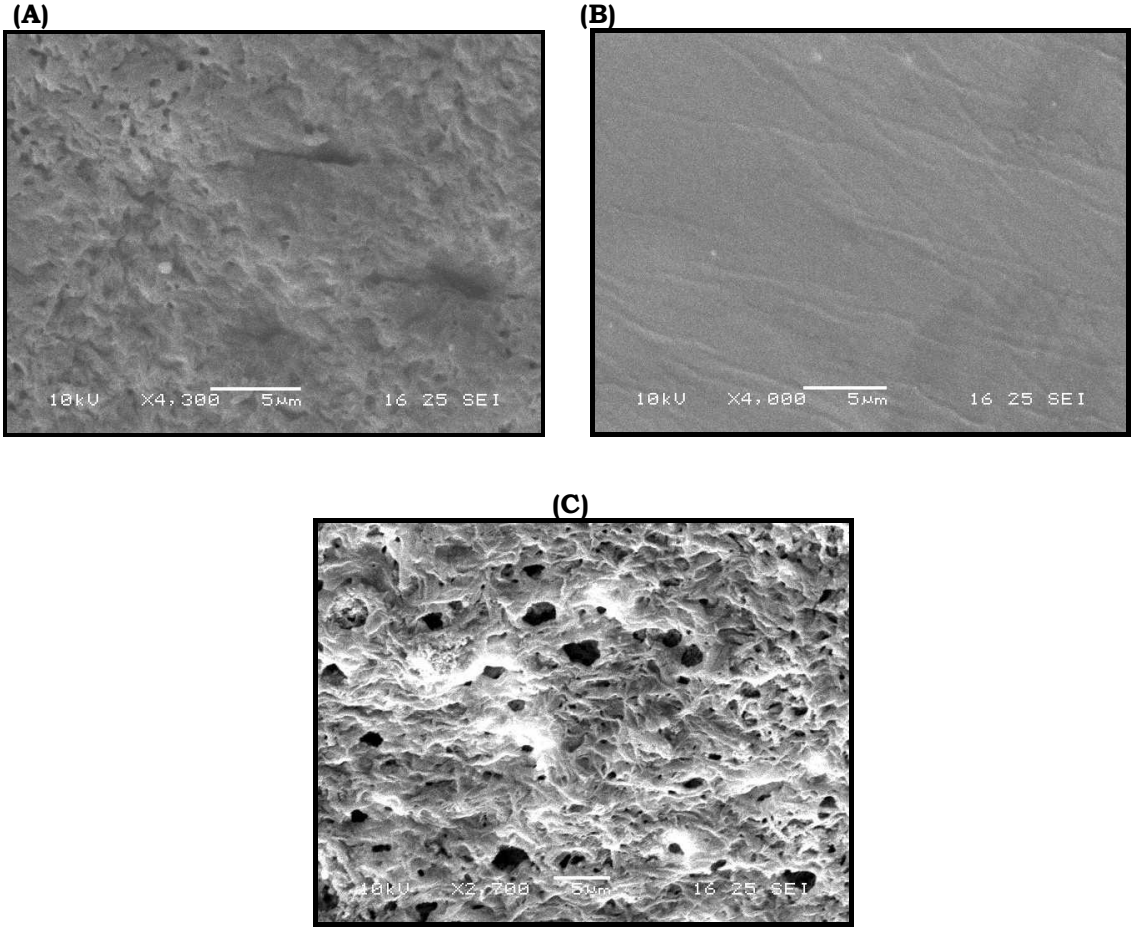

Figure 6.17: SEM scans of the blend and composite blend films as revealed by SEM analysis. 5 wt% P(HB)/1 wt% P(3HO) (B) 5 wt% P(3HO)/1 wt% P(3HB) and (C) 5 wt% P(3HO)/1 wt% P(3HB) composite film

This roughness of the blend and composite blend films were quantified using white light interferometry with the use of the instrument ZYGO® (**Figure 6.18**). The smooth surface of the blend 5 wt% P(3HO)/1 wt% P(3HB) film was confirmed by the lowest roughness value of 0.670µm obtained by the white light interferometry analysis. Similarly, the blend with a high % of the brittle P(3HB) i.e. 5 wt% P(3HB)/1 wt% P(3HO) had a surface roughness of 1.30 µm. The composite 5 wt% P(3HO)/1 wt% P(3HB) film had the highest roughness value of 12.46 µm.

(A)

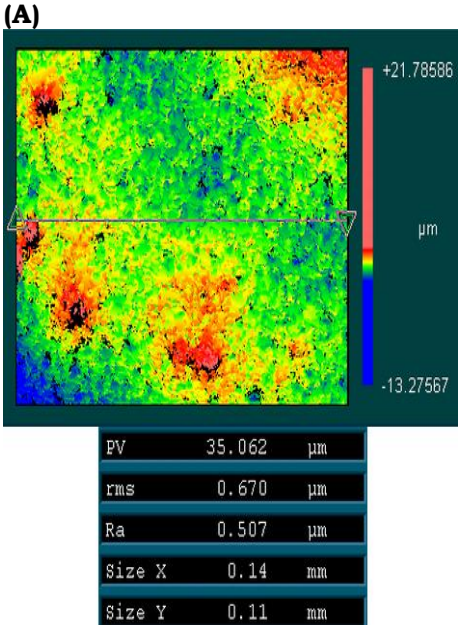

(B)

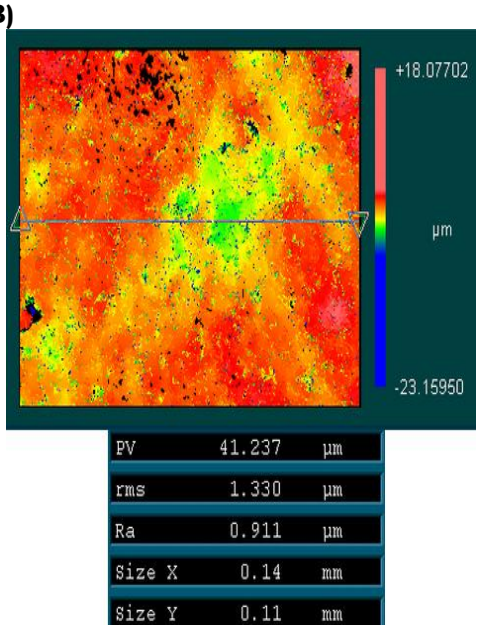

(C)

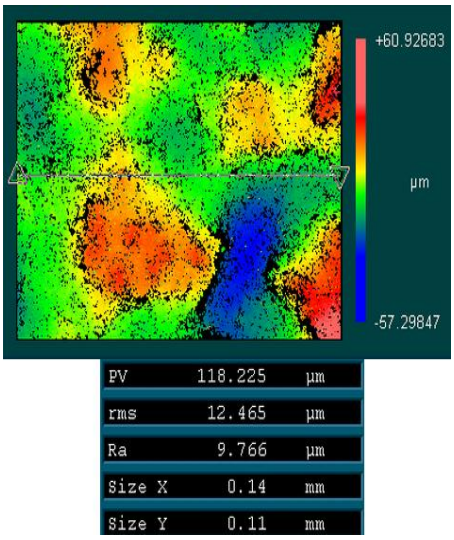

Figure 6.18: White light interferometry analysis of the surface topography of the blend and composite blend films: (A) 5 wt% P(3HO)/1 wt% P(3HB), (B) 5 wt% P(3HB)/1 wt% P(3HO) and (C) composite 5 wt% P(3HO)/1 wt% P(3HB) film.

Water contact angle studies of the films are shown in **Figure 6.19** show that the smooth 5 wt% P(3HO)/1 wt% P(3HB) film had the lowest contact angle value (θ_{H2O} = 86.9º). The rough 5 wt% P(3HB)/1 wt% P(3HO) film had a θ_{H2O} value of 81.97º. The composite 5 wt% P(3HO)/1 wt% P(3HB) had the lowest water contact angle of, θ_{H2O} = 71.06º.

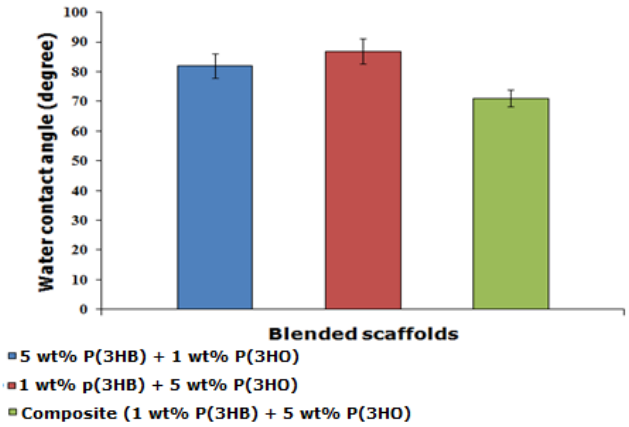

Figure 6.19: Contact angle measurement for blend and composite blend films: ■ 5 wt% P(3HB) + 1 wt% P(3HO), ■ 1 wt% P(3HB) + 5 wt% P(HO) and ■ Composite (1 wt% P(3HB) + 5 wt% P(3HO)

6.2.3.2 Mechanical characterisation.

Static mechanical test was carried out on the fabricated blend and composite blend films to understand their mechanical properties. The tensile tests were carried out on thin strips of the films; six repeats per sample. The initial load was set to 1 mN and then increased to 6000 mN at the rate of 200 mN min^{-1}. The results from the static test are compiled in the **Table 6.4** below.

Sample	Young's modulus (Pa)	% Elongation
5 wt% P(3HB) + 1 wt% P(3HO)	4.03E+08	2
1 wt% P(3HB) + 5 wt% P(HO)	3.25E+06	221.45
Composite(1 wt% P(3HB) + 5 wt% P(3HO)	3.91E+08	1.23

Table 6.6: The Young's modulus value of the fabricated films.

6.2.3.3. *In vitro* degradation study

In vitro degradation studies of the fabricated blend and composite blend films were carried out by thermostatically incubating the films in simulated body fluid at 37°C over a period of 15, 30 and 60 days. The weight lost, (WL), during degradation of the films was calculated as a percentage of weight loss from the original weight of the film. The % of water absorbed, (WA) and weight loss (WL) by the films are depicted in **Figure 6.20** and can be summarised as follows: (i) The water absorption for the films increased on prolonged immersion (ii) The water absorption was highest, 28 % for the composite blend film followed by 5 wt% P(3HB)+1 wt% P(HO), 26.5 % and 5 wt% P(3HO)+1 wt% P(3HB) 21 %. (iii) The weight loss by the films also increased progressively with time, with the same trend observed as that of water absorption. The highest WL was observed for the composite blend, 19 % followed by 5 wt% P(3HB)+1 wt% P(HO), 17 % and 5 wt% P(3HO)+1 wt% P(3HB), 16 %.

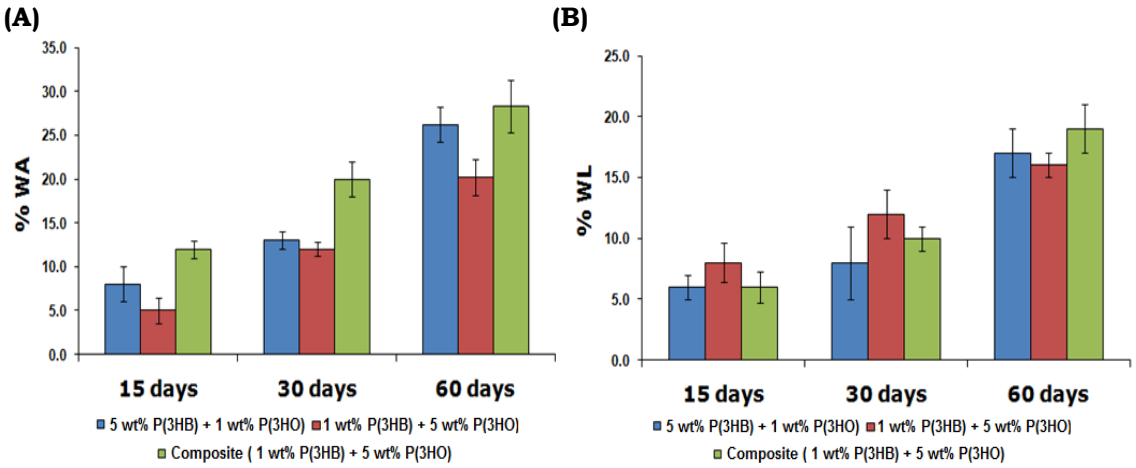

Figure 6.20: *In vitro* degradation study of the blend and composite blend samples in (A) DMEM and (B) DMEM^{KT} media. The study was carried out for a period of 15, 30 and 60 days: Water absorption =WA and weight loss = WL, ■ 5 wt% P(3HB) + 1 wt% P(3HO), ■1 wt% P(3HB) + 5 wt% P(HO) and ■ Composite(1 wt% P(3HB) + 5 wt% P(3HO)

6.2.3.4. Surface studies of the degrading films

SEM scans of the degrading films (**Figure 6.21**) were also carried out at the end of the 60 days of incubation. SEM scans reveal that the films were undergoing initial degradation which had started on the surface of the polymer.

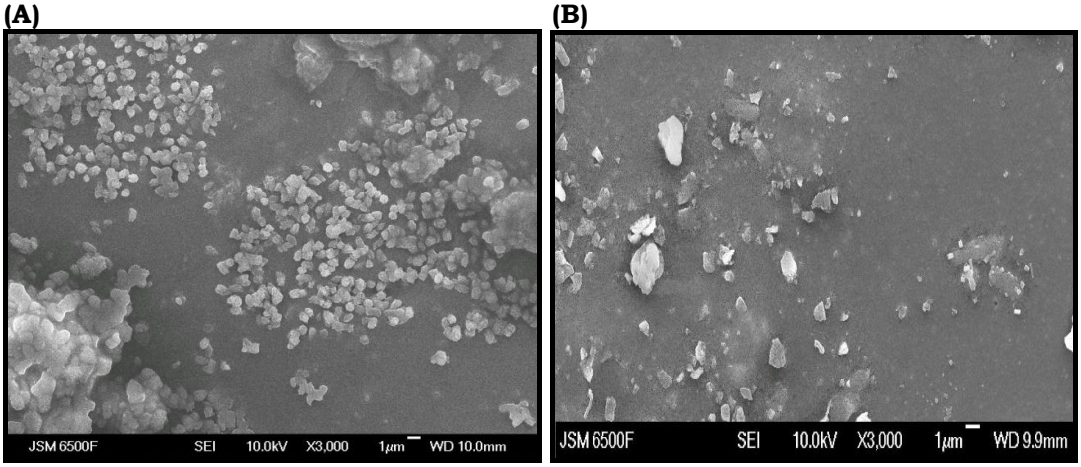

(C)

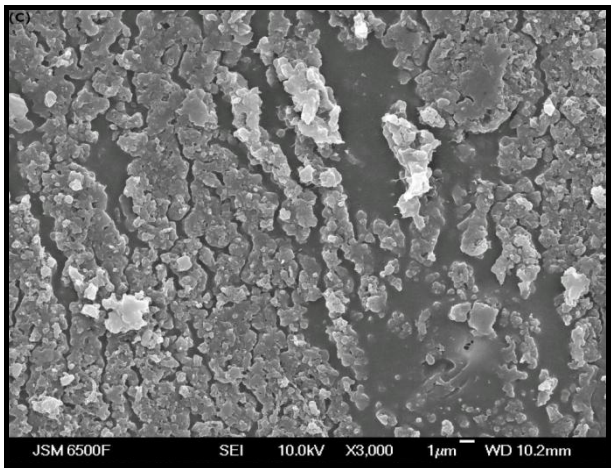

Figure 6.21: SEM scans of the degrading blend films after 60 days of incubation: (A) 5 wt% P(3HO)+1 wt% P(3HB), (B) 5 wt% P(3HB)+1 wt% P(HO) and (C) Composite/5 wt% P(3HO)+1 wt% P(3HB).

6.3. Discussion

In this section the results of the investigation on the modification of P(3HO) using the three approaches: (i) Treatment of the polymer using UV rays (ii) incorporation of n-BG into the polymer matrix to form P(3HO)/n-BG composite films and (iii) blending of the polymer with P(3HB) are discussed to assess their effects on the properties of the fabricated films.

6.3.1. Modification of P(3HO) using UV rays

UV treatment of the polymer caused chain scissions which had resulted in a decrease in M_w (337597 for the UV treated polymer) and caused an increase in the M_n (180901). The PDI value had also decreased from 2.07(control) to 1.87 (UV treated). Similar observations of reduced M_w was observed when Shangguan *et al.* (2006) carried out UV treatment of P(3HB-co-3HHx). The polymer UV treated for 8 to 16 hrs had it molecular weight reduced from 526 kD to 68.3 and 36.2 kD respectively. The UV treated polymer also exhibited a

broad PDI value of 6.4(8 hrs) and 4.8 (16 hrs) as opposed to the control value of 2.2 (Shangguan *et al.,* 2006).

6.3.1.1. Properties of the fabricated films

The UV treated P(3HO) was fabricated into P(3HO) neat films. XPS analysis was then carried out on the film to observe if modification of the polymer P(3HO) had taken place. The results of the analysis are depicted in **Figure 6.2** and compiled in **Table 1.** An increase in the amounts of C-OH, C=O, COOH bonds and a decrease in the C-C bonds on the UV P(3HO) neat (5 wt%) and UV P(3HO)/n-BG composite film (5 wt%) was observed as opposed to the film made from non UV treated P(3HO) (5 wt%). The increase in the C=O bonds would have occurred due to the scissions of ester linkages and due to the interaction of photons with the atmospheric oxygen which results in the incorporation of oxygen moieties in treated surfaces thus forming polar groups such as C=O on its surface (Ruiz and Martinez, 2005). Shangguan *et al*. (2006) observed that the P(3HB-co-3HHx) film made from UV treated P(3HB-co-3HHx) powder had an increase in the presence of polar C-O, C=O bonds and a decrease in the non polar C-C bonds when compared to P(3HB-co-3HHx) films made from non UV treated P(3HB-co-3HHx). Koo *et al*. (2008) also observed an increase in the surface oxygen content with the UV treated PLA surface as opposed to an untreated PLA surface. Koo *et al*. attributed this observation to the α-cleavage (breaking of the C-C bond adjacent to the carbonyl carbon) of the ester linkage due to UV irradiation (Koo and Jang, 2008).

UV treatment of the polymer in addition to increasing the polar group on its surface also increased the surface roughness of the fabricated films. SEM images of the UV P(3HO) neat film showed a rough surface when compared to the SEM images of P(3HO) neat film made from non UV treated polymer (**Figure 6.3**). White light interferometry analysis using ZYGO® confirmed

this increase in the roughness where by a typical RMS value of 0.324 μm was observed for the UV 5wt% neat film as opposed to 0.238 μm observed for the control 5 wt% neat film (made from non UV treated P(3HO). Therefore, the roughness of the UV 5wt% neat film had increased by 26.5%. Similarly, the roughness of the UV 5 wt% composite film was found to be 0.578 μm (**Figure 6.4(B)**. Its roughness had increased by 44% when compared to the UV 5 wt% neat film and by 24% when compared to the control 5 wt% composite film made (made from non UV treated P(3HO). Thus, the increase in the roughness of the UV 5 wt% composite film could be attributed to combined effects of exposure to UV rays and due to the incorporation of the n-BG which had introduced rough surface topography on the film surface. Exposure to UV rays could have increased the roughness due to the polymer chains scissions which result in shorter polymer chains which hence are more randomly oriented in the solvent cast film resulting in a less ordered structure leading to a rougher surface. The UV 10 wt% neat and UV 10 wt% composite films could not be assessed for roughness, however similar observations of increase roughnes due to UV exposure and incorporation of n-Bg could be expected.

For the UV fabricated films the increased polar groups on its surface also decreased the water contact angle significantly (n=4, *p<0.05) on these films as opposed to the control. The water contact angle, θ_{H2O} is an indicator of the wettability of a material surface. Wettability is the ability of a liquid to adhere to a solid and spread over its surface to varying degrees. Wettability with water is a surface property of a material as opposed to hydrophilicity which is considered a bulk property. However, in this present study as P(3HO) was first subjected to UV treatment and then fabricated into films, therefore wettability would reflect changes in the hydrophilicity i.e. the bulk property of the UV fabricated films. The reduced water contact angles on the films fabricated using UV treated polymer (UV 5wt% com = 67^o, UV 5wt% neat = 71.2^o , UV 10 wt% com = 69.35^o and Uv 10 wt% neat = 72^o) as opposed

to the non films made from non UV treated P(3HO) (5 wt% com = 75.39^{o}, 5 wt% neat = 77.4^{o}, 10 wt% com = 76.44^{o} and 10 wt% neat = 78.4^{o}) showed that UV treatment of P(3HO) had improved the wettability i.e. the hydrophilcity of the polymer. Similar observations of increase in wettability has been seen when other polymeric materials such as polyethylene, polypropylene, poly(ethylene terephthalate), nylon 6, polycarbonate, poly(Lactic acid) when exposed to UV rays (Heitz, 2006; Jang and Jeong, 2006; Shangguan *et al.*, 2006; Jaleh *et al.*, 2007; Koo and Jang, 2008).

Incorporation of n-BG also decreased the water contact angle on the UV composite films when compared to the UV neat films. This observation of increased wettability is due to the incorporation of the n-BG particles which are hydrophilic in nature. This increased wettability of the UV composite film is in agreement with the observations made in the previous study by Misra *et al.,* as discussed in Chapter 5 refer section 5.3.1. (Misra *et al.,* 2007; Misra *et al.,* 2008).

UV treatment of P(3HO) was found to increase the stiffness of the fabricated films. Static mechanical test revealed that there were a 9 and 12.42 % increase in the E value for UV 5 wt% composite film and UV 10 wt% composite film respectively when compared to the control 5 wt% and 10 wt% composite films made from non UV treated P(3HO). Higher relative increase in stiffness was seen for the UV P(3HO) neat films, 30 % for the UV 5 wt% neat film and 28.13 % for the UV 10 wt% neat film with respect to comparable films made from non UV treated polymer when compared to the UV P(3HO)/n-BG composite films. This increase in the stiffness of the UV fabricated films is most likely due to the crosslinking i.e. formation of covalent bonds between neighbouring P(3HO) chains when exposed to UV rays. This relatively lower increase in the E values observed for the UV P(3HO)/n-BG composites as opposed to that of the UV P(3HO) neat films could be because in the composites the presence of nBG resulted in relatively higher E values,

therefore the effect of the presence of crosslinks within the polymer chains does not change the E value as drastically. Also, the presence of n-BG in the polymer matrix as in the case of the composites presents a high interfacial surface area between the polymer and the glass inclusions. This could possibly interfere with cross linking and thus reduced the amount of cross linking taking place between the polymer chains. **Figure 6.26** shows a schematic representation of cross linked P(3HO) chains when exposed to UV radiation.

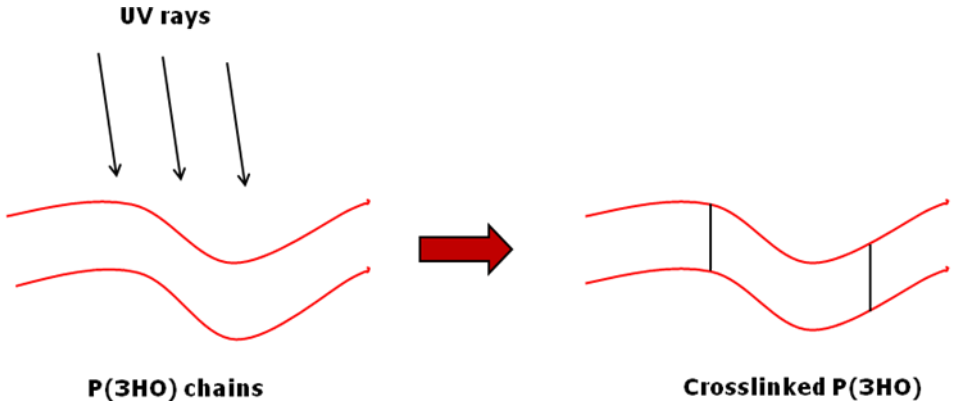

Figure 6.22: Schematic representation of crosslinking of P(3HO) chains using UV rays.

It has been discussed in literature that polymeric materials undergo crosslinking which can be mediated by chemicals, radiation and enzymes. Such crosslinking results in increased tensile strength and reduction in the flexibility of the polymer i.e. increase Young's modulus of the polymer (Bareil *et al.,* 2010). For example, irradiation of collagen with UV rays had been found to increase its tensile strength due to crosslinking (Weadock *et al.,* 1995; Ohan *et al.,* 2002). However, in the studies carried out by Shangguan *et al.* (2006) the Young's modulus value for the P(3HB-co-3HHx) film made from 8 hrs UV treated P(3HB-co-3HHx) was 140.9 MPa and from 16 hrs UV treated P(3HB-co-3HHx) was 147 MPa when compared to the non UV treated polymer with a Young's modulus value of172.5 MPa. Thus, the mechanical

strength of the UV fabricated P(3HB-co-3HHx) films had reduced when compared to the non UV treated P(3HB-co-3HHx).

For the UV composite films the increase in the stiffness could be associated to the crosslinking of the P(3HO) chains and (ii) due to the incorporation of the n-BG particles in the polymer matrix as discussed in previous chapter (chapter 5, section 5.3.1) and observed in previous studies of P(3HB)/n-BG composites carried out by Misra *et al*. (2008) and nanoscale tricalcium phosphate/PLGA composite (Loher *et al.,* 2006). The n-BG particles increase the stiffness by efficiently infiltrating the pores of the polymer matrix thereby sealing it and in the process strengthen the whole composite structure. Secondly, the incorporation of the n-BG into the polymer matrix provides a higher interfacial surface area which enhances the load transfer between the matrix and the stiff inclusions.

Thermal studies of the fabricated films, were also carried out to understand how UV treatment of P(3HO) affected the thermal properties of the fabricated UV P(3HO) neat and UV P(3HO)/n-BG composite films. The thermal properties of the films are depicted in **Figure 6.8** and summarised in **Table 2**.

As discussed in chapter 5 (section 5.3.1) the T_m peak appeared during the first heat scan because of the loss of ordered arrangements of the polymer chains in the crystalline region of the polymer as they melt. Once melted, the polymer chains are unable to rearrange themselves into ordered structures as a result of which no T_m peak is observed during the second heat scan. Incorporation of bioactive nanoglass particles in the polymer matrix resulted in the reduction of the melting temperature as compared to the UV neat films, thus indicating a decreased crystallinity for the UV composite as shown in **Figure 6.9** and **Table 6.1.** This decrease in the crystallinity of the P(3HO)/n-BG composites is due to the introduction of the filler n-BG in the crystalline

portion of the polymer matrix , decreasing the ordered arrangement in the composite. Therefore, as the crystallinity of the composite system gets reduced the polymer chains require less energy to fall out of their ordered structure. Hence, a decrease in the T_m is observed. These, observations were consistent with the observation made in Chapter 5 (section 5.2.3) and observations made by Misra *et al*. (2007), whereby the melting temperature for the composites of poly-3-hydroxybutyrate, P(3HB) and 45S5 Bioglass® (microsize) was lower as opposed to that of neat P(3HB) films (Misra *et al.,* 2007).

6.3.1.2. *In vitro* degradation study

The *in vitro* degradation of the UV fabricated films were carried out to assess how exposure of P(3HO) to UV rays would affect the degradation properties of the fabricated films. For these the films were thermostatically incubated at 37^{o}C in DMEM and DMEM^{KT} media for a period of 1, 2 and 4 months. The reasons for choosing these media have been described previously in chapter 5 (section 5.3.2)

Water absorption, weight loss studies and SEM scans of the films at the end of the 4 months of incubation showed that the films had undergone degradation. As the films were incubated in enzyme free media, the films had undergone hydrolytic degradation in a process autocatalysed by the generation of carboxylic acid end groups as discussed in Chapter 5. SEM images of the degraded films show that the hydrolytic degradation had commenced at the surface of the polymer. The results (**section 5.2.4.1, Figure 6.11**) show that the films absorbed water and lost weight during the incubation period. Both the water absorption and the weight loss increased progressively with time in both the media. Also, the water absorbed and weight loss was higher for the UV composite films as opposed to the UV neat films. Similar results of increased water absorption and weight loss have been

described in literature due to the incorporation of n-BG into the P(3HB) matrix (Misra *et al.,* 2007; Misra *et al.,* 2008). This increased water absorption observed for the composites as opposed to the neat films is due to the presence of n-BG in the composite films which creates large interfacial surface area between the filler phase and the matrix. The water then diffuses or enters through this interface and also due to the hydrophilic nature of the n-BG.

The pH of the media (DMEM and $DMEM^{KT}$) in which the films were incubated were found to increase with the incubation time. The increase in the pH of the media containing UV P(3HO) neat films was because of the degradation of the UV P(3HO) neat films into 3-hydroxyoctanoate. In this present study, like that observed in chapter 5 (section 5.3.2), the pH of the media was higher than that of pKa value for 3-hydroxyoctanoic acid (4.89). Therefore, most of the molecule would exist in the base form, i.e., 3-hydroxyoctanoate, leading to an increase in the pH of the media. However, the increase in the pH of the media in case the composite films is due to the of the leaching out of the Na and Ca ions from the incorporated n-BG particles leading to the formation of alkaline NaOH and $Ca(OH)_2$.

Exposure to UV rays had increased the hydrophilicity of the polymer P(3HO), however, the weight loss experienced by the films fabricated from the UV treated P(3HO) was lower than that of films fabricated from non UV treated P(3HO). The highest % of weight loss experienced by the UV films was 12.48% for the UV 5wt% composite film after 4months of incubation as opposed to 18% weight loss for the non UV 5wt% composite film for the same time point. This decrease in the rate of degradation of the films made from UV treated P(3HO) as opposed to films made from non UV treated P(3HO) is most likely due to the cross linking of the P(3HO) chains when exposed to UV rays. Cross linking of polymers by UV irradiation has been observed to increase the tensile strength, stiffness i.e. Young's modulus and decrease the rate of degradation (Ohan *et al.,* 2002). Thus, the reduced rate of degradation of the

films fabricated using UV treated polymer is most likely an effect of crosslinking of the P(3HO) chains. Thermal and mechanical analysis of the degraded UV films also revealed that the fabricated films were undergoing polymer ageing like that observed for the films made from non UV treated P(3HO) as observed in Chapter 5 (sction 5.2.4). The ageing of the polymer resulted in an increase in the stiffness of the UV fabricated films which increased progressively with time as depicted in **Figure 6.10**. Polymers can undergo change in their bulk properties such as macrostructural, enthalpy, mechanical and dielectric responses as a function of storage time at constant temperature, at zero stress and without any influence of external conditions (Hutchinson, 1995). This process is called ageing and have been reported in many polymers including PHAs such as P(3HB-co-8.1 mol% 3HHx), P(3HB) and P(3HB-co-3HV) (Biddlestone *et al.*, 1996; Asrar *et al.*, 2002; Alata *et al.*, 2007; Parulekar and Mohanty, 2007). Thermal analysis of the UV fabricated films also showed the appearance of a second glass transition temperature that occurred between a range of -51 to -56^{o}C over the incubation time period. This appearance of a second T_g peak indicates that the amorphous regions of the fabricated UV films were undergoing an additional secondary crystallisation due to polymer ageing.

6.3.1.3. Protein adsorption study and *in vitro* cell biocompatibility

Numerous studies have been carried out which have enabled increasing understanding of cell material interface relationships, particularly related to protein adsorption. Most mammalian cells are anchorage-dependent cells and need a biocompatible substrate for attachment, migration and differentiation to form new tissues. Therefore, protein adsorption studies were carried out to evaluate how UV modification of P(3HO) would have affected its biocompatibility and therefore its potential as a biomaterial for tissue engineering application. Protein adsorption studies showed that the amount of proteins adsorbed on the films fabricated from UV treated P(3HO) was

significantly higher than that adsorbed on the films fabricated from non UV treated P(3HO). Also, the amount of protein adsorbed on the UV composites films was also higher than that on the UV neat films. This increase in the adsorption of proteins on the UV fabricated films as opposed to the non UV treated films could have resulted from the nanostructural changes, increase in surface roughness and the increase in the hydrophilicity, of the UV fabricated film surface. Similarly, the higher adsorption of proteins on the UV composite films as opposed to the UV neat films also resulted from the incorporation of n-BG which increased the surface roughness of the films, the hydrophilcity and the surface area of the composite. This increased adsorption of proteins on the composite as opposed to the neat polymer is in agreement with the increased adsorption of proteins observed on composites of P(3HO)/n-BG (Chapter 5, section 5.3.3), P(3HB)/n-BG (Misra *et al.,* 2008), nanoscale hydroxyapatite/PLLA composite scaffold (Wei and Ma, 2004) and fibrous nanoscale tricalcium phosphate/PLGA composite scaffold (Schneider *et al.,* 2008).

The proteins adsorbed on the UV fabricated films as opposed to non UV fabricated were also analysed using XPS based on the amount of nitrogen present on the films before and after incubation with Foetal Bovine Serum (FBS). The presence of nitrogen can be related to the protein content and thus allows for an indirect evaluation of protein adsorption onto the surface layer of the films. The results in **Figure 6.16** show that, as expected, the amounts of nitrogen in both the UV P(3HO) neat and UV P(3HO)/n-BG composite increased post incubation in FBS. The amounts of nitrogen were also found to be higher for the UV fabricated films as opposed to the non UV fabricated films. The adsorption of proteins on the UV P(3HO) neat film was 46.43% higher than that of the comparable neat film made from non UV treated P(3HO). Similarly, the adsorption of protein on the UV P(3HO)/n-BG composite film was 31.22% higher than that of the comparable composite

films made from non UV treated P(3HO). These results show that modification of P(3HO) using UV rays has increased the surface roughness and hydrophilicity of the UV fabricated films which has led to an increased adsorption of the proteins as opposed to the non UV fabricated films. Also, as the protein adsorption was higher on the UV P(3HO)/n-BG composite films as opposed to the comparable UV P(3HO) neat films; the presence of n-BG in the polymer matrix has also contributed to an increased surface roughness, hydrophilicity and surface area of the composite as opposed to the neat UV films. Thus, the XPS studies were in agreement to the observations made in protein adsorption studies. However, XPS measurement (without sputtering) is a surface analysis technique with a depth of 5 nm and hence does not give the total protein adsorbed by the surface.

Biocompatibility studies on these UV fabricated films were evaluated by seeding HaCaT cells on the surface of the films and studying its proliferation for over a period of 1, 4 and 7 days. These results showed that the biocompatibility of the P(3HO) had significantly increased when subjected to modification by exposure to UV rays and with the addition of nBG as a filler. A rough and hydrophilic surface provides a better matrix for cell attachment and proliferation. Therefore, this increase in the biocompatibility of the UV fabricated films can be directly related to increased roughness and the hydrophilicity of the UV fabricated films. Functional groups and the charge they bear also influence the behaviour of both proteins and cells. It has been found that cells adhere well to surfaces with charged functional groups such as –COOH and $–NH_2$, whereas poorly to surfaces carrying $–CH_3$ groups (Ostuni *et al.*, 2001; Arima and Iwata, 2007; Pashkuleva *et al.*, 2010). Therefore, the increase of these charged functional groups COOH, C-OH and C=O on the surface of the film made from the UV treated P(3HO) also explains the increase of protein adsorption and cell growth observed on this surface.

The further increase in biocompatibility of the UV composite films is due to the incorporation of the n-BG which had introduced a rough surface topography, also n-BG has high surface to volume ratio that creates large interfacial area for cell attachment and also due to the increased hydrophilicity of the UV composite films as opposed to the comparable UV neat films. The cell proliferation results obtained thus suggest that a significant increase in the surface roughness and wettability of the P(3HO) surface due to its modification using UV rays (UV neat films) and also incorporation of n-BG (UV composite films) translates into the cytocompatibility of the HaCaTs.

SEM studies of the seeded HaCaT cells also confirmed that the polymer matrix was able to support cell adhesion, its proliferation and maturation. The HaCaTs had arranged themselves into horn sheets by day 4 in the UV composite films. However, on the UV P(3HO) neat films, confluent growth of the cells were observed but with few arrangement of horn sheets. Keratinocytes arrange themselves into four distinct layers. The outermost layer of arrangement is the horn sheets at which state the HaCaT cells are most mature. Therefore, arrangement of horn sheets in the composite films within day 4 indicates that the HaCaT cells have been able to grow and mature faster in the composite films. On the other hand the appearance of only few horn sheets in the neat UV films suggest that the HaCaT cells are growing and maturing comparatively slowly in the neat UV films as opposed to the UV composite films.

Thus the modification of P(3HO) using UV rays and incorporation of n-BG was successful in introducing microstructural changes in the polymer. The films were found to have increased surface roughness and hydrophilicity which aided in improved protein adsorption resulting in improved biocompatibility of the fabricated films. However, the UV treatment in addition to cleavage of ester linkages caused crosslinking of the P(3HO)

chains which increased its stiffness and lowered its degradation rate. The present study has shown the usefulness of controlled UV treatment and incorporation of a bioactive glass ceramic such as n-BG as a method of modification of the polymer, leading to improved biocompatibility.

6.3.2. Blending of P(3HO) with P(3HB)

Blending of polymers is a known method of polymer modification. In this study modification of the flexible P(3HO) by blending it with the hard and brittle P(3HB) produced from *B. cereus* SPV as well as incorporation of n-BG was carried out to assess how blending of these two polymers and incorporating n-BG to the blend would affect the properties of the individual polymers.

6.3.2.1. Properties of the fabricated films

Microstructural studies of the blend and the composite blend films revealed differences in their surface roughness and wettability. It was seen that 5wt% P(3HO)/1wt% P(3HB) film had a smooth surface, however on increasing the amount of P(3HB) from 1 wt% to 5 wt% and simultaneously decreasing the P(3HO) content from 5 to 1 wt%, the blend film revealed a highly rough surface (1.33 μm) as oppose to the 5 wt% P(3HO)/1 wt% P(3HB) film which had a roughness of 0.67 μm. This increase in roughness could be because scl-PHA like P(3HB) are inherently of rough texture and therefore have rough surfaces as oppose to mcl-PHAs like P(3HO) which are smooth in nature this possessing smooth surface. Incorporating n-BG in the blend film of 5 wt% P(3HO)/1 wt% P(3HB) had introduced a rough nanotopography with the roughness of the film being (12.46 μm). The increase roughness of the composite blend was expected as incorporation of n-BG as a filler in polymer matrix have been widely reported to increase the surface roughness of the composite system.

Water contact angle studies showed that the wettability of the composite blend film was the highest (71.06^{o}) when compared to other blend films in this study. This higher hydrophilicity of the composite blend film can again be due to the incorporation of the n-BG which have been reported to be hydrophilic in nature. The 5 wt% P(3HO)/1wt% P(3HB), had a contact angle 86.9^{o} as oppose to only 5 wt% P(3HO) film which had a contact angle of 77.3^{o} (Figure 5.6, chapter 5). Thus introducing P(3HB) 1 wt% to P(3HO) 5 wt% had deceased its wettability. 5wt% P(3HO)/1 wt% P(3HB), had a contact angle value of 86.9^{o}. Thus the blend films showed differences in their surface roughness and wettability.

The blend film with a higher wt% of P(3HO) and a lower wt% of P(3HB) i.e. 1 wt% P(3HB)/5 wt% P(3HO) had the lowest E value of 3.25 MPa and elongation to break of 221.45 %. The film exhibited such low stiffness because of the high P(3HO) content as P(3HO) are very flexible and elastomeric material in nature. Increasing amount of P(3HB) as in the case of 5 wt% P(3HB)/1 wt% P(3HO) increased the stiffness of the film (403 MPa). The % elongation of the film was also reduced to just 2 %. The could be because P(3HB) are hard and brittle in nature exhibiting % elongation of only 5% (Lee, 1995). Incorporating n-BG into this blend polymer matrix 1 wt% P(3HB)/5 wt% P(3HO) had increased the stiffness of the composite (1 wt% P(3HB)/5 wt% P(3HO)) film (E value of 391 MPa). The % elongation was also reduced to 1.23. As discussed in chapter 5, n-BG have been reported to increase the roughness of composite systems by being able to infiltrate the polymer chains thus strengthening it and also because the incorporation of the n-BG into the polymer matrix provides higher interfacial surface area which enhances the load transfer between the matrix and the stiff inclusions.

Water absorption and weight loss behaviour of the films were studied over the incubation time period of 60 days. The results (**Figure 6.24, 6.25**) show that the films did absorb water and lost weight during the incubation period thus

indicating, that the films were undergoing degradation. Here too the films were undergoing hydrolytic degradation. Both the water absorption and the weight loss increased progressively with time. The water absorption was highest for the composite 5 wt% P(3HO)/1 wt% P(3HB) followed by 5 wt% P(3HB)/1 wt% P(3HO) and 5 wt% P(3HO)/1 wt% P(3HB) respectively. Increased water absorption and weight loss experienced by the composite film could be due to the incorporation of n-BG into the polymer matrix which had increased surface roughness and improved wettability of the sample. Similar results of increased water absorption and weight loss have been found in literature due to the incorporation n-BG into the polymer matrix which creates large interfacial surface area between the filler phase and the matrix. The water then diffuses or enters through this interface and also due to the hydrophilic nature of the n-BG (Misra *et al.,* 2007; Misra *et al.,* 2008). Similarly, water absorption was higher on the 5wt% P(3HB)/1wt% P(3HO) as opposed to 5 wt% P(3HO)/1 wt% P(3HB) film. This is because of the high content of P(3HB) in the former than in the latter. P(3HB) having a shorter carbon chain (4 carbons) are comparaticely more hydrophilic than P(3HO) which possess a longer aliphatic carbon chain (8 carbons).

Thus P(3HO) showed marked differences in its surface roughness, wettability, mechanical strength and degradation when (i) blended with varying amounts of P(3HB) and (ii) with the incorporation of n-BG.

Chapter 7: Conclusions and Future works

7.1. Conclusion

In the current scenario of increasing environmental problems and shrinking petroleum reserves, polyhydroxyalkanoates are becoming the focus of attention as a potential substitute for non biodegradable polymers. The properties of biocompatibility, biodegradability and tailorability make PHAs a key player amongst the various bioplastics that are available in the market. PHAs have been used for a number of industrial, agricultural and medical applications. In fact research on the medical applications of PHAs is increasingly attracting interest. An interesting area of PHA application that has recently emerged is its possible use as biofuels. Thus, with new forays for PHA application emerging, many companies are now trading in PHAs. This present study was carried out with an aim of producing polyhydroxyalkanoates from bacteria and then using the polymer produced for medical applications.

B. cereus SPV was isolated in our laboratory and have been observed to accumulate short chain length, scl-PHAs when grown using different carbon sources (Valappil *et al.,* 2006; Valappil *et al.,* 2007). Nutrient(s) limitations play an important role in driving organisms to accumulate PHAs. Therefore, *B. cereus* SPV was subjected to different nutrient limitations of nitrogen, potassium, sulphur, and phosphate to assess the behaviour of the organism to accumulate PHAs under these nutrient limitations. The organism was able to accumulate PHAs under all these nutrient limitations. Good growth and maximum yield of the polymer (38% dcw) was achieved under nitrogen limiting conditions. When analysis of the extracted polymer produced under these nutrient limiting conditions were carried out using FTIR and GCMS, it was found that the organism had mainly accumulated 3-hydroxybutyrate. However, the polymer had accumulated monomers of 3-hydroxybutyrate and 3-hydroxyvalerate under potassium limitations. The production of such

copolymers using structurally unrelated carbon sources glucose will allow industrial production of these copolymers using cheap carbon sources.

Amongst the PHAs, scl-PHAs such as P(3HB), poly(4-hydroxybutyrate), P(4HB) and copolymer such as P(3HB-co-3HV), P(3HB-co-3HHx) have been studied extensively for medical applications. Scl-PHAs are however brittle and stiff and mcl-PHA are flexible and elastomeric. These properties of the mcl-PHAs make them suitable for soft tissue engineering. Therefore, studies were also carried out for the biosynthesis of mcl-PHAs using different *Pseudomoanas* sp. Five different *Pseudomonas* sp were initially studied for mcl-PHA production i.e. *P.putida, P. aeruginosa, P. fluorescens, P. oleovorans* and *P. mendocina.* Studies on these organisms showed that the organism show selective preference for a particular PHA production media to grow and accumulate PHAs. This selective preference of the media could be due to the carbon to nitrogenratio in a particular media. *P. aeruginosa* accumulated an interesting copolymer of 3-hydroxyoctanoate and 2-hydroxydodecanaote, 2(HDD) when grown in octanoate in ME2 medium. 2HDD is a very interesting monomer as occurrence of monomers other than 3-hydroxyacids is very rare. Both *P. putida* and *P. aeruginosa* were able to accumulate mcl-PHAs when grown on octanoate. Amongst these five organisms *P. mendocina* was mainly focussed for the production of mcl-PHAs. The organism was able to accumulate mcl-PHAs and its copolymer when grown in both structurally related (fatty acids) and unrelated (carbohydrate) carbon sources. The organism was able to accumulate a homopolymer of 3-hydroxyoctanoate, P(3HO), which has never been reported in literature previously. The maximum yield obtained for this polymer was 35 % of its dry cells weight. Such a production of a homopolymer of P(3HO) can help in improved understanding of the properties of pure mcl-PHAs as till date most of the mcl-PHA studies have been carried out on copolymers of mcl-PHAs such as P(3HB-co-3HHx), P(3HO) containing different mole fractions of

3(HHx) and 3(HD). Another interesting polymer accumulated by the organism was a copolymer of P(3HB-co-3HO), an scl-mcl copolymer from sucrose. Such a production of a copolymer containing scl and mcl monomers by PHA producers are very rare and can be related to the extraordinarily broad substrate specificity of PHA synthase present in *P. mendocina*. The polymers produced from the fatty acids also had lower melting temperatures and were therefore less crystalline than the polymers from carbohydrates which had higher melting temperatures. The downstream processing study showed that, the kind of extraction method employed does have an effect on the yield, thermal properties, molecular weight and LPS content of P(3HO). By subjecting the polymer to repeated purification, the LPS content of the polymer was reduced to 0.35 EU/ml which complies with the endotoxin requirements of the FDA for biomedical applications such as implants and drug delivery systems (U.S. Department of Health and Human Services, 1997). Physical characterisation of P(3HO) revealed that the polymer was a flexible elastomeric polymer with a Young's modulus value of 11.4 MPa and a crystallinity of 37.2%. Thus the homopolymer P(3HO) is less crystalline than the homopolymer P(3HB) which had a crystallinity of 46% and was hard and brittle (Misra *et al.,* 2007). Studies on the optimum production conditions for increasing the yield of P(3HO) was also carried out. These conditions were generated using the partial factorial design, considering three parameters of pH, C/N ratio and stirrer speed i.e. rpm with their lower and upper limits. The fermentation condition with pH=7.5, rpm = 150 and C/N ratio = 10: 1 resulted in highest yield of P(3HO), which was 35% of the dry cell weight.

The homopolymer P(3HO) was then studied as a potential biomaterial for medical applications. The polymer was fabricated into P(3HO) neat and P(3HO)/n-BG composite films by the solvent casting method. The neat film was assessed as a biomaterial for pericardial patch application. The composite film as a multifunctional wound dressing which would act both as a

biomaterial for skin tissue engineering and also provide a haemostatic effect. Microstructural studies showed a smooth surface for the neat films, whose roughness and wettability was increased by the incorporation of the bioactive nanobioglass particles in the case of composite films. The incorporated n-BG had introduced a rough surface topography on the surface of the film and was present both on the surface as well as in the polymer matrix. Both the neat and composite films had low Young's modulus values and had T_g values below the room temperature. This combined effect of low Young's modulus values and T_g below room temperature imparted elastomeric behaviour to the fabricated films. Importantly the mechanical properties of the fabricated 5 wt% neat film were also found to be suitable to be used as a cardiac patch material. Its Young's modulus value of 1.4 MPa was close to that of polyglycerol sebacate, PGS (1.2 MPa) which is currently being studied for cardiac patch applications (Chen *et al.,* 2008). In fact this fabricated neat P(3HO) has been chosen as one of the biomaterial for pericardial patch application studies in a research project funded by the European Commission (FP-7) in the area of cardiac tissue engineering and regeneration. Similarly, the flexible and elastomeric nature of the composite film also makes it suitable for skin tissue engineering. Such a flexible film can easily fit into difficult contours of the body. However, the mechanical strength of the fabricated composite films were low when compared to human skin. The incorporated n-BG in the polymer matrix was also found to have a haemostatic effect. It accelerated the clotting time, however a clot of weak strength was formed. Both the neat and composite films showed biocompatibility with the seeded HaCaT cells. The cells were able to successfully adhere, proliferate and mature on both the neat and composite films. However, relatively improved growth and proliferation of the HaCaT cells were seen on the composite films as opposed to the neat films. *In vitro* degradation studies revealed that the films undergo slow hydrolytic degradation which is initiated at the surface. The maximum weight loss after

4 months of degradation was 15% for the neat films and 18% for the composite films. The *in vitro* degradation studies also revealed that the films undergo ageing, which resulted in the occurrence of second glass transition and increased stiffness of the polymers. Polymer ageing have been reported in some PHAs such as P(3HB-co-3HHx), P(3HB) and P(3HB-co-3HV) (Biddlestone *et al.*, 1996; Asrar *et al.*, 2002; Alata *et al.*, 2007; Parulekar and Mohanty, 2007).

Studies on the modification of this homopolymer of P(3HO) was also carried out. This was done by exposing P(3HO) to UV rays, incorporating n-BG into the UV treated polymer matrix to form composites and by blending P(3HO) with P(3HB) produced from *B. cereus* SPV and incorporating n-BG into this blend polymer matrix. UV treatment of P(3HO) caused the C-C and ester bond to cleave thus increasing the proportion of the polar groups C-OH and COOH and decreasing the non polar group C-C as confirmed by XPS analysis. XPS analysis also confirmed the presence of C=O bond in the film made from UV treated P(3HO) which occurred from the photooxidation of P(3HO) by UV rays. This cleavage of the C-C bonds and ester linkage had decreased the M_w and increased the M_n of the polymer. As expected, because of the increase in the polar groups C-OH, COOH, incorporation of C=O and decreasing non polar group C-C, the static contact angle on these fabricated films made from the UV treated P(3HO) was reduced i.e. the films showed increased wettability. This increased wettability was also accompanied with increased surface roughness of the films. Also, as expected, within the films made using UV treated polymer, the composite films showed higher hydrophilicity and surface roughness when compared neat films. This was attributed to the incorporation of the n-BG particles in the UV P(3HO)/n-BG composite films. Owing to increased hydrophilicity and surface roughness, the seeded HaCaT cells showed improved growth on UV P(3HO) neat and UV P(3HO)/n-BG composite films as opposed to P(3HO) neat and P(3HO)/n-BG composite films

fabricated from non UV treated P(3HO). However, the stiffness of these UV fabricated films had increased compared to the films made from non UV treated P(3HO). The *in vitro* degradation studies of these films also showed the ageing effect as seen with films fabricated from non UV treated P(3HO). However, these UV fabricated films showed slower rate of degradation as opposed to the comparable films made from non UV treated P(3HO). This slowed degradation rate and increased stiffness could be due to the crosslinking of the polymer chains due to UV exposure. Therefore, although the biocompatibility of the polymer had increased, cross linking had caused an increase in the stiffness and reduced the degradation rate of the polymer.

Blending of the flexible and soft P(3HO) with the brittle and stiff P(3HB) was also carried out to understand the effect of incorporating P(3HB) into the polymer matrix of P(3HO). The surface properties of the blend films was greatly affected by the amounts of P(3HB) incorporated. The roughness was higher for the blend film containing higher wt% of P(3HB). The roughness was further increased with the incorporation of n-BG into this blend matrix.. The stiffness of P(3HO) increased due to the incorporation of P(3HB). *In vitro* degradation studies showed that the fabricated blend and composite blend films undergo hydrolytic degradation. The weight lost by these films at the end of 60 days was 17%, 16% and 19% for 5 wt% P(3HB)+1 wt% P(3HO), 1 wt% P(3HB)+5 wt%P(3HO) and composite (1wt% P(3HB)+5wt%P(3HO)) respectively.

7.2. Future work

The results obtained during this study have given an understanding on the biosynthesis of PHAs by the organisms studied. The homopolymer P(3HO) was assessed for its application as a biomaterial for medical applications and

showed promising results. Therefore based on these results the following experiments are suggested which could be carried out in the future.

7.2.1. Optimisation of P(3HO)

One of the major limiting factors in the applications of mcl-PHAs has been a low yield of mcl-PHAs.. In this present study, the homopolymer P(3HO) was produced for the very first time, which accumulated up to 35% of the bacterial dry cell weight. Initial studies have been carried out to find optimum fermentation condition for P(3HO) production based on partial factorial design. However, in the future, studies could be carried out for finding fermentation conditions based on a full factorial study using pH, C/N and rpm as the varying parameters. Ultimately surface response analysis could then be carried out on the data produced from the fermentation data generated in order to find the optimum condition for P(3HO) production.

7.2.2. *In vitro* degradation studies

The *in vitro* degradation studies showed that the films undergo hydrolytic degradation. After 4 months of incubation the maximum weight lost by these films ranged between 15 to 18%. Thus the films degrade very slowly and therefore, long term degradation studies need to be carried out in order to have a better understanding of the degradation behaviour and the physical and chemical changes taking place in the polymer whilst undergoing degradation. Studies could also be carried out on the degradation behaviour of this polymer in the environment.

7.2.3. Incorporating suitable plasticizers

P(3HO) like many other PHAs was found to age with time. These ageing caused the stiffness of the films to increase which may not be favourable for the proposed applications. Therefore, suitable plasticizers could be incorporated into the polymer matrix in order to inhibit this ageing effect. Therefore, studies should be carried out to find suitable plasticizers which would not interfere with the desired properties of the fabricated films, for a particular application. Some suggested plasticizers which have been used with PHA and other polymers such as PLA are poly(ethyleneglycol) and glucosemonoesters.

7.2.4. Applications of P(3HO)

Roughness, wettability and porosity of films and scaffolds influence cell adhesion and proliferation. Therefore, in the future, biocompatibility of these fabricated P(3HO) films could be enhanced by incorporating pores in it. This could be done by fabricating films using the solvent casting method and leaching out the incorporated salts and sugars. Also by varying the size of the incorporated salts or sugars we could also vary the pore size in these films.

In this study the biocompatibility of the neat films was studied with HaCaTs cell line. However, different cells can behave differently on a similar surface, therefore for pericardial patch application; studies must also be carried out to check the biocompatibility of the fabricated neat films with cardiac cell lines. The films must be able to support the adhesion, proliferation and maturation of the seeded cardiac cells.

For wound dressing application, the incorporated n-BG accelerated blood clotting time but the clot formed was of weak strength. From Ostomel's studies we have seen that the haemostatic effect of bioglass is affected by the

Si to Ca ratio and that the bioglass with Si to Ca ratio of 80 was more haemostatic than with Si to Ca ratio of 60. In this present study the Si to Ca ratio of the incorporated bioactive nanosize 45S5 Bioglass® was 1.69, therefore studies need to be carried out on the composition of the n-BG with desirable Si to Ca ratio, (to start with Si to Ca ratio of 60) which can result in both accelerated clotting time and strong clot formation. In this present study the haemostatic assessment of only the n-BG was carried out, but because the n-BG is to be incorporated into the polymer matrix and then used for the proposed application, therefore studies must also be carried out to assess if the haemostatic property of the n-BG is affected because of its incorporation in the polymer matrix i.e. haemostatic effect of the whole composite system must be assessed.

7.2.5. Modification of P(3HO)

Modification of P(3HO) was found to increase the hydrophilicity and the surface roughness of the fabricated films, which resulted in an increase in biocompatibility. However, cross linking of the P(3HO) occurred due to UV radiation which resulted in increasing the stiffness of the polymer and also lowered its degradation rate. Therefore, other approaches could be used for improving the hydrophilicity and biocompatibility of the polymer as described in section 1.11.

7.2.6. Long term goals

The homopolymer P(3HO) has been proposed as a biomaterial for the fabrication of neat 2D films as cardiac patch and by introducing filler, bioactive 45S5 Bioglass® to form the P(3HO)/n-BG composite film for multifunctional wound dressing. In line of these proposed applications following studies need to be carried out:

7.2.6.1. Fabrication

An ideal construct for the cardiac patch must be able to mimic native human myocardium. Therefore, fabrication studies must be carried out where the patch can replicate myocardium like features. For example possess mechanical properties similar to cardiac muscles, have anisotropic properties, able to orient cardiac cells in the right orientation and provide *in vivo* like oxygen supply to the seeded cells in the patch construct.

Similarly, the P(3HO)/n-BG composite film, must be fabricated to possess mechanical properties similar to that of human skin.

7.2.6.2. Cell

For the cardiac patch application many questions centre around 'cell' that need to be addressed; like what cells can be seeded onto the construct? As cardiac cells do not regenerate one option is to seed the constructs with stem cells differentiate *in vitro* into cardiac cells and suture onto the heart. Another question to look at is, at what stage should the cells be seeded onto the construct and similarly at what stage of the seeded cells in the construct should it be sutured onto the infarcted heart. To find, a reliable and safe source of cells and to find optimum cell density in the construct.

One major limitation of skin tissue engineering is the long waiting time to regenerate skin tissues. Therefore, comprehensive studies need to be carried out where skin regeneration can be carried out efficiently reducing waiting time.

7.2.6.3. Analysis

Further analysis need to be carried out to assess the potential of these fabricated neat and composite films. Since in both the proposed applications the construct will be under constant stress, therefore fatigue studies need to be carried out to assess the creep effect on these constructs. Both the applications require the constructs to enable high oxygen mass transfer, therefore gas permeability assessment of the fabricated neat and composite

films must be carried out. Another important aspect to assess would be the haemocompatibility of these fabricated films.

7.2.6.4. *In vivo* studies

In vivo studies: *In vivo* studies must be carried out in suitable animal models to assess the performance of these constructs in a dynamic environment and to study the physiological and biological reactions that the constructs may evoke.

7.3. Concluding remarks

This study has helped to provide an insight into the accumulation of PHAs by *B. cereus* SPV under different a single nutrient limitations. The PHA accumulation behaviour of the relatively unexplored organism *P. mendocina* was extensively studied. The homopolymer P(3HO) was produced during this study, for the first time. Fabrication of P(3HO) into neat films and P(3HO)/n-BG composites were studied for the first time for medical applications. The fabricated films were found to be biocompatible, a crucially important property for a biomaterial. Thus, the research carried out during this study have therefore successfully resulted in the production of a homopolymer P(3HO) with potential for biomedical applications.

Reference

Abraham G. A., Gallardo A., Roman J. S., Olivera E. R. and Jodra R. (2001). "Microbial synthesis of poly(ß-hydroxyalkanoates) bearing phenyl groups from *Pseudomonas putida*: chemical structure and characterization." Biomacromolecules **2**: 562-567.

Alata H., Aoyama T. and Inoue Y. (2007). "Effect of Aging on the Mechanical Properties of Poly(3-hydroxybutyrate-co-3-hydroxyhexanoate)." Macromolecules **40**: 4546-4551.

Anderson A. J. and Dawes E. A. (1990). "Occurrence, Metabolism, Metabolic Role, and Industrial Uses of Bacterial Polyhydroxyalkanoates." Microbiological Reviews **54**: 450-472

Arima Y. and Iwata H. (2007). "Effects of surface functional groups on protein adsorption and subsequent cell adhesion using self assembled monolayers." Journal of Materials Chemistry **17**(38): 4079–87.

Asrar J., Valentin H. E., Berger P. A., Tran M., Padgette S. R. and Garbow J. R. (2002). "Biosynthesis and Properties of Poly(3-hydroxybutyrate-co-3-hydroxyhexanoate) Polymers." Biomacromolecules **3**: 1006-1012.

Ballistreri A., Giuffrida M., Guglielmino S. P. P., Carnazza S., Ferreri A. and Impallomeni G. (2001). "Biosynthesis and structural characterization of medium-chain-length poly(3-hydroxyalkanoates) produced by *Pseudomonas aeruginosa* from fatty acids." International Journal of Biological Macromolecules **29**: 107-114.

Bang F. B. (1953). "The toxic effect of a marine bacterium on Limulus and the formation of blood clots." The Biological Bulletin **105**: 361-362.

Bareil R. P., Gauvin R. and Berthod F. (2010). "Collagen-Based Biomaterials for Tissue Engineering Applications." Materials **3**: 1863-1887.

Barham P. J. and Keller A. (1986). "The relationship between microstructure and model of fracture in polyhydroxybutyrate " Journal of Polymer Science Physics Education **24**: 69-77.

Bayram C. and Denbas E. B. (2008). "Preparation and Characterization of Triamcinolone Acetonideloaded Poly(3-hydroxybutyrate-co-3-hydroxyhexanoate) (PHBHx) Microspheres." Journal of Bioactive and Compatible Polymer **23**: 334-347.

Bello Y. M., Falabella A. F. and Eaglstein W. H. (2001). "Tissue engineered Skin Current status in wound healing." American Journal of Clinical Dermatology **2**: 305-313.

Berger E., Ramsay B. A., Ramsay J. A. and Chavarie C. (1989). "PHB recovery by hypochlorite digestion of non-PHB biomass,." Biotechnology Techniques. **3**: 227–232.

Bhurke A. S., Askeland P. A. and Drzal L. T. (2000). Annual Meeting of the Adhesion Society, Myrtle Beach, SC.

Biddlestone F., Harris A. and Hay J. N. (1996). "The Physical Ageing of Amorphous Poly(hydroxybutyrate)." Polymer International **39**: 221-229.

Bing O. H. L., Matsushita S., Fanburg B. L. and Levine H. J. (1971). "Mechanical properties of rat cardiac muscle during experimental hypertrophy." Circulation Research **28**(2): 234–45.

Blaker J. J., Bismarck A., Boccaccini A. R., Young A. M. and Nazhat S. N. (2010). "Premature degradation of poly(a-hydroxyesters) during thermal processing of Bioglass-containing composites." Acta Biomaterialia **6**: 756-762.

Boccaccini A. R., Gerhardt L. C., Rebeling S. and Blaker J. J. (2005). "Fabrication, characterisation and assessment of bioactivity of poly(D,L lactid acid) (PDLLA)/TiO2 nanocomposite films." Composites **36**: 721–727.

Borah B., Thakur P. S. and Nigam J. N. (2002). "The influence of nuritional and environmental conditions on the accumulation of poly-beta-hydroxybutyrate in Bacillus mycoides RLJ B-017." Journal of Applied Microbiology **92**: 776-783.

Brandl H., Gross R. A., Lenz R. W. and Fuller R. C. (1988). "*Pseudomonas oleovorans* as a source of poly(b-hydroxyalkanoates) for potential applications as biodegradable polyesters." Applied and Environmental Microbiology. **54**: 1977–1982.

Brandl H., Knee J., Fuller R. C., Gross R. a. and Lenz R. W. (1989). "Ability of the phototrophic bacterium *Rhodospirillum rubrum* to produce various poly(ß-hydroxyalkanoates): potential sources of biodegradabl polyesters." International Journal of Biological Macromolecules **11**: 49-55.

Braunegg G., Sonnleitner B. and Lafferty R. M. (1978). "A rapid gas chromatographic method for the determination of poly-ß-hydroxybutyric acid in microbial biomass." European Journal of Applied Microbiology and Biotechnology **6**: 29-37.

Browne N. and Dowds B. C. A. (2002). "Acid stress in the food pathogen Bacillus cereus." Journal of Applied Microbiology **92**: 404 - 414.

Byrom D. (1987). "Polymer synthesis by microorganisms: technology and economics." Trends in Biotechnology **5**: 246-250.

Caballero K. P., Karel S. F. and Register R. A. (1995). "Biosynthesis and characterisation of hydroxybutyrate-hydroxycaproate copolymers." International Journal of Biological Macromolecules **17**: 86-92.

Carr M. E. and Alving B. M. (1995). "Effect of fibrin structure on plasmin-mediated dissolution of plasma clots." Coagulation Fibrinolysis **6**(6): 567-73.

Chen G. Q. (2005). Polyhydroxyalkanoates, in Biodegradable Polymers for Industrial Applications. Florida, USA, CRC

Chen G. Q. and Qiong W. (2005). "The application of polyhydroxyalkanoates as tissue engineering materials." Biomaterials. **26**: 6565–6578.

Chen J. Y., Liu T., Zheng Z., Chen J. C. and Chen G. Q. (2004). "Polyhydroxyalkanoate synthases PhaC1 and PhaC2 from *Pseudomonas stutzeri* 1317 had different substrate specificities." FEMS Microbiology Letters **234**: 231-237.

Chen J. Y., Song G. and Chen. G. Q. (2006). "A lower specificity of PhaC2 synthase from *Pseudomonas stutzeri* catalyses the production of copolyesters consisting of short-chain-length and medium chain- length 3-hydroxyalkanoates." Antonie van Leeuwenhoek **89**: 157-167.

Chen Q., Roether, J.A., Boccaccini, A.R. (2008). Tissue Engineering Scaffolds from Bioactive Glass and Composite Materials

Chen Q. Z., Bismarck A., Hansen U., Junaid S., Tran M. Q., Harding S. E., Ali N. N. and Boccaccini A. R. (2008). "Characterisation of a soft elastomer poly(glycerol sebacate) designed to match the mechanical properties of myocardial tissue." Biomaterials **29**(47-57).

Choi G. G., Kim H. W. and Rhee Y. H. (2004). "Enzymatic and non-enzymatic degradation of poly (3-hydroxybutyrate-co-3-hydroxyvalerate) copolyesters produced by *Alcaligenes* sp MT-16." Journal of Microbiology. **42**: 346–352.

Choi M. H. and Yoon S. C. (1994). "Polyester Biosynthesis Characteristics of Pseudomonas citronellolis Grown on Various Carbon Sources, Including 3-Methyl-Branched Substrates." Applied and Environmental Microbiology **60**(9): 3245-3254.

Clarinval A. M. and Halleux J. (2005). Classification of biodegradable polymers, in Biodegradable Polymers for Industrial Applications. CRC Fl USA.

Clupper D. C. and Hench L. L. (2003). "Crystallization kinetics of tape cast bioactive glass 45S5." Journal of Non-Crystalline Solids **43**: 318.

Conte E., Catara V., Greco S., Russo M., Alicata R., Strano L., Lombardo A., Silvestro S. D. and Catara A. (2006). "Regulation of polyhydroxyalkanoate synthases (phaC1 and phaC2) gene expression in *Pseudomonas corrugata*." Applied and Environmental Microbiology **72**: 1054-1062.

Cromwick A. M., Foglia T. and Lenz R. W. (1996). "The microbial production of poly(hydroxyalkanoates) from tallow." Applied Microbiology and Biotechnology **46**: 464–469.

de Koning G., Kellerhals M., vanMeurs C. and Witholt B. (1997). "A process for the recovery of poly(hydroxyalkanoates) from Pseudomonads. 2. Process development and economic evaluation." Bioprocess Engineering **17**: 15-21.

de Koning G. J. M. and Witholt B. (1997). "A process for the recovery of poly (hydroxyalkanoates) from Pseudomonads. 1. Solubilization." Bioprocess Engineering **17**: 7-13.

de Smet M. J., Eggink G., Witholt B., Kingma J. and Wynberg H. (1983). "Characterization of intracellular inclusions formed by *Pseudomonas*

oleovorans during growth on octane." Journal of Bacteriology **154** 870–878.

Degelau A., Scheper T., Bailey J. E. and Guske C. (1995). "Fluorometric measurement of poly-b-hydroxybutyrate in Alcaligenes eutrophus by flow cytometry and spectrofluorometry." Applied Microbiology and Biotechnology **42**: 653–657.

Deng Y., Lin X. J., Zheng Z., Deng J. G., Chen J. C., Ma H. and Chen G. Q. (2003). "Poly(hydroxybutyrate-co-hydroxyhexanoate) promoted production of extracellular matrix of articular cartilage chondrocytes in vitro." Biomaterials. **24**: 4273-4281.

Deng Y., Zhao K., Zhang X. F., Hu P. and Chen G. Q. (2002). "Study on the three-dimensional proliferation of rabbit articular cartilage-derived chondrocytes on polyhydroxyalkanoate scaffolds." Biomaterials **23**: 4049-4056.

Diard S., carlier J. P., Ageron E. and Grimont P. A. D. (2002). "Accumulation of poly(3-hydroxybutyrate) from Octanoate in different Pseudomonas Belonging to the rRNA Homology Group I." System Applied Microbiology. **25**: 183-188.

Doi Y. (1990). Fermentation and analysis of microbial polyesters. Microbial Polyesters. New York, VCH Publishers**:** 11-16.

Doi Y., Kanesawa Y., Kawaguchi Y. and Kunioka M. (1989). "Hydrolytic degradation of microbial poly(hydroxyalkanoates." Makromol Chem Rapid Commun **10**: 227–230.

Doi Y., Kanesawa Y., Kunioka M. and Saito T. (1990). "Biodegradation of microbial copolyesters: poly (3-hydroxybutyrate-co-3-hydroxyvalerate) and poly(3-hydroxybutyrate-co-4-hydroxybutyrate)." Macromolecules **23**: 26–31.

Doi Y., Kitamura S. and Abe H. (1995). "Microbial synthesis and characterization of poly(3-hydroxybutyrate-co-3-hydroxyhexanoate)." Macromolecules **28**: 4822–4828.

Doi Y., Kunioka M., Nakamura M. and Soga K. (1986). "Biosynthesis of polyesters by Alcaligenes eutrophus: incorporation of 13C labelled acetate and propionte." Journal of the Chemical Society, Chemical Communications. **23**: 1696-1697.

Durner R., Zinn M., Witholt B. and Egli T. (2000). "Accumulation of poly[(R)-3-hydroxyalkanoates] in Pseudomonas oleovoransDuring Growth in Batch and Chemostat Culture with Different Carbon Sources." Biotchnology and Bioengineering. **72**(3): 278-288.

Durner R., Zinn M., Witholt B. and Egli T. (2001). "Accumulation of poly[(R)-3-hydroxyalkanoates] in Pseudomonas oleovoransDuring Growth in Batch and Chemostat Culture with Different Carbon Sources." Biotchnology and Bioengineering **72**(3): 278-288.

Ehmsen J. M., Peterson K. L., Kedes L., Whittaker P., Dow J. S., Long T. I., Laird P. W. and Kloner R. A. (2002). "Rebuilding a damaged heart-long-term survival of transplanted neonatal rat cardiomyocytes after

myocardial infarction and effect on cardiac function." Circulation **105**(14): 1720-6.

Elbahloul Y. and Steinbüchel A. (2009). "Large-Scale Production of Poly(3-Hydroxyoctanoic Acid) by *Pseudomonas putida* GPo1 and a Simplified Downstream Process." Applied and Environmental Microbiology. **75**(3): 643-651.

Etzion S., Battler A., Barbash I. M., Cagnano E., Zarin P., Granot Y., Kedes L. H., Kloner R. A. and Leor J. (2001). "Influence of embryonic cardiomyocyte transplantation on the progression of heart failure in a rat model of extensive myocardial infarction." J Mol Cell Cardiol **33**(7): 1321-30.

Findlay R. H. and White D. C. (1983). "Polymeric hydroxyalkanoates from environmental samples and *Bacillus megaterium*." Applied and Environmental Microbiology. **45**: 71-78.

Flachskampf F. A., Chandra S., Gaddipatti A., Levine R. A. and Weyman A. E. (2000). "Analysis of shape and motion of the mitral annulus in subjects with and without cardiomyopathy by echocardiographic 3-dimensional reconstruction." Journal of the American Society of Echocardiography **13**(4): 277-87.

Fritzsche K. and Lenz R. W. (1990). "Bacterial polyesters containing branched poly(ß-hydroxyalkanoate) units." Int J Biol Macromol. **12**: 92-102.

Fujimoto K. L., Tobita K., Merryman W. D., Guan J. J., Momoi N. and Stolz D. B. (2007). "An elastic, biodegradable cardiac patch induces contractile smooth muscle and improves cardiac remodeling and function in subacute myocardial Infarction." Journal of the American College of Cardiology **49**(23): 2292-300.

Furrer P., Hany R., Rentsch D., Grubelnik A., Ruth K., Pankeb S. and Zinn M. (2007). "Quantitative analysis of bacterial medium-chain-length poly([R]-3-hydroxyalkanoates) by gas chromatography." Journal of Chromatography.: 199–206.

Furrer P., Maniura K., Zeller S., Panke S. and Zinn M. (2006). "Medium chain length polhydroxyalkanoate: a bacterial biopolyester for medical applications?" European Cells and Materials. **11**(Suppl 2): 4.

Furrer P., Pankeb S. and Zinn M. (2007). "Efficient recovery of low endotoxin medium-chain-length poly([R]-3-hydroxyalkanoate) from bacterial biomass." Journal of Microbiological Methods. **xx** xxx–xxx.

Gagnon K. D., Lenz R. W. and Farris R. J. (1992). "The mechanical properties of a thermoplastic elastomer produced by the bacterium *Pseudmonas oleovorans*." Rubber Chemistry and Technology. **65**(4): 761-777.

Garlotta D. A. (2001). "literature review of poly(lactic acid)A " Journal of Polymers and the Environment **9**(2): 63–84.

Grage K., Jahns A. C., Parlane N., Palanisamy R., Rasiah I. A., Atwood J. A. and Rehm H. A. (2009). "Bacterial Polyhydroxyalkanoate Granules: Biogenesis, Structure, and Potential Use as Nano-/Micro-Beads in

Biotechnological and Biomedical Applications." Biomacromolecules. **10**(4): 660-669.

Grage K. P., V.; Palanisamy, R.; Rehm, B. H. A. ; Ed.; : United Kingdom, 2009; pp (2009). In Microbial production of biopolymers and biopolymer precursors. United Kingdom, Caister Academic Press.

Gross R. A., DeMello C., Lenz R. W., Brand H. and Fuller R. C. (1989). "Biosynthesis and Characterization of Poly@-hydroxyalkanoates) Produced by *Pseudomonas oleovoran*." Macromolecules. **22**: 1106-1115.

Hahn S. K., Chang Y. K., Kim B. S. and Chang H. N. (1994). "Optimization of microbial poly (3-hydroxybutyrate) recovery using dispersions of sodium hypochlorite solution and chloroform." Biotechnology and Bioengineering. **44**: 256-261.

Hahn S. K., Chang Y. K., Kim B. S., Lee K. M. and Chang H. N. (1993). "The recovery of poly (3-hydroxybutyrate) by using dispersion of sodium hypochlorite solution and chloroform." Biotechnology Techniques. **7**: 209–212.

Hahn S. K., Chang Y. K. and Lee S. Y. (1995). "Recovery and characterization of poly (3-hydroxybutyric acid) synthesized in *Alcaligens eutrophus* and recombinant *Escherichia coli*." Applied and Environmental Microbiology. **61**: 34-39.

Hang X., Lin Z., Chen J., Wang G., Hong K. and Chen G. Q. (2002). "Polyhydroxyalkanoate biosynthesis in *Pseudomonas pseudoalcaligenes* YS1." FEMS Microbiology Letters. **212**: 71-75.

Hartmann R., Hany R., Pletscher E., Ritter A., Witholt B. and Zinn M. (2006). "Tailor-made olefinic medium-chain-length poly[(R)-3-hydroxyalkanoates] by *Pseudomonas putida* Gpo1: batch versus chemostat production." Biotechnology and Bioengineering **93**: 737-746.

Haywood G. W., Anderson A. J., Ewing D. F. and Dawes E. A. (1990). "Accumulation of polyhydroxyalkanoate containing primarily 3-hydroxydecanoate from simple carbohydrate substrates by Pseudomonas sp. strain NCIMB 40135." Applied and Environmental Microbiology. **56**: 3354–3359.

Hazenberg W. and Witholt B. (1997). "Efficient production of medium-chain-length poly(3-hydroxyalkanoates) from octane by *Pseudomonas oleovorans* : economic considerations." Applied Microbiology and Biotechnology **48**: 588-596.

He W., Tian W., Zhang G., Chen G. Q. and Zhang Z. (1998). "Production of novel polyhydroxyalkanoates by Pseudomonas stutzeri 1317 from glucose and soybean oil." FEMS Microbiology Letters. **169**: 45-49.

Heitz J. (2006). "Irradiating polymers improves biocompatibility." Biomedical Optics and Medical Imaging Retrieved 4 June 2010, 2010, from http://spie.org/x8635.xml?ArticleID=x8635.

Hocking P. J. and Marchessault R. H. (1994). Biopolyesters in: Chemistry and Technology of Biodegradable Polymers. Glasgow, Blackie.

Holland S. J., Jolly A. M., Yasin M. and Tighe B. J. (1987). "Polymers for biodegradable medical devices. II. Hydroxybutyrate-hydroxyvalerate copolymers: hydrolytic degradation studies." Biomaterials **8**: 289–295.

Holmes P. A. (1988). Biologically produced R(3)-hydroxyalkanoate polymers and copolymers. . Development in crystalline polymers. Bassett D. C. London, Elsevier**:** 1-65.

Hong K., Sun S., Tian W., Chen G. Q. and Huang W. (1999). "A rapid method for detecting bacterial polyhydroxyalkanoates in intact cells by Fourier transform infrared spectroscopy." Applied Microbiology and Biotechnology **51**: 523-526.

Hong K., Sun S., Tian W., Chen G. Q. and Huang W. (1999). "A rapid method for detecting bacterial polyhydroxyalkanoates in intact cells by fourier transform infrared spectroscopy." Applied and Environmental Microbiology. **51**: 523-526.

Huijberts G. N. M., De Rijk T. C., De Waard P. and Eggink G. (1994). "13C nuclear magnetic resonance studies of Pseudomonas putida fatty acid metabolic routes involved in poly(3-hydroxyalkanoate) synthesis." Journl of Bacteriology **176**: 1661-1666.

Huijberts G. N. M. and Eggink G. (1996). "Production of poly(3-hydroxyalkanoates) by *Pseudomonas putida* KT2442 in continuous cultures." Applied and Environmental Microbiology. **46**: 233-239.

Huijberts G. N. M., Eggink G., De Waard P., Huisman G. W. and Witholt B. (1992). "Pseudomonas putida KT2442 cultivated on glucose accumulates poly(3-hydroxyalkanoates) consisting of saturated and unsaturated monomers." Applied and Environmental Microbiology. **58**: 536–544.

Huisman G. W., Leeuw O. D., Eggin G. and Witholt B. (1989). "Synthesis of Poly-3-Hydroxyalkanoates Is a Common Feature of Fluorescent Pseudomonads." Applied and Environmental Microbiology. **55**(8): 1949-1954.

Huisman G. W., Wonink E., Meima R., Kazemier B., Terpstra P. and Witholt B. (1991). "Metabolism of poly(3-hydroxyalkanoates) (PHAs) by *Pseudomonas oleovorans*." The Journal of Biological Chemistry **266**: 2191–2198.

Hutchinson J. M. (1995). "Physical ageing of polymers." Progress in Polymer Science **20**: 703-760.

Jaleh B., Parvin P., Sheikh N., Zamanipour Z. and Sajed B. (2007). "Hydrophilicity and morphological investigation of polycarbonate irradiated by ArF excimer laser." Nuclear Instruments and Methods in Physics Research **265**: 330-333.

Jang J. and Jeong Y. (2006). "Nano roughening of PET and PTT fabrics via continuous UV/O3 irradiation." Dyes and Pigments **69**: 137-143.

Jendrossek D., Frisse A., Behrends A., Andermann M., Kratzin H. D., Stanislawsk T. and Schlegel H. G. (1995). "Biochemical and Molecular

Characterization of the Pseudomonas lemoignei Polyhydroxyalkanoate Depolymerase System." Journal of Bacteriology.: 596-607.

Jendrossek D. and Handrick R. (2002). "Microbial degradation of polyhydroxyalkanoates." Annual Review of Microbiology **56**: 403–432.

Ji Y., Li X. T. and Chen G. Q. (2008). "Interactions between a poly(3-hydroxybutyrate-co-3-hydroxyvalerate-co-3-hydroxyhexanoate) terpolyester and human keratinocytes." Biomaterials. **29**: 3807-3814.

Jiang X., Ramsay J. A. and Ramsay B. A. (2006). "Acetone extraction of mcl-PHA from Pseudomonas putida KT2440." Journal of Microbiological Methods. **67**: 212-219.

Jung K., Hany R., Rentsch D., Storni T., Egli T. and Witholt B. (2000). "Characterisation of New Bacterial Copolyesters Containing 3-hydroxyalkanoates and Acetoxy-3-hydroxyalkanoates." Macromolecules. **33**(23): 8571-8575.

Kannan L. V. and Rehacek Z. (1970). "Formation of poly-beta-hydroxybutyrate by Actinomycetes." Indian Journal of Biochemistry. **7**: 126-129.

Kansiz M., Jacob H. B. and Mc Naughton D. (2000). "Quantitative Determination of the Biodegradable Polymer Poly(b-hydroxybutyrate) in a Recombinant Escherichia coli Strain by Use of Mid-Infrared Spectroscopy and Multivariative Statistics." Applied and Environmental Microbiology **66**(8): 3415–3420.

Kato M., Fukui, T. and Doi, Y. (1996). "Biosynthesis of polyester blends by Pseudomonas sp. 61-3 from alkanoic acids." Bulletin of the Chemical Society of Japan **69**: 515-520.

Kessler B. and Witholt B. (2001). "Factors involved in the regulatory network of polyhydroxyalkanoate metabolism." Journal of Biotechnology. **86**: 97-104.

Kim B. S. (2002). "Production of medium chain length polyhydroxyalkanoates by fed-batch culture of *Pseudomonas oleovorans*." Biotechnology Letters. **24**: 125-130.

Kim B. S., Lee S. C., Lee S. Y., Chang H. N., Chang Y. K. and Woo S. I. (1994). "Production of poly(3-hydroxybutyric acid) by fed-batch culture of *Alcaligenes eutrophus* with glucose concentration control." Biotechnology and Bioengineering **43**: 892–898.

Kim D. Y., Kim H. W., Chung M. G. and Rhee Y. H. (2007). "Biosynthesis, Modification, and Biodegradation of Bacterial Medium -Chain-Length Polyhydroxyalkanoates." The Journal of Microbiology. **45**(2): 87-97.

Kim D. Y., Kim Y. B. and Rhee Y. H. (2000). "Evaluation of various carbon substrates for the biosynthesis of polyhydroxyalkanoatesbearing functional groups by *Pseudomonas putida*." International Journal of Biological Macromolecules **28**: 23-29.

Kim D. Y., Kim Y. B. and Rhee Y. H. (1998). "Bacterial Poly(3-hydroxyalkanoates) Bearing Carbon-Carbon Triple Bonds." Macromolecules. **31**: 4760-4763.

Kim G. J., Lee I. Y., Yoon S. C., Shin Y. C. and Park Y. H. (1997). "Enhanced yield and a high production of medium chain length poly(3-hydroxyalkanoates) in a two-step-fed-batch cultivation of *Pseudomonas putida* by combined use of glucose and octanoate." Enzyme and Microbial Technology. **20**: 500-505.

Kim H. W., Chung C. W., Hwang S. J. and Rhee Y. H. (2005). "Drug release from and hydrolytic degradation of a poly(ethylene glycol) grafted poly(3-hydroxyoctanoate)." International Journal of Biological Macromolecules **36**: 84-89.

Kim H. W., Chung C. W., Kim S. S., Kim Y. B. and Rhee Y. H. (2002). "Preparation and cell compatibility of acrylamide-grafted poly(3-hydroxyoctanoate)." International Journal of Biological Macromolecules **30**: 129-135.

Kim S. N., Shim S. C., Hammer W. J. and Newmark R. A. (1996). "Microbial synthesis of poly(beta-hydroxyalkanoates) containing fluorinated side-chain substituents." Macromolecules. **29**: 4572-4581.

Kim S. W., Kim P., Lee H. S. and Kim J. H. (1996). "High production of poly-beta-hydroxybutyrate (PHB) from *Methylobacterium organophilum* under potassium limitation." Biotechnol Letters **18**: **25-30**.

Kim Y., B; and Lenz R. W. (2001). Polyesters from Microorganisms. Advances in Biochemical Engineering Biotechnology. Babel W. and Steinbuchel A. Berlin, Heidelberg, Springer-Verlag. **71:** 52-79.

Kim Y. B., Kim D. Y. and Rhee Y. H. (1999). "PHAs produced by *Pseudomonas putida* and *Pseudomonas oleovorans* grown with n-alkanoic acids containing aromatic groups." Macromolecules. **32**: 6058-6064.

Kim Y. B., Lenz R. W. and Fuller R. C. (1992). "Poly(ß-hydroxyalkanoates) copolymers containing brominated repeating units produced by *Pseudomonas oleovorans*." Macromolecules. **25**: 1852-1857.

Kim Y. B., Rhee Y. H., Han S. H., Heo G. S. and Kim J. S. (1996). "Poly-3-hydroxyalkanoates produced from *Pseudomonas oleovorans* grown with ω-phenoxyalkanoates." Macromolecules. **29**: 3432-3435.

Klinke S., de Roo G., Witholt B. and Kessler B. (2000). "Role of phaD in accumulation of medium-chain-length poly(3-hydroxyalkanoates) in Pseudomonas oleovorans " Applied and Environmental Microbiology **66**(9): 3705-3710.

Klinke S., Guy D. R., Witholt B. and Kessler B. (2000). "Role of phaD in Accumulation of Medium-Chain-Length Poly(3-Hydroxyalkanoates) in *Pseudomonas oleovorans*." Applied and Environmental Microbiology. **66**(9): 3705–3710.

Knoll M., Hamm T. M., Wagner F., Martinez V. and Pleiss J. (2009). "The PHA Depolymerase Engineering Database: A systematic analysis tool for the diverse family of polyhydroxyalkanoate (PHA) depolymerases." BMC Bioinformatics. **10**: 89.

Koh G. Y., Klug M. G., Soonpaa M. H. and Field L. J. (1993). "Differentiation and long-term survival of C2c12 myoblast grafts in heart." J Clin Invest **92**(3): 1548–54.

Kominek L. A. and Halvorson H. O. (1965). "Metabolism of Poly-ß-Hydroxybutyrate and Acetoin in Bacillus cereus." Journal of Bacteriology. **90**: 125-1259.

Koo G. H. and Jang J. (2008). "Surface Modification of Poly(Lactic Acid) by UV/Ozone Irradiation." Fibers and Polymers **9**(6): 674-678.

Kranz R. G., Gabbert K. K. and Madigan M. T. (1997). "Positive selection systems for discovery of novel polyester biosynthesis genes based on fatty acid detoxification." Applied and Environmental Microbiology **63**: 3010–3013.

Labuzek S. and Radecka I. (2001). "Biosynthesis of PHB tercopolymer by *Bacilllus cereus* UW85." Journal of Applied Microbiology **90**: 353-357.

Lageveen R. G., Huisman G. W., Preusting H., Ketelaar P., Eggink G. and Witholt B. (1988). "Formation of Polyesters by *Pseudomonas oleovorans*: Effect of Substrate on Formation and Composition of Poly-(R)-3-Hydroxyalkanoates and Poly-(R)-3-Hydroxyalkanoates." Appled Environmental Microbiology. **54**(12): 2924-2932.

Langer R. and Vacanti J. P. (1993). Science**:** 260-920.

Laposata M., Hicks D. G. and Connor A. M. (1989). Clinical haemostasis handbook, Year Book medical Pub.

Law J. H. and Slepecky R. A. (1961). "Assay of poly-ß-hydroxybutyric acid." Journal of Bacteriology. **82**: 33-36.

Lee E. Y., J, Jendrossek D., Schirmer A., Choi C. Y. and Steinbüchel A. (1995). "Biosynthesis of copolyesters consisting of 3-hydroxybutyric acid and medium-chain-length 3-hydroxyalkanoic acids from 1,3-butanediol or from 3-hydroxybutyrate by *Pseudomonas* sp. A33." Applied Micobiology and Biotechnology **42**: 901-909.

Lee S. Y. (1995). "Review Bacterial Polyhydroxyalkanoates." Biotechnology and Bioengineering **49**: 1-14.

lee S. Y. and Chang H. N. (1995). "Production of poly-(hydroxyalkanoic acids)." Advances in Biochemical Engineering/Biotechnology **52**: 27-58.

Lee S. Y., Wong H. H., il Choi J., Lee S. H., Lee S. C. and Han C. S. (2000). "Production of Medium-Chain-Length Polyhydroxyalkanoates by High-Cell-Density Cultivation of *Pseudomonas putida* Under Phosphorous Limitation." Biotechnology and Bioengineering. **68**(4): 466-470.

Lee S. Y., Wong H. H., Lee S. H., Lee S. C. and Han C. S. (2000). "Production of Polyhydroxyalkanoates by High -Cell-Density Cultivation of *Pseudomonas putida* Under Phosphorous Limitation." Biotechnology and Bioengineering. **68**: 466-470.

Lee T. R., Lin J. S., Wang S. S. and Shaw G. C. (2004). "PhaQ, a New Class of Poly-ß-Hydroxybutyrate (PHB)-Responsive Repressor, Regulates phaQ and phaP (Phasin) Expression in Bacillus megaterium through Interaction with PHB." Journal of Bacteriology **186**(10): 3015-3021.

Lemoigne M. (1926). "Products of dehydration and of polymerization of β–hydroxybutyric acid." Bulletin de la Société de chimie biologique **8**: 770-782.

Levin J. and Bang F. B. (1968). "Clottable protein in Limulus: its localization and kinetics of its coagulation by endotoxin." Thrombosis et diathesis haemorrhagica journal 186-197.

Li H. and Chang J. (2004). "Fabrication and characterization of bioactive wollastonite/PHBV composite scaffolds." Biomaterials. **25**: 5473–5480.

Li Z. T., Zhang Y. and Chen G. Q. (2008). "Nanofibrous polyhydroxyalkanoate matrices as cell growth supporting materials." Biomaterials. **29**: 3720-3728.

Liebergesell M., Schmidt B. and Steinbu¨chel A. (1992). "Isolation and identification of granule-associated proteins relevant for poly(3-hydroxyalkanoic acid) biosynthesis in *Chromatium vinosum* D." FEMS Microbiology Letters **78**: 227-232.

Loher S., Reboul V., Brunner T. J., Simonet M., Dora C. and Neuenschwander P. (2006). "Improved degradation and bioactivity of amorphous aerosol derived tricalcium phosphate nanoparticles in poly(lactide-co-glycolide)." Nanotechnology **17**: 2054-2061.

Lopez J. G., Rubia T. D., La Ballesteros F. and Cormenzana A. R. (1986). "Growth of *Bacillus megaterium* in phosphate limited medium." Folia Microbiology **31**: 98-105.

Luthen F., Lange R., Becker P., Rychly J., Beck U. and Nebe B. (2005). "The influence of surface roughness of titanium on b1-and b3-integrin adhesion and the organisation of fibronectin in human osteoblastic cells. Biomaterials." Biomaterials **26**: 2423-40.

Macrae R. M. and Wilkinson J. R. (1958). "Poly-b-hydroxybutyrate metabolism in washed suspensions of *Bacillus cereus* and *Bacillus megaterium*." Journal of General Microbiology **19**: 210-222.

Madison L. L. and Huisman G. W. (1999). "Metabolic engineering of poly(3-hydroxyalkanoates): from DNA to plastic." Microbiology and Molecular Biology Reviews **63**: 21-53.

Marcacci M., Kon E., Moukhachev V., Lavroukov A., Kutepov S. and Quarto R. (2007). Tissue Engineering **13**(5): 947-955.

Marcal H., Wanandy N. S., Sanguanchaipaiwong V., Woolnough C. E., Lauto A., Mahler S. M. and Foster L. J. R. (2008). "BioPEGylation of Polyhydroxyalkanoates: Influence on Properties and Satellite-Stem Cell Cycle." Biomacromolecules **9**: 2719–2726.

Marchessault R. H., Monasterios C. J., Morin F. G. and Sundarajan P. R. (1990). "Chiral poly(beta-hydroxyalkanoates): an adaptable helix influenced by the alkane side-chain." International Journal of Biological Macromolecules **12**(2): 158-65.

Marois Y., Ze Zhang., Vert M., Deng X., Lenz R. and Guidone R. (2000). "Mechanism and rate of degradation of polyhydroxyoctanoate films in

aqueous media: A long-term in vitro study." Journal of biomedical materials research **49**(2): 216-24.

Martin D. P. and Williams S. F. (2003). "Medical applications of poly-4-hydroxybutyrate; a strong flexible absorbable biomaterial." Biochemical Engineering Journal. **16**: 97-105.

Matsusaki H., Manji S., Taguchi K., Kato M., Fukui T. and Doi Y. (1998). "Cloning and molecular analysis of the poly(3-hydroxybutyrate) and poly(3-hydroxybutyrate-co-3- hydroxyalkanoate) biosynthesis genes in *Pseudomonas* sp. strain 61-3." J. Bacteriol **180**: 6459–6467.

Mc Cool G. J. and Cannon M. C. (2001). "PhaC and Pha R are required for polyhydroxyalkanoic Acid Synthase Activity in *Bacillus megaterium*." Journal of Bacteriology **183**: 4235-4243.

McLafferty F. W. (1956). "Mass Spectrometric Analysis: Broad Applicability to Chemical Research." Anal. Chem **28**: 306-316.

Mei N., Zhou P., Pan L. F., Chen G., Wu C. G., Chen X., Shao Z. Z. and Chen G. Q. (2006). "Biocompatibility of poly (3-hydroxybutyrate-co-3-hydroxyhexanoate) modified by silk fibroin." Journal of Materials Science: Materials in Medicine. **17**: 749-758.

Misof K., Landis W. J., Klaushofer K. and Fratzl P. (1997). "Collagen from the osteogenesis imperfecta mouse model (oim) shows reduced resistance against tensile stress." Journal of Clinical Investigation **100**(1): 40-5.

Misra S. K., Mohn D., Brunner T. J., Stark W. J., Philip S. E., Roy I., Salih V., Knowles J. C. and Boccaccini A. R. (2008). "Comparison of nanoscale and microscale bioactive glass on the properties of P(3HB)/Bioglass® composites." Biomaterials **29**: 1750-1761.

Misra S. K., Nazhat S. N., Valappil S. P., Torbati M. M., Wood R. J. K., Roy I. and Boccaccini A. R. (2007). "Fabrication and Characterization of Biodegradable Poly(3-hydroxybutyrate) Composite Containing Bioglass." Biomacromolecules **8**(7): 2112–2119.

Misra S. K., Ohashic F., Valappil S. P., Knowles J. C., Roy I., Silva S. R. P., Salih V. and Boccaccini A. R. (2009). "Characterization of carbon nanotube (MWCNT) containing P(3HB)/bioactive glass composites for tissue engineering applications " Acta Biomaterilia.

Misra S. K., Philip S. E., Chrzanowski W., Nazhat S. N., Roy I., KNowles J. C., Salih V. and Boccaccini A. R. (2009). "Incorporation of vitamin E in poly(3hydroxybutyrate)/Bioglass composite films: effect on surface properties and cell attachment." Journal of the Royal Society Interface **6**(33): 401-9.

Misra S. K., Valappil S. P., Roy I. and Boccaccini A. R. (2006). "Polyhydroxyalkanoate (PHA)/Inorganic Phase Composites for Tissue Engineering Applications." Biomacromolecules **7**(8): 2249-2258.

Mochizuki M. and Hirami M. (1997). "Structural effects on the biodegradation of aliphatic polyesters." Polymers for advanced technologies **8**(4): 203-209.

Nagueh S. F., Shah G., Wu Y., Torre-Amione G., King N. M. P. and Lahmers S. (2004). "Altered titin expression, myocardial stiffness, and left ventricular function in patients with dilated cardiomyopathy." Circulation **110**(2): 155-62.

Nair L. S. and Laurencin C. T. (2006). "Polymers as Biomaterials for Tissue Engineering and Controlled Drug Delivery." Advances in Biochemical Engineering/Biotechnology **102**: 47-90.

Nakano K., Sugawara M., Ishihara K., Kanazawa S., Corin W. and Denslow S. (1990). "Myocardial stiffness derived from end-systolic wall stress and logarithm of reciprocal of wall thickness. Contractility index independent of ventricular size." Circulation **82**(4).

Navarro M., Aparicio C., Harris C. M., Ginebra P., Engel E. and Planell J. A. (2006). "Development of biodegradable composite scaffold for bone tissue engineering: physiochemical, topographical, mechanical, degradation and biological properties. ." Advances in Polymer Science **200**: 209-31.

Nelson T., Kaufman E., Kline J. and Sokoloff L. (1981). "The extraneural distribution of γ-hydroxybutyrate." Journal of Neurochemistry **37**: 1345-1348.

Ng K., Rham W., Lim T. C. and Hutmacher W. D. (2005). "Assimilating cell sheets and hybrid scaffolds for dermal tissue engineering." Journal of Biomedical Materials Research Part A **75**: 425–438.

Nocolais L. and Mashelkar R. A. (1977). "Prediction of the Slope Discontinuity in Stress-Strain Behaviour of Polymeric Composites with Spherical Inclusions " International Journal of Polymeric Materials **5**(4): 317-324.

Ohan M. P., Weadock K. S. and Dunn M. G. (2002). "Synergistic effects of glucose and ultraviolet irradiation on the physical properties of collagen." Journal of Biomedical Materials Research **60**: 384–391.

Ostle A. G. and Holt J. G. (1982). "Nile Blue A as a fluorescent stain for poly-b-hydroxybutyrate." Applied and Environmental Microbiology **44**: 238–241.

Ostomel T. A., Shi Q., Tsung C. K., Liang H. and Stucky G. D. (2006). "Spherical Bioactive Glass with Enhanced Rates of Hydroxyapatite Deposition and Hemostatic activity." Small **2**(11): 1261-1265.

Ostomel T. A., Shi Q., Tsung C. K., Liang H. and Stucky G. D. (2006). "Spherical Bioactive Glass with Enhanced Rates of Hydroxyapatite Deposition and Hemostatic activity." Small **2**(11): 1261-1265.

Ostuni E., Chapman R. G., Holmlin R. E., Takayama S. and Whitesides G. M. (2001). " A survey of structure-property relationships of surfaces that resist the adsorption of protein." Langmuir **17**: 5605-20.

Ouyang S. P., Luo R. S., Chen S. S., Liu Q., Chung A., Wu Q. and Chen G. Q. (2007). "Production of Polhydroxyalkanoates with High 3-Hydroxydodecanoate Monomer Content by *fadB* and *fadA* Knockout

Mutant of *Pseudomonas putida* KT2442." Biomacromolecules **8**: 2504-2511.

Page W. J. and Knosp O. (1989). "Hyperproduction of poly-β-hydroxybutyrate during exponential growth of *Azotobacter vinelandii* UWD." Applied and Environmental Microbiology **55**: 1334-1339.

Palleroni N. J., Doudoroff D. and Stainer R. Y. (1970). "Taxonomy of the aerobic pseudomonas: the properties of the *Pseudomonas stutzeri* group." Journal of General Microbiology **60**: 215-231.

Pandey J. K., Kumar A. P., Misra M., Mohanty A. K., Drzal L. T. and R.P. S. (2005). "Recent advances in biodegradable nanocomposites." Journal of Nanoscience and Nanotechnology **5**: 497–526.

Parulekar Y. and Mohanty A. K. (2007). "Extruded Biodegradable Cast Films from Polyhydroxyalkanoate and Thermoplastic Starch Blends: Fabrication and Characterization." Macromolecular Materials and Engineering **292**: 1218-1228.

Pashkuleva I., Marques A. P., Filipe V. and Reis R. L. (2010). "Surface modification of starch based biomaterials by oxygen plasma or UV-irradiation." Journal of Materials Science: Materials in Medicine **21**: 21–32.

Peoples O. P. and Sinskey A. J. (1989). "*Poly-β-hydroxybutyrate biosynthesis in Alcaligenes eutrophus H16. Characteristion of the genes encoding β-ketothiolase and acetoacetyl-CoA reductase*." Journal of Biological Chemistry **264**: 15293-15297.

Peschel G., Dahse H. M., Konrad A., Wieland G. H., Mueller P. J., Martin D. P. and Roth M. (2007). "Growth of keratinocytes on porous films of poly(3-hydroxybutyrate) and poly(4-hydroxybutyrate) blended with hyaluronic acid and chitosan." Journal of biomedical materials research: 1073-1081.

Peters V. and Rehm B. H. A. (2005). "In vivo monitoring of PHA granule formation using GFP-labeled PHA synthases." FEMS Microbiology Letters. **248**: 93-100.

Philip S., Keshavarz T. and Roy I. (2006). "Polyhydroxyalkanoates: biodegradable polymers with a range of applications." JCTB.

Philip S., Keshavarz T. and Roy I. (2007). "Polyhydroxyalkanoates: biodegradable polymers with a range of applications." Journal of Chemical Technology and Biotechnology **82**(3): 233- 247.

Philip S., Sengupta S., Keshavarz T. and Roy I. (2009). "Effect of Impeller Speed and pH on the Production of Poly(3-hydroxybutyrate) Using Bacillus cereus SPV." Biomacromolecules. **10**: 691-699.

Pozo C., Toledo M. V. M., Rodelas B. and Löpez J. G. (2002). "Effects of culture conditions on the production of polyhydroxyalkanoates by *Azotobacter chroococcum* H23 in media containing a high concentration of alpechín (wastewater from olive oil mills) as primary carbon source." Journal of Biotechnology **97**(2): 125-131.

Pratten. J., Nazhat S. N., Blaker J. J. and Boccaccini A. R. (2004). "*In Vitro* Attachment of Staphylococcus Epidermidis to Surgical Sutures with and without Ag-Containing Bioactive Glass Coating." Journal of Biomaterials Applications **19**(47).

Preusting H., Nijenhuis A. and Witholt B. (1990). "Physical Characteristics of Poly(3-hydroxyalkanoates) and Poly(3-hydroxyalkenoates) Produced by *Pseudomonas oleovorans* Grown on Aliphatic Hydrocarbons." Macromolecules **23**: 4220-4224.

Prieto M. A., Buhler B., Jung K., Witholt B. and Kessler B. (1999). "PhaF, a polyhydroxyalkanoate-granule-associated protein of Pseudomonas oleovorans GPo1 involved in the regulatory expression system for pha genes." The Journal of Bacteriology **181**: 858-868.

Qi Q. and Rehm B. H. A. (2001). "Polyhydroxybutyrate biosynthesis in Caulobacter crescentus: molecular characterization of the polyhydroxybutyrate synthase " Microbiology **147**: 3353-3358.

Qu X. H., Wu Q. and Chen G. Q. (2006). "*In vitro* study on hemocompatibility and cytocompatibility of poly(3-hydroxybutyrate-co-3-hydroxyhexanoate)." Journal of Biomaterials Science, Polymer Edition **17**(10): 1107-1121.

Ramires P. A., Romito A., Cosentino F. and Milella E. (2001). "The influence of Titania/Hydroxyapatite Composite Coatings on *in vitro* Osteoblasts Behaviour." Biomaterials **21**(12): 1467-1474.

Ramsay B. A., Langlade V., Carreau P. J. and Ramsay J. A. (1993). "Biodegradability and mechanical-properties of poly-(beta-hydroxybutyrate-co-betahydroxyvalerate) starch blends." Applied and Environmental Microbiology **59**(4): 1242–6.

Ramsay B. A., Saracovan I., Ramsay J. A. and Marchessault R. H. (1991). "Continuous production of long-side-chain poly-ß-hydroxyalkanoates by *Pseudomonas oleovorans*." Applied and Environmental Microbiology. **57**: 625–629.

Ramsay B. A., Saracovan I., Ramsay J. A. and Marchessault R. H. (1992). "Effect of nitrogen limitation on long-side chain poly-b-hydroxyalkanoate synthesis by *Pseudomonas resinovorans*." Applied and Environmental Microbiology **58**: 744–746.

Ramsay J. A., Berger E., Voyer R., Chavarie C. and Ramsay B. A. (1994). "Extraction of poly-3-hydroxybutyrate using chlorinated solvents." Biotechnology Techniques.(8): 589-594.

Randriamahefa S., Renard E., Gue´ rin P. and Langlois V. (2003). "Fourier Transform Infrared Spectroscopy for Screening and Quantifying Production of PHAs by Pseudomonas Grown on Sodium Octanoate." Biomacromolecules **4**: 1092-1097.

Reddy S. V., Thirumala M. and Mahmood S. K. (2009). "A novel Bacillus sp. accumulating poly (3-hydroxybutyrate-co-3-hydroxyvalerate) from a single carbon substrate." J Ind Microbiol Biotechnol **36**: 837–843.

Rehm B. H. A. (2003). "REVIEW ARTICLE Polyester synthases: natural catalysts for plastics." Biochem. J. **376**: 15-33.

Ren Q., de Roo G., Witholt B., Zinn M. and Meyer L. T. (2009). "Overexpression and characterization of medium-chain-length polyhydroxyalkanoate granule bound polymerases from *Pseudomonas putida* GPo1." Microbial Cell Factories **8**(60).

Renard E., Walls W., Guerin P. and Langlois V. (2004). "Hydrolytic degraation of blends of polyhydroxyalkanoates and functionalized polyhydroxyalkanoates." Polymer Degradation and Stability **85**: 779-787.

Reusch R. N. (2002). Non-storage poly-(R)-3-hydroxyalkanoates (complexed PHAs) in prokaryotes and eukaryotes. Weinheim Germany, Wiley-VCH.

Roeder B. A., Kokini K., Sturgis J. E., Robinson J. P. and Voytik-Harbin S. L. (2002). "Tensile mechanical properties of three-dimensional type I collagen extracellular matrices with varied microstructure." J Biomech Eng Trans ASME **124**(2): 214-22.

Rouf M. and Stokes J. (1962). "isolation and identification of the sudanophile granules of Sphaerotilus natans." Journal of Bacteriology **83**: 343-347.

Ruiz M. D. L. and Martinez J. M. M. (2005). "Surface modification of EVA copolymer by UV treatment." International Journal of Adhesion & Adhesives **25**: 139-145.

Ryu H. W., Hahn S. K., Chang Y. K. and Chang H. (1997). "Production of poly(3-hydroxybutyrate) by high cell density fed-batch culture of *Alcaligenes eutrophus* with phosphate limitation." Biotechnol Bioeng. **55**: 28–32.

Sánchez R., Schripsema J., da Silva L. F., Taciro M. K., Pradella G. C. and Gomez G. C. (2003). "Medium-chain-length polyhydroxyalkanoic acids (PHAmcl) produced by *Pseudomonas putida* IPT 046 from renewable sources." European Polymer Journal **39**: 1385-1394.

Schlegel H. G., Lafferty R. and Krauss I. (1970). "*The isolation of mutants not accumulating poly-b-hydroxybutyric acid*." Arch Mikrobiol. **71**: 283-294.

Schmack G., Gorenflo V. and Steinbüchel A. (1998). "Biotechnological production and characterization of polyesters containing 4-hydroxyvaleric acid and medium-chain-length hydroxyalkanoic acids. ." Macromolecules **31**: 644–649.

Schneider O. D., Loher S., Brunner T. J., Uebersax L., Simonet M. and Grass R. N. (2008). "Cotton wool like nanocomposite biomaterials: in vitro bioactivity and osteogenic differentiation of human mesenchymal stem cells." Journal of Biomedical Materials Research B **84B**: 350-62.

Scott G. and Gilead D., Eds. (1995). Degradable Polymers Principles and Applications. London, Chapman and Hall.

Senior P. J. and Dawes E. A. (1971). "Poly-ß-hydroxybutyrate biosynthesis and the regulation of glucose metabolism in *Azotobacter beijerinckii*." Biochemical Journal **125**: 55-66.

Senior P. J. and Dawes E. A. (1973). "The regulation of poly-ß-hydroxybutyrate metabolism in *Azotobacter beijerinckii*." Biochemical Journal **134**(1): 225-238.

Sezer A. D., Hatipoglu F., Cevher E., Ogurtan Z., Bas A. L. and Akbuga J. (2007). "Chitosan Film Containing Fucoidan as a Wound Dressing for Dermal Burn Healing: Preparation and In Vitro/In Vivo Evaluation." AAPS PharmSciTech **8**(2).

Shangguan Y. Y., Wang Y. W., Wu Q. and Chen G. Q. (2006). "The mechanical properties and in vitro biodegradation and biocompatibility of UV-treated poly(3-hydroxybutyrate-co-3-hydroxyhexanoate)." Biomaterials **27**: 2349–2357.

Shin H. D., Lee J. N. and Lee Y. H. (2002). "In vivo blending of medium chain length polyhydroxy-alkanoates and polyhydroxybutyrate using recombinant *Pseudomonas putida* harboring

phbCAB operon of *Ralstonia eutropha*." Biotechnology Letters **24**: 1729–1735.

Sodian R., Hoerstrup S. P., Sperling J. S., Daebritz S., Martin D. P., Moran A. M., Kim B. S., Schoen F. J., Vacanti J. P. and Mayer J. E. (2000). "Early in vivo experience with tissue-engineered trileaflet heart valves." Circulation **102**: 22-29.

Sodian R., Loebe M., Hein A., Martin D. P., Hoerstrup S. P., Potapov E. V., Hausmann H., Leuth T. and Hetzer R. (2002). "Application of stereolithography for scaffold fabrication for tissue engineered heart valves." ASAIO J. **48**: 12-16.

Steinbüchel A. and Eversloh T. L. (2003). "Review: Metabolic engineering and pathway construction for biotechnological production of relevant polyhydroxyalkanoates in microorganisms." Biochemical Engineering Journal **16**: 81-96.

Stock U. A., Nagashima M., Kahalil P. N., Nollert G. D., Herden T., Sperling J. S., Moran A. M., Lien B., Martin D. P., Schoen F. J., Vacanti J. P. and Mayer J. E. (2000). "Tissue engineeed valved conduits in the pulmonary circulation." Journal of Thoracic and Cardiovascular Surgery **119**(4): 732-740.

Stock U. A., Wiederschain D., Kilroy S. M., Tim D. S., Khalil P. N., Vacanti J. P., Mayer J. E. and Moses M. A. (2001). "Dynamics of Extracellular Matrix Production and Turnover in Tissue Engineered Cardiovascular Structures." Journal of Cellular Biochemistry **81**: 220-228.

Sudesh K., Abe H. and Doi Y. (2000). "Synthesis, structure and properties of polyhydroxyalkanoates: biological polyesters." Progress in Polymer Science **25**: 1503-1555.

Sun J., Dai Z., Zhao Y. and Chen G. Q. (2007). "*In vitro* effect of oligo-hydroxyalkanoates on the growth of mouse fibroblast cell line L929." Biomaterials. **28**(28): 3896–3903.

Sun Z., Ramsay J. A., Guay M. and Ramsay B. (2007). "Increasing the yiled of mcl-PHA from nonanoic acid by co feeding glucose during the PHA

accumulation stage in two stage fed bacth fermentatons of *Pseudomonas putida* KT2440." Journal of Biotechnology.

Taguchi K., Aoyagi Y., Matsusaki H., Fukui T. and Doi. Y. (1999). "Over-expression of 3-ketoacyl-ACP synthase III or malonyl-CoAACP transacylase gene induces monomer supply for polyhydroxybutyrate production in Escherichia coli HB101." Biotechnology letters **21**(7): 579±84.

Taguchi K., Tsuge T., Matsumoto K., Nakae S., Taguchi S. and Doi Y. (2001). "Investigation of metabolic pathways for biopolyester production." Riken review. **42**: 71-74.

Tajima K., Igari T., Nishimura D., Nakamura M., Satoh Y. and Munekata M. (2003). "Isolation and characterization of Bacillus sp. INT005 accumulating polyhydroxyalkanoate (PHA) from gas field soil." Journal of Bioscience and Bioengineering **95**: 77-81.

Tang H., Ishii D., Mahara A., Murakami S., Yamaoka T., Sudesh K., Samian R., Fujita M., Maeda M. and Iwata T. (2008). "Scaffolds from electrospun polyhydroxyalkanoate copolymers: Fabrication, characterization, bioabsorption and tissue response." Biomaterials **29**: 1307-1317.

Terskiih V. V. and Vasiliev A. V. (1999). "Cultivation and transplantation of epidermal keratinocytes." International Review of Cytology **188**: 41-72.

Tian W., Hong K., Chen G. Q., Wu Q., Zhang R. Q. and Huang W. (2000). "Production of polyesters consisting of medium chain length 3-hydroxyalkanoic acids by *Pseudomonas mendocina* 0806 from various carbon sources." Antonie van Leeuwenhoek. **77**: 31-36.

Tim D. S., Stock U., Hrkach J., Shinoka T., Lien B., Moses M. A., Stamp A., Taylor G., Moran A. M., Landis W., Langer R., Vacanti J. P. and Mayer J. E. (1999). "Tissue Engineering of Autologous Aorta Using a New Biodegradable Polymer." The Annals of Thoracic Surgery. **68**: 2298-2305.

Timm A. and Steinbuchel A. (1990). "Formation of polyesters consisting of medium-chain-length 3-hydroxyalkanoic acids from gluconate by *Pseudomonas aeruginosa* and other fluorescent *pseudomonads*." Applied and Environmental Microbiology **56**: 3360-3367.

Timm A. and Steinbuchel A. (1990). "Formation of polyesters of mediumchain-length 3-hydroxyalkanoic acids from gluconate by Pseudomonas aeruginosa and other fluorescent pseudomonads." Appl. Environ. Microbiol **56**: 3360–3367.

Tobin K. M. and O' Connor K. E. (2005). "Polyhydroxyalkanoate accumulating diversity of *Pseudomonas* species utilising aromatic hydrocarbons." FEMS Microbiology Letters **253**: 111-118.

Tokiwa Y. and Calabia B. P. (2004). "Degradation of microbial polyesters." Biotechnology letters **26**: 1181 - 1189.

Türesin F., Gürsel I. and Hasirci V. (2001). "Biodegradable polyhydroxyalkanoate implants for osteomyelitis therapy: in vitro

antibiotic release." Journal of Biomaterials Science, Polymer Edition **12**(2): 195-207.

Valappil S. P., Boccaccini A. R., Bucke C. and Roy I. (2006). "Polyhydroxyalkanoates in Gram-positive bacteria:insights from the genera Bacillus and Streptomyces." Antonie van Leeuwenhoek: DOI 10.1007/s10482-006-9095-5.

Valappil S. P., Misra S. K., Boccaccini A. R., Keshavarz T., Bucke C. and Roy I. (2007). "Large-scale production and efficient recovery of PHB with desirable material properties, from the newly characterised *Bacillus cereus* SPV." Journal of Biotechnology **132**(3): 251-258.

Valappil S. P., Misra S. K., Boccaccini A. R. and Roy I. (2006). "Biomedical applications of polyhydroxyalkanoates, an overview of animal testing and *in vivo* responses." Expert Review of Medical Devices **3**(6): 853-868.

Valappil S. P., Peiris D., Langley G. J., Herniman J. M., Boccaccini A. R., Bucke C. and Roy I. (2006). "Polyhydroxyalkanoate (PHA) biosynthesis from structurally unrelated carbon sources by a newly characterized Bacillus spp." Journal of Biotechnology **127**(3): 475-487.

Valappil S. P., Rai R., Bucke C. and Roy I. (2007). "Polyhydroxyalkanoate biosynthesis in *Bacillus cereus* SPV under varied limiting conditions and an insight into the biosynthetic genes involved." Journal of Microbiology.

van der Walle G. A. M., de Koning G. J. M., Weusthuis R. A. and Eggin G. (2001). "Properties, Modifications and Applications of Biopolyesters." Advances in Biochemical Engineering/Biotechnology. **71**: 263-291.

Verlinden R. A. J., Hill D. J. H., Kenward M. A., Williams C. D. and Radeclka I. (2007). "Review article: Bacterial synthesis of biodegradable polyhydroxyalkanoates." Journal of Applied Microbiology: 1365-5072.

Vogel H. J. and Bonner D. (1956). "Acetylornithinase of Escheria coli: Partial purification and some properties." The journal of biological chemistry **218**: 97-106.

Volova T. (2004). Polyhydroxyalkanoates Plastic Material of the 21st Century. Andronic M. and Razmadze R. New Tork, Nova Science Publishers Inc.

Wakisaga Y., Masaki E. and Nishimoto Y. (1982). Applied and Environmental Microbiology **43**: 1473-1479.

Wakisaka Y., Masaki E. and Nishimoto Y. (1982). "Formation of δ-endotoxin or poly-β-hydroxybutyric acid granules by asporogenous mutants of Bacillus thurungiensis." Applied and Environmental Microbiology **43**: 1473-1480.

Wall S. T., Walker J. C., Healy K. E., Ratcliffe M. B. and Guccione J. M. (2006). "Theoretical impact of the injection of material into the myocardium-a finite element model simulation." Circulation **114**(24): 2627-35.

Wallen L. L. and Rohwedder W. K. (1974). "Poly-b-hydroxyalkanoate from activated sludge." Environmental Science and Technology **8**: 576-579.

Wang F. and Lee S. Y. (1997). "Poly(3-hydroxybutyrate) production with high productivity and high polymer content by a fed-batch culture of *Alcaligenes latus* under nitrogen limitation." Applied and Environmental Microbiology **63**: 3703–3706.

Wang Y. D., Ameer G. A., Sheppard B. J. and Langer R. A. (2002). " A tough biodegradable elastomer." Nature Biotechnology **20**(6): 602–6.

Wang Y. W., Qiong W., Chen J. and Chen G. Q. (2005). "Evaluation of three-dimensional scaffolds made of blends of hydroxyapatite and poly(3-hydroxybutyrate-co-3-hydroxyhexanoate) for bone reconstruction." Biomaterials **26**: 899–904.

Wang Y. W., Wu Q. and Chen G. Q. (2005). "Gelatin Blending Improves the Performance of Poly(3-hydroxybutyrate-co-3-hydroxyhexanoate) Films for Biomedical Application." Biomacromolecules **6**: 566-571.

Wang Y. W., Wu Q. O. and Chen G. Q. (2004). "Attachment, proliferation and differentiation of osteoblasts on random biopolyester poly(3-hydroxybutyrate-co-3-hydroxyhexanoate) scaffolds." Biomaterials. **25**: 669-675.

Wang Y. W., yang F., Wu Q., Cheng Y. C., Yu P. H. F., Chen J. and Chen G. Q. (2005). "Effect of composition of poly(3-hydroxybutyrate-co-3-hydroxyhexanoate) on growth of fibroblast and osteoblast." Biomaterials. **26**: 755-761.

Wang Z., Itoh Y., Hosaka Y., Kobayashi I., Nakano Y., Maeda I., Umeda F., Yamakawa J., Kawase M. and Yagi K. (2003). "Novel Transdermal Drug Delivery System with Polyhydroxyalkanoate and Starburst Polyamidoamine Dendrimer." Journal of Bioscience and Bioengineering **95**(5): 541-543.

Ward P. G., De Roo G. and Connor K. E. O. (2005). "Accumulation of Polyhydroxyalkanoate from Styrene and Phenylacetic Acid by Pseudomonas putida CA-3." Applied and Environmental Microbiology.: 2046–2052.

Weadock K. S., Miller E. J., Bellincampi L. D., Zawadsky J. P. and Dunn M. G. (1995). "Physical crosslinking of collagen fibers: Comparison of ultraviolet irradiation and dehydrothermal treatment." Journal of Biomedical Materials Research **29**: 1373-1379.

Webb A. R., Yang J. and Ameer G. A. (2004). "Biodegradable polyester elastomers in tissue engineering." Expert Opinion on Biological Therapy **4**(6): 801–12.

Webster T. J., Ergun C., Doremus R. H., Siegel R. W. and Bizios R. (2000). "Specific Proteins Mediate Enhanced Osteoblast Adhesion on Nanophase Ceramics." Journal of Biomedical Materials Research. **51**(3): 475-483.

Wei G. and Ma P. X. (2004). "Structural and properties of nano-hydroxyapatite polymer composite scaffolds for bone tissue engineering." Biomaterials **25**: 4749-57.

Wiliamson D. H. and Wilkinson J. F. (1958). "The isolation and estimation of poly-ß-hydroxybutyrate inclusions in *Bacillus* species." Journal of General Microbiology **19**: 198-209.

Williams S. F. and Martin D. P. (2005). Applications of PHAs in medicine and pharmacy Weinheim, Germany, Marchessault RH (Eds) Wiley-VCH.

Williams S. F., Martin D. P., Horowitz D. M. and Peoples O. P. (1999). "PHA applications: addressing the price performance issue I. Tissue engineering." International Journal of Biological Macromolecules **25**: 111-121.

Witholt B. and Kessler B. (1999). "Perspectives of medium chain length poly(hydroxyaIkanoates), a versatile set of bacterial bioplastics." Current Opinion in Biotechnology. **10**: 279-285.

Woo K. M., Wei G. and Ma P. X. (2002). "Enhancement of Fibronectin- and Vitronectin-adsorption to Polymer/Hydroxyapatite Scaffolds Suppresses the Apoptosis of Osteoblasts." Jonurnal of Bone and Mineral Research **17**(1): S407–S407.

Wu Q., Huang H., Hu G. H., Chen J., Ho K. P. and Chen G. Q. (2001). "Production of poly-3-hydroxybutyrate by *Bacillus* sp. JMa5 cultivated in molasses media." Antonie van Leeuwenhoek **80**: 111-118.

Wu S., Liu Y. L., Cui B., Qu X. H. and Chen G. Q. (2007). "Study on Decellularized Porcine Aortic Valve/Poly (3-hydroxybutyrate-co-3-hydroxyhexanoate) Hybrid Heart Valve in Sheep Model." Artificial Organs **31**(9): 689-697.

Xi J., Zhang L., Zheng Z., Chen G., Gong Y., Zhao N. and Zhang X. (2008). "Preparation and Evaluation of Porous Poly(3-hydroxybutyrateco-3-hydroxyhexanoate)–Hydroxyapatite Composite Scaffolds." Journal of Applied Biomaterials Applications **22**: 293-307.

Yamane T., Fukunage M. and Lee Y. W. (1996). "Increased PHB productivity by high-cell-density fed-batch culture of *Alcaligenes latus*, growth-associated PHB producer." Biotechnology and Bioengineering **50**: 197-202.

Yang F., Li, X., Li, G., Zhao, N., Zhang, X. (2002). "Study on chitosan and PHBHHx used as nerve regeneration conduit material." Journal of Biomedical Engineering **19**: 25-29.

Yang X. S., Zhao K. and Chen G. Q. (2002). "Effect of surface treatment on the biocompatibility of microbial polyhydroxyalkanoates." Biomaterials **23**: 1391-1397.

Yao J., Zhang G., Wu Q., Chen G. Q. and Zhang R. (1999). "Production of polyhydroxyalkanoates by Pseudomonas nitroreducens." Antonie van Leeuwenhoek **75**: 345–349.

Yasotha K., Aroua M. K., Ramachandran K. B. and Tan I. K. P. (2006). "Recovery of medium-chain-length polyhydroxyalkanoates (PHAs) through enzymatic digestion treatments and ultrafiltration." Biochemical Engineering Journal. **30**: 260-268.

Yin F. C., Dpurgeon H. A., Weisfeldt M. L. and Lakatta E. G. (1980). "Mechanical properties of myocardium from hypertrophied rat hearts. A comparison between hypertrophy induced by senescence and by aortic banding." Circulation Research **46**: 292-300.

York G. M., Stubbe J. and Sinskey A. J. (2001). "New Insight into the Role of the PhaP Phasin of Ralstonia eutropha in Promoting Synthesis of Polyhydroxybutyrate " Journal of Bacteriology. **183**(7): 2394-2397.

Yun S. I., Gadd G. E., Latella B. A., Lo V., Russel R. A. and Holden P. J. (2008). "Mechanical Properties of Biodegradable Polyhydroxyalkanoates/Single Wall Carbon Nanotube Nanocomposite Films." Polymer Bulletin

Yung A. (2010). Retrieved 15 April, 2010, from http://dermnetnz.org/pathology/skin-structure.html.

Zhang L., Xiong C. and Deng X. (2003). "Biodegradable polyester blends for biomedical application." Journal of Applied Polymer Science **56**(1): 103-112.

Zhao K., Deng Y., Chen J. C. and Chen G. Q. (2003). "Polyhydroxyalkanoate (PHA) scaffolds with good mechanical properties and biocompatibility." Biomaterials: 1041-1054.

Zhao K., Deng Y., Chen J. C. and Chen G. Q. (2003). "Polyhydroxyalkanoate (PHA) scaffolds with good mechanical properties and biocompatibility." Biomaterials **24**: 1041-1045.

Zhao K., Yang X., Chen G. Q. and Chen J. C. (2002). "Effect of lipase treatment on the biocompatibility of microbial polyhydroxyalkanoates." Journal of Materials Science: Materials in medicine **13**: 849-854.

Zheng Z., Bei F. F., Deng Y., Tian H. L. and Chen G. Q. (2005). "Effects of crystallization of polyhydroxyalkanoate blend on surface physicochemical properties and resulting biocompatibility for chondrocytes." Biomaterials **26**: 3537-3548.

Zinn M., Witholt B. and Egli T. (2001). "Occurrence, synthesis and medical application of bacterial polyhydroxyalkanoate." Advanced Drug Delivery Reviews. **53**: 5-21.

Appendix

1. Standard curve for glucose estimation

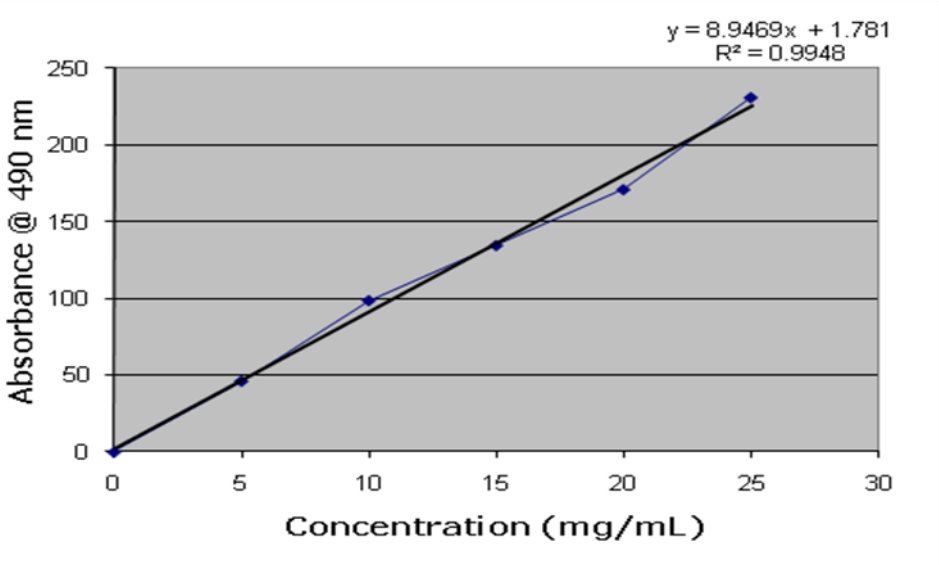

Figure 1: Standard curve for glucose

2. Standard curve for sucrose estimation

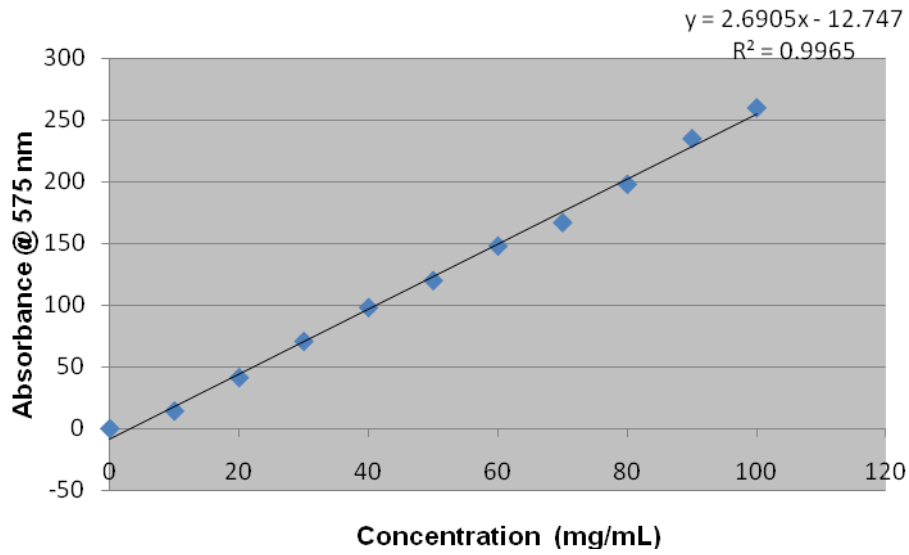

Figure 2: Standard curve for sucrose

3. Standard curve for fatty acid estimation

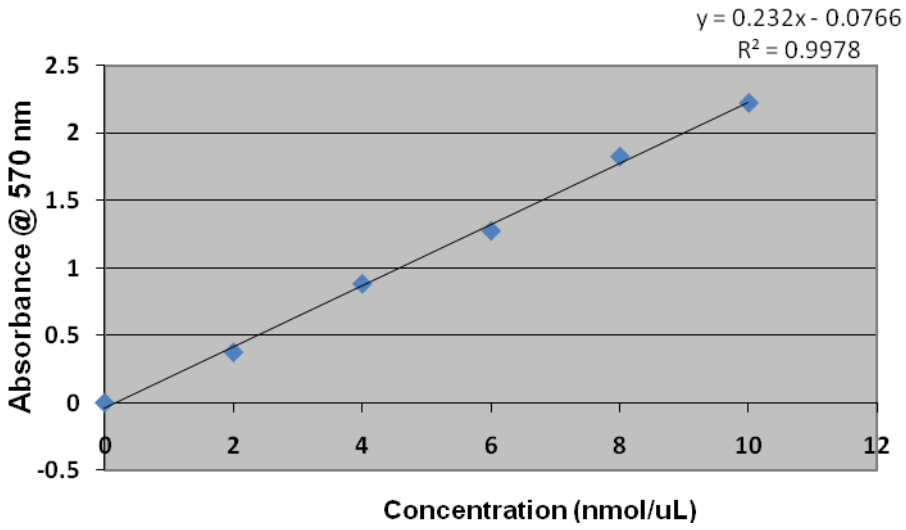

Figure 3: Standard curve for fatty acid

4. Standard curve for endotoxin estimation

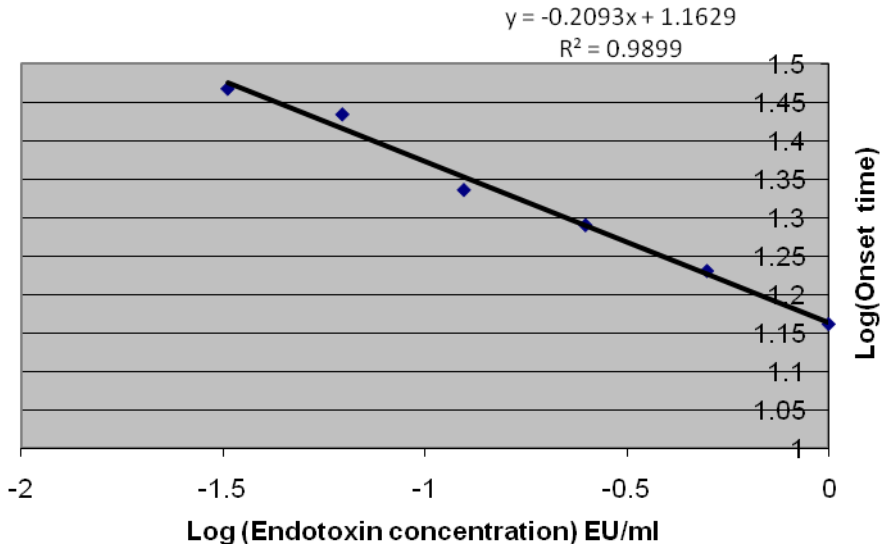

Figure 4: Standard curve for endotoxin

5. Standard curve for nitrogen estimation

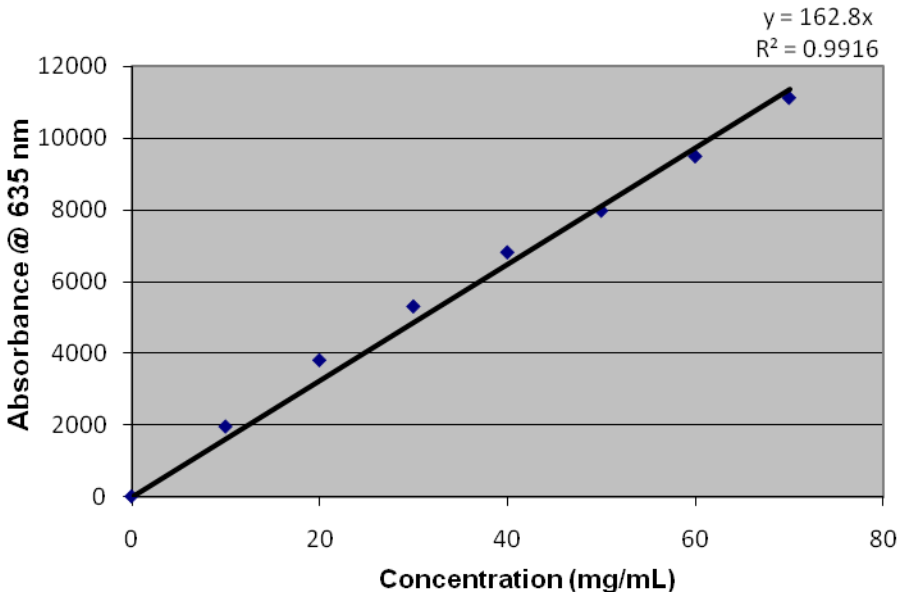

Figure 5: Standard curve for nitrogen

6. Standard curve for protein estimation

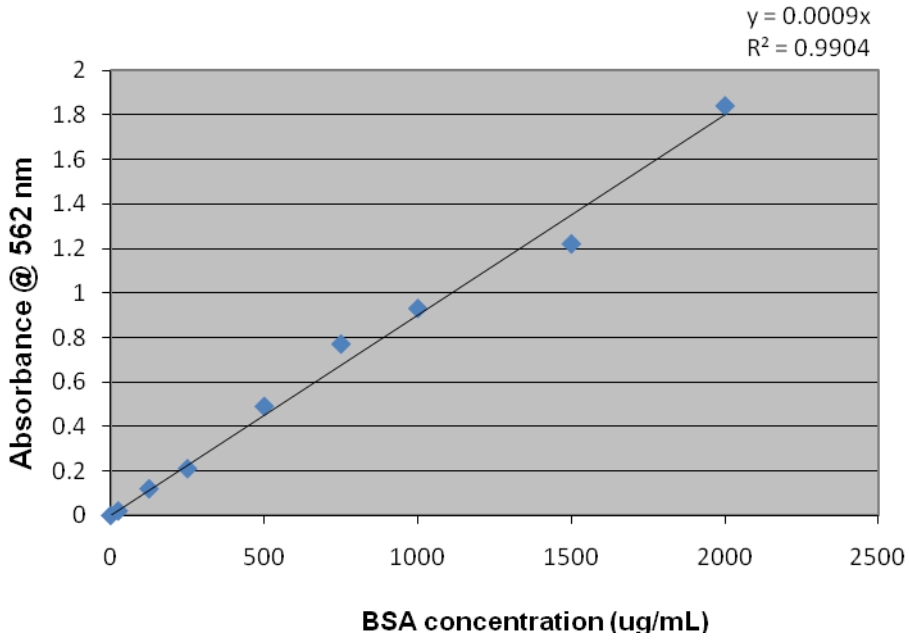

Figure 6: Standard curve for protein

Publications

Peer reviewed publication:

1. Valappil, S. P., **Rai, R**., Bucke, C. and Roy, I. (2008). "Polyhydroxyalkanoate biosynthesis in *Bacillus cereus* SPV under varied limiting conditions and an insight into the biosynthetic genes involved." Journal of Applied Microbiology: 104(6), pp.1624-35.

2. Rai, R and Roy, I. (2010). "Polyhydroxyalkanoates, the emerging new green polymers of choice". In Handbook of Applied Biopolymer Technology: Synthesis, Degradation & Applications. Sharma, S.K., Mudhoo, A. (eds) Royal Society of Chemistry, UK. **(Submitted)**.

3. Rai, R., Keshavarz, T., Roether, J.A., Boccaccini, A.R and Roy, I. (2009). Medium chain length polyhydroxyalkanoates, promising new biomedical materials for the future. Material Science and Engineering: R: Reports **(Submitted).**

4. Thomson, N., Channon , K., Staniewicz, L., Mokhtar , A., **Rai, R**., Roy, I., Summers, D., Sivaniah, E. The application of wet scanning-transmission electron microscopy for imaging internal features of whole, un¯xed bacteria. Journal of Bacteriology **(Submitted).**

Conference publications:

1. Rai, R., Boccaccini, A.R., Knowles, J.C., Locke, I.C., Gordge, M.P., Cormick, A.M., Salih, V., Mordon, N., Keshavarz, T., Roy, I. 2010 "Fabrication of a novel poly(3-hydroxyoctanoate) / nanoscale bioactive glass composite film with potential as a multifunctional wound dressing." In: Proceedings of International Conference on Times of Polymer and Composites. Ischia, Italy.

2. Rai, R., Keshavarz, T., and Roy, I. 2008 "Production of Medium Chain Length Polyhydroxyalkanoates using *Pseudomonas* species" In: Proceedings of International Conference on Biodegradable Polymers: their production, characterisation and application; Auckland, New Zealand.

3. Philip S., Keshavarz T., Bucke C., Francis L., **Rai, R.**, Akaronye E., Valappil S., Misra S., Bucke C., I. Roy 2008 "Microbial biosynthesis of PHAs and their applications" In: Proceedings of Westfocus conference on Health and well-being, University of Westminster, U.K.

4. Rai, R., Keshavarz, T., and Roy, I. 2007 "Production of Medium Chain Length Polyhydroxyalkanoates using *Pseudomonas* species UOW0417398 In: Proceedings of International Conference on Biodegradable Polymers: their production, characterisation and application"; SCI, London, U.K.

5. Rai R., Padinhara S.V., Keshavarz T. and Roy I. 2007 "Production of Polyhydroxyalkanoates from *Bacillus cereus* SPV under different nutrient limiting conditions." In Proceedings of COST 868 Symposium, Graz, Austria.